FORCED CONVECTIVE HEAT TRANSFER FROM AN INCLINED SHELTER ROOF EXPOSED TO SOLAR RADIATION

By

HARRY JOHN BRAUD, JR.

Bachelor of Science in Agricultural Engineering
Louisiana State University
1957

Master of Science in Agricultural Engineering
Louisiana State University
1959

Submitted to the Faculty of the Graduate School of
the Oklahoma State University
in partial fulfillment of the requirements
for the degree of
DOCTOR OF PHILOSOPHY
May, 1962

FORCED CONVECTIVE HEAT TRANSFER FROM AN INCLINED SHELTER ROOF EXPOSED TO SOLAR RADIATION

Thesis Approved:

B. J. Nelson
Thesis Adviser

E. U. Schroeder

Earl E. Marshall

J. W. Bragg

Roger L. Landgrebe

Lloyd Nordeen
Dean of the Graduate School

PREFACE

This study evolved from research projects conducted at the Oklahoma Agricultural Experiment Station dealing with environmental control for animal comfort during summertime hot weather. The investigation was financed through Oklahoma Agricultural Experiment Station Project 834.

Sincere appreciation is extended to Professor Gordon L. Nelson of Agricultural Engineering Department who served as advisor for the investigation. His guidance and direction were invaluable. Thanks is expressed to Professor E. W. Schroeder, Head of the Agricultural Engineering Department for his cooperation and administrative direction of the project.

The writer wishes to thank Professors J. H. Boggs, Head of the Mechanical Engineering Department, R. L. Flanders of the Civil Engineering Department, and C. E. Marshall, Head of Statistics Department for serving on the advisory committee.

The assistance rendered by the personnel of the Computing Center is acknowledged, especially the program writing by Messrs. Gene Pulley and Edgar Butler. Professor J. G. Porterfield of the Agricultural Engineering Department also gave valuable aid in the computing work. Robert Peace, Consultant Meteorologist for the Agricultural Experiment Station gave technical assistance and helpful suggestions concerning

the instrumentation for metering thermal radiation.

To the Agricultural Engineering Department draftsmen, J. I. Fryrear and Don McCrackin, goes a word of thanks for care and patience while preparing the illustrative material.

LIST OF FIGURES

CHAPTER I

INTRODUCTION

Artificial shade shelters are in widespread use in livestock producing areas for reducing the thermal stress on livestock. Especially for conditions of high productivity such as steers on feed wherein the heat production of the animal is high, thermal radiation is a significant part of the heat load. Designers of animal shelters are concerned with finding the shelter configuration and selection of materials which minimize the discomfort of the animals.

A hot weather shelter must protect the animals from the heat of the sun's rays and enhance cooling by allowing free air circulation. Variables involved in the performance of a shade structure are absorptivity of surfaces, shelter configuration, surface textures, orientation of structure with respect to wind direction, and orientation with respect to the direct rays of the sun. Studies by Bond et al. (3) have shown that hot roof surfaces on an unceiled, uninsulated shelter contribute significantly to the heat load on the livestock underneath the shelter.

Investigations have been made to evaluate the effect of surface absorptivity on the heat gain of a solar heated

roof surface. Bond et al. (3), and Ittner and Kelly (27), made studies of the portion of radiant energy absorbed by various surface materials. Nelson et al. (47) and Evans (16) studied the effects of openings in walls on a shelter on the air movement in the shelter.

Shelter configuration has received little attention in studies of the aerodynamic aspects of objects placed in a gradient wind stream. Studies can be found in which the force exerted on various structure components have been investigated, but the thermal behavior or cooling of surfaces as influenced by geometrical relations of the structural elements of shelter forms has not been investigated. The cooling due to wind-induced movement of air over a solar heated surface involves the interplay of three physical phenomena: radiant heat transfer by which the roof gains heat by irradiation, forced convection heat transfer which regulates the cooling due to wind currents, and a fluid flow system which describes the gross flow pattern of the wind over the structure.

The Problem

When solar radiation impinges on a solid surface such as a roof, part of the thermal energy is reflected to the sky and part of the energy is absorbed by the surface, causing an increase in the surface temperature. The surface temperature rises above the ambient air temperature and there is heat flow to the air adjacent to the surface. The rate of heat

flow depends on the temperature difference and the character of the air movement over the surface.

The importance of the cooling effect due to the movement of air over a solar heated roof surface has escaped serious study. Some investigators recognized the effect of surface texture on the heat pickup, but few have compared the heat losses from roof surfaces with different textures. In their studies of surface absorptivity, Bond et al. reported that a shelter with a roof covered with coarse hay was consistently cooler than other materials with better reflecting qualities.

When a prevailing wind direction exists, the orientation of a roof surface with respect to the wind direction influences the wind pattern over the surface and should therefore affect the rate of heat pickup by the air currents. Angle of inclination, height above ground, and roof length are variables the designer can usually adjust at will. With changes in these variables, the nature of air flow over the roof surface should change and thus influence the heat loss from the surface. In a shade shelter designed for optimum summer comfort, what is the proper roof material, orientation, texture, slope angle, and roof height?

Analytical and experimental analyses of heat transfer have well described the heat transfer from a flat smooth surface to a moving air stream. A purely analytical determination of the heat flow from an irregular surface such as a corrugated metal roof does not seem feasible due to the unpredictable disturbance to uniform air movement offered by the corrugations.

A roof surface is usually inclined with respect to the main wind stream. The effect of inclining a surface to the air stream introduces a new variable to the heat transfer system and likewise adds to the complexity of describing the heat transfer rate. Due to the large number of variables involved, an analytical approach to determining the rate of heat transfer from a solar heated roof surface would require unrealistic simplifications and approximations to actual conditions.

Because the roof temperature depends on the magnitude of the solar and sky radiation, on the emissive and absorption properties of the roof material, on the character and properties of the air flowing, and on several parameters of the construction of the structure, a basic relation by which the temperature rise of a roof could be correlated with the magnitude of the pertinent variables would be of value for designers of animal shelters. Also such a correlation would be of value for defining the effect of these variables.

Objective and Procedure

The objective of this study was to make an experimental analysis of the convective cooling of a solar heated shelter roof in a wind stream. The investigation was designed to show in what way the absorptivity, slope, height and texture of the roof of an animal shelter structure affect the temperature rise of the roof when there are air currents moving over the roof. The specific objective was to develop prediction

equations from which the temperature rise of the roof can be determined from observations of radiation intensity, air properties, wind velocity, and absorptive and textural properties of the surface.

In view of the many variables which influence the rate of heat loss from a solid surface to a moving air stream, dimensional analysis was used to arrange dimensionless groups of parameters for simplification of the experimental work. The major portion of the experimental work was conducted with a scaled-down model of a shelter structure. The plan was to operate the model in a wind tunnel which had incandescent heat lamps installed in the ceiling of the tunnel to heat the model roof as the sun heats an actual shelter.

Measurements of the temperature rise on a full size structure and an intermediate shelter were also made to extend the range of variation of the independent variables associated with the gross building size and to check the compatibility of the three test systems. The model system offered conditions in which the wind velocity and intensity of radiation could be controlled readily. The operation of the full size shelter and intermediate size shelter under natural sunshine and in a natural wind provided observations under conditions as they occur in nature.

Limitations

Any research data to be used in design work should be general and widespread in application so that a large portion

of the conditions and circumstances encountered in actual practice fit the range of validity of the research results. On the other hand, limitation of the extent of experimentation is often necessary to allow concentrated study of certain variables so the basic relations among the variables can be realized. With these thoughts in mind the following limitations were pre-assigned to the investigation:

1. Only one type of shelter construction was studied. The shelter type was an open, unceiled pole frame structure with a symmetrical gable roof. No other roof forms were included. This choice of shelter was governed by the availability of an actual shelter building on which measurements in a system with large geometric dimensions could be obtained. The full size shelter had no walls and no ceiling. It was in use for housing turkeys at the Perkins Branch of the Oklahoma Agricultural Experiment Station.
2. Wind direction was taken as normal to eave direction only. Orientation of the shelter with respect to wind direction was not a variable for the study. Most shade structures in use face the prevailing summer breezes.
3. Only thin, uninsulated metal roofing was studied. Many shade shelters consist only of light framing with metal roofing on widely-

spaced purlins. Free air circulation underneath the roof tends to cool a roof just as the air currents above the roof do.

4. The three surface treatments were plain, aged, galvanized steel, aged aluminum, and galvanized steel covered with outside white paint. These treatments gave surfaces with varying degrees of absorption for solar and sky radiation. The prototype shade shelter had strips of each of these kinds of roofing. Thus, the temperature rise of three kinds of materials with different absorption coefficients was investigated.
5. Three surface textures were used. A flat roof and two sizes of corrugated sheet metal were included to learn the effect of surface texture on the cooling effect of the wind currents.
6. Observations of the temperature rise were confined to the areas in the central portion of the roof where the air flow pattern was thought to be two dimensional. Regions near the side edges of a roof are in mixed flow regions due to edge effects.
7. The study was limited to conditions of forced convection heat transfer. No observations were taken with zero wind velocity.

CHAPTER II

REVIEW OF THE LITERATURE

The fundamentals of heat transfer and fluid flow and the information obtained from other sources which form the basis for this study fall into distinct categories. First, there are studies dealing with shade shelters in general which give an evaluation of the performance of a shade shelter in relation to enviromental climatic conditions. The analysis of the mechanics of convective cooling of a solid surface by a moving air stream is a problem in itself and deserves thorough consideration. This cooling effect is actually a thermal effect superimposed on an aerodynamic effect, making the two effects so interrelated that both can be treated as one topic. Boundary layer theory and heat transfer theory comprise the second section of this chapter. An aspect of forced convection heat transfer is the condition of the free wind stream. An account of the character of wind as it occurs in nature is given in the third section. The fourth section reviews the pertinent aspects of solar and sky radiation, radiometers, and the fundamentals of radiant heat transfer applicable to the problem of the heating of a roof exposed to solar and sky radiation. In the fifth section the principles of dimensional analysis and requirements for

physical similarity are discussed.

Related Studies

Animal Shelters

Hot weather shelters for livestock are common in areas of the United States where high environmental temperature and high solar heat loads place thermal stress on livestock. A shade shields the animals from the direct rays of the sun and dissipates the intercepted energy by reflection, reradiation and convection to the air. Kelly, Bond, and Heitman (35) reported that a standard shade lowered the radiant heat load on an animal's horizontal back by 50 to 65 per cent. Reduction in the radiant heat load is also gained by shading the ground around the animals.

A series of studies beginning in 1946 by the University of California in cooperation with the United States Department of Agriculture was conducted to study the factors affecting the performance of shade shelters for livestock. A series of tests reported by Kelly and Ittner (36) at California was a comparison of four types of shades. The types were a wood slat shade, a hay-covered shade, an aluminum shade, and a galvanized iron shade. Each one was 16 x 24 feet and 10 feet high, all with a flat or nearly flat roof. A hemispherical radiometer was placed 3 feet above the ground under the center of the shade to measure the total incoming radiation on a horizontal plane at that point. Observations made at

the hottest part of the day showed that the radiation reaching the flat plate was 181 Btu/hr sq ft under the hay shade, 190 under the aluminum, 193 under the galvanized, and 223 under the wood slat. Measurements of the temperature of the shade surfaces indicated that the galvanized shade average 26 F above air temperature, the aluminum 10 F, wood slat 9 F, and the hay 5 F. As these data were only preliminary measurements for a more detailed study of shade shelters, no significant conclusions were drawn from the findings.

In the following report, Bond, Kelly and Ittner (3) gave design procedure for determining the radiant heat load on an object under an open type shade. Radiant heat exchange shape factors were presented for a rectangular shade with the underside of the shade surface material as a heat source. The analysis was developed for conditions of little or no convective cooling of the shade surfaces. The authors pointed out that wind currents would cool the shade and thereby reduce its radiation downward to the animals under the shade.

Bond, Kelly, and Ittner (3) and Bond and Kelly (2) proceeded to make comparative measurements of the effect of absorptive power of the shade material on the temperature rise of the material and the radiant heat load under the shade. The shades were placed in an open field where wind effects were equal on each shade treatment. A globe thermometer was used for evaluating total radiation received under the shade, and thermocouples were installed to measure the temperature rise of each shade material.

White painted aluminum sheets were found to be as much as 15 F cooler than unpainted aluminum when exposed to the sun; painted galvanized steel sheets were found to be 50 F coller than unpainted galvanized iron. For a minimal radiant heat load under a shade a white-painted top surface with a black-painted bottom surface was found to be superior to other combinations. The shade material that proved invariably cooler than the metal shades was hay. When hay was placed over a metal sheet the radiant heat load under that shade was less than under the others. The hay temperature remained very close to air temperature and as much or 25 F lower than the surface temperature of the plain aluminum shade. The arthors presumed that the rough character of the hay caused much heat loss by convection.

The California studies pointed out the advantage of a highly reflecting surface for reducing the absorption of solar energy. While no attempt was made to evaluate the effect of wind currents for reducing the temperature of the shade, the investigators did point out that wind velocity is an important factor.

Dale and Giese (10) made investigations of the heat gain of insulated airtight compartments under different kinds of roofing. Experimental measurements were taken of the roof surface temperature and air tamperature in the enclosed space under the roof. Using the fundamental laws of heat transfer an analytical analysis was used to predict the heat gain to the insulated compartments. Nine treatments of surfacing material

and types of decking were used in the experiments. The average maximum temperatures reached by the different types of roofing were: galvanized steel, 139.4 F; asphalt shingles, 136.3 F; wood shingles, 129.9 F; asbestos-cement shingles, 123.1 F; aluminum with spaced sheathing, 111.2 F; and aluminum with solid sheathing, 112.2 F. The wind velocity over the period of the test time was given as 6.5 mph on the average. Conclusions drawn from the experiments were that characteristics of a roofing material which affect its solar heat transmission to the interior include absorptivity for solar energy and emissivity. A high outside emissivity and low inside emissivity were found to be most desirable.

Also reported by Dale and Giese was a series of measurements of the temperature under open shade shelters with the five types of roofing. It was reported that little if any difference in temperatures occurred if the wind was blowing as much as two or three mph.

Wind increases the rate of heat loss from the outside surface of the roofing material thereby lowering its surface temperature. With aluminum roofing, sheathing was found to have a negligible effect on the heat transmitted.

Sol-Air Temperature

The engineer who must calculate the cooling load on a building in the summertime needs data on the expected solar and sky radiation in that area, air temperature and humidity, and the wind velocity that can be expected. The interrelation of all variables which affect the heat gain to a building in

the summertime is complicated and has been the subject of much research. Design data computed by the American Society of Heating and Air Conditioning Engineers are extensive. A useful concept utilized in calculation of the heat flow through walls and roofs exposed to solar and sky radiation and cooled by wind currents is the sol-air concept.

Mackey (41) developed the sol-air temperature concept as a logical combination of the factors which influence the rate of heat transfer from the outer surface of a wall or roof. The sol-air temperature is defined by Mackey as:

> ...The temperature of outdoor air, which, in contact with the shaded surface of any building material that does not transmit solar radiation, would give the same rate of heat transfer and the same temperature distribution through that material as exists with the actual outdoor surface and solar radiation incident upon the sunlit surface. (41, p. 75).

For either steady or unsteady heat flow, the rate of heat entry into the outside of an opaque surface is

$$\frac{q}{A} = bI + h\,(t_a - t_s)$$

where q/A = heat flow rate, Btu/hr ft^2
b = absorptivity of the surface for solar radiation
I = intensity of incident solar radiation, Btu/hr ft^2
h = film coefficient for heat transfer between air and the surface, Btu/hr ft^2 F
t_a = outdoor air temperature, F
t_s = surface temperature, F.

Rearranging the right side of the above equation, one gets

$$bI + h\,(t_a - t_s) = h\left(\frac{b}{h} I + t_a - t_s\right)$$

The sol-air temperature is defined to be $t_e = t_a + \frac{bI}{h}$

The rate of heat flow can now be given in terms of the sol-air temperature as

$$\frac{q}{A} = h(t_e - t_s).$$

Dimensionally bI/h is equivalent to a temperature. The ratio b/h is a characteristic of the material surface while I is characteristic of the orientation of the surface. Mackey gave tabulated values of the expected sol-air temperature for a horizontal surface at New York City, based on weather bureau records of solar intensity and air temperatures for that area. The data were developed for unit values of absorptivity. Other tabulations give the sol-air temperature for a vertical surface of various orientations. In another article (42) design sol-air temperatures are presented for Lincoln, Nebraska, based on weather bureau information obtained there. All sol-air temperature tabulations were compiled with an assumed value or the film coefficient of 4 Btu/hr ft^2 F which was based on the results of Rowley, Algren and Blackshaw (56) taken as the correct value for a parallel movement of air past a rough (wood) surface for a 5 mph wind or a 10 mph wind on a glass or painted wood surface.

Sol-air temperature data serve a useful purpose in design calculations of the expected heat flow through building materials for different climatic areas. Because the computations of the sol-air temperature are of primary use in design work, the values of solar intensity and air temperatures used are either maximums or average values accordingly as

which yields safe design requirements. Precise evaluation of the sol-air temperature depends on instantaneous values of solar intensity, film coefficient, wind velocity, air temperature and on the absorption coefficient of the material.

Nelson et al. (47) used the sol-air temperature as a criterion for evaluating the performance of different types of masonry construction and three types of metal roofing for animal shelter construction. As the sol-air temperature is a measure of the rate of heat gain by the outside surface of a material, quantitative evaluation of the sol-air temperature of specimens of a material is an indication of the heat gain of the material on a building if orientation is the same for the specimen and the material on the building and if the wind velocity influence is similar for both.

Sol-air temperature was measured with a sol-air thermometer of the type developed by Mackey and Wright (40). It consists of a 12-inch aluminum foil-covered cork block with a recess on the top surface for installation of the material specimen. The temperature of the material is measured when the specimen is exposed to a known intensity of radiation. With negligible heat flow into the block the sol-air temperatures can be computed from measurements of I and air temperature.

Correlations of sol-air temperature of the roof samples to wind velocity by Nelson et al., showed that the heat gain of a material becomes somewhat independent of absorption coefficient at brisk wind velocities. Enameled steel had the

lowest sol-air temperature, followed by aluminum and then galvanized steel. Sol-air temperature difference among the specimens was more pronounced at low wind velocity than at high wind velocity.

Review

Several of the studies have pointed to the significance of wind currents for reducing the temperature rise of a heated roof surface. The tests of surface absorption by Bond et al. were comparative tests in which equal wind treatments were assumed by placing the test shelters in similar exposures and by making observations when wind currents were nil. Dale and Giese found no differences in environmental temperatures under five test shelters with different roof types when wind velocity exceeded 2 or 3 mph.

The sol-air temperature concept is an attempt to define the heat gain of a material for conditions under which the material would be when in use on a building. This procedure gets nearer to the problem of expressing the true heat gain since it takes into account both the radiative and convective properties pertinent to heat transfer. For design work sol-air temperatures based on weather data of solar intensity in various areas have been developed. These data are necessarily general and of limited value for specific application.

In view of the cooling process in operation when wind blows over the solar heated roof of an open shelter a specification of the film coefficient and surface orientation

characteristics necessary in the sol-air technique is not the usual condition with cooling at only one surface. The occurrence of heat loss from the underside of the metal makes the sol-air technique appear inadequate to define the cooling process. Cooling of the underside of the roof is unpredictable. Furthermore, the leeward roof is not in a direct wind stream which would make specification of a film coefficient a bit difficult. No specific information on the effect of roof configuration on the temperature rise under combined solar heating and wind cooling was found. Dale and Giese (10) found that wind currents tend to cancel the effect of differences in roof absorptivity as far as resultant heat load under a shelter roof is concerned. These results served as a stimulus to an investigation of shelter roof preformance which takes into account all pertinent variables, with the objective of learning the combined effect these variables have on the temperature rise of a shelter roof.

Boundary Layer and Heat Transfer

Introduction

When the movement of a fluid over a solid surface is caused by effects other than the heating or cooling of the fluid, the type of heat transfer is termed forced convection. The wind cooling of a heated roof surface would fall under the classification of forced convection. Since heat transfer is so dependent on the character of flow near the roof surface a review

of the character of fluid flow near a solid surface is in order. Flow near a surface is markedly different from flow in regions away from the surface effects. The name boundary layer is used to define the region near a surface which is under the influence of the surface effects.

Assuming no change of state will occur, properties of a fluid pertinent to boundary exchange phenomena are density, viscosity, thermal conductivity and diffusivity, and temperature. Variables of the solid surface include temperature, area, roughness, and inclination with respect to flow direction. Parameters which describe a flow condition are mean velocity, velocity gradient, and the degree of turbulence. At a point at a given time in a fluid, a particular flow direction can be assigned so specification of a mean velocity of a region of the fluid is more definitive of the gross flow condition. The degree of turbulence specifys what portion of the total fluid particles are conforming to the mean of all velocities as time progresses.

In the boundary layer near a surface, flow characteristics can be described at each point in the boundary layer. Characteristics may change with distance from the surface and also with position along the surface. Problems in heat transfer have commonly been broadly classified as either laminar heat transfer or turbulent heat transfer in accordance with the character of the flow in the boundary layer. In the laminar boundary layer the velocity of flow parallel to the surface varies linearly with distance from the surface. The flow

can be described as sheets of fluid sliding past one another. In the turbulent boundary layer the motion of fluid particles is erratic, and there is movement of particles normal to the surface as well as parallel to it. This mixing effect increases the heat exchange between the fluid and solid.

Boundary Layer Theory

Study of the behavior of flow in the boundary layer has been extensive. In 1874 Osborne Raynolds (52) suggested that heat and momentum are transferred in a similar manner. Prandtl was the first to consider these matters analytically, and his work together with the early studies of Pohlhausen (50) laid the basis for the quantitative interpretation of boundary flows. (9).

The first semi-empirical theory of turbulent skin friction was given in 1921 by Prandtl and Von Karman. Von Karman further developed the work in a 1934 publication (33). The work was based on the theorem that friction between a fluid and a solid is accompanied by an equivalent change in momentum of the fluid. For a flat plate the drag or friction force F_x due to fluid flow in the x direction over the surface was given by Von Karman as

$$F_x = b \int_0^\infty \rho\, u(U - u)\, dy$$

where F_x = friction force, lb
b = width of plate, ft
U = uniform velocity before disturbance, ft/sec
u = velocity parallel to plate at some height y above the plate, ft/sec

y = distance above the plate, ft
ρ = density of fluid, lb_m/ft^3.

The friction force per unit area is the same as the shear stress, hence

$$\tau_o = (1/b)\left(\frac{dF}{dx}\right) = \frac{d}{dx}\left(\int_o^\infty \rho\, u(U - u)\, dy\right)$$

where τ_o = shear stress of fluid, lb/ft^2
dF = force acting on a strip bdx.

For solution Von Karman evaluated the integral from $y = o$ to $y = \delta$, where δ is the boundary layer tickness. In the region beyond δ the velocity defect $(U - u)$ was assumed to be small. The problem of skin friction was then reduced to a problem of velocity profile measurement over the boundary layer. Prandtl had previously derived a mathematical description of the velocity distribution for laminar flow. Von Karman thus obtained for a laminar boundary a coefficient of local friction c_f as

$$c_f = 0.664/(U\, x/\upsilon)^{\frac{1}{2}}$$

where c_f = friction coefficient, dimensionless
υ = kinematic viscosity, ft^2/sec
x = distance along plate in flow direction, ft.

For turbulent flow in the boundary layer Von Karman used the same procedure as for laminar flow except that the velocity distribution was assumed to be described by a function of the form $u = Uf(y/\delta)$, f denoting "function of."

The relation for the velocity distribution had been obtained experimentally so that the coefficient for turbulent

skin friction was presented as

$$c_f = C/(Ux/\upsilon)^{m/m+1}$$

where C a constant and m would be determined from experimental results. For a smooth plate Prandtl and Von Karman obtained

$$c_f = 0.059/(Ux/\upsilon)^{1/5}$$

This result checked with tests on smooth plates in the range for $Ux/\upsilon = 3x10^6$. For larger values Ux/υ the exponent was found to change. New theoretical work was needed to describe phenomena over a larger range of conditions.

Reynolds had shown that the momentum transport in unit time and through unit area due to fluctuations in the velocity components could be represented by an apparent shear stress, of magnitude $\tau = -\rho \overline{u' v'}$

where u' and v' are fluctuations of the velocity components in the x and y directions respectively, and the dash indicates a temporal mean value of the product. The negative sign indicates that shear τ is positive if the fluid at a diatance y from the wall is accelerated by the outside flow. Von Karman recognized the need for a correct length parameter to characterize the flow at a point x on the surface:

> ... we have to introduce a further characteristic parameter of the turbulent flow: namely a length which is characteristic for the size of the region involved in the turbulent exchange: i.e. in the turbulent momentum transfer. (33, p.5).

Recognizing the fact that at high Reynolds number for flow in a pipe the laminar friction is a negligible part of the total friction causing pressure drop, Von Karman concluded that the turbulent exchange is independent of the viscosity of the fluid. For velocity at the center of the pipe denoted by U, velocity at distance y from wall by u, inside radius r, and wall friction by τ_o

$$(U - u) / (\tau_o / \rho)^{\frac{1}{2}} = f\ (y/r)$$

where ρ is fluid density and f represents a functional relationship. The term $(\tau_o / \rho)^{\frac{1}{2}}$ was called the friction velocity.

The requirement that velocity at the wall be zero led Von Karman to conclude that u is fully determined by τ_o, y, ρ, and υ. Dimensional analysis led to the arrangement

$$u = ((\tau_o / \rho)^{\frac{1}{2}}\ g((\tau_o / \rho)^{\frac{1}{2}}\ y/\upsilon)$$

where g denotes a functional relationship. The parameter $((\tau_o/\rho)^{\frac{1}{2}}\ y/\upsilon)$ was called the friction distance parameter and was attributed to Prandtl. It is similar to a Reynolds number because it contains a friction velocity, distance from the surface as a length term, and the kinematic viscosity.

The critical Reynolds number for transition was known to depend also on the turbulence in the outside stream and on the condition of the leading edge of the plate. Thickness of boundary δ was given by Von Karman as:

$$\delta = 0.38 \times (C_f)^{\frac{1}{2}}$$

In the last two decades hundred of papers have been written on research on boundary layer flow. The development of the hot-wire anemometer provided a sensitive tool for measuring velocity transients in the boundary layer. Knowledge gained of momentum transfer was useful in explaining heat transfer because of the similarity of the transfer mechanisms. The growth of the aeronautical sciences gave the greatest impetus to interest in boundary layer phenomena.

With a sensitive hot-wire anemometer Dryden (12) measured the velocity profile near a thin flat plate. The mean velocity measured corresponded to that derived by Blasius from Prandtl's laminar flow equation. The flow was found to vary from laminar to turbulent at a Reynolds number which was greatly affected by turbulence of the free air stream. Increasing air stream turbulence caused a decrease in Reynolds number for transition. Dryden found the turbulence in the free air stream also caused fluctuations in the u-velocity component in the laminar boundary layer.

Dryden's apparatus for velocity measurement was an improvement over the usual pitot tubes for measuring instantaneous velocity components at a point. The response of the anemometer was recorded with an oscillograph for defining the flow at a point; i.e. according to the size and frequency of the fluctuations the flow could be specified as laminar or turbulent. Correlation with fluctuations in the free air stream could be made.

Hinz (22) supported the observation that free stream turbulence has an effect on the laminar boundary layer and the point of transition but little or no effect on the turbulent boundary region. He referred to experiments by Edwards and Furber (14) who measured heat transfer from a flat plate in an air stream which could be made turbulent by means of grids installed upstream from the plate. No effect at all on the rate of heat transfer in the turbulent region of the boundary layer was observed, but a significant effect in the laminar region was noted. With an intensity of free stream turbulence of 5 per cent, the transition occurred at Reynolds number based on distance from the leading edge of approximately 10^5 whereas with no turbulent-producing grid transition occurred at 10^6. The greatest increase in the Nusselt number amounted to 70 per cent at Reynolds number of 2.5×10^5.

Establishment of a turbulent boundary layer along a smooth surface requires a high Reynolds number of flow and sufficient length of plate for viscous drag along the surface to disrupt the stability of the laminar flow. If the upstream edge of the surface is roughened turbulence will ensue sooner, Klebanoff and Diehl (37) glued sandpaper on the first two feet of a smooth plate to promote turbulence. Using hot-wire anemometers and pitotmeters the mean velocity profile and fluctuations were measured in the artifically established turbulent layer. The roughness caused the development of a boundary layer nearly three inches thick, making measurements across the profile easier than in a

Prandtl's modulus other than unity (11).

Von Karman (32) used Reynolds' analogy of heat and momentum transfer to correlate fluid friction with heat transfer. Results of the analysis were expressed in dimensionless groups with a Nusselt number as a function of a Reynolds number and a Prandtl number. The relation was

$$N_n = (0.04\ R_e^{3/4}\sigma)/(1 + 1.74\ R_e^{-\frac{1}{4}}\ (\sigma - 1))$$

where

N_n = Nusselt number, hD/k

R_e = Reynolds number, UD/υ

σ = Prandtl number, υ/α

h = heat transfer coefficient for surface, Btu/hr/ft^2 F

D = suitable length parameter, ft

k = conductivity of fluid, Btu/hr ft F

U = undisturbed velocity, ft/hr

υ = kinematic viscosity, ft^2/hr

α = thermal of diffusivity, ft^2/hr.

In comparison Dittus and Boelter had obtained the empirical formula

$$N_n = 0.0254\ R_e^{0.8}\ \sigma^{0.35}$$

by averaging the results of many experimenters. Agreement between the two relations is good for $\sigma \leq 25$.

A thorough study of heat transfer to air flow past a

surface was made by Jakob and Dow (28). Instead of using a flat plate a solid cylinder with an unheated nosepiece was used for the test specimen. A cylindrical surface is free from edge losses. For turbulent flow in the boundary layer the relation obtained was

$$N_n = 0.028\ R_e^{0.8}\left(1 + 0.40(L_{st}/L_{tot})^{2.75}\right)$$

where L_{st}= length of unheated leading edge

L_{tot}=total length of specimen and

R_e is based on total surface length.

The maximum value of the bracketed term is 1.4 which gives a somewhat high value for the expression. For no unheated leading edge the above expression reduces to

$$N_n = 0.028\ R_e^{0.80}$$

In the laminar flow range Jakob and Dow obtained

$$N_n = 0.590\ R_e^{0.5}$$

which is in good agreement with Pohlhausen's analytic solution for a flat plate which can be expressed

$$N_n = 0.592\ R_e^{0.5}$$

In the turbulent range Latzko had obtained

$$N_n = 0.0356\ R_e^{.08}\sigma$$

with the restriction that σ is equal to 1. For air $\sigma \cong 0.71$

which gives a coefficient to R_e= 0.0253.

Jakob and Dow presented the results of several analytical and experimental investigations of a flat plate to show that their cylindrical specimen gave comparable results. Works referred to were Colburn (7), Latzko (39), Elias (15), Pohlhausen (50) and others.

To study heat transfer from a vertical plate in a parallel air stream at moderate velocities and temperatures, Slegel and Hawkins (59) used an eight-by-ten inch heated brass plate. A film temperature defined as the average of surface and bulk air temperatures was used for determining physical properties of air necessary for correlation. With N_n and R_e based on plate length the test results were expressed in the form

$$N_n = 0.0299\ R_e^{0.817}$$

Jakob (30) in a discussion of the above result suggested that high values for heat loss obtained was probably due to the flow mixing at the edge of the plate. With the thermocouples placed on the center of the plate some heat losses near the edge were unaccounted for.

In order to obtain more exact data on the heat transmission for flat, smooth, glass surfaces Parmlee and Huebscher (49) measured heat flow from a flat plate in a parallel air stream. The restrictions followed included: (1.) The study was limited to a smooth flat plate. (2.) The air stream was undisturbed before encountering the leading edge of the plate. (3.) The flow of air along the plate was such that

the velocity distribution was characteristic of turbulent flow.

Parmlee and Huebscher arranged their data so that it could be correlated with skin friction for flat plates. Colburn (7) had shown that the friction factor can be correlated with heat transfer by

$$N_s N_p^{2/3} = \tfrac{1}{2} C_f$$

Where N_s = Stanton number, $h/c\rho v$

N_p = Prandtl number as before

C_f = friction factor, dimensionless

c = specific heat of air, Btu/lb F

ρ = air density, lbs/ft^3

v = free air stream velocity, ft/sec.

Goldstein's expression (20) for relating C_f to R_e is

$$C_f = 0.455/(\log_{10} R_e)^{2.58}$$

where R_e is based on plate length. Solving for f gives

$$N_s N_p^{2/3} = 0.228/(\log_{10} R_e)^{2.58}$$

This relation gives a method of relating the Stanton and Prandtl number to the Reynolds number. The Stanton and Prandtl numbers are composed of quantities related to heat transfer, the Reynolds number contains quantities descriptive of the type of flow.

Correlation of the experimental data of Parmlee and Huebscher with the above equation was good when the distance

from the leading edge to the test point was taken into account. Curves were developed for the mean heat transfer coefficient versus length of surface for air velocities from 5 to 25 mph. These curves were presented mainly to show that length of surface affects the coefficient. The authors pointed out that the mean heat transfer coefficient changes with velocity to 0.8 power and inversely as length of surface to 0.2 power.

Parmlee and Huebscher noted that heat transfer coefficients developed under controlled wind tunnel conditions would have to be used with caution to describe heat transfer under natural conditions. The effect of roughness characteristic of the type of material and also general roughness caused by window ledges, mortar joints, etc. is uncertain. Consideration should also be given to angle of air flow approach. Of prime importance and not understood is the effect of large scale turbulence or eddying of the air stream.

Seban and Doughty (58) used crystalline grit on the leading edge of the plate to establish turbulence near the leading edge.

Tests were made with a constant free stream velocity with natural transition in the boundary layer, and the results obtained were in substantial agreement with the Colburn and Von Karman analogies for heat flow to a turbulent boundary layer.

Heat Flow From Inclined Surfaces

A roof surface is usually not parallel to the direction

of the main wind stream under natural conditions. The investigations of heat losses from inclined surfaces have been less extensive than for horizontal and vertical surfaces.

Rowley and Eckley (57) evaluated an over-all surface heat coefficient for a test surface at different angles of incidence between wind direction and surface orientation. The heated test surface was fifteen inches square with a wing placed on the leading edge to direct air passage over the surface and to prevent disturbing eddy currents from forming at the leading edge. Plate glass and smooth pine surfaces were used.

For zero angle of incidence and zero air velocity the surface coefficients were essentially the same as reported by Houghten and McDermott (23). Increase in angle of incidence produced a slight decrease in surface coefficient. The authors stated:

> On a whole, the reduction in the numerical value of the coefficient was not as much as anticipated, and for practical purposes, the coefficients as obtained for parallel flow would be satisfactory. (57, p. 37).

At a given wind speed the coefficient was largest for zero angle of incidence and least for 60° angle of incidence while the air velocity parallel to the surface decreased in magnitude as the angle of incidence increased. No large difference in coefficient due to surface type was noted although the pine surface had a slightly higher coefficient than the glass. Flow visualization photographs showed that esentially streamline flow existed over the surface for angles of incidence less than 60°. A stagnation area developed before the plate for angles greater than 60°.

Drake (11) in a 1949 publication reviewed the literature and found no data available for heat transfer from inclined plates. He proceeded to measure the point unit heat transfer coefficients for inclined plates. The experiments were limited to a study of laminar flow with the plate inclined and a study of turbulent flow over a horizontal plate. A smooth plate 18 inches long was placed in a variable wind stream. The leading edge of the plate was sharpened to cause the turbulent boundary layer to begin at the same point as the incipient thermal effects for the case of zero angle of incidence. No attempt was made to maintain an isothermal surface during the tests.

Data were presented in log-log curves of N_{n_x} versus R_{e_x} and $N_{n_x}/(R_{e_l})^{\frac{1}{2}}$ versus x/l

where N_{n_x} = Nusselt number at point x, $h_x\, x/k$,

R_{e_x} = Reynolds number at point x, $U_o\, x/\upsilon$

R_{e_l} = Reynolds number for plate, $U_o\, l/\upsilon$

x = distance to point x from leading edge, ft

l = length of plate, ft

h = unit heat transfer coefficient, Btu/hr/ft^2 F

U_o = free stream velocity, ft/hr

k = thermal conductivity of air Btu/hr/ft F.

A line was fitted to the point on the log-log plot of $N_{n_x}/(R_{e_l})^{\frac{1}{2}}$ versus x/l. Laminar flow was defined by adherence of data points to a linear variation, and turbulent flow was indicated by deviation of data from the linear relationship. Curves were plotted for zero angle of incidence, for a ten

degree angle of incidence, and for each ten degree increment up to ninety degrees. Drake concluded that the effect of inclining the plate was to cause the boundary layer to remain laminar further downstream due to the decreasing pressure gradient in the direction of flow.

Drake showed that for forced convective heat transfer in the laminar boundary layer of a non-isothermal inclined plate the relation among variables can be represented by an equation of the type

$$N_{n_x}/R_{e_l}^{\frac{1}{2}} = C(x/l)^n$$

where C and n were constants determined from the log-log curves. The value of C was found to increase from 0.652 at 10 degree angle of inclination to 1.025 at 90°, n increased from 0.640 at 10 degrees to 1.00 at 90 degrees. Comparison of the experimental results to an analytical expression developed by Eckert for an isothermal plate indicated that the experimental results were thirty per cent above the analytical values.

A qualitative investigation of Drake's curves shows that the effect of inclination of a plate surface is that near the leading edge the rate of heat loss is higher for small angles of incidence than for large ones. As the point in consideration is taken further from the leading edge the higher rate of heat loss occurs at large angles of inclination.

Bosworth (4) claimed that the effect of inclining a

surface to the moving fluid stream is to increase the heat transfer coefficient seven or eight fold, presumably by reducing the thickness of the stagnation film. This conclusion is in contradiction to Rowley and Eckley's experimental results but in accord with Drake's findings.

Experimental Investigations of the Heat Transfer from Roof Materials

Flow of heat through roof materials has long been a concern of the American Society of Heating and Ventilating Engineers (now named the American Society of Heating and Air Conditioning Engineers). In 1928 reports of experimental work to determine heat transfer coefficients were reported (24), (25). Using a Nicholls heat flow meter, inside and outside surface conductance coefficients were evaluated. Values of outside surface conductance coefficients were obtained which were thought to be of limited accuracy due to the complexity of heat flow from a roof surface. Wind data were recorded during the tests but no correlation of the wind effect on the coefficient was found.

In 1930 Rowley et al., (55) studied the effect of air velocity on the surface coefficient of heat transfer. The authors recognized the fact that air velocity would vary with angle of inclination. In order to standardize to some practical condition the air stream was directed parallel to the horizontal test surface.

Results of trial runs showed that measurement of the air temperature one inch from the test surface would yield the

same value of surface coefficient as air temperature measured in the free air stream up to eight inches away from the test surface. For a test surface of smooth pine the f value increased from 1.34 at 0 mph to 9.4 at 35 mph, when wind was parallel to the test surface.

In a later publication (56) of the same year Rowley et al. reported the results of tests on glass, brick, smooth pine, painted pine, concrete, rough plaster and stucco surfaces. For smooth glass the coefficient increased linearly from approximately 1.5 at 0 mph to 9.0 at 35 mph. In contrast the rough brick surface coefficient changed from approximately 2.0 at 0 mph to 15.0 at 35 mph. The rough plaster and stucco behaved similarly to the brick.

Houghten and McDermott (23) proceeded with tests of coefficients for sand-coated surfaces and smooth pine boards. At 30 mph air speed the sand-coated surface coefficient was 12 Btu per hour per ft^2 per ^0F. At 0 mph both the smooth and rough surfaces had a coefficient of 1.6. Summarizing their work and the works of Rowley et al., it was concluded that the surface conductance f will vary from 1.4 and 2.1 for still air and between the extreme values obtained from the simple equation

$$f = 1.4 + 0.281V$$

$$f = 2.1 + 0.515V$$

where V is wind velocity parallel to surface, miles per hour. It was noted that film conductance is largely a function of

surface roughness and could probably be expressed as a function of surface roughness.

Resume'

Theoretical analyses and experimental investigations have led to descriptions of convective heat transfer of two forms: laminar and turbulent. For skin friction-produced flow in the boundary layer the rate of heat transfer is generally correlated to the other variables in a dimensionless form using a Nusselt number and Reynolds number,

$$N_n = C\ R_e^{\ n}$$

where a representative laminar flow value for C is 0.590 and for n is 0.50. For turbulent flow characterized by fine scale mixing of fluid particles in the boundary layer, the heat transfer rate at any point is related to system variables by an equation form containing a Nusselt, Reynolds and Prandtl number

$$N_n = C\ R_e^{\ n}\ P_r^{\ 1/3}$$

where the constant C has a value 0.030 and n a value of 0.80 for a uniform air stream free from eddies and for a smooth flat surface. Transition from laminar flow to turbulent flow depends on conditions of leading edge and surface roughness. The maximum Reynolds number for laminar flow is given as 500,000.. Turbulence exists at a much lower Reynolds number if the free air stream is turbulent and can occur for moderate

wind velocities.

As pointed out by Parmlee and Huebsher (49), heat transfer studies can be divided into two categories: (1) The air approaching the test surface is in a non-uniform pattern. (2) The air approaches with no previously developed velocity gradient. If the test surface is installed in the wall of a duct or wind tunnel there is a velocity profile developed before the air strikes the test surface. Such a case belongs to the first category. If a plate is installed in the center of a wind tunnel such that there are no effects produced by the walls of the tunnel or by other disturbances, this type of study belongs to the second.

The researches of Houghten and Zobel (24), (25), Rowley et al., (55) Houghten and McDermott (23), belong to the first category. The works of Elias (15), Rowley and Eckley (57), Seban and Doughty (58), Jakob and Dow (28), Slegel and Hawkins (59), Parmlee and Huebsher (49), and Drake (11) belong to the second category.

For inclined surfaces contradictory experimental results were found. Drake's experiments apparently under close-controlled wind tunnel conditions indicated an increase in heat transfer with slope angle for laminar conditions. No reports for inclined surfaces with turbulent transfer were found.

For an inclined roof surface subjected to a natural wind stream the heat transfer to the wind currents would be difficult to specify. To judiciously select a heat transfer

coefficient obtained from past wind tunnel studies applicable to a natural wind stream would require knowledge of the character of a natural wind stream before a compatible wind tunnel investigation could be chosen. Other variables that must be considered include slope angle, surface texture, and surface length.

No information was found in the literature even partly concerned with heat flow in a wake region such as occurs over a leeward surface of a gable roof.

The influence of free stream turbulence on the convection process was reported to be limited to the laminar boundary region. Its effect on the transition point is to trigger turbulence at a lower Reynolds number.

Cooling at the top and bottom surfaces of a metal roof occurs simultaneously. The lower side cooling is probably influenced by shelter height, configuration, etc. Separate definition of heat transfer to air stream above the roof and to air stream below the roof would be necessary if an analytical analysis were attempted. The two effects are not independent since the material surface temperature is common to both convection processes. To define the convective heat loss from a leeward roof surface by analytical methods appears more formidable than for the windward roof. An experimental investigation under representative conditions seems more realistic.

Solar and Sky Radiation and Radiative Heating of Roofs

Meteorologists have long studied the quantity and quality of irradiation received at the earth's surface. Atmospheric conditions modify the sun's rays. Correct interpretation of the energy spectrum reaching the earth requires some recognition of atmospheric phenomena. Various types of radiometers in use respond differently to the solar and sky spectrum of radiation. Quantitative measurements therefore have little meaning unless the spectral sensitivity of the instrument is known.

In the present study, the sun and sky are the heat sources which heat the roof of the animal shelter. Consideration of the characteristics of the heat source is necessary for accurate definition of the heat transfer system. The interchange of thermal energy between a solid surface and its environment by electromagnetic radiation depends not only on the radiosity of the environment but also on the absorptive and emissive properties of the surface. Cognizance of the interrelation of all factors pertinent in the radiative heat transfer process is necessary for adequate description of the heat load on a roof due to solar and sky radiation.

Solar and Sky Radiation

If a plane surface were set normal to the sun's rays outside the earth's atmosphere, it would receive solar radiation in an amount of about 420 Btu/sq ft hr. (21). Dust particles, water vapor, and other substances in the atmosphere scatter and absorb part of the direct radiation so that the

amount received at the earth's surface is less. The energy intensity at the outer edge of the atmosphere is more or less constant as the earth remains practically a constant distance from the sun.

Observations show that the solar spectrum is wavelengths between 0.15 and 4.0 microns. (1). This range covers the electromagnetic spectrum from the ultraviolet (less than 0.4 micron) through the visible light region (o.4 to 0.7 micron) to the infrared or heat region (above 0.7 micron). The sun has an estimated temperature of 10,000 degrees Rankine, and it radiates nearly like a black body. Planck's law for monochromatic emission indicates the peak emission for a radiator at 10,000 R to be near 0.5 micron, which is in agreement with observations of the solar spectrum. Electromagnetic radiation travels in straight lines, and the sun is sufficiently far from the earth that direct sun rays can be assumed to be parallel.

Close investigation of the solar spectrum shows absorption bands caused by products in the atmosphere. Quantitatively, about half the direct radiation reaching the earth is in the visible region and over 40 per cent is in the infrared region. (60).

Sky radiation is composed partly of a portion of direct solar radiation which is scattered on passage through the atmosphere. According to Kelly (35) reflection from clouds and radiation from atmospheric gases are components of sky radiation, too. He termed the radiation from atmospheric

gases "atmospheric" radiation. Sky radiation strikes a horizontal surface from a hemisphere of space.

Kelly pointed out that the radiation absorbed by the earth is reradiated to the sky in long wavelengths due to relatively low temperature of the earth. The peak wavelength is 10 microns. This long wave radiation is readily absorbed by atmospheric gases. Brunt (6) indicated that water vapor, oxygen, and carbon dioxide in the atmosphere absorb all energy in the spectrum between wavelengths of 5.5 and 7.0 microns and wavelengths of more than 14 microns. Partial absorption occurs for 7.0 to 8.5 and 11 to 14 microns. This absorbed energy reradiated to earth and outer space is called "atmospheric" radiation by Kelly.

Radiation incident on a roof is the sum of the direct beam and diffuse short wave radiation from the sun and the long wave diffuse sky radiation coming from 2π space. Tabular values of the solar intensity to be expected at different locations in the United States are given by Moon (45). The intensity at any given time depends on atmospheric conditions, cloud cover, and solar angle. Correlation of solar intensity with other observed phenomena would require direct observation rather than reliance on values tabulated for design work. Sky radiation intensity varies through the day with solar altitude. Measurements of sky radiation can be made by placing a radiometer in a horizontal position and shielding the sensing surface from the direct beam solar rays. The instrument then responds only to the hemisphere

of sky radiation which it can "see".

Radiometers for Solar and Sky Radiation

Two types of radiation meters are in common use for measuring solar and sky radiation. The Eppley pyrheliometer responds to the wavelengths of the solar spectrum, and it is the accepted standard instrument of the United States Weather Bureau. The Gier and Dunkle total hemispherical radiometer responds to all wavelengths of radiation, and it is in widespread use for thermal radiation measurements.

Selectivity of the Eppley pyrheliometer is achieved by a clear lime glass sphere which encloses the sensing element. Transmission of the glass envelope for wavelengths less than 0.28 micron and greater than 5.0 micron is nil, making the pyrheliometer highly biased to the solar spectrum. The Gier and Dunkle total hemispherical radiometer has an unshielded sensing surface which responds to all wavelengths of energy.

Data for radiation intensity on a horizontal plane by Moon (45), were developed from pyrheliometric data. It should be noted that such measurements give the energy contributed by direct solar radiation and short wave diffuse sky radiation. The long wave sky radiation, being rejected by the pyrheliometer, is unaccounted for by pyrheliometric measurements as pointed out by Kelly (35).

Gier and Dunkle (19) made comparative measurements of the irradiation on a horizontal surface as indicated by a pyrheliometer and a total radiometer. The total radiometer recorded

values as high as 410 Btu/hr ft^2 at midday while the pyrheliometer reached a maximum of about 290 Btu/hr ft^2.

Kelly and Ittner (36) reported measurements of total solar and sky radiation, including long wave atmospheric radiation as high as 527 Btu/hr ft^2 in the Imperial Valley in California. This observation leads to an interesting question. If the intensity of radiation received at the outer edge of the atmosphere is of the order of magnitude of 425 Btu/hr ft^2, how can a larger value be observed at the earth's surface? The direct beam radiation is attenuated by absorption and scattering. Scattering by the atmosphere is uniform in all directions and causes no build-up of radiant flux at any location. Kelly in personal correspondence (62) explained that the total hemispherical radiometer responds to total incoming radiation. Radiation incident on the ground is reflected partly back to the sky which in turn radiates and reflects to the sensing element of the radiometer. In other words, the response of the instrument is to the total of direct and diffuse solar radiation, long wave sky radiation, and reflected radiation from the ground.

Heat Gain of a Roof

The radiative heat balance of a roof exposed to solar and sky radiation follows the fundamental laws of heat transfer which were formulated by Planck, Wein, and Stefan and Boltzmann.

Radiation from the sun and sky is a wide spectrum of wavelengths. Let the monochromatic radiation received by the roof surface be denoted by E_λ. The total energy density

incident on the roof would be E_t where

$$E_t = \int_0^\infty E_\lambda \, d\lambda$$

If the roof were a black body it would absorb all the radiation of all wavelengths and its energy gain would be E_t. But this incident radiation is partially reflected away. The monochromatic absorptivity of the surface, α_λ, is defined as the fraction of the energy incident on the surface between wavelengths λ and $\lambda + d\lambda$ which is absorbed by the surface. Total absorptivity is then defined

$$\alpha_t = 1/E_t \int_0^\infty \alpha_\lambda E_\lambda \, d\lambda.$$

Absorption depends on the spectral qualities of the incident radiation. Precise calculation of the amount of incident radiation absorbed would require knowledge of α_λ and E_λ. Very limited data of this sort have been collected.

Fortunately, many materials encountered in engineering practice can be assumed to be grey bodies, which means that the absorption coefficient is independent of the wavelength of the incident radiation and independent of the temperature of the body.(44). Thus $\alpha_t = \alpha_\lambda$ for a grey body.

Radiation from the roof to sky occurs simultaneously with the solar and sky heating of the roof. The Stefan-Boltzmann law expresses the radiation from a body as

$$E_r = \epsilon \sigma T^4$$

where E_r = intensity of emitted radiation, Btu/hr ft^2

ϵ = emissive power of the surface, dimensionless

σ = Stefan-Boltzmann constant, Btu/hr ft R^4

T = temperature of the surface, degree Rankine

Emissive power of a surface depends on wavelength emitted and surface temperature, but again for many engineering materials it can be assumed a property of surface characteristics alone. (44). If no convection or conduction cooling were present the temperature of a roof would rise until the outgoing radiation E_r would equal E_t and equilibrium would be achieved.

McAdams (44) has tabulations of the emissive power of numerous materials. As the cleanliness and degree of oxidation on a surface affects the emissive power, caution should be exercised in using tabulated values for matching actual materials.

Radiation from a metal roof could be evaluated analytically only if correct values of the emissive power of the particular material were available. Surface oxidation soon destroys the smooth polish finish on aluminum and galvanized steel roofing, making the surface which radiates and absorbs energy behave more like an oxide than a polished metal.

The Wind Near the Ground

The natural movement of air over the ground is a familiar phenomena. This air current is the heat sink which carries off heat from warm building surfaces.

Small structures such as animal shelters are entirely

immersed in the regions of air movement in which the viscous drag of the earth's surface has a pronounced effect on the flow pattern. Such structures are actually in the boundary layer of the wind flow, and some aerodynamic theories of the boundary layer are accepted as applicable to atmospheric flow phenomena.

Wind Character

As in any gas there is molecular motion present in air. Under atmospheric conditions the mean free path of the air molecules is of the order of 10^{-4} millimeter. Molecular motion is so small in relation to large scale motions which exist that a gas is assumed to be a continuous medium and heat transfer on a molecular scale can be assumed to be a conduction process.

There are secondary motions present in a natural wind, however. According to Gieger (18) the air almost without exception is in a turbulent state. Thermal stratification in the lower layers of the atmosphere causes rise of warm air which creates eddy currents. Heat is removed from the earth's surface many times faster by the eddy diffusion process than by molecular conduction alone.

In engineering practice eddies are usually defined as a rotating fluid motion superimposed on the mean flow. The term "eddy" is often used interchangeably with vortex. Meteorologists use the term "eddy" for any disturbance to uniform flow of air. This definition includes rotating motions, convective currents, and any other type of disturbance. (5). In this

presentation the engineering definition will be adhered to. The meterologists' definition of eddying for description of a flow condition is somewhat similar to engineer's definition of turbulent flow as in pipes. But in atmospheric phenomena the cause of disturbances to steady flow are more than just viscous skin friction, for convection currents and large scale irregularities of the earth's surface complicate the problem of adequately assigning a proper name to the type of fluid flow.

Large objects such as trees and buildings disrupt the flow pattern of the natural wind and produce eddies downwind from the objects. Small objects such as grass and stones cause small eddies to form. The size of the eddy produced by an object is of order of magnitude of the size of the object which produces it. Under certain conditions of the atmosphere the eddies are damped out immediately after formation. The criterion for the dissipation of the eddies is the stability of the atmosphere. If the air stream encounters successive objects along the flow path new eddies are formed by each object regardless of the rapidity of the dissipation of the eddies.

Air density stratification is the governing factor in atmospheric stability. When the ground is warmer than the air above it the air layers in contact with the ground are heated, causing convective rise of the warmed air. Colder air must descend to replace the warm air removed. Such is the case for unstable equilibrium. Stable equilibrium occurs when there are no differences in air temperature great enough to cause vertical exchange. Stable equilibrium occurs when the lower

layers of the air are cooler and likewise more dense than the layers above. In this instance vertical exchange is resisted by the stable density stratification.

Temperature stratification is an indication of stability, and several investigations have correlated thermal stratification to the wind velocity profile. Keast and Wiener (34) give methods for relating the wind profile in the lower 30 ft of the atmosphere to air temperature measurements taken at two heights. Their scheme is valid for a low uniform ground cover only.

Even under stable conditions the propagation of eddies downstream from an object is hard to specify. Brooks (5) stated that a weather station 5 ft above the ground in a forest clearing is not considered in an open exposure unless the clearning is one-half mile in diameter. Over open ground the fine-scale eddies formed by the ground surface tend to dissipate faster than larger scale eddies such as those produced by trees. Brooks gave a sketch of a natural profile as shown in Figure 1.

Nearly all buildings and shelters are surrounded by adjacent buildings, trees, or fences. Jensen (31) in wind tunnel tests found that up to eight to ten times the height downwind from a solid barrier eddying occurred with velocity fluctuations of up to 30 per cent of the unobstructed velocity.

Wind Profile

The largest scale motion of air in a natural wind is movement parallel to the ground surface. For given surface

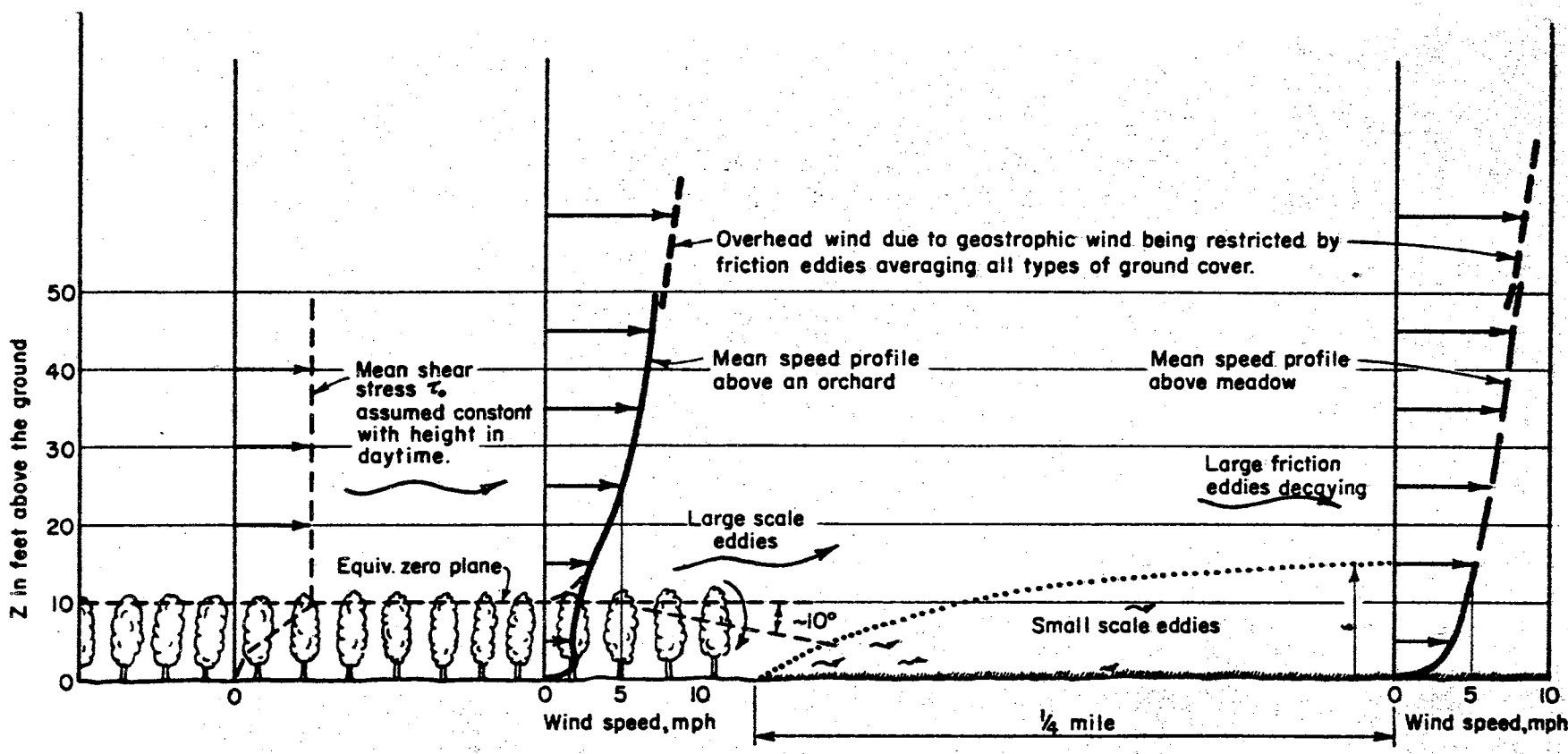

Figure 1. Brook's representation of a natural wind profile. From Reference (5, page 98).

features several profile laws have been developed to describe wind velocity variation with height above ground. The literature reviewed here is limited to those studies dealing with winds in the lower 30 ft of the atmosphere.

If air were inviscous the proximity of the earth to the air would have no effect on the wind flow. The braking action of the earth's surface is transferred from layer to layer by viscous drag. Through turbulent diffusion the retardation effect is transmitted upward, moving slow particles among the faster particles with a resulting dissipation of velocity energy. This momentum transfer process is similar to that of the turbulent boundary layer of a smooth plate, the exception being that few aerodynamically-smooth surfaces exist at the ground surface.

To describe the variation of mean wind speed with height Gieger (18) presented an exponential variation of the form.

$$V_y = V_1(y)^a$$

where V_y signified the mean wind velocity at height y above the ground and V_1 is the velocity at some reference height. There is sufficient experimental evidence to support this relationship if temperature variation, time of day, and other factors are taken into account. Sutton (60) pointed out that the value of "a" in Gieger's expression depends on the temperature gradient in the vertical direction. Sutton presents evidence that the value of "a" changes over a period of a day and also changes from season to season of the year.

Gieger reviewed the works of several researches and concluded that the value of "a" can vary from 1/5 to 1/3 depending on the ground cover. For smooth ground cover such as snow cover a value of 1/5 was proposed. The value 1/3 was given for a ground texture similar to a turnip field.

Prandtl's development of skin friction theory led to logarithmic profile law which is accepted equally well as the power law. For turbulent momentum exchange caused by skin friction, the boundary layer profile presented by Prandtl (51) for the atmospheric profile is

$$V = V_* (5.75 \log_{10}(y/K) + C)$$

where V = velocity at height y

V_* = shearing velocity at $y = 0$, τ/ρ

τ = shear stress at $y = 0$

y = height above ground

K = a length dimension representative of roughness condition of the ground: height of trees, houses, etc.

C = A constant which depends on K, with values between 5 and 8.5

ρ = fluid density

Experiments by W. Paeschke for winds over natural vegetation suggested that the C value in Prandtl's expression should be 5.0 if K is taken as the height of vegetation.

An approximation for the logarithmic law is the one-seventh power law which has been established for the boundary profile in pipes for turbulent flow. Several modifications of

the power and logarithmic laws can be found in the literature.

Brooks (5) pointed out that the wind profile is related to the foliage layer which absorbs the drag force and is rather independent of the sheltered ground surface. Therefore, the height of an anemometer should be taken as the height above the foliage covering and not the height above the ground surface. The profile power law is modified to the form

$$V_y/V_1 = (y-d)^p/(y-d) \qquad y \geq d$$

where d is the height above ground level of the "equivalent zero plane".

For neutral stability, when no large scale eddies are present Brooks agreed that p = 1/7.

For conditions of thermal turbulence resulting from warm air eddies rising from a warm ground, Brooks recommended p = 0.1 or less. For stable equilibrium p = 0.5 was recommended.

In review, it should be noted that a profile law is at best as statistical derivation of a phenomena which is erratic and unsteady in behavior. Of several means of describing the mean wind profile, the power law appears adequate. Definition of the exponent has been accomplished for fairly smooth ground surfaces such as meadows and fields. For stable conditions the exponent may be as high as 0.50. For neutral conditions the 1/7 power is adequate. When rising warm air currents occur an exponent as low as 0.10 is thought to best describe the mean profile.

Brooks (5) warns that any profile law is only a time

average of an instantaneous erratic distribution of velocities. Gieger points to this fact, too, by recalling that velocity measurements over a long period of time may not adequately represent the true velocity at any given time. But no matter how elusive the profile is, its existence is accepted by meteorologists and aerodynamicists.

Dimensional Analysis and Physical Similarity

A heat process involving a gradient wind stream, radiative heating, and a non-parallel surface is a system with numerous variables. An experimental approach to investigations that include many variables can be aided by the application of dimensional reasoning. Dimensional analysis provides the foundation for testing for similarity among physical systems, which is the basis for model studies. The bulk of research in physical sciences is concerned with finding the relationships among the quantities involved in physical systems. Problems can be approached either from the analytic viewpoint which draws on mathematical and rational reasoning or from the experimental viewpoint which draws on measurement and observation or from a combined theoretical and experimental analyses in which theoretical reasoning directs the experiments that in turn test the theory. In all approaches the axioms for dimensional equality place severe restrictions on the validity of quantitative and qualitative measurements of physical phenomena.

Dimensional Analysis

The formulation of dimensional analysis as an analytical tool has been attributed to Buckingham and Lord Rayleigh. Murphy (46) stated the axioms of dimensional analysis as follows: (1.) Absolute numerical equality of quantities may exist when the quantities are similar qualitatively, and (2.) The ratio of magnitudes of two like quantities is independent of the units of measurement used, as long as the same units are used for evaluating each. These axioms are somewhat self-evident.

Many physical quantities encountered in engineering practice and theory can be expressed in five basic entities: mass, length, time, temperature, a heat unit, and electric charge. For example, velocity is length per unit time. The system of measurements used for defining the magnitudes of quantities is arbitrary. A physical quantity has magnitude with respect to some system of measurement and also has dimensions which are composed of combinations of the basic entities. The entities are independent attributes. Their units of measurement have been arbitrarily described for all scientific work.

Equality in physical quantities requires not only a numerical equality, but also dimensional equality. This follows from the axioms of dimensional analysis. Dimensional equality serves as check on the validity of equations and formulas which express relationships among physical quantities. Any valid relationship or expression among the variables which represents the action of a system must be consistent in dimensions.

This requirement rests on the axiom of equality of dimensions.

When a large number of physical quantities are pertinent to the operation of a physical system, a dimensional investigation of the requirements for equality in dimensions usually gives some insight to the dependence of some quantities on others.

The value of dimensional analysis in experimental work is that the number of experiments which must be conducted to learn the relationships among the variables in a system can often be reduced. When several quantities are combined to form a dimensionless group, the dimensionless group can be considered a variable in the problem instead of each individual quantity. An aggregation of all pertinent quantities into dimensionless groups reduces the number of variables to a minimum. Experiments to determine the correct relationships among the dimensionless groups will often yield a maximum amount of information from a minimum amount of experimentation.

The omission of a pertinent quantity in an analysis can lead to wrong conclusions about the apparent relationship among the variables and the independent variables. The larger the number of pertinent quantities involved in a system, the larger is the problem of correctly relating them. Dimensional incompatibility offers some evidence that a selection of quantities may be imcomplete and additional quantities may be necessary to completely define the physical system. The procedure for organizing dimensionless groups of quantities in a study follows from the Buckingham Pi Theorem.

The Buckingham Pi Theorem

According to the Buckingham Pi Theorem the number of independent groups of dimensionless products which can be formed from a group of quantities is equal to the number of quantities minus the number of basic dimensions necessary to formulate these quantities. Each dimensionless group is called a pi term. If

n = total number of quantities

b = number of basic dimensions involved

s = number of pi terms

by the Buckingham Pi Theorem

$$s = n - b.$$

In mathematical parlance, if the correct pertinent quantities are contained in the pi terms, correct description of the action of the system is given by

$$F(\pi_1, \pi_2, \pi_3, \ldots, \pi_s) = 0$$

where F denotes an implicit function and s denotes the total number of pi terms. The Buckingham Pi Theorem has been refined by Langhaar who showed that

> ....the number of dimensionless products in a complete set is equal to the total number of variables minus the rank of their dimensional matrix. (38, p.31).

For any group of quantities there is no unique set of pi terms, because it is usually possible to form many different groups

or pi terms from the set of quantities. The Buckingham theorem makes no stipulation as to the most appropriate set of pi terms to be used. If no evidence is available to give information on a reasonable grouping of quantities the experimenter may have to use rational reasoning to arrive at reasonable set of pi terms. Fortunately, in most studies the physical system is at least akin to systems which are subject to analysis by the usual physical laws. Any set of pi terms consistent in number and form with the Buckingham theorem is a valid set. The investigator should arrange the quantities into dimensionless groups that will facilitate experimental analysis for determining the functional relationship among the dimensionless groups. Some dimensionless groups which occur again and again in different fields of engineering science have become familiar. For instance, Reynolds number and the Nusselt number are dimensionless groups of quantities which have physical significance in fluid flow and heat flow, respectively. It should be pointed out that the Buckingham theorem can only be applied to a problem after the pertinent quantities have been listed. An application of the Buckingham theorem depends fully on the completeness of the list of pertinent quantities. Omission of the pertinent quantities will sometimes be pointed out when the formation of dimensionless groups in accordance with the theorem is not possible.

An accurate way to define a physical system is to express the entire set of pertinent quantities involved. A physical system might be defined as a phenomena in which the pertinent

groups of physical quantities bear a unique relationship to each other.

Compatibility and Similarity

The conditions of compatibility and similarity among physical systems follows at once from the Buckingham theorem. If a physical system is described by a particular set of pertinent quantities, such that a group of pi terms represents the system, then the action of the system is represented by some implicit function

$$F_1(\pi_{11}, \pi_{12}, \pi_{13}, \cdots, \pi_{1s}) = 0.$$

If another physical system contains the same physical quantities as the first and no more, a similar group of pi terms π_{21}, π_{22}, π_{23}, $\cdots$, π_{2s} can be formed, and the Buckingham theorem again leads to the result

$$F_2(\pi_{21}, \pi_{22}, \pi_{23}, \cdots, \pi_{2s}) = 0.$$

Now if system 2 is operated in such a manner that sufficient observations are taken to yield the function F_2 over a particular range of values of the pi terms, this function is a valid representation of system 1 when the magnitudes of the pi terms fit into the range for which F_2 is valid. System 2 can be thought of as a model of system 1. But to be more specific the two systems are actually samples of a general system in which the samples may differ in magnitudes of certain of the pi terms.

Compatibility is defined as the condition that exists when the same set of pi terms correctly represents the phenomena in both systems. Compatibility among systems is achieved if they contain the same physical quantities. The problem of demonstrating or testing similarity among compatible systems is an experimental and mathematical one because unless the same magnitudes of dimensionless parameters exist among the systems, behavior beyond a range of testing is usually unpredictable. Numerical equality of pi terms is the interpretation of similarity.

By these definitions, compatibility is asserted by the component physical quantities. Similarity is ascertained by numerical equality of dimensionless groups of quantities. Compatibility implies the presence of the same pi terms. Compatibility must be established before similarity can be confirmed.

The use of models for study is a matter of convenience in making observations. Unless the system is well enough understood, justification of similarity between model and prototype is usually a necessary part of the experimentation.

Systematic investigation on several systems to learn whether they are models of a general system is a powerful test for similarity and an expedient means of evaluating the performance of variables at widely different magnitudes. If compatibility can be established, the observations taken for the several systems can be pooled for analysis with a resultant functional relationship applicable for a general system for

which the several test systems are samples.

Prediction Equations

Dimensional analysis offers a sound approach to developing prediction relations. If a set of pi terms π_1, π_2, π_3, . . ., π_s are formed for a set of quantities pertinent to action in a system, the implicit relationship

$$F(\pi_1, \pi_2, \pi_3, \ldots, \pi_s) = 0$$

can be rearranged to an explicit form

$$\pi_1 = f(\pi_2, \pi_3, \pi_4, \ldots, \pi_s) = 0.$$

It is expedient to think of one term as a dependent variable and the others as independent variables, although this symbolic relation does not imply that the function will define pi_1 in mathematically explicit form. Sufficient observations of π_1, π_2, π_3, . . ., π_s may be analyzed to learn the prediction relation if the analysis is not too formidable. At any rate, the preceding equation form is a desirable one for a prediction equation because it compresses the pertinent quantities into a minimum number of independent terms.

Experimentation for determining the prediction equations should be designed with a two fold objective: (1.) To test the hypothesis that the chosen set of pertinent quantities includes all physical quantities which influence the action of the system and (2.) To correlate the variables for as wide a range of values of the variables as the range in which the

prediction relation is to be relied on. The first objective is necessary unless beforehand evidence is available to substantiate the chosen quantities. The reason for a wide range of variation in the independent variables is to insure the validity of the prediction relation over a wide enough range of values to make extrapolation unnecessary. There is no stipulation that the function will be continuous or finite over an extended region. Rouse (54) pointed to the Blasius formula for smooth pipes as a fine example of the danger of extrapolation.

The determination of a prediction relationship can also be accomplished with a model system whereas the application of the equation may be only in a prototype system. Murphy (46) presented applications of model techniques based on pi term similarity and numerical equality for a wide range of physical applications. Dependability of model data for accurate prototype predictions requires compatibility of the two systems. In complex systems compatibility can usually be verified by the success of model predictions on prototype observations.

CHAPTER III

EXPERIMENTAL DESIGN

Introduction

Dimensional analysis and the principles of similarity present a systematic approach to problems involving the presence of several physical quantities. The application of the pi theorem gives insight on the inter-dependence of physical quantities and serves as a logical starting point for developing the appropriate experimental technique for analyzing the action of a physical system.

A roof heated by solar and sky radiation and cooled by moving air currents is a problem in which the resulting temperature rise of the roof at any point is related to the magnitude of the other physical quantities. It is a variable whose magnitude can be uniquely defined by specifying the magnitudes of the other physical quantities necessary for definition of the system. This is just a statement of the fact that a measurement of a physical quantity has no meaning in itself; only when a measurement of one quantity in relation to other quantities involved in a phenomenon does a physical quantity have significance.

In this chapter is given the selection of independent variables of the heat and transfer flow processes which based

on findings presented in the previous chapter are thought to be definitive of the behavior of the system. The first part of the analysis contains a statement of these selected quantities which are presented as a unique definition of the physical system for study. This selection of physical quantities to be considered is really the heart of the study because it defines the variables which were measured and accounted for in the investigational procedure. An application of the pi theorem was used for the formation of dimensionless groups. Then a presentation of the experimental design is given.

Selection of Pertinent Quantities

The System

In general terms the physical system can be described as an open type pole-framed building which is heated by solar and sky radiation and cooled by a natural wind. The roof is a symmetrical gable roof with thin sheet metal roofing on widely spaced purlins. Wind direction is taken normal to eave direction, and the building is long enough so that the gross wind flow might be described in two dimensional coordinates. A definition sketch is given in Figure 2. Table I contains the listing of quantities thought to be necessary for complete system definition.

The system is assumed to be a forced convection system, that is, one in which the wind velocity is sufficient to insure forced momentum exchange in the boundary layer. A

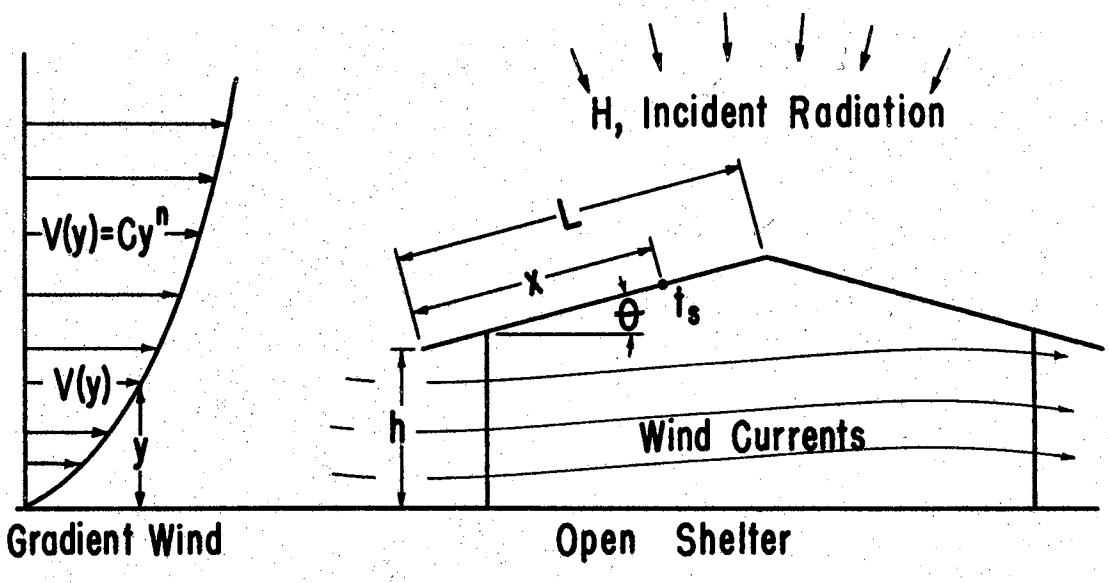

Figure 2. Definition sketch of the shelter system. Shelter has no ceiling and a thin metal roof.

TABLE I
PERTINENT QUANTITIES FOR THE PHYSICAL SYSTEM
(Definition sketch in Figure 2.)

No.	Symbol	Description	Dimension
		(The dependent variable)	
1.	Δt	Difference in surface temperature t_s, measured at ridge of corrugation at distance x up roof slope, and free stream air temperature, t_a, $\Delta t = t_s - t_a$	θ
2.	x	Distance up roof slope to point t_s is measured.	L
		(Total incoming radiation)	
3.	H	Total incoming radiation incident on roof. Should be constant over a given roof side.	$BL^{-2}T^{-1}$
		(Shelter Configuration)	
4.	h	Height of eave	L
5.	L	Length of roof	L
6.	θ	Roof slope angle	---
7.	s	Purlin width	L
8.	z	No. of purlins	---
		(Properties of the roof material)	
9.	α	Absorption coefficient of surface for incident radiation	---
10.	ϵ	Emissive power of surface	---
11.	r	Corrugation pitch. Distance between corrugations of roof	L
12.	k_m	Conductivity of roof material.	$BL^{-1}T^{-1}\theta^{-1}$
13.	t	Roof thickness.	L
		(Air properties)	
14.	ρ	Air density	ML^{-3}
15.	μ	Air viscosity	$ML^{-1}T^{-1}$
16.	c_p	Air specific heat	$BM^{-1}\theta^{-1}$
17.	k^p	Air conductivity	$BL^{-1}T^{-1}\theta^{-1}$
18.	t_a	Air temperature. Measured upstream	θ
		(Wind character)	
19.	V	Wind velocity at eave height	LT^{-1}
20.	n	Exponent for wind velocity profile law	---

Dimensions: θ - Temperature, T - Time, L - Length, M - Mass, B - Heat.

Note: System of units employed for this study was the engineer's system with mass unit=slug, length=ft and time=sec. Density, ρ, is slugs/ft^3, viscosity, μ, is lbfsec/ft^2 = slugs/ft-sec.

steady state condition is assumed which means that thermal and dynamic equilibrium are established before observations of temperatures would be taken.

List of Pertinent Quantities for the Windward Roof

A. Definition of $\triangle t$, the Dependent Variable

In this study the measure of effective cooling at any point on the roof is defined as the difference in surface temperature t_s, and free air temperature t_a. It is the dependent variable whose magnitude is to be related to the observed magnitude of the other quantities in the system. Usually in heat transfer a film heat transfer coefficient is considered the dependent variable. For a roof cooled by convection on both top and bottom sides a measure of overall cooling would have to be expressed with two coefficients, one for the top side and one for the bottom side if coefficients were used. According to the theory and numerous experimental investigations the heat transfer coefficient at any point along a surface is a function of air velocity, surface texture, and air properties. One can say that the film coefficient, is a function of the independent quantities, V, ρ , μ , x, c_p, etc. It is a derived quantity which gives a measurement of a ratio of heat flow to temperature difference.

Radiation heat transfer problems encountered in animal shelter engineering require knowledge of surface temperatures. A prediction of the temperature rise of the roof is a more useful quantity than a convective coefficient.

Any quantity which is pertinent in a phenomena must be subject to measurement or have a known magnitude. The stipulation of the dependent variable implies that its magnitude is defined by the magnitude of the independent variables. For the system with quantities listed in Table I,

$$\Delta t = f(x, H, h, \ldots V, n).$$

Verification of the completeness of the list of quantities was then a necessary part of the investigation. To adequately define this functional relationship is a restatement of the objective of the study as was stated in the first chapter.

To locate the point on the roof at which Δt is measured, the quantity, x, distance up roof slope from leading edge is used.

B. Total Incoming Radiation

As the sun and sky are the radiant heat source, the total incident radiant energy level affects the temperature rise of the roof. The total incoming radiation incident on the roof is denoted by the quantity H. It is the intensity integrated over wave length and direction incident on the plane of the roof surface. It can be evaluated by placing a non-selective radiometer on the roof so that the plane of the sensing element is parallel to the roof plane.

C. Quantities Describing the Geometry of a Symmetrical Gabled Structure

With only three variables the geometry of a gabled roof can be quantitatively specified. These are height of eave, h, length of roof, L, and the slope angle, θ. Two-dimensional

coordinates are sufficient only because the structure is assumed to be long enough to rule out end effects as being important. Because wind currents underneath the roof surface affect the temperature rise of the roof we have to attach significance to the presence of the purlins. For conventional types of construction, statement of the width of purlins and their spacing is sufficient. The presence of purlins alters the air currents on the underside of the roof and should therefore be recognized. The amount of contact area for thermal conduction to the purlins is small for corrugated sheet metal, and since wood is a poor conductor the presence of purlins is only of interest inasmuch as they do hinder convective cooling on the underside of the roof.

D. Properties of the Roof Material

For radiant heat transfer the total absorption coefficient, α, of a material is an important quantity. This quantity is a measure of the fraction of incident radiation integrated over all wavelengths of the source and over 2π space which is absorbed by the surface. The emissive power, ϵ, is likewise significant.

Corrugation pitch, r, is an index of the surface texture. Texture was studied because the ratio of projected area to actual area available for cooling is unequal for corrugated metal. Corrugation size is defined for corrugated metal by the pitch length. Texture on a finer scale could be investigated, but this study only included commercial sheet roofing materials.

With wind cooling on the underside of the roof, the rate of heat flow through the roof material is affected by the

conductivity, K_m, and the metal thickness, t. The temperature of the lower surface is a quantity which would be a function of radiation intensity, wind velocity, and the other variables listed in Table 1. It was not considered because it is not an independent quantity and it is uniquely defined in terms of the other chosen quantities for the heat transfer system.

E. Air Properties

Studies in forced convective heat transfer have verified the following air properties as pertinent to the heat transfer process: density, viscosity, conductivity, and specific heat. In keeping with the common notation ρ, μ, k, and c_p denote density, viscosity, conductivity, and specific heat, respectively. All these properties were evaluated at the free stream air temperature.

In a combined radiant and convective heat transfer process some absolute temperature reference is necessary because radiant exchange depends on absolute temperatures. Convective theory makes no stipulation of the absolute temperatures in a system. Only differences are important. The fundamentals of radiant heat exchange place importance on absolute temperature, making both temperature differences and the location on the absolute temperature scale pertinent. For this study absolute air temperature was chosen as a pertinent temperature index. Surface temperature, t_s, might be more consistent with conventional thinking but t_s is uniquely defined by Δt the chosen dependent variable and t_a the independent variable by $t_s = t_a + \Delta t$. With this explicit definition only two of the temperature values

need to be specified; the third is uniquely defined.

In view of the turbulent properties of a natural wind the question arises as to whether a quantity describing the degree of turbulence was necessary. According to Brooks (5) an open reach upstream with no objects to disrupt the wind stream produces a profile characterized by only fine scale turbulence associated with surface drag. Hinze (22) pointed out the unimportance of free stream turbulence on heat transfer in the turbulent boundary layer. With a corrugated leading edge, non-laminar free air stream, and somewhat unsteady flow, the largest portion of a roof would be thought to be exposed to turbulent boundary layer heat transfer only.

F. Wind Character

The profile assumed by a natural wind can be defined with two new physical quantities. For an exponential profile law of the form $V_{(y)} = C(y)^n$, where $C = V_{(h)}$, h = eave height for reference height. The specification of V and n with h already present was sufficient to define a profile. Steady state conditions were assumed.

Pertinent Quantities for the Leeward Roof

The leeward roof had to be considered as a separate system from the windward roof although the experiments could be run on the two roofs simultaneously. It experiences a temperature rise just as the windward does. The quantities presented as pertinent for the windward roof apply equally well for the leeward roof when defined for the leeward roof system. To

locate a point on the leeward roof distance up roof slope from eave edge is sufficient. The same notation, x, for this quantity was used. Radiation intensity incident on the leeward roof carries the same symbol H. Wind velocity at eave height, air properties measured upstream, etc., have their same meaning.

Temperature measurements on the leeward roof would reveal interesting information on the thermal behavior of a roof surface in a wake region. The air currents striking the leeward roof are modified in temperature by the windward roof heat loss, making the downstream roof side not independent of the windward roof behavior. Conditions representative of an actual shelter exposed to natural hot weather can be produced by a radiation level nearly equal for both roofs. This is the case for a high summer sun at midday. The plan was to observe temperature rise on both roof sides when radiation level was approximately equal for the two sides. The two roofs are identified as the windward roof and the leeward roof, respectively, to differentiate observations on the two roof sides.

Formation of Pi Terms

Application of the Buckingham Theorem to a group of quantities yields the number of independent dimensionless groups of quantities which can be formed. These dimensionless groups, commonly referred to as pi terms, are the parameters which were to be investigated.

There are 20 pertinent quantities listed in Table 1 which

are proposed as the necessary ones to adequately define the system. With 20 quantities expressed in 5 basic dimensions the number of pi terms is 20 - 5 = 15. This number was found equal to the rank of the dimensional matrix, as required by Langhaar's refinement to the theory.

Any 15 independent pi terms are valid. Independence implies that no pi term can be formed from linear combinations of the others. For any 15 independent pi terms

$$F (\pi_1, \pi_2, \pi_3, \ldots, \pi_{15}) = 0$$

which means that these 15 terms uniquely define the action of the system expressed in entirety by the quantities from which the pi terms are composed.

The dimensionless groups chosen from the list of quantities in Table 1 were formulated by seeking to find those groups which have significance from the standpoint of heat transfer theory.

Referring to Table II in which the selected dimensionless groups are listed, the groups are denoted in the conventional pi term notation.

The first pi term, π_1, bears resemblance to the reciprocal of the Nusselt number so common in forced convective heat transfer. It contains the dependent variable Δt which was defined as the dependent quantity of the study.

For the second group, the ratio of the absolute air temperature to Δt was chosen. This pi term can be thought of as an index of the potential for radiant heat transfer from the

TABLE II

SELECTED PI TERMS FOR SHELTER SYSTEM

Pi Term No.		(Description)
(Groups Containing Major Variable Quantities)		
1	$\pi_1 = k\Delta t/Hx$	
2	$\pi_2 = t_a/\Delta t$	
3	$\pi_3 = V\rho x/\mu$	Reynolds Number
4	$\pi_4 = x/L$	Location of temperature measurement
(Parameters of Shelter Configuration and Material Type)		
5	$\pi_5 = \theta$	
6	$\pi_6 = r/L$	
7	$\pi_7 = h/L$	
8	$\pi_8 = \alpha$	
9	$\pi_9 = \epsilon$	
(Parameter assumed unimportant for thin roofs)		
10	$\pi_{10} = t/L$	
(Groups with constant value)		
11	$\pi_{11} = k/k_m$	
12	$\pi_{12} = s/L$	
13	$\pi_{13} = z$	
14	$\pi_{14} = \mu c_p/k$	Prandtl Number
15	$\pi_{15} = n$	

roof.

Pi-three is a Reynolds number based on distance up the roof from the leading edge. It is a common parameter appearing in fluid flow and heat transfer processes.

The geometric dimensions of the building are related in π_5, π_6, and π_7.

The absorption coefficient, α, and emissive power of the roof material, ϵ, are both intrinsic dimensionless ratios, and each is a property of the roof material. Each should stand alone as a pi term because emission and absorption do not precisely have a constant relationship. Pi-ten relates roof thickness to roof length. Ratio of air to material conductivity is expressed in pi-eleven.

Number of roof purlins and purlin spacing are characterized by π_{12} and π_{13}.

A Prandtl number is given in π_{14}. This parameter is often encountered in forced convection theory and experiment.

The last pi term denotes the wind gradient law. It is an index of the slope of the profile.

The selected groups were based on the assumed general similarity to other heat transfer systems thought to be somewhat related to the roof cooling problem. Although the dependent quantity Δt appears in two dimensionless parameters, experiments could be conducted to find the functional relation among the selected parameters. If an implicit relation were obtained, algebraic manipulation could rearrange the relation to produce a form which gives Δt as a function of the other

variables in the system.

Experimental Design

The first four pi terms contain quantities which would be thought to be quite variable in nature. Radiation intensity, difference in surface and air temperature, wind velocity, and other quantities in these terms would be expected to vary for any given system. These four pi terms were caused to vary over a wide range of values in order that their effects might be thoroughly understood. Since there was interest in finding how the temperature of the surface varied over the length of the roof, the surface temperature was measured at several points along the roof. This gave several values to the fourth pi term.

The thicknesses of commercial sheet metals used for roofing are all small, making the ratio of thickness to roof length, pi-ten, appear to be an unimportant parameter. For thin metal roofing it was assumed that the thickness of the metal, t, had no significant effect on the thermal behavior of the system. No attempt was made to vary roof material thickness in the experiments. The full size shelter used in the study was already in use in other experiments, and its design dictated the general type of geometrical structure for study. The shelter was a symmetrical, gabled-roofed open type shelter. It had white-painted galvanized corrugated metal roofing, except for one strip each of aluminum roofing and unpainted galvanized steel. Thermocouples were installed to

measure the temperatures along each of the three kinds of roofing. The eave direction was east-west. Roof slope was four-on-twelve.

In order to utilize the three kinds of roofing in the full size system three kinds of surfacing were included in the model system. This gave three assigned values for π_8 and π_9. To test the effects of slope angle, three values of π_5 were used: Three-on-twelve, four-on-twelve, and five-on-twelve. To learn the effect of surface texture the plan was to use three values for π_6: sizes corresponding to 2½ inch pitch corrugations, 1¼ inch pitch corrugations, and a flat sheet. Two values of π_7, roof height, were studied.

With three values for π_9, three for π_5, three for π_6 and two for π_7 there were

$$3 \times 3 \times 3 \times 2 = 54$$

possible configuration and material selection combinations possible. With no interest in testing for interactions, fewer combinations would yield information on treatment effects. In view of the major interest in π_1, π_2, π_3, and π_4, only eight configuration and material selection combinations were used. This was the minimum number which allowed evaluation of the configuration and material selection parameter effects. Table III gives the number of pi term combinations which were studied. For each combination π_1, π_2, π_3, and π_4 were investigated in detail with the objective of obtaining enough data to establish a separate prediction relation for each configuration

and material selection combination. The possibility of including the configuration variables into the equation as independent parameters was considered since they would have made the predictions more general in application.

TABLE III

SCHEDULE OF COMBINATIONS OF PI TERMS FIVE TO NINE

Combination No.	$\pi_5=\Theta$	$\pi_6=r/L$	$\pi_7=h/L$	$\pi_8=\alpha$ $\pi_9=\epsilon$
		Value No.		
1	1	1	1	1
2	1	1	1	2
3	1	1	1	3
4	1	2	1	1
5	1	3	1	1
6	1	1	2	1
7	2	1	1	1
8	3	1	1	1

Note: The table gives a representation of the eight combinations chosen for study. Note that each combination differs from any other in at least one pi term value. Table IV contains the numerical values of the pi terms used in the study.

CHAPTER IV

EXPERIMENTAL PROCEDURE

Introduction

The bulk of the experimental investigation was conducted with a scaled-down model of a shelter structure by making measurements of the temperature rise of the roof when controlled wind currents passed over the roof of the model which was heated by an artificial source of controlled thermal radiation. The model was tested in a low speed wind tunnel with infrared heat lamps installed in the ceiling of the tunnel over the model to heat the roof radiantly. A wind profile similar to a natural wind was developed by placing round bars across the tunnel section to block the cross section area of the tunnel in such a way that a suitable profile was developed.

Before the model was installed in the tunnel a series of calibration curves for the intensity of radiation incident on the model were made using a total hemispherical radiometer. Calibration curves for wind speed at the leading edge of the model roof were also made, along with necessary corrections for wind speed reduction due to the presence of the model in the tunnel.

For determining the cooling effect of the wind, the temperature rise was measured for predetermined conditions of

radiation intensity, wind speed and properties of the air. Control of the intensity of radiation incident on the model roof was obtained by varying the voltage supplied to the bank of heat lamps.

A series of measurements on a prototype shelter was made on clear, bright days when the wind was blowing from the desired direction with fairly constant velocity.

Following a preliminary analysis of model and full size shelter results, certain discrepancies in behavior were found. Experiments were conducted on an intermediate size shelter in an attempt to resolve these discrepancies.

The Wind Tunnel

A low speed, open return wind tunnel belonging to the Oklahoma State University Agricultural Engineering Department was utilized for the model studies. The tunnel has a 4 x 4 x 50 ft test section with a 9 ft 9-3/4 in square entrance section. An anti-turbulence screen covers the entrance section to dampen out large scale turbulence of the entering air stream. With a 22 x 22 mesh, the screen has openings of 50.5 per cent of the gross area.

The fan system consists of a five ft diameter, axial flow, sixteen blade fan driven through a variable speed drive by a 15 hp electric motor. Blade pitch can be changed to vary the range of wind speeds available in the tunnel. By changing the drive ratio in the variable speed drive the rpm of the fan can be adjusted anywhere from 280 to 1200 rpm. Figure 3 gives

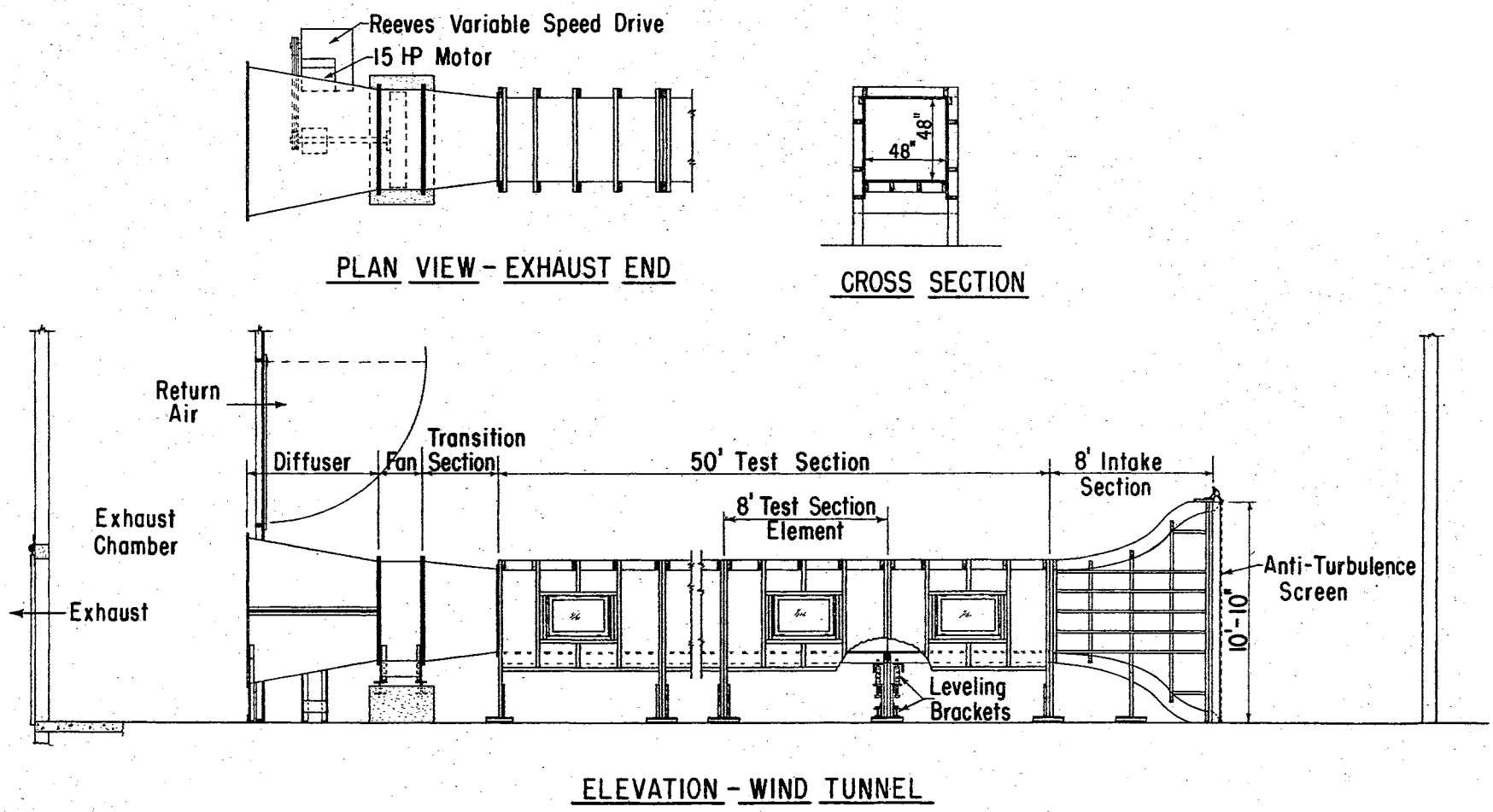

Figure 3. The Agricultural Engineering Research Wind Tunnel.

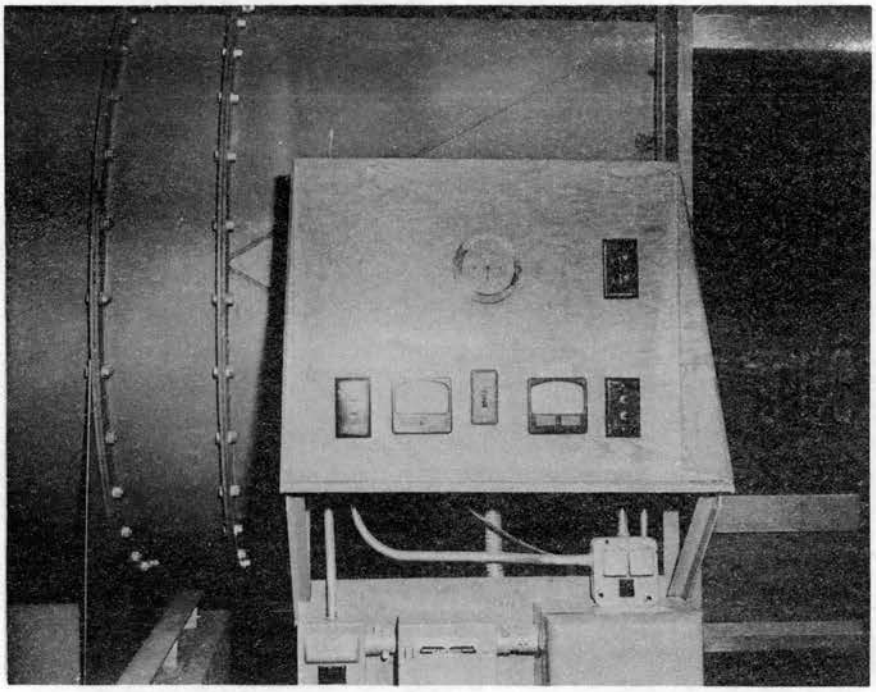

Figure 4. Control panel for the wind tunnel fan drive.

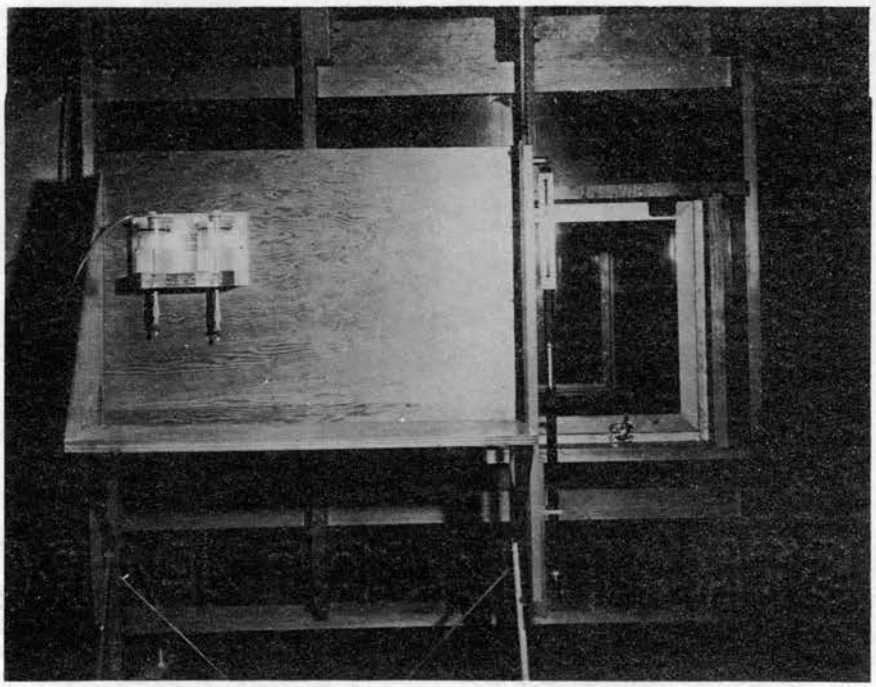

Figure 5. Micromanometer for sensing piezometer static pressure.

a diagram of the wind tunnel. The control panel is shown in Figure 4.

For measuring the mean velocity in the tunnel, a piezometer ring with nine static pressure taps monitors the static pressure drop at the downstream end of the test section. A precision micromanometer gages the pressure drop sensed by the piezometer ring.

A pitot tube and micromanometer are used for measuring velocity at any point in the windstream. A view of the manometer is shown in Figure 5.

When in operation, the air discharged from the tunnel exit returned through the laboratory room back to the entrance end of the tunnel. No means of controlling the properties of the air were attempted except for temperature which could be held fairly constant by closing all doors and windows to the laboratory and adjusting the heaters used for warming the laboratory.

The Infrared Heater

For heating the model roof a bank of eighteen infrared heat lamps was installed in the ceiling of the wind tunnel where the radiant energy could be beamed down on the roof of the model. With the lamps directly over the model, the condition was similar to an overhead sun on a summer day near midday. The initial plan was to uniformly heat an area of 8 sq ft in which the model would be placed. Design calculations indicated that eighteen lamps in a bank spaced eight inches apart would

give an intensity of 800 Btu/hr/sq ft three feet away from the lamps. The standard industrial type heat lamp has a tungsten filament which operates at 2500 to 2700 degrees Kelvin. Approximately 11 per cent of the emitted radiation is in the visible region, and approximately 77 per cent in the infrared region. (61). This is a lower temperature source than the sun which emits radiation as a 6,000 degree Kelvin radiator. A comparison of the spectrum of the sun and an infrared lamp is shown in Figure 6. There are lamps available which are rich in shorter wave lengths but the power output at the short wave lengths is extremely small. For instance, a sunlamp produces 72 per cent of its total visible radiation in the region 0.5 to 0.6 micron, but the power output for this band of radiation is only 2.3 per cent of the lamp watts. Only 11 per cent of the lamp wattage is radiated in the entire region 0.38 to 0.76 micron. (61). An extremely large bank of such lamps would be needed to get a flux density on the model roof as high as the natural solar irradiation.

The choice of the infrared lamps was based on their long life and adaptability to voltage control. Other lamps than tungsten filament lamps are designed for constant voltage. This limitation would have made changes in the radiation incident on the model roof difficult to achieve without affecting the uniformity of the flux pattern over the model roof if other types of lamps had been used.

Figure 6 shows that the spectrum of the infrared lamp is different from the solar spectrum. Metal roofs except when new

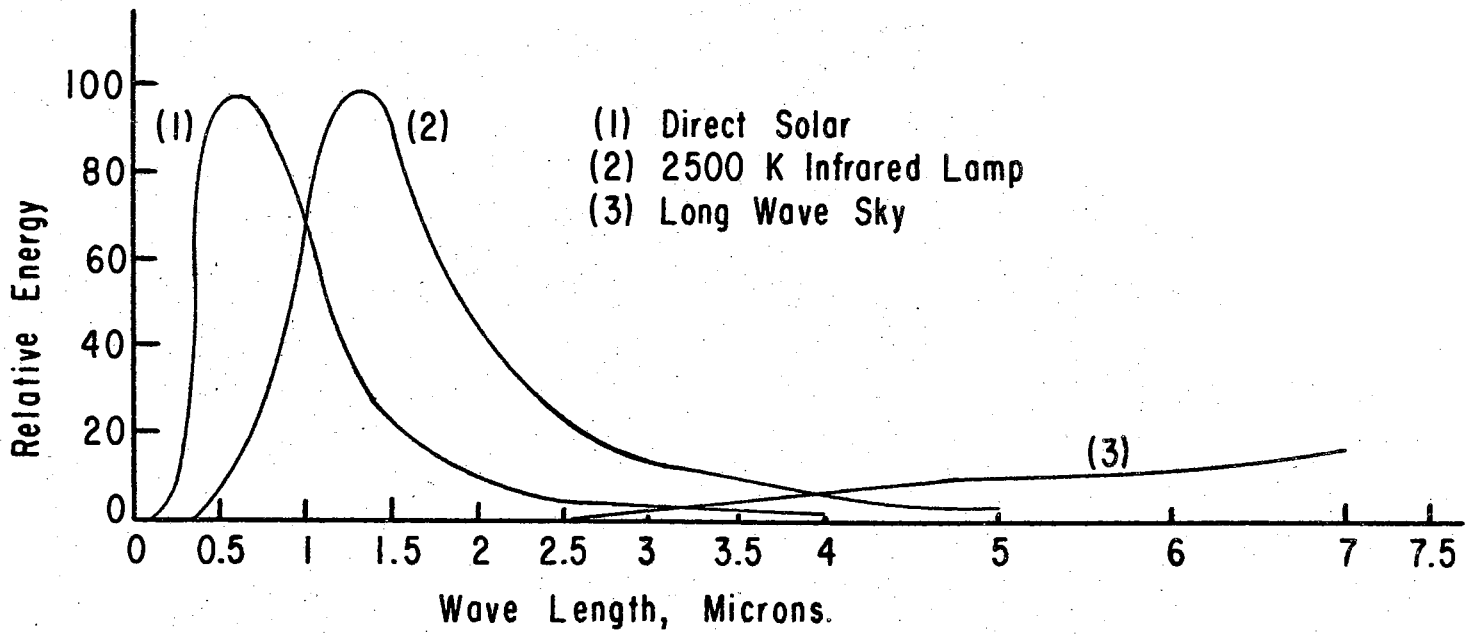

Figure 6. Spectral distribution curves for solar, sky, and infrared lamp radiation. Curve (1) and (3) plotted from data by Kelly et. al., (35, p. 566) and curve (2) was plotted from data by Weitz, (61, p. 36).

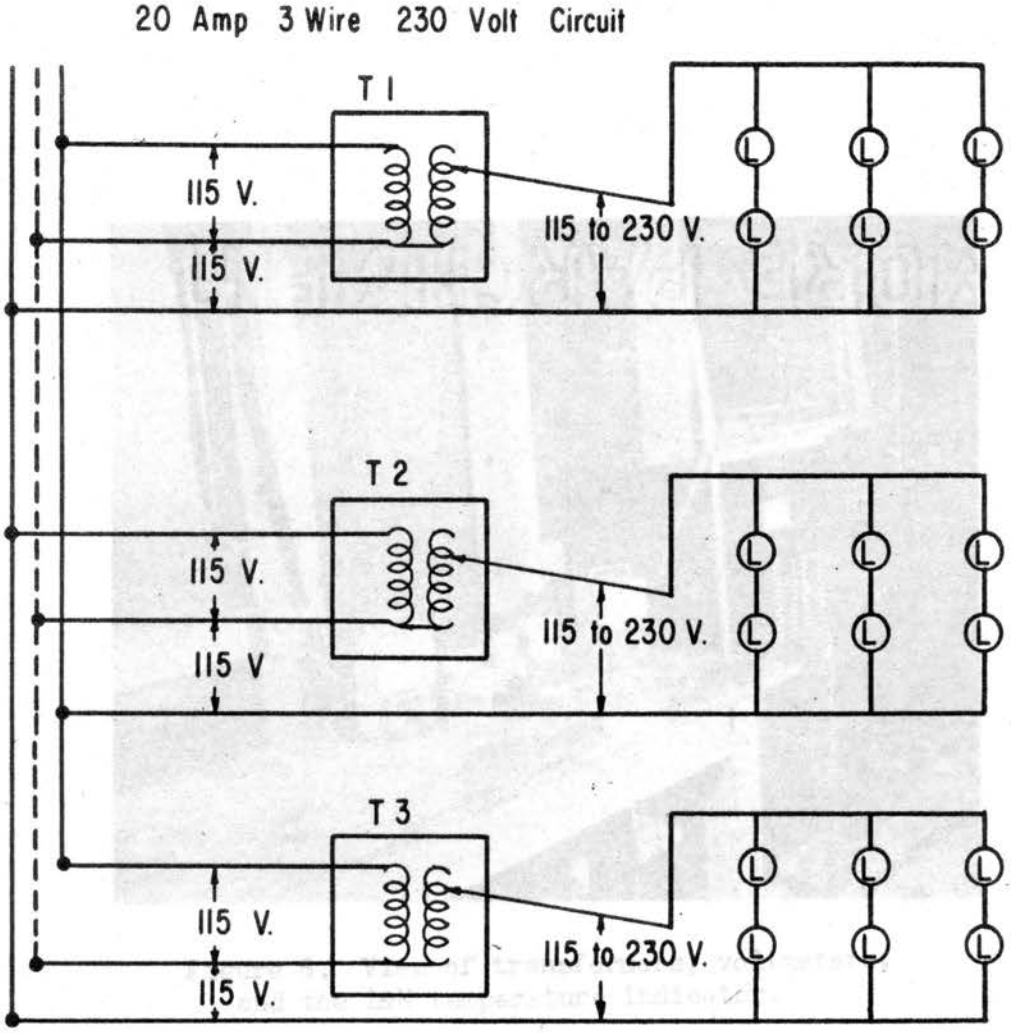

Figure 7. Control circuit for infrared heat lamps. Voltage measurement was output of transformer.

these two pi terms were equal in magnitude in both model system and prototype system.

For a scale ratio of "n" the thickness of the model roof would have to be 1/n times the prototype roof thickness. For a sheet metal prototype roof, it would have been necessary to use an extremely thin foil for the model roof. Structural strength problems would have arisen. To avoid the use of extremely thin model roof components, it was necessary to distort this pi term.

For thin, highly conducting materials such as boiler tubing or thin sheet metal the thermal resistance is largely dependent on the fluid films in contact with the surface. The thermal resistance of the material itself is insignificant in relation to the film resistance. The film resistance is of the order of magnitude of one thousand times larger than the resistance of sheet metal roofing. As long as a sheet of roofing is sufficiently thin, the gauge of metal has an insignificant effect on the thermal behavior.

Twenty-six gage sheet metal similar to the thickness of the roofing on the full size shelter was used for the model roof. This thickness, t = 0.00157 ft, was a constant for all model and full size shelter treatments.

Working with the scale ratio of 27, a model was built with a symmetrical gable roof 12.375 inches long and 36 inches wide. While the prototype roof was only 48 ft wide, the model width was similar to a building 71 ft wide. Two dimensional flow was thought to exist near the center of the roof.

The purlin and rafter sizes and locations were similar for the model and prototype. The other structural members were thought to have little effect on the air flow pattern, so lower chord members and other bracing were not included in the model.

To facilitate changes in slope angle and height of the roof on the model, the model was installed on a plywood platform, Figure 9, with the poles extending down through the platform through cut-out slots to clamps underneath the platform. A small metal rod served as a hinge along the ridge line of the roof, and piano-type hinges were used to attach the roof section to the plate girders. By loosening the clamps below the platform, the height of the roof and the pitch angle could be adjusted by moving the poles upward and downward or forward and backward. Details of the model are shown in Figure 10. A sheet metal cover was fitted over the cut-out slots to give the poles a snug fit and to remove irregularities on the platform surface.

The roof surfacing materials were made in panels four inches wide so that removal and replacement of panels could be made easily. Each roof panel was attached to the roof with 4-36 machine screws. The screws were placed only along the edges of the panels, away from the center where temperature measurements were taken. While the screw heads did protrude above the roof the effect on the air stream at the panel midpoint was thought to be small. Views of the model installed on the platform in the tunnel under the heat lamps are shown

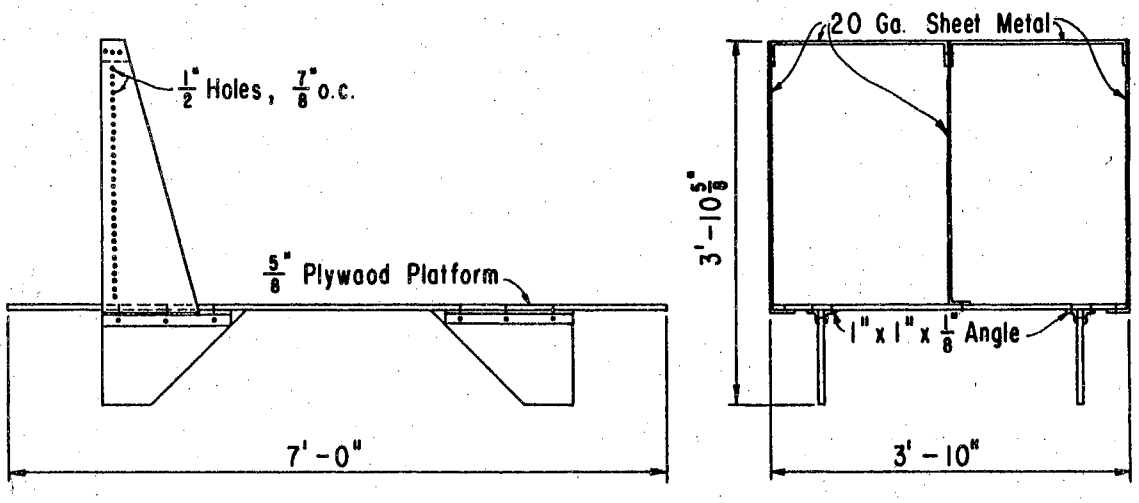

Figure 9. Construction details for model platform.

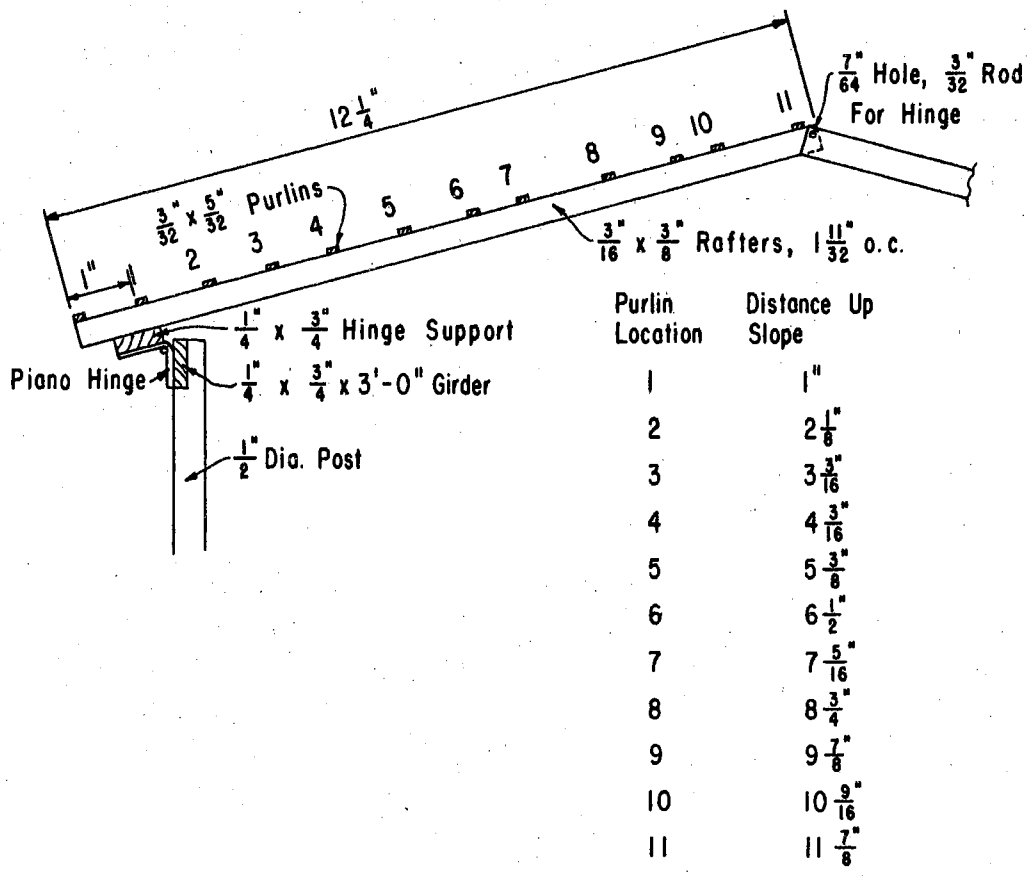

Figure 10. Model construction details.

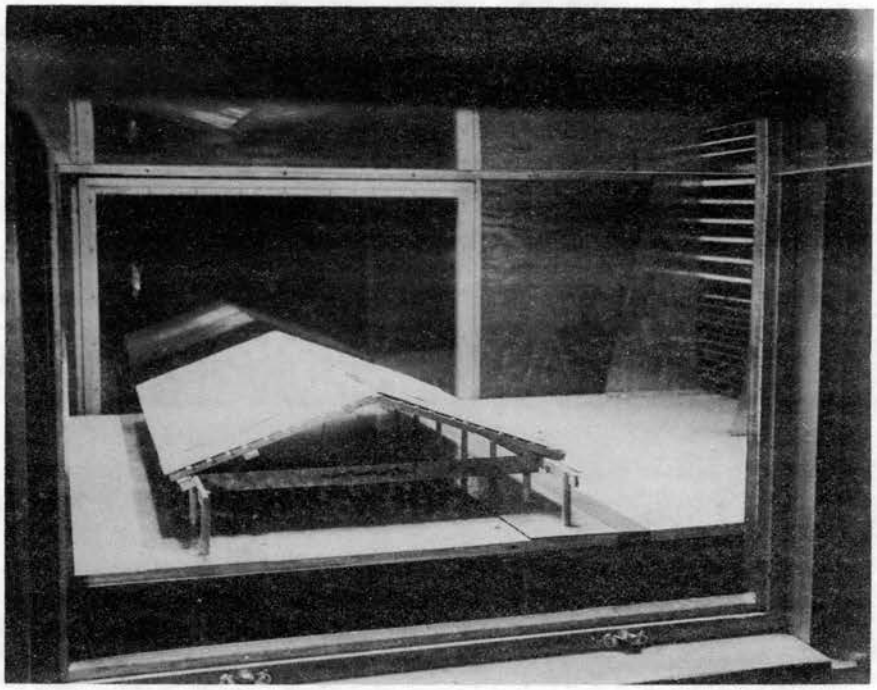

Figure 11. Model in position for temperature measurements.

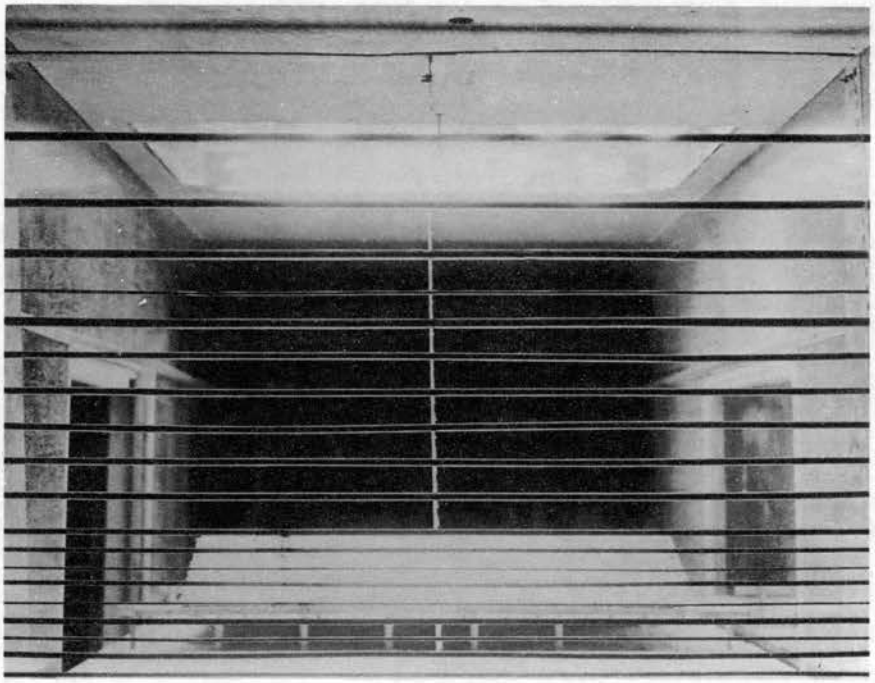

Figure 12. Model viewed from upstream location ahead of the profile bar rack.

in Figures 11 and 12.

Model Roof Panel Treatments

Pi term six called for a scaled-down corrugation size. For the 2½ inch corrugation pitch on the prototype roof, a 2.5/27 = 0.0926 inch pitch spacing had to be obtained for the model roof. A 1¼ inch prototype corrugation pitch would require 1.25/27 = 0.0463 inch model pitch. The smaller pitch would be extremely difficult to produce on a thin roof panel of sheet metal, so consideration of a treatment corresponding to 1¼ inch pitch roofing was abandoned. The 0.0926 inch pitch corrugations were produced by a small set of sheet rollers machined to groove the sheet metal. With the success of the small rolling mill, it was decided to also use a roof covering with larger corrugations. A corrugation size of 0.1852 inch pitch was decided upon. This corresponds to a five inch pitch in a 27 ft long roof system. Rollers machined to the 0.1852 inch pitch were used for producing the large corrugations.

New 26 gage sheet metal was used for the model roof panels. After the rolling process was completed, the galvanized steel samples were pickled with diluted hydrochloric acid to remove the oil finish and to start the oxidation process. A set of galvanized panels were given two coats of outside white paint. The paint was sprayed on with an air gun. Several methods were tried to get a uniform cover of paint but in all cases the paint accumulated in the corrugation

grooves, leaving the ridges somewhat uncovered.

After surface preparation, the samples were placed outdoors for six weeks for aging under natural weather elements. In a week a noticeable oxide coating appeared on the plain galvanized samples and the aluminum samples lost their glossy shine. A set of six panels of each treatment were prepared to provide three for each roof side.

Shelter Treatment Combinations

The model roof panel section treatments were scheduled to meet the shelter roof combinations as called for in the experimental design. It was decided to use the plain galvanized treatment in more combinations since this surfacing was expected to give the largest temperature rise. A 4/12 slope angle corresponded to the full size shelter configuration, giving it precedence in the combinations over the other slopes. Table IV gives the specific configurations used in the model study. A particular combination of pi terms five to nine in Table IV defines the treatments which are hereafter referred to as shelter treatments.

The configuration and material properties for the full size shelter are also presented in Table IV. It is seen that the first three model treatments are similar in configuration and material properties to the full size shelter.

Temperature Measurements

In order to determine the temperature of the roof panel

TABLE IV

SHELTER TREATMENT SCHEDULE AS DEFINED IN DIMENSIONLESS PARAMETERS

Treatment No.	$\pi_5=\theta$	$\pi_6=r/L$	$\pi_7=h/L$	$\pi_8=\alpha$ $\pi_9=\epsilon$
		(Model Shelter)		
1	4/12	0.0989	0.264	AL*
2	4/12	0.0989	0.264	G
3	4/12	0.0989	0.264	PS
4	4/12	(flat)	0.264	G
5	4/12	0.1978	0.264	G
6	3/12	0.0989	0.264	G
7	5/12	0.0989	0.264	G
8	4/12	0.0989	0.750	G
		(48 ft x 48 ft Shelter)		
9	4/12	0.0989	0.264	AL
10	4/12	0.0989	0.264	PS
11	4/12	0.0989	0.264	G

*AL means aluminum roofing, PS white-painted steel, G plain, aged galvanized steel. Numerical value of absorptivity and emissivity not needed.

when exposed to the thermal radiation and the wind cooling, iron-constantan thermocouples were soldered to the under surface of each test panel. The couples were of No. 30 gage wire, and they were soldered to the galvanized panels with regular lead-tin solder. A liquid cold solder was used for attaching the couples to the aluminum panels. The couples were placed on the panels at points not coinciding with purlin locations. Distance from the leading edge, x, in relation to total length of the roof panel at which couples were attached is shown in the following table.

TABLE V

VALUES OF x/L FOR THE EIGHT THERMOCOUPLES

Couple No.							
1	2	3	4	5	6	7	8
0.0606	0.120	0.2288	0.3885	0.5222	0.654	0.793	0.919

All thermocouple leads from a panel were laced together. When the roof panel sheets were placed on the model roof, the leads passed up the roof to the ridge where the leads from both the windward and leeward roof panel were joined together and passed downward through a drilled hole in the platform. All panels were wired individually prior to the test runs so that exchanging panels could be done without need for making new junctions.

The potentiometer used for monitoring the thermocouples was a self-balancing Leeds and Northrup 48 point temperature indicator with a least count of 0.5 F and a range of 0 to 250 F.

It is shown in Figure 8.

For measurement of air temperature t_a, four thermocouples were placed in the windstream ahead of the platform on which the model rested. These couples were placed so that thermal stratification of the air stream, if any, could be detected.

Other Instrumentation

For measuring air properties a mercurial barometer and a sling psychrometer were used. From barometric pressure and wet and dry bulb temperature measurements, the density of air could be computed. Viscosity as a function of temperature was found in tabulated data in the literature. Thermal conductivity is also a function of temperature and its value is given in texts. Plots of viscosity and thermal conductivity of air which were used for quick reference are contained in Appendix A.

A Beckman and Whitley total hemispherical radiometer was used for measuring the intensity of radiation under the heat lamps. The radiometer is nonselective and responds to all wavelengths of energy. Its operating principle is that of a heat flow meter. The calibration factor for the particular instrument is 25.72 Btu/hr sq ft per millivolt output of the thermopile. A single thermal junction measures the temperature of the sensing surface for a correction factor which is given by the manufacturer.

The output of the thermopile was monitored with a Leeds and Northrup precision null balance potentiometer reading to

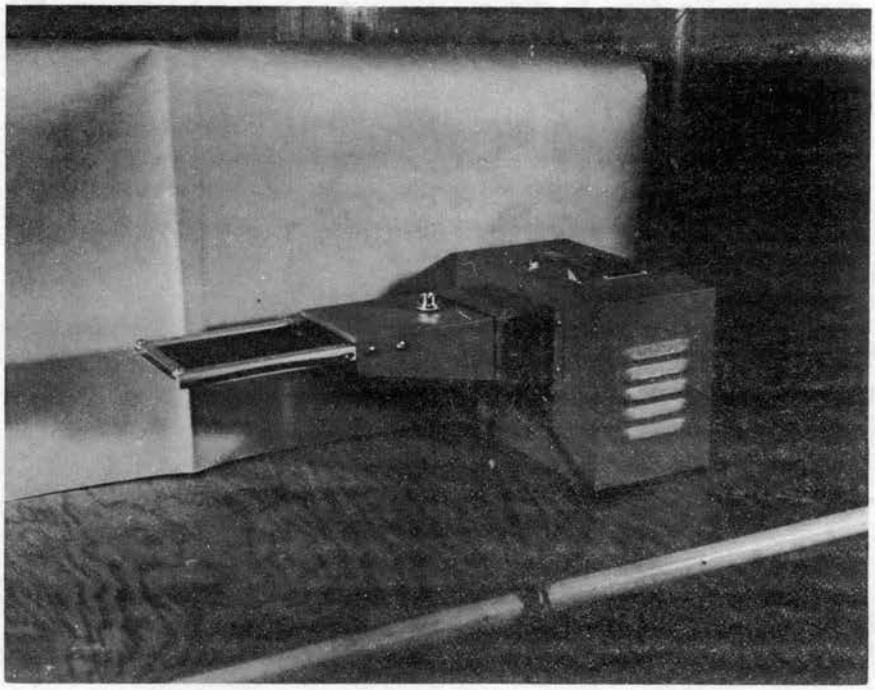

Figure 13. Beckman and Whitley flat plate radiometer.

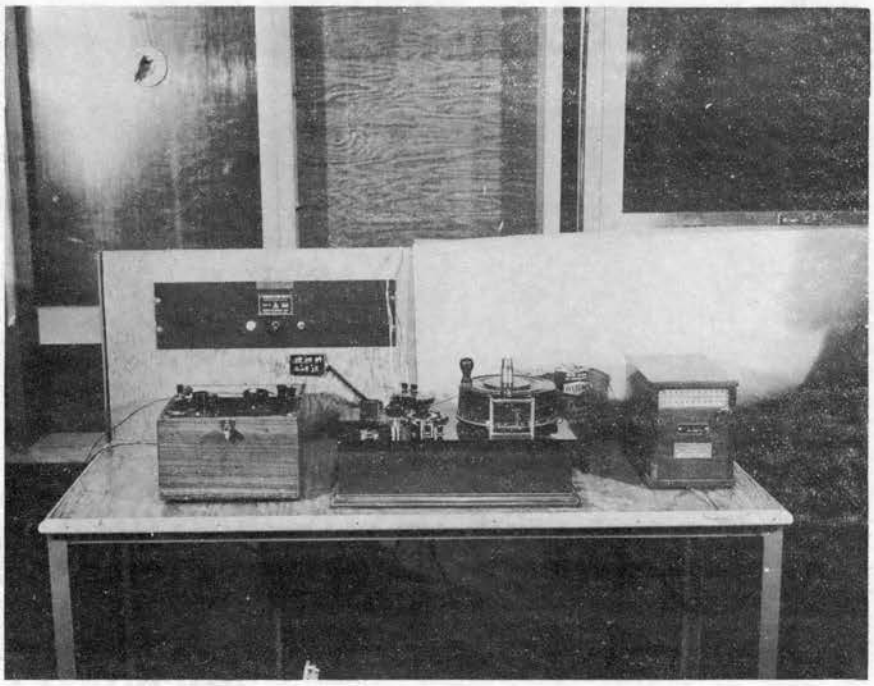

Figure 14. Potentiometers for sensing radiometer thermopile emf and the temperature of the sensing element.

the nearest 0.0001 volt. The radiometer is shown in Figure 13 and the potentiometers in Figure 14.

Wind Profile

Adherence to similarity of conditions as they exist in nature required that the velocity pattern for the model system be similar to that of an actual wind.

In wind tunnel experiments by Rice (53) and O'Neill (48) a profile was produced by placing round bars varying in diameter from 1/16 to 1/2 inch across the tunnel section to retard velocity near the bottom of the air stream. By using different size bars and by varying the spacing between bars the blockage produced could be controlled.

According to Brooks (5), on hot days when convective air currents from the warm ground are rising, the profile of the natural wind is described by an exponential law with an exponent of 0.25 to 0.10 or less. For the present study, by trial and error, bars placed across the tunnel were rearranged until a profile with an exponent of 0.20 was obtained. The profile bars were placed 32 inches ahead of the model's leading roof edge. A pitot tube was used for determining the velocity by traversing the wind stream in a vertical direction at the location of the model roof's leading edge, before the model was placed on the platform.

Once a desired profile was obtained, the shape of the profile was checked at three different wind speeds to learn if changes in velocity changed its shape. A graph of the final

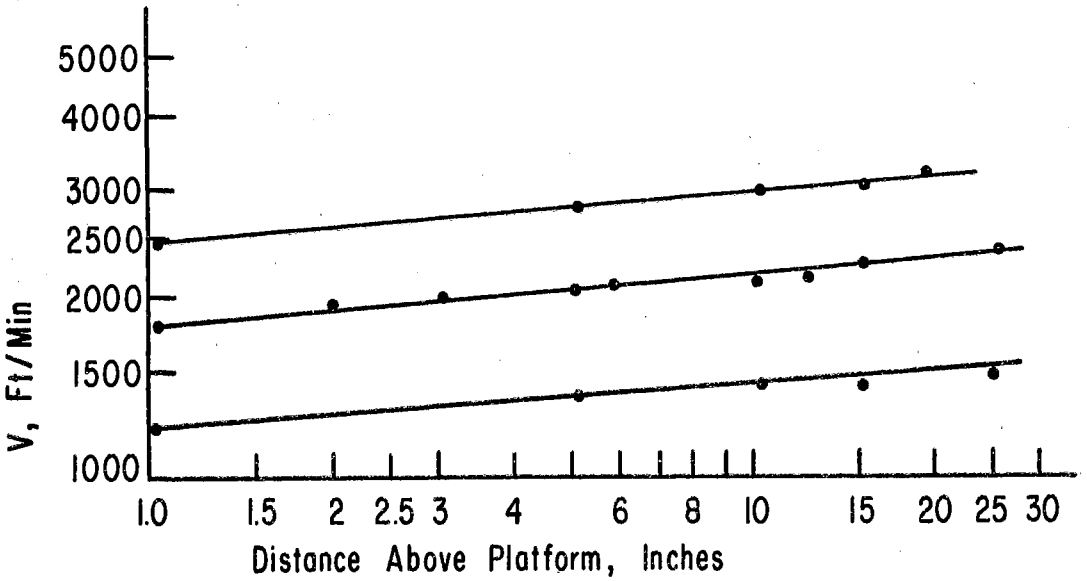

Figure 15. Curves of wind profile at three fan speeds. Average slope of lines is 0.20. Upper curve represents profile measured 32 inches behind profile bars for fan speed of 800 rpm, middle curve 600 rpm, and lower curve 400 rpm.

profile for three wind speeds is shown in Figure 15. No measurements of the eddies or turbulence caused by the bars were made. Once the calibration of the profile was made, the bars were not removed from the arrangement found suitable.

Maher (43) in previous use of the wind tunnel made investigations of the turbulence in the wind stream with hot wire anemometry. He found fine scale turbulence at all fan speeds. With turbulence-producing screens installed in the test section the velocity fluctuations associated with eddies formed by the screens were damped out 15 mesh diameters downstream from the screen.

For the present experiments the largest bar size used was 1/2 inch diameter. With the profile rack 32 inches upstream from the model the eddies formed by the bar were

thought to be damped out, in accordance with Maher's results.

Calibration of the Wind Speed at Model Eave Height

Before the model was placed on the platform, a calibration of wind speed at the height of the model eave versus piezometric head was made for a 3.25 inch eave height and a 9.312 inch eave height. With the model installed, the pitot tube could not be placed low enough to the platform to coincide with the eave height. For set conditions in the wind tunnel the static pressure drop sensed by the piezometer ring at the downstream end of the test section was an accurate criterion of mean velocity at any point in the tunnel air stream if simultaneous measurements of the two were made.

With the model in place on the platform, additional blockage of the tunnel cross section would occur and thereby reduce the velocity of the air stream. The piezometric readings would not be a true indication of velocity at eave height on the model because part of the pressure drop would be consumed by viscous drag on the model.

Significant disturbances in the flow pattern caused by placing the model in the windstream would occur only downstream from the model. If velocity at a given point upstream from the model were measured over a range of fan speeds with the model present and again with the model removed, the reduction in velocity due to the model at the upstream point would be equal to the velocity reduction at eave height just ahead of the model.

On the basis of the foregoing hypothesis, velocity upstream from the model was measured for both model-in and model-out the tunnel conditions. The plot of piezometer head versus pitot reading for the two conditions is given in Figure 16. The reduction factor for the upstream point was applied to the piezometer head versus velocity-at-eave-height curve. The corrected velocity-at-eave-height curve gives the value of the quantity V. Piezometric head readings could be determined readily for any test run. Corrected velocity-at-eave-height curves are plotted in Figure 17. When utilizing the velocity curves during the testing, density corrections were made when air density differed from 0.0704 lbs/ft^3.

Radiation Intensity

The quantity H as defined in the section on pertinent quantities is the total incoming radiation incident on the roof surface. On an actual roof the incident radiation is approximately equal over any portion of each roof plane, but on a gable roof the incident radiation is different on the two roof planes unless the sun altitude is 90°.

Spot measurements of the intensity of radiation under the bank of heat lamps showed that the radiant energy level was higher in the center of the heated area than near the edges of the area. By tilting the center lamps away from the central area the intensity near the edge was increased. While the bank of lamps did tend to uniformly heat the entire area occupied by the model, no attempt was made to get a perfectly uniform

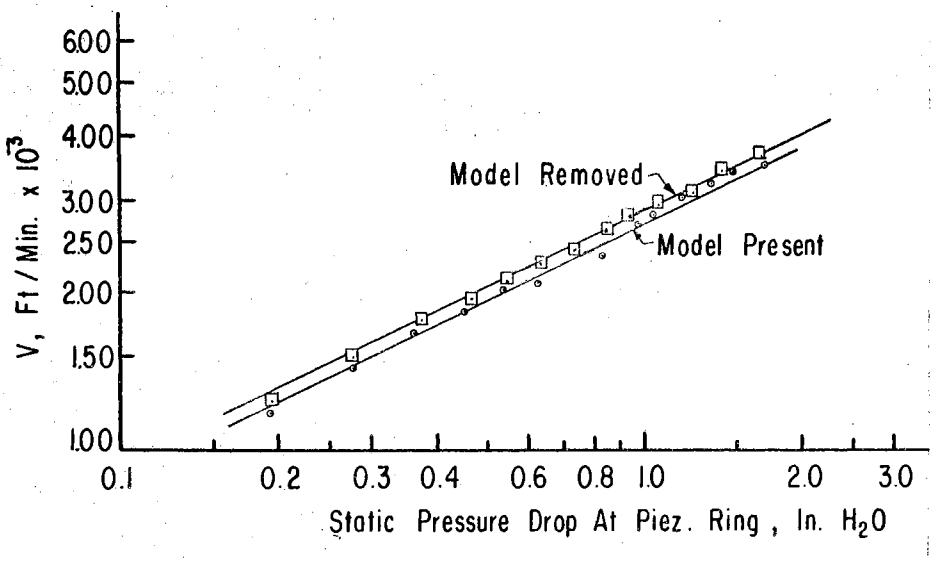

Figure 16. Wind velocity at center of tunnel section 8 ft upstream from the profile bar rack. Analysis of covariance indicated that the regression lines are parallel @ 97.5% confidence level. Difference in adjusted means = 0.016865. This is the velocity reduction factor due to blockage offered by the presence of the model in the tunnel section.

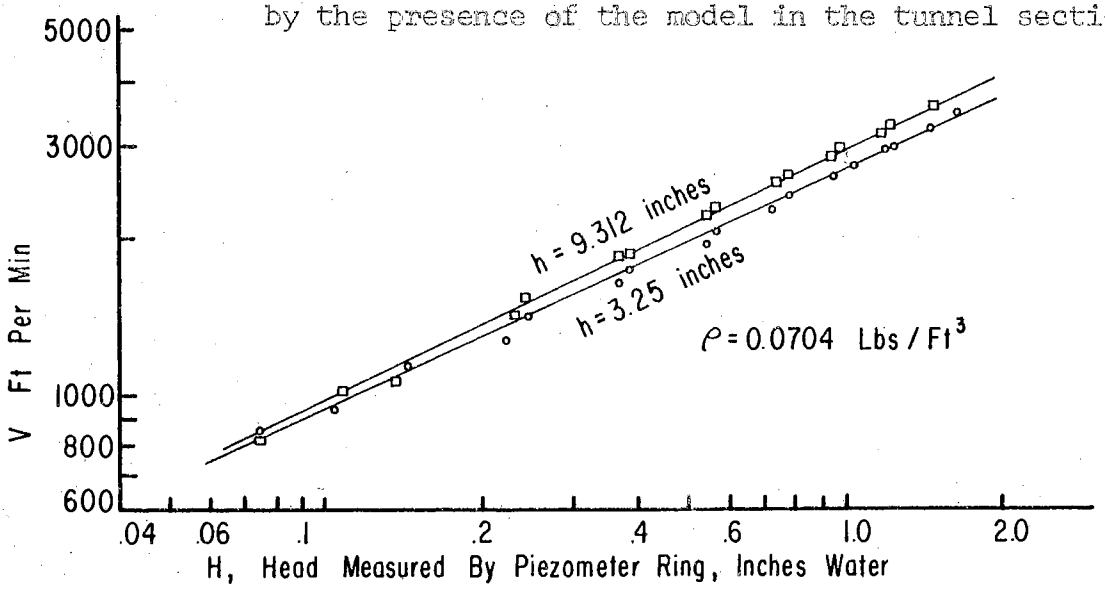

Figure 17. Velocity at eave height vs. piezometric head. Plotted curves represent velocity at model eave height after use of the blockage correction factor. Regression equations after blockage reduction:

h=3.25 inches: $V=2585.4\ H^{0.4765}$

h=9.312 inches: $V=2852.0\ H^{0.4970}$

where V=ft/min, H=deflection of piezometer ring, inches H_2O.

intensity over the entire roof area. Adjustments were made on the lamp beam directions until the radiation was uniform over the center roof panels which had the thermocouples attached.

A small photometer which responded readily to the lamp output was used for checking uniformity of flux over the plane area which the test panels would occupy. When a uniform flux pattern was obtained over the test area, the photometer was replaced by the radiometer for quantitative measurement of the incident thermal radiation.

By placing the radiometer on a tilting table, the sensing element of the meter could be placed at the exact spot under the bank of lamps that the test roof panels would occupy. With the meter in the correct position, the incident radiation received was plotted against lamp voltage setting. By trial and error procedure, the lamps were directed so that the intensity of radiation on the windward roof was approximately equal to the intensity on the leeward roof. As the lamps used have a long rated life and the voltages used were equal to or lower than rated voltage, the calibrations of lamp volts versus intensity of radiation were thought to be stable with time. Two vacuum tube voltmeters were employed in the voltage measurements.

To place the meter in the location of the model roof during calibration, the platform on which the model rested was moved upstream in the tunnel, giving a flat area on the rear of the platform upon which the radiometer on the tilting table could be placed. When calibrations were completed the platform was

returned to its original position, putting the model roof where the sensing element was positioned during calibration. Figure 18 shows the radiometer in position for making a calibration.

Calibration curves for each combination of roof eave height and slope were made, but not all prior to all the experiments. After all model data had been taken for one condition of height and slope the radiation intensity was measured for the other conditions of height and slope angle after re-setting some of the lamp beam directions as necessary to get uniform radiant energy distribution over the test panels for the new conditions of height and slope. The calibration curves are given in Appendix A.

With a calibration of radiation intensity complete, the model set-up was ready for the first run of experimentation.

Test Run for Model Treatment No. 1

For the first experimental run for the model, the aluminum test panels were installed on the model roof. The eave height was set at 3.25 inches and the slope angle 4/12. These conditions correspond to Treatment No. 1 in Table IV.

After all thermocouples were checked for faults, the model was ready for operation. The fan was turned on and the wind speed set at an intermediate value. The plan was to hold the velocity constant while the temperature rise of the model roof was measured for changes in H, the intensity of radiation normal to the model roof surface. In the π term notation this procedure gave a measure of π_1 for changes in π_2 π_3 held

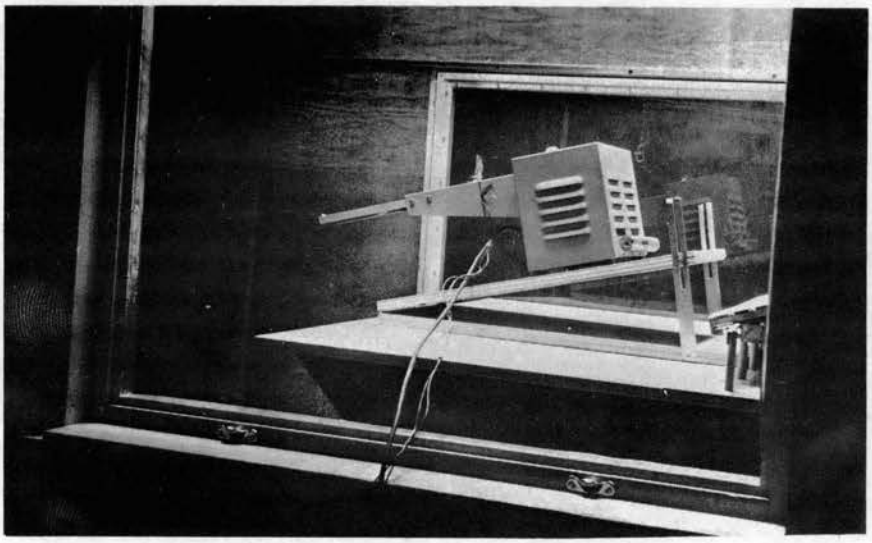

Figure 18. Radiometer on the tilting table in position for sensing radiation received at the particular location under the lamp bank.

constant.

When the wind velocity in the tunnel was set at an arbitrary value the heat lamps were turned on with the voltage set at a low value. After waiting several minutes for thermal equilibrium to be established, the temperature measurements were made. First the air stream was checked for thermal stratification. If there were differences in air temperature in excess of half a degree F, air circulation fans were turned on in the laboratory to mix the cool air near the floor with the warm air near the ceiling. This procedure appeared effective for giving a uniform temperature distribution to the air sucked into the entrance section. The quantity t_a, air temperature, was taken as the average value measured at four points in the air stream ahead of the model.

The order of taking temperature measurements was as follows: First the air temperature at one point upstream, then the eight surface temperatures on the windward roof panel, then two measures of air temperature upstream, then the eight temperature measurements on the leeward roof panel, and finally another air temperature measurement upstream from the model.

Other data for a run included deflection of the micromanometer on the piezometer ring and lamp voltage. Barometric pressure and wet and dry bulb temperature were measured only once per several runs of data.

Next, the lamp voltage setting was increased, and after equilibrium was established the same temperature measurements and other readings described above were repeated. This procedure

was repeated for eight different runs corresponding to eight different intensities of radiation on the model roof, giving a total of 64 observations of the temperature rise for each roof side.

On the windward roof when the system was in operation the surface temperatures were found to be lower near the eave and highest near the ridge. This was consistent with the laws of convection, since the air next to the surface was warmed as it passed along the sample, lowering the air-surface temperature difference. In conventional practice the heat transfer coefficient correlated through a Nusselt number decreases with distance from the leading edge of a surface.

The temperature gradient on the leeward roof was found similar to the windward roof: low surface temperature near the eave and an increasing surface temperature with distance up the roof length.

Eight runs were then conducted with radiant energy level constant and wind velocity varying from run to run.

With an expected value of Δt encountered in actual shelter systems in use in the range 5 to 50 F, control on radiation intensity and wind velocity was enacted to produce Δt values in this range. Radiation intensity could be varied from approximately 5 to 12 Btu/min-ft^2, and wind velocity from 500 to 3800 ft/min with the wind tunnel setup. Values of Δt smaller than 2 or 3 degrees F were subject to a large percentage error since surface temperature and air temperature could only be read to the nearest half degree with estimation

to the nearest tenth. For this reason radiation intensity was varied over the entire range possible, and wind velocity was kept in a range from 800 to 3400 ft/min during the experimentation to effect a Δt in a range of 2 to 60 F.

Test Run for Model Treatment No. 2

For the second test run the plain galvanized, corrugated roof panels were installed on the model. Roof slope was left at 4/12 and the eave height at 3.25 inches corresponding to Treatment No. 2 in Table IV.

After testing the thermocouple points on the roof panels for faults the system was ready for operation. Following the procedure outlined for the aluminum roof panels the temperature rise for the plain galvanized panels was obtained. Preliminary analysis of the data test run No. 1 indicated that the temperature rise of the roof panels varied consistently with changes in the control quantities. The systematic technique of changing wind velocity with radiation held constant and then changing radiation intensity with wind velocity constant produced wide range of variation in the dimensionless parameters π_1, π_2, and π_3. By observing the temperature rise at eight points a change in the value of π_4 at which observations were taken was effected. No evidence was available to warrant a change in the technique to a different one from that of the first test run.

The temperature rise experienced by the plain galvanized panels was larger than for the aluminum roofing as would be

expected.

Test Run for Model Treatment No. 3

For system Treatment No. 3 the corrugated, white-painted roof panels were installed on the model. With the same slope angle and eave height setting the temperature rise for the white-painted samples was recorded along with the measure of the other quantities in the system. Contrary to expectation the temperature rise of the white-painted samples was larger than the rise for the aluminum. One factor which was suspected to cause high absorption was the thin, non-opaque paint coverage at the ridge of the corrugations due to imperfect paint coverage.

Test Run for Treatments No. 4 and No. 5

Placing the flat, plain galvanized samples on the roof provided conditions for Treatment No. 4. The usual 128 observations of temperature rise were made for the flat samples.

In like manner, the large corrugated samples, corresponding to $\pi_6 = r/L = 0.1852$, were placed on the model roof and the controlled observations taken with these samples. With the completion of the fifth treatment all testing at the 4/12, 3.25 inch height configuration was completed, and the heat lamp position settings could be modified to produce a uniform flux pattern for some other configuration.

Test Run for Treatment No. 6

Treatment No. 6 is characterized by a 3/12 roof slope angle. Spot measurements showed that the pattern used in the 4/12 slope tests was not uniform for a 3/12 model roof slope. Using the photometer for reference, the beam direction of several of the lamps were altered until the response of the photometer was constant everywhere over the area a test panel with 3/12 slope would occupy. A calibration for total incoming radiation for the 3/12 slope condition determined by the flat plate radiometer is given in Appendix A.

Treatment No. 6 called for the small corrugated, plain galvanized panels set at h = 3.250 inches and 3/12 slope. For this condition the sixteen runs were made over the usual range of velocity and radiation intensity.

Test Runs for Treatments No. 7 and No. 8

These two treatments required separate calibration curves for radiant energy incident on roof vs. lamp voltage. After the setup was used for conditions corresponding to Treatment No. 7 with slope angle 5/12, the lamps were arranged to provide a uniform pattern for the eighth treatment with h/L = 0.750. Technique of measurement of the pertinent quantities was similar to test run No. 1.

In review, observations of the temperature rise on selected treatments of a shelter roof were made with a model system operated in a controlled wind stream with an adjustable radiant heat source supplying thermal energy. Eight treatment combinations of configurations of the model shelter, surface

texture, and kinds of material were utilized. Certain treatments were in correspondence with a full size shelter which was a replication of these treatments in a system with geometric dimensions 27 times larger than the model and exposed to conditions of natural wind and solar and sky irradiation.

Observations in the Full Size System

The full size system utilized for this study was a 48 ft x 48 ft open type pole frame shelter used for housing turkeys at the Perkins Experiment Station, Figure 19. It was a 48 ft x 48 ft structure with a 4/12 roof slope and 7 ft 2 in roof height. Its corrugated metal roofing was white-painted except for a strip each of aluminum and galvanized roofing on the south slope. There were a few tall trees about 300 ft south of the shelter which due to their sparse foliage were not thought to offer much blockage to the wind pattern. A few brooder houses 100 ft south and 30 ft east of the shelter were expected to cause some disturbance to the wind character. The pi term connotation for the shelter is given in Table IV.

Thermocouples of 20 gage iron-constantan wire had already been taped to four points along each roof type for previous experiments, so four more 30 gage couples were added at intermediate points as shown in Figure 20. The couples were taped to the underside of the roof metal with plastic adhesive tape. Attempts at soldering the couples to the roof in the inaccessible place in the dusty open attic space were futile. Two couples were placed near the eave in the shade to measure the

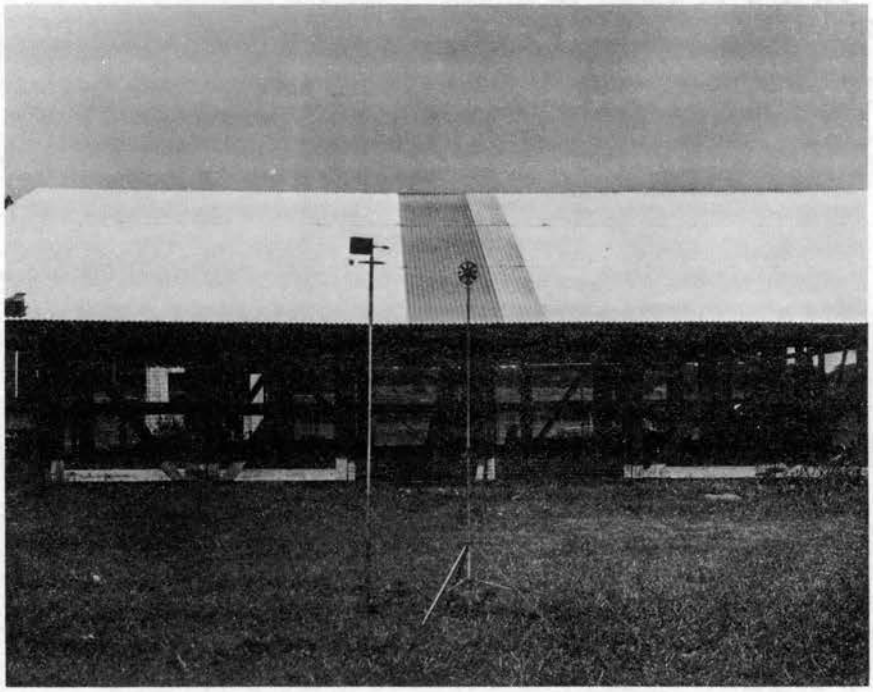

Figure 19. The 48 ft. x 48 ft. shelter. A wind direction vane and an anemometer are shown in the foreground.

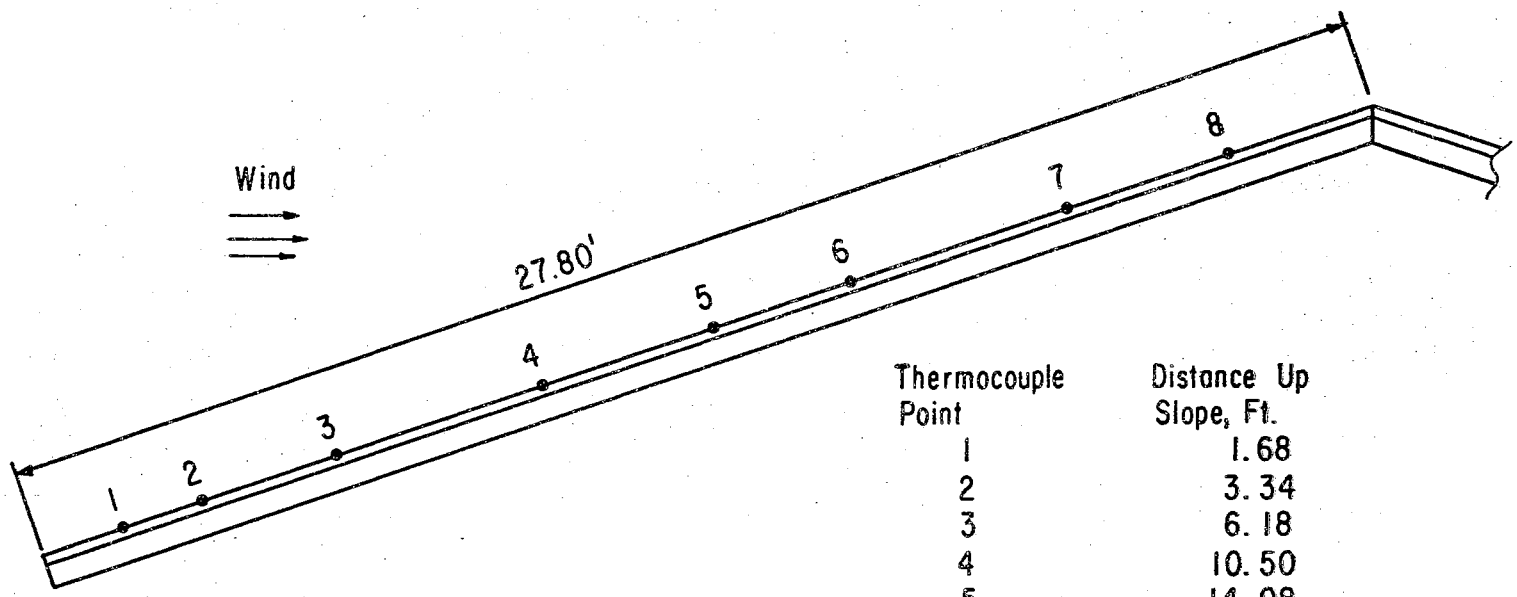

Thermocouple Point	Distance Up Slope, Ft.
1	1.68
2	3.34
3	6.18
4	10.50
5	14.08
6	16.90
7	21.43
8	24.81

Prototype Thermocouple Locations

Figure 20. Thermocouple points along the 48 ft x 48 ft shelter roof. Even number points were 20 gage wire couples and odd numbers were 30 gage wire couples.

temperature of the air stream. The 24 surface temperature measuring junctions and the two air temperature couples were connected to the 48 point Leeds and Northrup precision temperature indicator which was placed inside the shelter.

No data were obtained for the north or leeward roof. It was desired to make a more complete observation of the windward roof slope rather than fewer observations on each of two slopes.

On days free from cloud cover when the wind was brisk and blowing from the south, the instrumentation was set up for use. The hemispherical radiometer was placed on the roof of the shelter such that its sensing element was parallel to and above the plane of the windward roof. Incoming radiation was read by the emf output of the radiometer. A vane type anemometer and a wind direction vane were set at eave height 30 ft upwind to measure wind velocity and direction. With the temperature indicator connected, the apparatus was ready for operation.

A preliminary series of test runs was completed to check the technique for taking the readings of the several instruments and to detect errors in the set-up.

For a set of observations, the anemometer was turned on, the 26 temperature measurements taken, incident radiation metered, and air properties necessary for density computations were recorded. The anemometer which measured total wind passage was allowed to run three minutes, the time interval necessary for recording the temperature indications. This procedure

gave the wind passage in feet for a measured time period from which the mean wind speed for the run could be computed. The non-steady character of wind velocity made several repetitions of test runs necessary for reducing error due to velocity fluctuations over the chosen time period. As the reading of the temperature points required a full three minutes, no shorter time interval for wind passage seemed appropriate as one mean wind velocity reading was used for a whole run of temperature observations.

A test run was initiated every 15 minutes, starting immediately after noon on two days when the sun altitude was nearly 90^{o} and starting at about 10:00 a.m. on a third day. For each day eight test runs were completed which were judged to be representative of a reasonably steady natural wind. Readings were discarded if the wind direction changed from true south during a run.

Some trouble was experienced keeping the 20 gage couples in intimate contact with the roof metal. The stiffness of the wire prevented the tape from effecting a pressure contact. The flexible 30 gage couples caused no trouble. A review of the temperature measurements showed that some of the points sensed by 20 gage couples were consistently lower in temperature than other points nearer the leading edge where 30 gage junctions were attached. With the possible error in measurement induced by the 20 gage junctions, the measurements at these points were later discarded from the analysis, leaving the four 30 gage observations per run per roof sample available.

With four observations per run, eight runs per day and three days of data-taking, a total of 96 observations of the pertinent quantities were gathered for each of the three roof samples on the windward roof of the 48 ft x 48 ft shelter.

Wind velocity during the test runs varied from 270 to 490 ft/min based on the three minute time average. Radiation intensity incident on the roof was in the range 6.0 to 8.0 Btu/min-ft^2, typical of a hot summer sun.

Observations in the Intermediate Size Shelter System

Following a preliminary analysis of the model and full size system results as given in Chapter V, there appeared to be need for further investigation of the effect of roof length on the shelter system behavior. The model and full size systems were in disagreement by what appeared to be a factor associated with the gross length of the roof surface. This initiated the plan to construct and test a shelter system with a roof length intermediate to the model and full size shelter roof length.

The intermediate size system consisted of a shelter constructed geometrically similar except for purlin location to the full size shelter on a 1/5 scale, L = 66.8 inches. The roof height was set at 0.75 L, giving π_7 = 0.75 instead of 0.264. Built of light framing material the shelter was mounted on skids to facilitate orientation to face the shelter into the prevailing wind. A drawing of the shelter is shown in Figure 21.

Rather than attempt to meet a corrugation scale-down

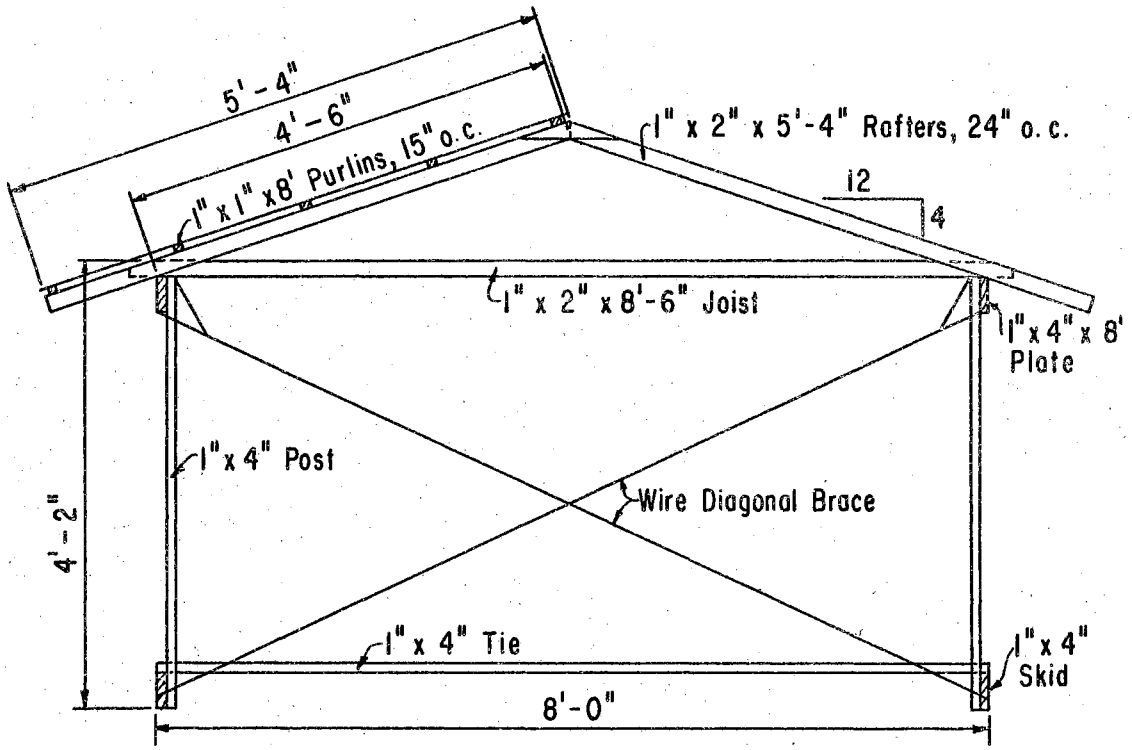

Figure 21. Construction details of the 8 ft x 8 ft shelter. Purlin spacing was not scaled.

requirement, the shelter was covered with flat, galvanized sheet metal. The metal sheets were acid-pickled to accelerate the aging condition. After the oxidizing process, the sheets were exposed to the natural elements for three weeks. After that time the sheets appeared to have a dull grey coating, typical of aged galvanized metal except for a few spots where the zinc coating was apparently oil-covered thick enough to prevent thorough acid penetration.

Thermocouples were soldered to the underside of the sheet metal at ten points along the roof in the central portion of the shelter's windward roof at distances up from eave given in Table VI. The thermocouples were wired to a Brown automatic temperature recorder which scanned the ten points every two minutes. Again only the windward roof side was studied. Further instrumentation consisted of the anemometer set at eave height, and the radiometer set on the roof to meter incoming radiation.

On a clear day with strong wind, observations of the pertinent quantities were taken. The measurements of air properties, wind velocity, incident radiation, and surface and air temperature were taken. Mean wind velocity was obtained by measuring wind passage over a one minute period. Velocities encountered were 300 to 500 ft/min on one day and 800 to 1300 ft/min on another day. Figure 22 shows the shelter ready for testing. Incident radiation was in the range of 6.5 to 7.5 Btu/min ft^2 during the runs.

TABLE VI

THERMOCOUPLE LOCATIONS ON WINDWARD
ROOF OF INTERMEDIATE SIZE SHELTER

Thermocouple No.	1	2	3	4	5	6	7	8	9	10
Distance from eave, x, in	1.0	4.05	6.25	8.02	9.06	14.82	25.18	33.80	42.35	51.60

Note: 1. Length of roof = 66.8 inches
2. Roof metal thickness, t = 0.00157 ft.

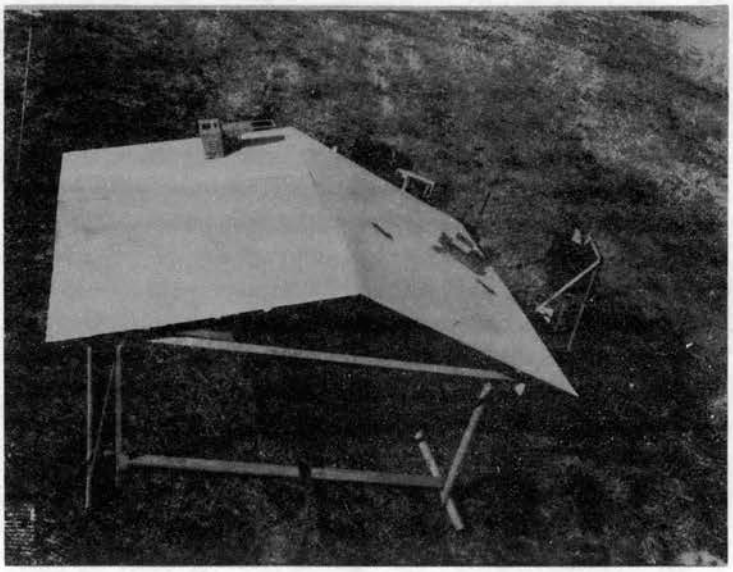

Figure 22. The intermediate size shelter ready for testing. This shelter is also called the 8 ft. x 8 ft or middle size shelter.

Thermocouples attached under roof areas that were shiny and not completely oxidized gave slightly lower readings than the other junctions. The four readings where the surface treatment was visibly non-representative of aged roofing were not discarded.

CHAPTER V

ANALYSIS

After collection of sufficient data from the model system and the full size shelter system, a preliminary analysis was made to test the adequacy of the experimental observations for yielding functional relations for describing the interrelation of pi terms one to four for a particular system treatment. This analysis led to the supplementary investigational study of the behavior of the intermediate size shelter.

Preliminary Analysis for the Windward Roof

After the completion of the experimental observations on the full size system and on two treatments of the model system an analysis of the data was initiated to find prediction relations for the chosen groups of dimensionless parameters and to search for behavior in the system unaccounted for by the measurement of the selected quantities. Early analysis was desirable to avoid gathering large amounts of insufficient data and to give some guidance on techniques for possible improvement to the data collection scheme.

For the preliminary analysis the data gathered for the windward roof from model and full size shelter observations were arranged in tabular form for systematic computation of the dimensionless parameters. Slide rule values were

considered adequate for the rough computations.

With pi terms ten to fifteen constant and terms five to nine constant for a system treatment the action of the system was hypothesized to be a function of the first four parameters

$$F (\pi_1, \pi_2, \pi_3, \pi_4) = 0.$$

Since $\pi_1 = k\Delta t/Hx$ is descriptive of the rate of convected heat flow from the surface it is convenient to think of it as a dependent parameter and the other three pi terms as independent parameters. Thus

$$\pi_1 = f (\pi_2, \pi_3, \pi_4)$$

where $\pi_2 = t_a/\Delta t$ is an index of radiant heat transfer from the roof to the surround, $\pi_3 = V\rho x/\mu$ is a Reynolds number based on distance up roof slope from the leading edge, and $\pi_4 = x/L$ is the ratio of distance to point where surface temperature was measured to total roof length.

Experiments had been run in the model system with π_3 constant and π_2 varying. Repeated observations at any temperature point gave constant values for π_4. With π_2 varying and π_3 and π_4 constant π_1 is some function of π_2

$$\pi_1 = f (\pi_2, \bar{\pi}_3, \bar{\pi}_4)$$

with the bar to denote constant values.

A plot of π_1, versus π_2 on rectangular coordinates indicated a non-linear relationship among the variables. When plotted on log-log paper there appeared to be strong evidence

of exponential variation as evidenced by the straight line fit in Figure 23 for the plain galvanized roof treatment. A similar plot for aluminum model roof data produced the same evidence of exponential relation. This result is consistent with much heat transfer phenomena in which dimensionless parameters combine as products of parameters to particular powers. For instance the Nusselt number is related to the Reynolds and Prandtl number by the relation

$$N_n = C(Re)^n(Pr)^m.$$

For the present system it was hypothesized that an adequate functional form for the prediction equation was

$$\pi_1 = K(\pi_2)^{b_1}(\pi_3)^{b_2}(\pi_4)^{b_3}$$

where log-log plots could be used to determine the values K, b_1, b_2, b_3. In Figure 23 the slope of the line for π_1, versus π_2 with π_3 and π_4 constant yields the value of exponent b_1. For the chosen equation form

$$\pi_1/\pi_2^{b_1} = f(\pi_3, \overline{\pi_4})$$

which could be investigated by observing π_1 and π_2 for changes in π_3 with π_4 held constant. The experimental runs with radiation intensity constant and wind velocity varying produced data with π_3 as a running variable. This data when plotted on a log-log paper gives a relation as shown in Figure 24 of the form

$$\pi_1/\pi_2^{b_1} = K_1(\pi_3)^{b_2}, \qquad \pi_4 = \text{constant}$$

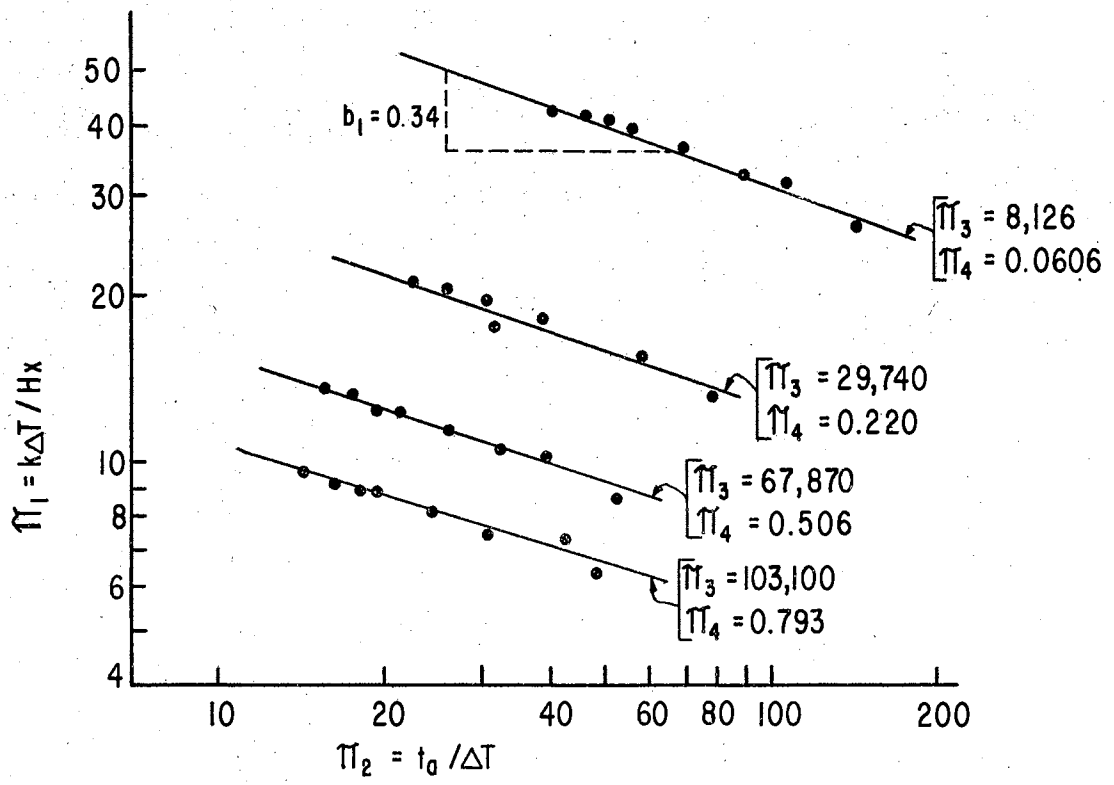

Figure No. 23. Pi-one versus pi-two for four values of x with wind velocity constant.

where b_2 is given by the slope of the line. A plot of the values of $\Pi_1 / \Pi_2^{b_1} \Pi_3^{b_2}$ versus Π_4 values yields the variation with Π_4. This gives a final value for K and the exponent b_3 as shown in Figure 25.

A complete prediction equation for the model behavior is then

$$\Pi_1 = 0.228 \ \Pi_2^{-0.34} \ \Pi_3^{-0.40} \ \Pi_4^{-0.65}$$

which correctly represents the model system for this roof treatment.

The inadequacy of the model observations for predicting

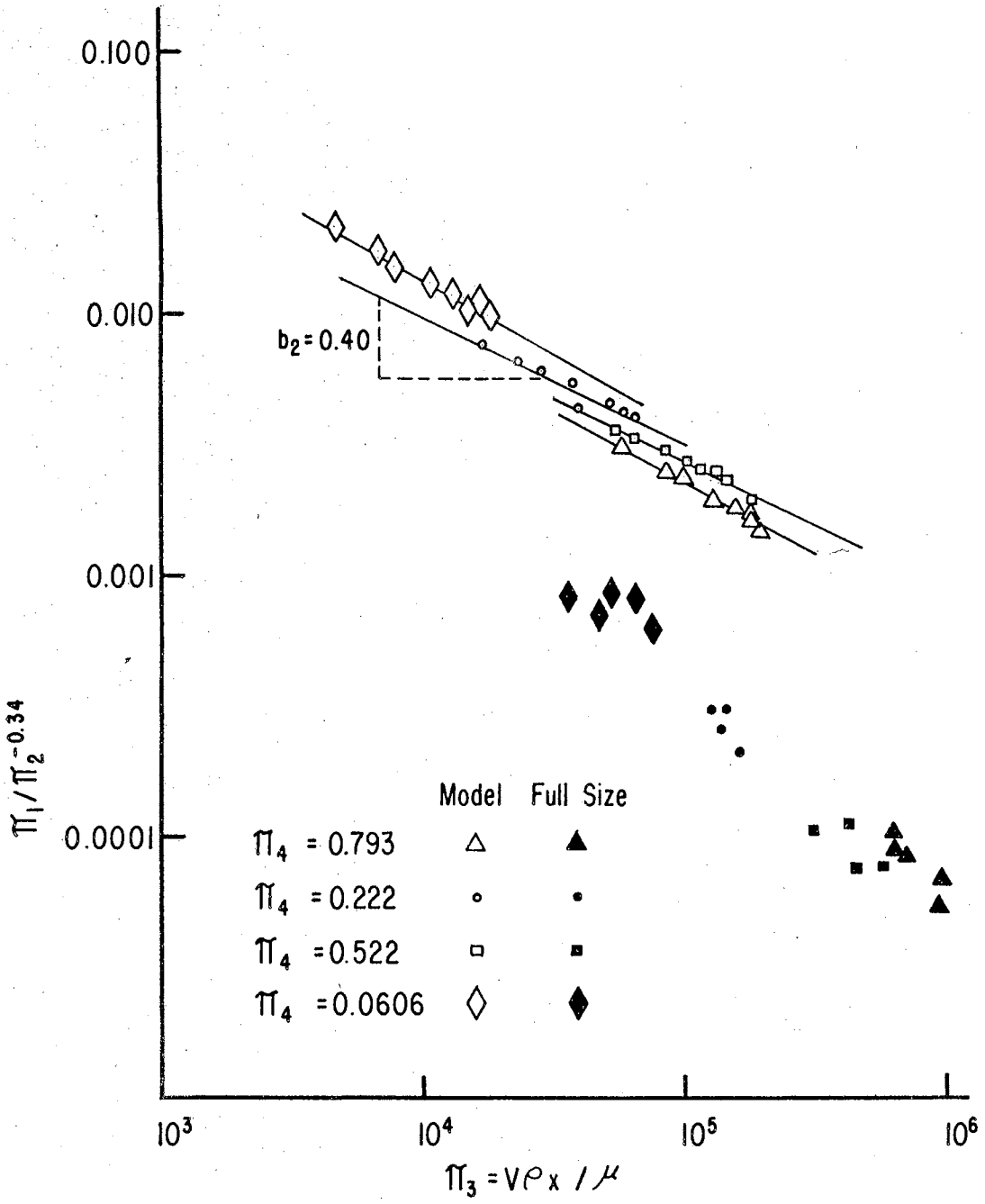

Figure No. 24. Plot for determining b_2. Test conditions were intensity of radiation constant and wind velocity varying. Pi-four = x/L.

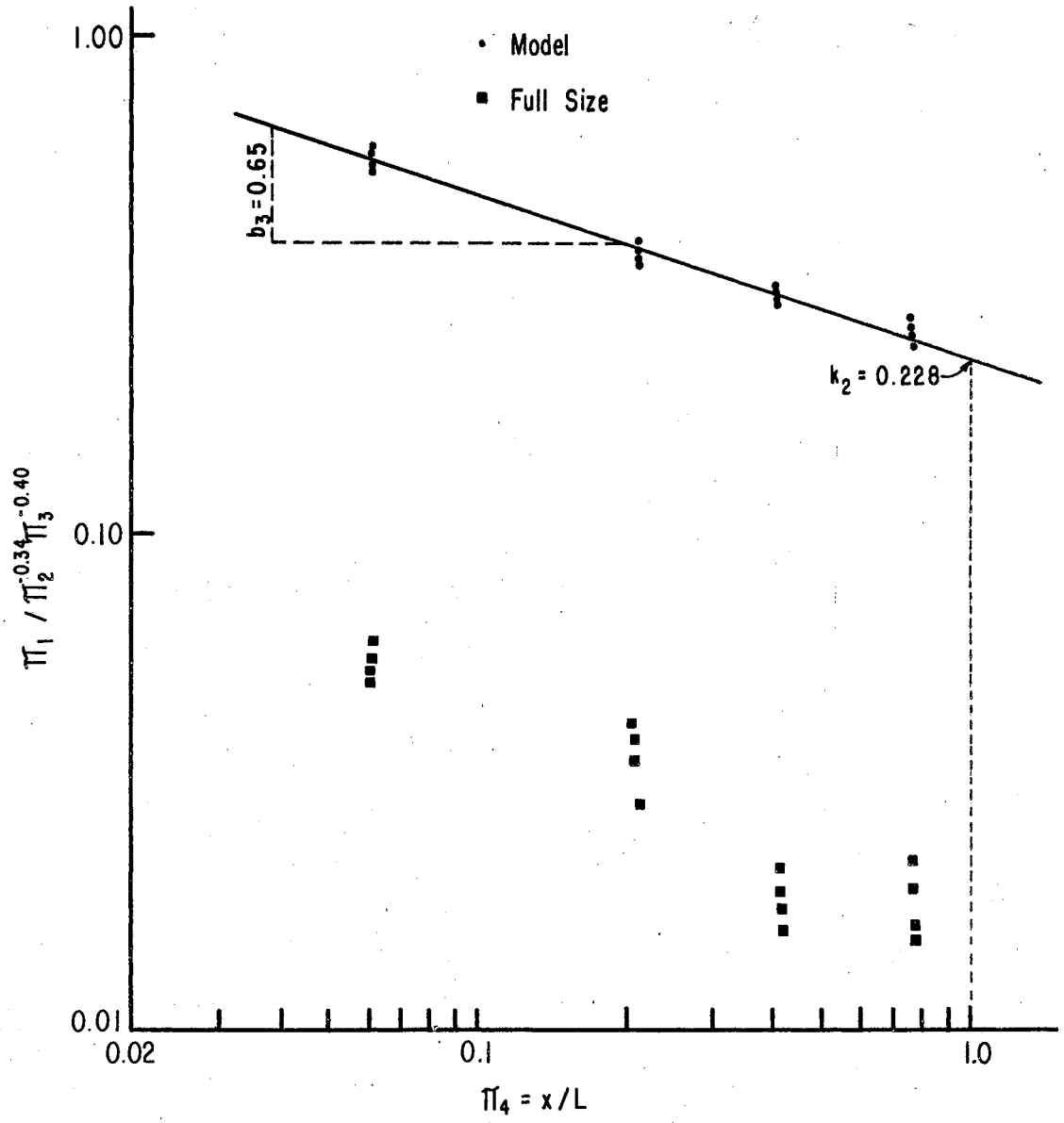

Figure No. 25. Plot for determining b_3 and K_2.

full size shelter behavior is shown in Figure 25 where a few values from the full size system were plotted along with the model data. For corresponding values of $\pi_4 = x/L$ in the two systems the prototype points should fall on the lines representing model data of the prediction relation developed from the model system if the model prediction would correctly define the prototype behavior. A discrepancy is evident.

Since the comparisons were not in the same range of magnitude of π_2 and π_3 one could suspect that the extrapolation of the prediction equation for the model system is unreliable for use with the values of π_2 and π_3 encountered in the full size system. Graphic techniques for curve fitting define the fit over the range of values encountered, giving no strength to any procedure for extrapolations.

Based on the evidence of the data presented thus far three conclusions might be drawn. The first is that the model system altogether fails to simulate the full size system. This conclusion would be premature based on this preliminary analysis. A second conclusion might be that the chosen equation form while adequate to fit the model data is just a simplification of a more general equation which would accurately describe the response of both systems. This is a situation always encountered in curve fitting analysis. A curve fit over a given range of values might be only an approximation to a higher order fit which would be required for a larger range in variation of the independent variables. Thirdly, the discrepancy might be due to the selected dimensionless parameters. There is evidence to

support this third conclusion.

In the model system the quantities H, V, and x were varied. Quantities that were constant were air properties, geometric lengths and material properties. In the full size system these same variations occurred. With little changes in air properties in either system the quantity most likely suspect in the first four pi terms was length of roof, L. In the model system with L equal to a constant value for the entire set of model observations, the behavior of the system was well defined by the equation form. When applied to the full size system with a much larger value of L there was no agreement.

The most elegant means of evaluating the effect of L would be to have it as a running variable. This could have been accomplished by using several systems with different roof lengths but equivalent in all dimensionless parameters. The suspicion that roof length has pertinent influence on the convective cooling of the shelter led to the plans to investigate the thermal behavior of the intermediate size shelter as described in the preceding chapter.

Re-Definition of Pi-Four

After observations were made on the intermediate size shelter new data were available on the response of the systems to the combined radiant heating and convective cooling. The intermediate shelter height was not in exact correspondence with the model and full size systems but the effect of gross shelter size and shelter roof height was assumed to be small

in comparison to effects measured in the first four pi terms.

Because of the definite, consistent response in the model system to changes in the independent variables the equation developed for the model system was applied to observations in the intermediate size system with the results shown in Figure 26. The ordinate $\pi_1/\pi_2^{-0.34}$ used as determined from model data, when used for intermediate size and full size systems implies that -0.34 is the correct exponent for them. The plotting of $\pi_1/\pi_2^{b_1}$ versus π_3 for all systems gives a decisive response for the model system, but nothing is learned from the intermediate and full size system points because for a given π_4 value, π_3 did not vary over a range large enough to establish a trend for the system. Only a scatter of points was evident. Again assuming that -0.34 is the correct exponent for all systems the lack of fit is attributed to the inadequacy of π_4 as a position parameter.

An alternative in line with dimensional reasoning is to find a new group of quantities chosen from the list of pertinent quantities which is to replace x/L with a parameter which defines the location of a temperature observation. In all three systems the thickness of the metal, t, was the same throughout the experimentation. Formation of a parameter x/t gives x as a running variable which defines the location of the point of temperature measurement.

Using the parameter x/t in place of x/L the variable $\pi_1/\pi_2^{b_1}\ \pi_3^{b_2}$ was plotted against x/t for data from the three systems as shown in Figure 27. Now it appears evident

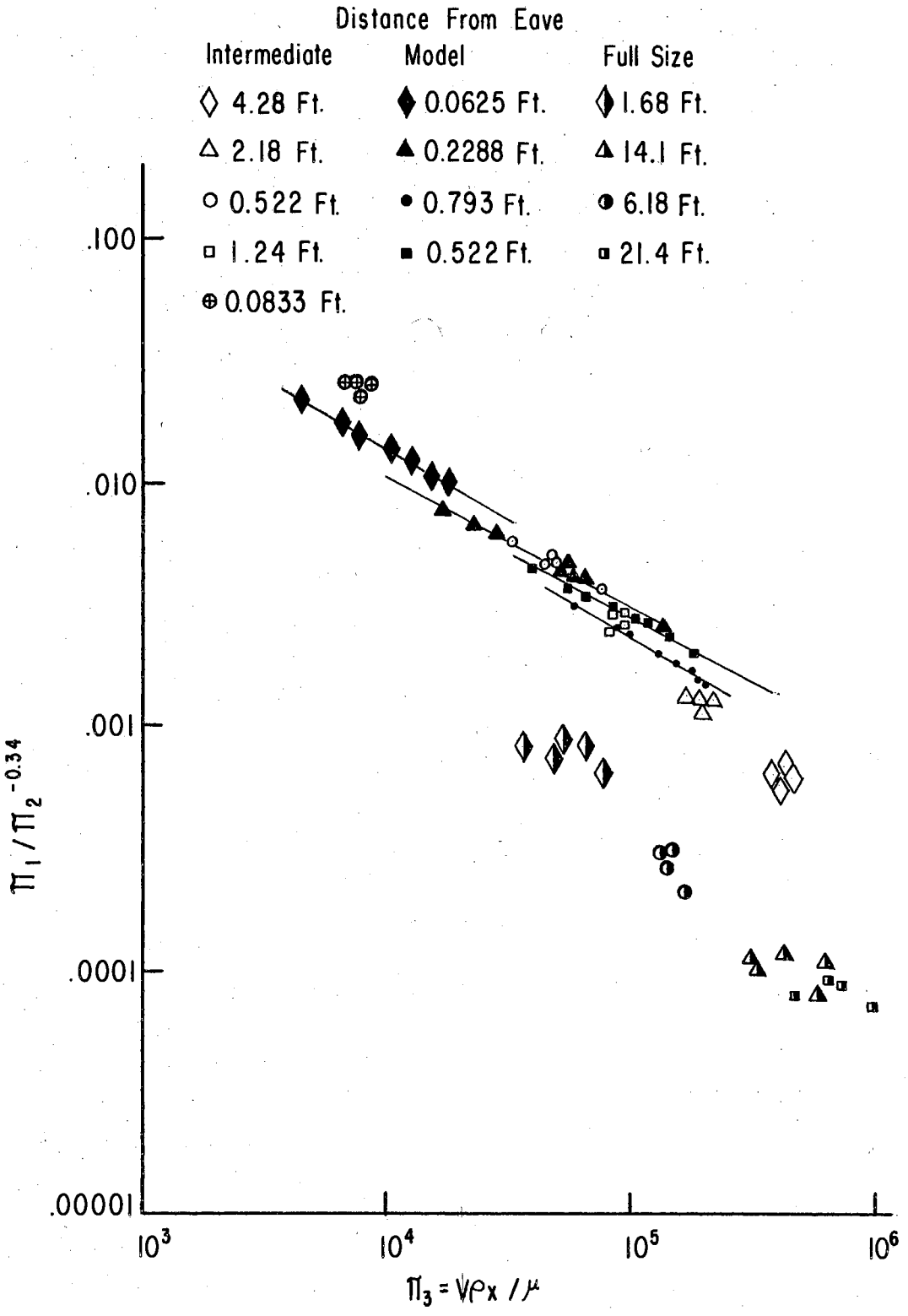

Figure No. 26. Prediction equation plot for three test shelters. Note effect of distance from eave edge on relative height of points.

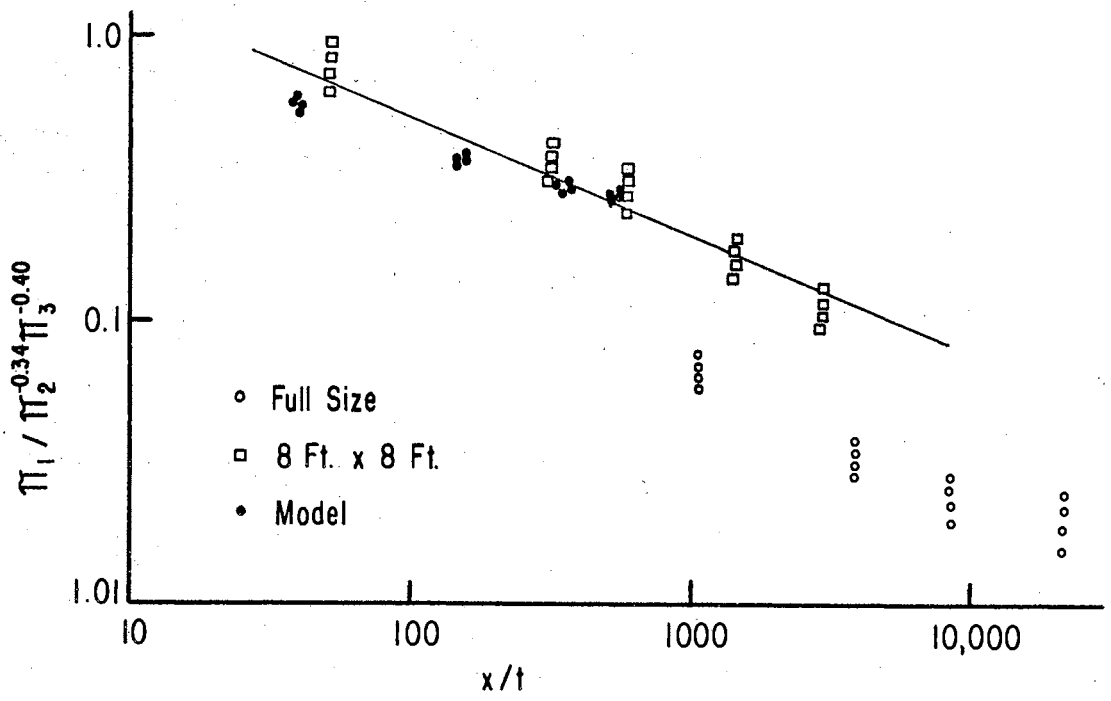

Figure No. 27. Response to variable $\pi_4 = x/t$ for the model, intermediate (8 ft x 8 ft), and full size shelters.

that a parameter which specified point location in ratio to roof thickness gives a variable by which the behavior of at least the model and intermediate size shelter systems can be expressed in an equation of the form

$$\pi_1 = K \ \pi_2^{b_1} \ \pi_3^{b_2} \ \pi_4^{b_3} \qquad (1)$$

where π_4 now has the components x/t. The full size system points still do not coincide with points in the other two systems.

The prediction equation form was found by a systematic

method of determining the effect of one variable at a time on the dependent variable. The exponent b_1 was derived from the model system where a control on π_3 and π_4 could be effected. Exponent b_2 was derived from the controlled model system where observations of π_1 and π_2 were taken with π_3 varying. A plot of $\pi_1 / \pi_2^{b_1} \pi_3^{b_2}$ versus $\pi_4 = x/t$ gave the value of K and b_3.

With agreement at least between model and intermediate size shelter behavior based on this rough graphical procedure alone, it was concluded that the equation form (1) was adequate to correlate the variables. Several other equation forms were tried and abandoned when they were found to be inferior to equation (1) for producing any consistent plots of pi term variations.

The Statistical Model

The equation form obtained in the preliminary analysis offered good evidence of an appropriate statistical model for analyzing the general physical system from which the three systems were thought to be samples. A combination by products of parameters was palatable from the viewpoint of dimensional reasoning, since the parameters being linearly independent they would be thought to be independent in effect and to exhibit no interaction in effect on the response of the system. The equation form (1) is the simplest form which seemed adequate to describe the phenomena.

For exponential relations a logarithmic transformation

eases mathematical operations. Let the logarithm of the pi terms be defined as follows:

$$\text{Log}_{10}\ \pi_1 = Y \qquad \text{Log}_{10}\ \pi_2 = X$$

$$\text{Log}_{10}\ K = b_o \qquad \text{Log}_{10}\ \pi_3 = Z$$

$$\text{Log}_{10}\ \pi_4 = S$$

The exponential form of equation (1) now is expressed in a linear form. In the new notation,

$$Y = b_o + b_1 X + b_2 Z + b_3 S$$

is the statistical model to which the data were fitted. With observed values of Y, Z, X, S, the coefficients b_o, b_1, b_2, and b_3 were to be estimated. A multiple regression analysis was immediately applicable to the problem of finding the coefficients.

Computational Procedure

Faced with the laborious task of having to repeatedly compute the dimensionless parameters from the measurements of the component physical quantities made in the investigation, the possibility of arranging the data in systematic form for utilizing the electronic computer belonging to the university's Computing Center became obvious. Via a computational program the dimensionless parameters and their logarithms could be rapidly computed and subjected to a regression analysis by feeding back to the computer the values of Y, X, Z, and S, with a regression program.

The raw experimental data were organized in tabular,

systematic form for placement on cards. A card was punched for every observation of surface temperature and the corresponding value of air temperature, wind velocity, radiation intensity, air properties, distance of roof to point, roof thickness, and an indentification number. These cards were called the raw data cards since they contained the actual raw data as obtained in the experiments.

A special computational program was written by computing center personnel to compute the values of π_1, π_2, π_3, and π_4, and Y, X, Z, and S from the raw data. For each raw data card two output cards were obtained, one with the π_1, π_2, π_3 and π_4 values and the other with Y, X, Z, and S corresponding the raw data values.

All the experimental data obtained from the model shelter, intermediate shelter, and full size shelter were put on cards. The computational program and raw data cards were read into the IBM 650 Computer which calculated the pi terms and their logs. Appendix B contains a tabulation of the values of π_1, π_2, π_3, and π_4 for the entire investigation. In the model experiments observation of the temperatures on the leeward and windward roof were made simultaneously, although the data listing in the appendix contains the pi terms values for the leeward roof separate from the windward roof.

Multiple Regression Analysis

A response surface described by an equation form

$$Y = b_o + b_1 X + b_2 Z + b_3 S$$

could be subjected to a statistical analysis and then

fitted to the observational values by a least square method which minimized the sums of squares of deviations of the observed values of the independent variables from the response surface.

With the experimental data all on punched cards and the values Y, X, Z, and S for each observation made during the experiments on cards, the standard COR IV program was used to compute sums of squares and cross products, sums, and standard deviations. By reading into the computer the COR IV program and a deck of data cards (values of Y, X, Z, and S) the computer made the calculation of the regression quantities for the set of observations. The output of the analysis was put on punched cards, making use of a matrix inversion program applicable to solve for the regression coefficients directly from the COR IV output cards. With this procedure a regression analysis on, say, 128 observations of the four variables could be completed in about three minutes.

Prior to the regression analysis the data cards were grouped into decks for easy identification. For one treatment of the model roof, decks were formed one for the windward roof for the run with wind velocity constant, a similar deck for the leeward roof, a deck for windward roof with radiation intensity constant, and a similar deck for the leeward roof. With 64 cards in a group, 128 cards per treatment per roof side were decked for use with the COR IV program. A combination of decks read into the computer could be used to find regression estimates based on any combined groups of data.

CHAPTER VI

RESULTS

Range of Variation in the Three Shelter Systems

The range of values encountered in the investigation of the dimensionless parameters was not equal in the three test systems. In the model system radiation intensity was varied from about 6.0 to 13.0 Btu/min-ft^2, providing a means of varying π_1 readily for any set conditions of the other variables. For the other two shelter systems H was always in the range 6 to 8 Btu/min-ft^2, typical of the hot summer sun. The control of H produced a wide range of variations in $\pi_2 = t_a/\Delta t$ for the model system. Air temperature t_a, changed but little. As shown in Figure 28, π_2 varied from 10 to 500 in the model tests, and 10 to 30 in the intermediate shelter system, and 10 to 100 in the full size system. Reynolds number π_3 being inflated by large x values for the full size system varied from 50 x 10^3 to 1000 x 10^3 and from 10 x 10^3 to 600 x 10^3 for the intermediate size shelter. In the model system the small x values were offset somewhat by large wind velocity values. In the model system Reynolds number fell in the range 5 x 10^3 to 300 x 10^3. There was more overlap for π_3 than for the other dimensionless groups.

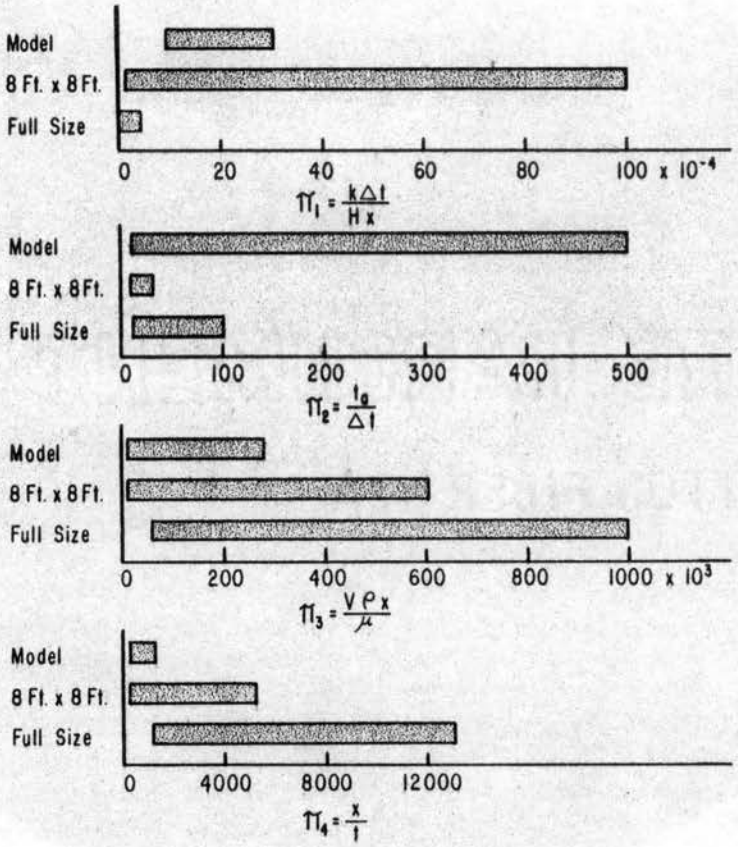

Figure No. 28. Range of values for which observations of the pertinent quantities were made for the model, intermediate (8 ft x 8 ft) and full size shelter systems.

For π_4 = x/t there was overlap only in values for model and intermediate size shelter systems; the x/t values in the full size shelter system were all larger than any x/t value in the model. With roof thickness t = 0.00157 ft for all systems, π_4 varied directly as x for each.

The range of values of π_2, π_3, and π_4 presented in Figure 28 produced values of π_1 different in each system as shown in the figure.

This presentation of the range of variation encountered

in the three test systems precedes the discussion of the equation fitting since recognition must be given to the range of values over which the variables were observed and over which equations were fitted.

Regression Estimates for the Windward Roof Model System

The first analyses completed were the multiple regressions for finding b_o, b_1, b_2, and b_3 for the windward roof of the model shelter for each of the eight shelter treatments. There were 128 observations of the pertinent quantities on each roof side for each treatment. Table VII contains a tabulation of the eight sets of coefficients obtained from the regression analyses. A separate program known as the Dolittle Program was used to compute the multiple correlation coefficient R^2 for each treatment analysis. The multiple correlation coefficient is a measure of the fraction of the variation in the dependent variable accounted for by the regression equation for the chosen independent variables. A high value of R^2, $(0 \leq R^2 \leq 1)$, is good indication that no other independent variables are necessary to account for variation in the dependent variable. In a surface fitting problem R^2 is an indication of the closeness of fit of the response surface to the experimental data.

For any treatment the equation gives the estimate of the dependent variable Y over the experimental range of values of the independent variables. The high R^2 values indicate that the

TABLE VII

COEFFICIENTS AND EXPONENTS FROM REGRESSION ANALYSES FOR THE WINDWARD MODEL ROOF

Treatment[1] No.	K	b_1	b_2	b_3	Number of Observations	Multiple Correlation Coefficient, R^2
		(Model Shelter)				
1	2.883	-0.5526	-0.3859	-0.4203	128	0.995
2	3.301	-0.3559	-0.5000	-0.2210	128	0.997
3	0.122	-0.2565	-0.4931	-0.1604	128	0.992
4	2.226	-0.3500	-0.4226	-0.3037	128	0.997
5	3.291	-0.3479	-0.5071	-0.2130	128	0.995
6	4.037	-0.3701	-0.5178	-0.2167	128	0.982
7	2.648	-0.3230	-0.4880	-0.2291	128	0.998
8	2.276	-0.2854	-0.4910	-0.2053	128	0.994

Note: 1. Treatment schedule defined in Table IV.
2. Values of K, b_1, b_2, and b_3 apply to equation (1).

coefficients obtained from the multiple regression analyses are adequate for use in the basic functional equation to predict system behavior for the range of variations encountered.

Windward Roof Model Behavior

As shown in Table VII each model shelter treatment is characterized by a coefficient and three exponents for the equation form

$$k\Delta t/Hx = K(t_a/\Delta t)^{b1}(V\rho x/\mu)^{b2}(x/t)^{b3}. \qquad (1)$$

It is expedient to compare these values to inclined plate studies found in the literature. For the windward roof the exponents for π_4, the temperature position parameter, were generally in the range 0.160 to 0.420. Drake (11) found that the heat transfer rate from an inclined plate expressed in a Nusselt number varied as distance from leading edge to the 0.652 power at 0 angle of incidence to 1.025 to 90 degrees incidence. Drake found a dependence of Nusselt number on Reynolds number (based on plate length) of 0.50. It should be noted that Drake's values represent a laminar flow boundary layer. For the present investigation the exponent of Reynold's number based on distance from leading edge is near 0.50 for all test runs for the model windward roof. This equivalence in exponents offers some evidence of laminar heat transfer from the windward model roof side. Convection theory has lead to a 1/2 power of Reynolds power for laminar boundary heat transfer.

It was possible that the roof surface near the leading edge was in a laminar region but near the ridge was sometimes

in a turbulent region. With the regression estimates based on all points along the roof the exponents are the estimates which fit the whole of the measurements on the roof side.

With a corrugated leading edge and a turbulent wind stream the occurence of transition would be expected at a relatively low value of Reynolds number. The bulk of the model experimental observations were made at Reynolds number less than 10^5.

In comparison to Drake's results there is equivalence of exponents for Reynolds number but for the roof system the dependence on a position parameter π_4, is characterized by exponents from 0.160 to 0.420 in comparison to Drake's values of 0.652 to 1.025.

Because no velocity or temperature measurements were made in the boundary layer only the value of the exponents in comparison to other heat transfer studies can be utilized to ascertain the probably characteristic boundary layer behavior for the windward roof system.

Rearrangement of the Prediction Equation Form

The prediction equation form (1) can be rearranged to give Δt as an explicit function of the other quantities. The high multiple correlation coefficients obtained in the regression analyses offer strong evidence that the chosen equation form is a valid one. By algebraic manipulation equation (1) can be put in the explicit form

$$\Delta t = K^{(1/b_1+1)}(Hx/k)^{(1/b_1+1)}(t_a)^{(b_1/b_1+1)} (V\rho x/\mu)^{(b_2/b_1+1)}(x/t)^{(b_3/b_1+1)} \qquad (2)$$

For Model Treatment No. 1 the experimentally observed values of Δt were plotted against Δt predicted by equation (2) using K and b values for the treatment. Figure 29 shows that the prediction form fits the data within close limits. This plot gives a visual demonstration of the adequacy of the equation and a check on computational errors.

Dependence of Temperature Rise on Pertinent Quantities

The rate of change of Δt as predicted by the equation for changes in wind velocity, radiation intensity, and distance up roof slope is of interest. The values of the exponent for the components of the right side of equation (1) are given in Table VII. Since radiation intensity appears in only one group the term $(1/b_1+1)$ is the exponent of H. For any treatment, Δt varies with $H^{(1/b_1+1)}$. With V contained in only one group Δt varies as $V^{(b_2/b_1+1)}$. The quantity x appears in three groups. However, it can be factored out as x to the $(1/b_1+1) + (b_2/b_1+1) + (b_3/b_1+1)$ power. The values of the exponents for x, V, and H for the treatments are listed in Table VIII.

It is seen that Δt did not vary linearly with H. In convection the coefficient $h = q/\Delta t$, where q is rate of heat flow per unit area, is independent of the magnitude of Δt. If convection is equally prevalent for all values of Δt, then the radiative aspects of the roof's thermal behavior has to be considered. The absorption rate of a material is usually higher for long wave radiation than for short wave radiation.

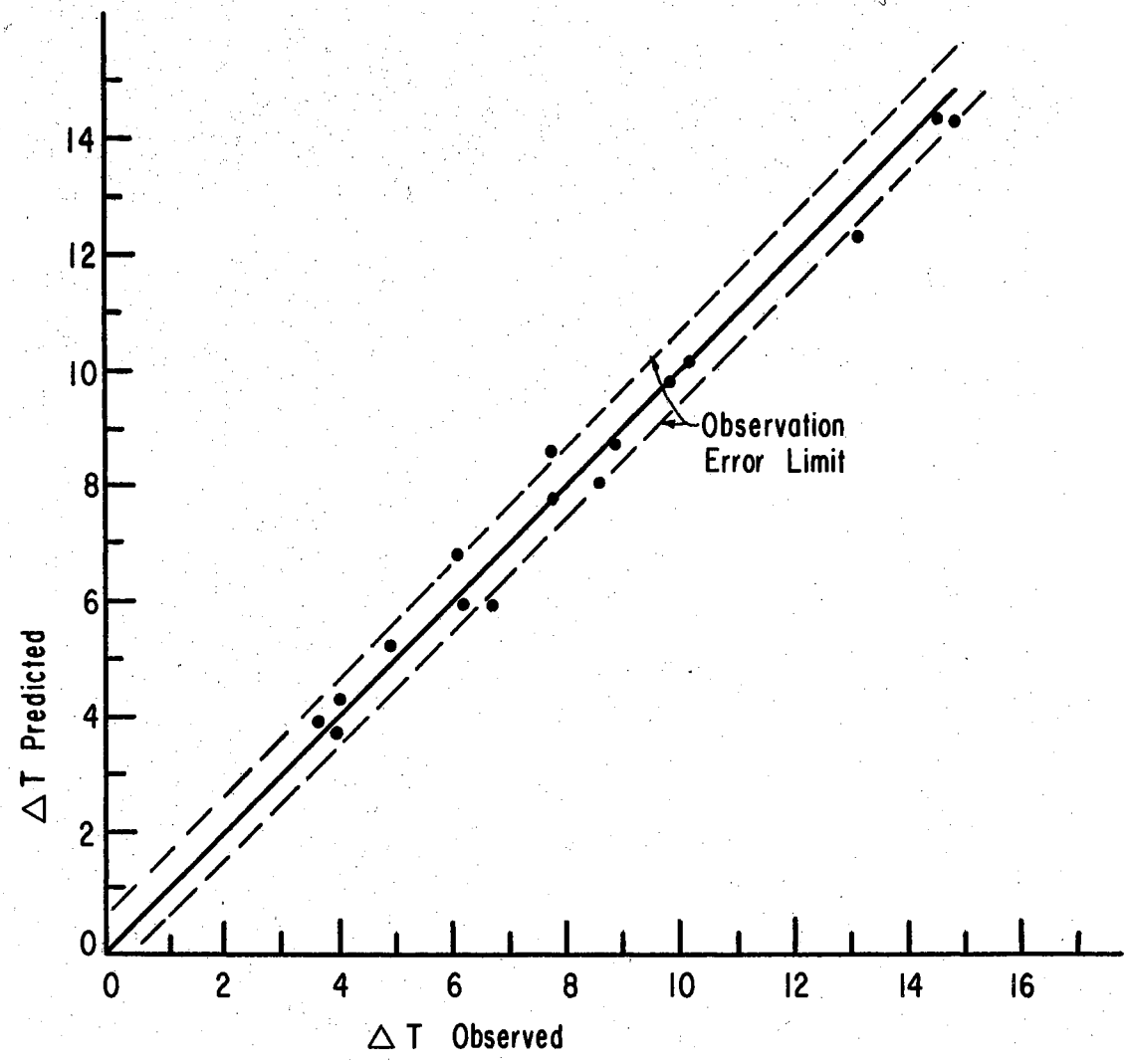

Figure No. 29. Check on prediction equation in factored form. Solid line is line of perfect agreement between a Δt value predicted by solving the equation with particular values of the independent variables and an observed value. Data from Model Treatment No. 1.

TABLE VIII

EXPONENTS FOR QUANTITIES X, V, AND H RESULTING FROM FACTORING PREDICTION EQUATION (2) FOR THE WINDWARD MODEL ROOF

Shelter Treatment No.	Quantity		
	X	V	H
	Exponent		
1	0.4333	-0.8624	2.235
2	0.4332	-0.7763	1.553
3	0.4661	-0.6632	1.345
4	0.4210	-0.6502	1.538
5	0.4292	-0.6632	1.533
6	0.4219	-0.8222	1.588
7	0.4178	-0.7209	1.477
8	0.4294	-0.6864	1.398

Note: Table IV contains shelter treatment schedule.

With voltage control on the heat lamps during the model experiments the radiation at low voltage and resulting low filament temperature was more characteristically long in wavelength compared to radiation at high voltages with higher filament temperatures. If variation in spectral absorption occurred, the value of Δt would be relatively smaller as H increases, for the spectrum of lamp output moves to shorter wavelengths and most materials absorb long wavelength radiation more readily than short wavelengths. This is in contradiction to what actually occurred.

One might suspect that for the exterior surface of an inclined roof the bouyancy of the heated air would promote thermal exchange. On the underside of the roof the effect would be reversed. With warm air in contact with the underside of the roof additional heating of the surface warms the air and decreases its density causing a pocket of warm air to remain under the roof. Mixing with the cool air streaming through the shelter would be inhibited.

Windward Roof Shelter Treatment Effects

Since each prediction equation is characterized by a coefficient and four exponents, differences in response of Δt to shelter size and shape effects can be demonstrated by assigning particular values to all but one independent quantities. Then the response to changes in the one independent quantity can be calculated. Assuming wind velocity = 11 mph, radiation intensity = 450 Btu/hr-ft^2, and 90 F air

temperature, Figure 30 shows a plot of Δt versus x, distance up roof, for three model roof treatments. These plots were obtained from equation (2) using the proper coefficient and exponents from Table VII.

From the model tests, little if any differences in temperature rise are noted for changes in roof slope angle in the range 3/12 to 5/12. In terms of the behavior of an actual shelter structure, the angle of incidence of direct solar irradiation at midday is affected by the slope angle of the roof.

A comparison of the response for the three surface texture treatment graphs in Figure 31 indicates corrugation size has little influence on the heat transfer to the air stream. Except for disturbances at the eave edge, wind flow parallel to corrugation direction is probably not influenced to a significant degree by presence or lack of corrugations. Perhaps with wind flow across the corrugations, thermal exchange would be influenced by corrugation configuration.

Figure 32 shows a plot of temperature rise versus distance up roof for the three kinds of materials used in the model tests. These graphs were made from solutions to the regression equation for each material. Galvanized roofing is the warmest followed by white-painted steel and then aluminum. In other studies reported in the literature, aluminum usually had a larger temperature rise than bright, white-painted roof specimens. There was evidence that the model white samples used for this study were not representative of the usual condition of a

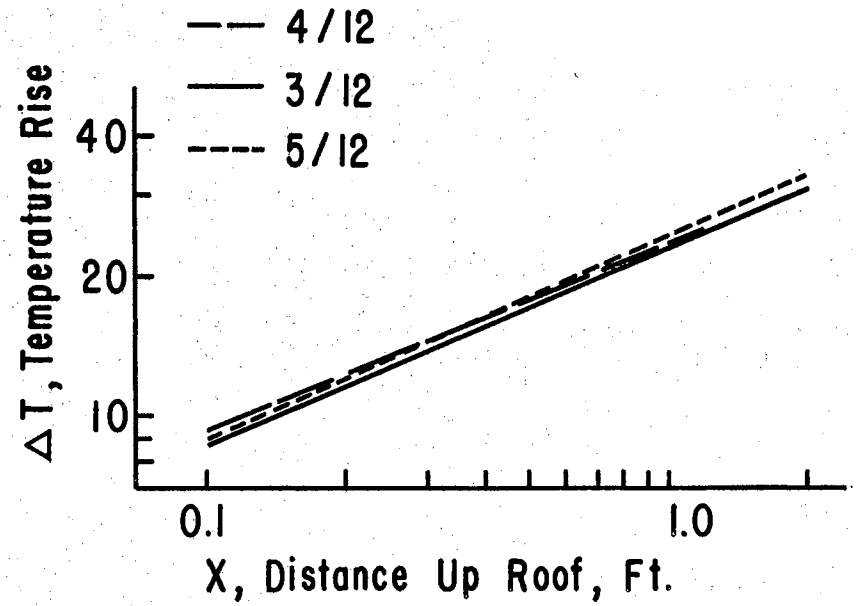

Figure No. 30. Temperature rise for three roof slope angles. Model comparisons with plain galvanized roof treatments. Conditions: V=1000 ft/min, H=75 Btu/min-ft^2, Small Corr. h=0.26 L t_a=550R, ρ=0.075 lbs/ft^3.

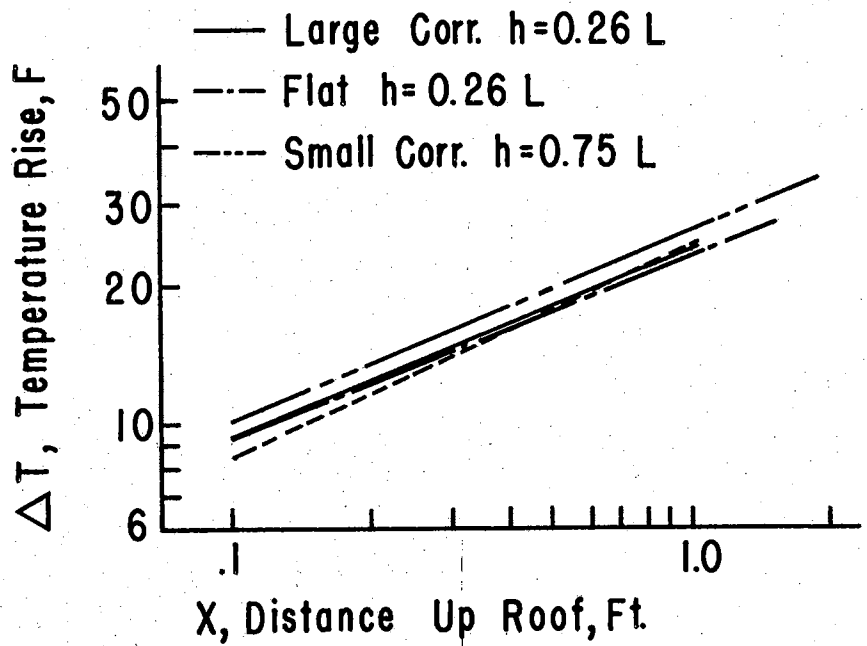

Figure No. 31. Comparison of three surface textures and two roof heights. Texture comparison made at height h=0.264L. Conditions: Same as Figure 30.

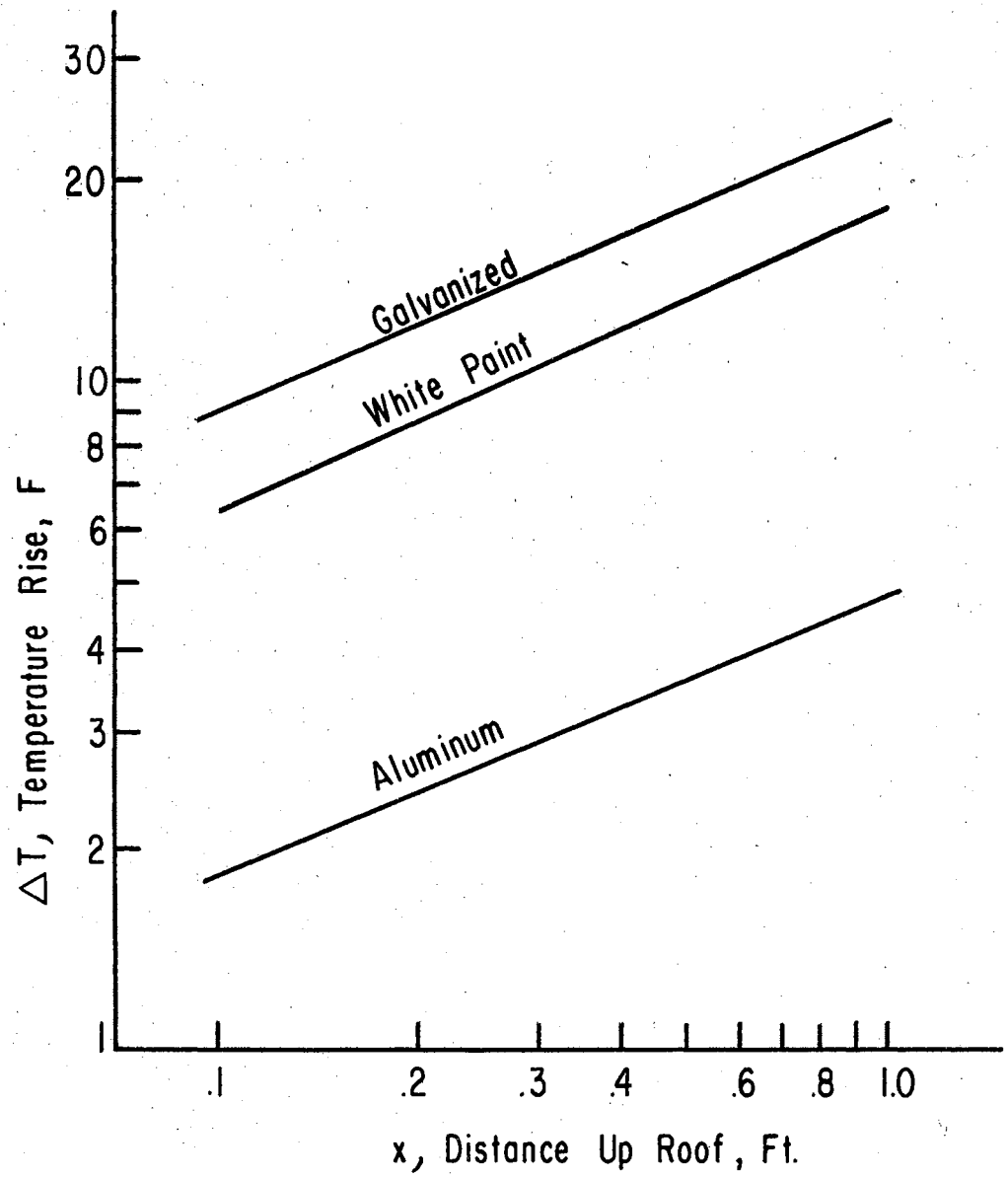

Figure No. 32. Temperature rise for three kinds of roofing used on the model. Curves are plots of regression equation for each material. Conditions: V=1000 ft/min, H=7.5 Btu/min ft^2, t_a=550R, ρ=0.075 lbs/ft^3.

white-painted galvanized steel prototype roof. When the paint was applied to the scaled-down corrugations the paint flowed into the valleys and left the corrugation ridges somewhat bare. Two light coats had been applied but the flat white surface noticable on the full size shelter roof was not achieved.

Further evidence of the apparent non-representative confitions of the painted sample is given in Figure 34 where the temperature rise of the three kinds of material are shown for the full size shelter system. For compatible conditions of radiative heating and wind cooling galvanized roofing is about 17 F warmer than aluminum and 20 F warmer than white-painted roofing. The galvanized roofing curve for the model data, Figure 32, averages about 17 F above the aluminum curve, but only 4 F above the white paint response curve. With agreement in galvanized-aluminum separation, the discrepancy appears to be in white paint results. A poor paint covering on oxidized galvanized steel would display high absorption properties. The white paint results for the model roof point out the importance of thorough paint coverage for reflecting incident solar radiation.

Shelter roof eave height had a small influence on thermal behavior. The model treatment with h = 0.75L experienced a larger temperature rise than the ones with h = 0.264L as shown in Figure 31. The intermediate size shelter with h = 0.75L produced similar results. Wind velocity was measured at eave height in the experiments. These height effect comparisons are made at equal wind velocity values. In an actual shelter,

higher roofs are in a zone of higher wind velocity which enhances cooling significantly.

It is of interest to investigate how the thermal behavior of an inclined surface changes with magnitude of incident radiation. Table VIII contains the exponents for the quantity H which show that incident radiation has strong influence on temperature rise.

In review, small differences due to slope angle and corrugation size were noted. Wind velocity, intensity of incoming radiation, and absorption properties of the roof material stand out as the major variables affecting the temperature rise of the windward roof.

Model Operation at Low Air Temperature

During the experimentation an auxiliary set of observations was taken for Treatment No. 8 with air temperature at a value lower than for the usual test runs. The objective was to measure the thermal behavior of the system with a lower value of air temperature than for the other runs. For the low temperature run the laboratory windows were opened on a winter day when air temperature outside was near 40 F. The air in the wind tunnel was thus held near to 42 to 45 F for the run. Measurement of wind velocity, incident radiation, etc., were taken as for the usual test runs. Observed values of the dimensionless parameters for the low air temperature run are listed in Appendix B with the other data.

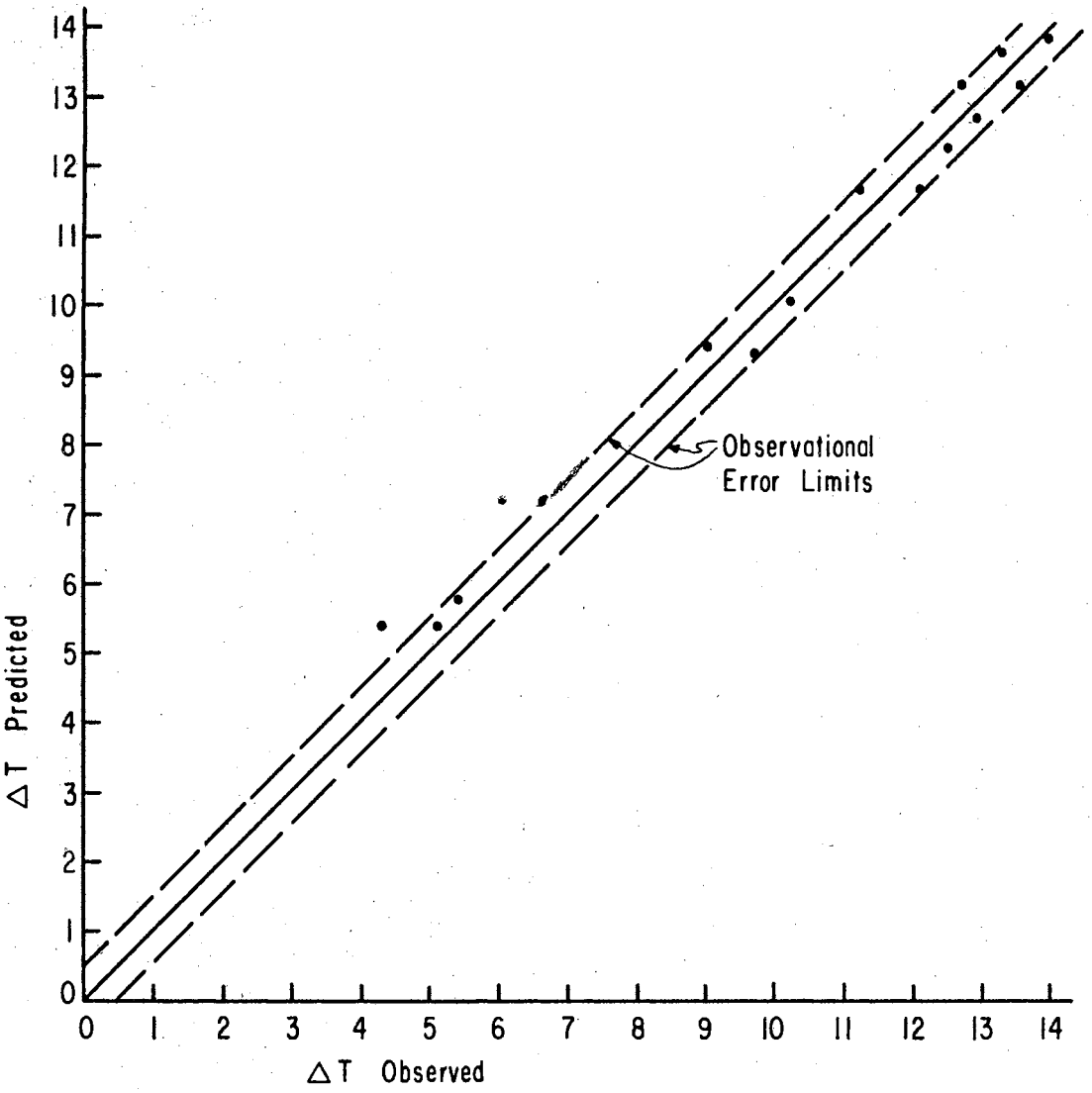

Figure No. 33. Predicted temperature rise at low air temperature. Prediction equation developed from runs with air temperature of 70 F is applied to observations of the variables at an air temperature of 42 F. Model Treatment No. 8.

The prediction equation derived from the observations with air temperature near 70 F was then applied to the observations made at the 42 F run. Figure 33 shows a plot of predicted versus observed values of Δt. A predicted value of Δt was obtained from equation (2) using the value of K, b_1, b_2, and b_3 obtained for the Treatment No. 8 model data. Good agreement between predicted and observed values offers evidence that air temperature is properly included in the equation. In absolute values 70 F = 530 abs, 42 F = 502 abs with a 5.3% difference in absolute value. With temperatures up to 98 F experienced during the full size shelter observations at least the range of air temperature likely to be encountered in actual shelter use was covered. There was a possible error in any Δt measurement of approximately 1 F. The validity of the dimensionless arrangement for adequate predictions is not known for values of t_a outside the range encountered in the experiments.

Regression Estimates for the Leeward Roof Model System

Observations of the temperature rise on the leeward roof provided information for the behavior of the leeward roof. Table IX gives the regression coefficients for the eight treatments for leeward roof observations. For the leeward roof the temperature rise over the roof length was found to correlate with the same dimensionless parameters as the windward roof so that the same statistical model was used for the

TABLE IX

COEFFICIENTS AND EXPONENTS OBTAINED FROM REGRESSION ANALYSES FOR THE LEEWARD MODEL ROOF

Shelter Treatment No.	K	b_1	b_2	b_3	Multiple Correlation Coefficient, R^2
1	4.007	-0.5947	-0.3409	-0.5252	0.995
2	5.774	-0.3725	-0.4671	-0.3686	0.994
3	2.909	-0.2524	-0.5190	-0.2547	0.989
4	3.333	-0.3638	-0.3880	-0.4245	0.995
5	5.709	-0.3615	-0.5133	-0.2777	0.993
6	6.209	-0.2671	-0.5464	-0.2954	0.999
7	5.548	-0.3273	-0.5204	-0.2896	0.995
8	4.952	-0.3085	-0.5145	-0.2755	0.995

Note: 1. Table IV contains the shelter treatment schedule.
2. Each treatment regression analysis based on 128 observations of the component quantities.

leeward roof data. As shown in Table IX the multiple correlation coefficients for leeward roof treatments are equally high as for windward roof, giving confidence to the selection of the same equation form for both roof sides. Figure 28 gave the general range of values of the variables for the model roof observations. The range for both roof sides was the same for π_3 and π_4 because they are formed from the same quantities. And for π_1, and π_2 the range encountered in the experimentation was nearly equal.

Behavior of the Model Leeward Roof

The eight roof treatments provided information on the thermal response of the leeward roof as well as the windward. For the leeward roof the quantity x is defined as the distance up roof slope from leeward eave edge. Radiation intensity is the magnitude of incident radiation on the leeward roof. In the experiments, the intensity of radiation was approximately equal on both roof sides, and produced conditions representative of a hot midday sun.

Table IX gives the exponents for Reynolds number, b_2, ranging from 0.3409 for Treatment No. 1 to 0.5464 for Treatment No. 6. With the leeward roof in a sheltered wake region the possibility noneddying flow on the leeward side of the roof was small.

It is interesting to note that the coefficients and exponents for the leeward roof are strikingly similar to those for the windward roof. Based on magnitude of exponents alone,

there is apparent evidence of a laminar flow condition for the leeward roof as exemplified by the nearness to the 0.50 power for Reynolds number characteristic of laminar transfer in the boundary layer. Table X contains the exponents for x, V, H which result from factoring equation (2) for individual quantities.

In all model tests the temperature rise of the leeward roof was smallest near the eave and largest near the ridge. In wind force studies up flow along leeward roofs are often encountered. Upflow for the present model study may have occurred as evidenced by the observed temperature variation on the leeward roof.

Table XI gives particular solutions to the regression equations for the leeward roof treatments. Small differences due to slope angle and texture are evident (treatments 1 to 7) and a small height influence (treatment 8 compared to 2). Aluminum was cooler than white-painted steel as for the windward roof.

Regression Estimates for the Intermediate Size Shelter and Full Size Shelter

With 160 observations of the pertinent quantities per treatment for the intermediate size shelter system and 96 observations per treatment of the full size shelter an estimate of the regression coefficients was obtained by using the same regression analysis for these systems as for the model.

The results of the analysis are given in Table XII. No

TABLE X

EXPONENTS FOR QUANTITIES X, V, AND H RESULTING FROM FACTORING PREDICTION EQUATION (2) FOR THE LEEWARD MODEL ROOF

Shelter Treatment No.	Quantity		
	X	V	H
	Exponent		
1	0.3307	-0.8412	2.467
2	0.2946	-0.7444	1.593
3	0.3027	-0.6943	1.338
4	0.2947	-0.6099	1.572
5	0.3272	-0.8041	1.566
6	0.2518	-0.7456	1.364
7	0.2824	-0.7735	1.486
8	0.3037	-0.7441	1.446

Note: Table IV contains the treatment schedule.

TABLE XI

LEEWARD ROOF COEFFICIENTS AND EXPONENTS FOR TEMPERATURE RISE AS A FUNCTION OF X, DISTANCE UP ROOF, FOR CONSTANT VALUES OF OTHER QUANTITIES

$$\Delta t = Cx^n$$

CONDITIONS: V = 1000 ft/min, H = 7.5 Btu/min-ft^2, t_a = 90 F, ρ = 0.075 lbs/ft^3.

Shelter Treatment No.	C	n
	Galvanized	
2	21.82	0.302
4	22.81	0.307
5	24.68	0.327
6	21.02	0.2158
7	21.93	0.282
8	25.51	0.304
	Aluminum	
1	4.50	0.331
	White Paint	
3	17.58	0.303

Note 1. These values result from solving equation (2) with the values listed above and exponents for the treatments from Table IX. (See Table IV for treatment schedule.)

2. $n = 1/b_1+1 + b_2/b_1+1 + b_3/b_1+1$.

TABLE XII

COEFFICIENTS AND EXPONENTS OBTAINED FROM REGRESSION ANALYSES FOR INTERMEDIATE AND FULL SIZE SHELTERS

Shelter Treatment No.	K	b_1	b_2	b_3	Number of Observations	Multiple Correlation Coefficient, R^2
			(8 ft x 8 ft Shelter)			
12	12.698	-0.9203	-0.0590	-0.9471	160	0.982
			(48 ft x 48 ft Shelter)			
9	2.529	-0.7278	+0.0245	-0.9673	96	0.994
10	3.770	-0.7568	-0.0023	-0.9705	96	0.995
11	2.826	-0.5980	-0.0328	-0.9188	96	0.994

Note: 1. Shelter treatments are defined in Table IV.
2. K, b_1, b_2, and b_3 apply to equation (1).

explanation was found for the positive value of b_2 for Treatment No. 9 except perhaps the possibility of several surface temperature readings having occurred during a lull in wind movement, causing a instantaneous high Δt reading which was correlated to the three minute time-averaged velocity reading. A review of the temperature measurements revealed no highly inconsistent reading when compared to readings for the galvanized roof and white painted roof treatments adjacent to the aluminum on the roof. A computational check run on the final equation form, equation (2), detected no computational errors.

With air temperature not caused to vary in the course of the experiments in the two systems, little can be concluded about the value of the exponent for π_2. Only small changes in Δt occurred causing little changed in π_2.

Intermediate Size Shelter and Full Size Shelter Behavior

Operating conditions for the intermediate and full size shelter systems were typified by unsteady wind velocity with mean wind velocity and radiation intensity not varying over a large range. With larger roof lengths than in the model, the possible variation in the quantity x was greater for these systems than for the model. Under natural sun and wind conditions no control on the variables H and V could be effected. The range of variations for velocity was approximately 350 to 1150 ft per min for the intermediate shelter and 270 to 489 ft per min in the full size shelter system.

Radiation intensity experienced a change of about 6.0 to 8.5 for both intermediate and full size systems.

The variation of Δt with x is characterized by the exponents listed in Table XIII for the shelter treatments. In most cases temperature increased with x as evidenced by positive exponents. On the intermediate size shelter roof there were three thermocouples in the central portion of the roof which gave lower readings than some nearer the eave edge. Probably a bright, reflecting spot over these couples caused lower absorption of incident radiation at these points. The non-representative values at these points were counteracted by seven other thermocouple junctions where the temperature variation with x was a consistent increase with distance. As the low reading points were high up the roof slope they apparently caused the regression fit to yield the slight negative exponent for x.

In both intermediate size and full size systems, radiation intensity did not vary over a large range of values. Measurements of temperature rise were made in the middle of the day to get large temperature differences more free from measurement error. Little significance can be attached to the exponents for H because radiation intensity varied so little that its variation was almost undistinguishable in the regression analysis. When quantities do not vary over a wide range of values in the course of experiments the exponents resulting from curve fitting (regression analysis in this case) bear little physical significance.

TABLE XIII

EXPONENTS FOR QUANTITIES X, V AND H RESULTING FROM FACTORING PREDICTION EQUATION (2) FOR INTERMEDIATE AND FULL SIZE SHELTERS

Shelter Treatment No.	Quantity		
	X	V	H
	Exponent		
	(Intermediate Shelter)		
12	-0.077	-0.7415	12.55
	(Full Size Shelter)		
9	-0.2099	-0.0898	3.673
11	0.1147	0.0816	2.488
10	0.1120	0.0938	4.111

Note: Table IV contains treatment schedule for full size shelter. Middle size shelter had a flat roof material, 4/12 slope, ratio of eave height to roof length of 0.75.

For the three full size shelter treatments the variations of temperature rise with x is flatter than the model treatment responses as indicated by the exponents in the range 0.112 to 0.209. The thermocouple locations on the shelter roof were at distances up roof slope between x values of 1.5 ft and 25 ft wherein large values of Reynolds number occurred for low wind velocities. In contrast the model temperature measurements were made in a region of x between 0.08 ft and 1 ft and for the middle size shelter in ranges of x values between 0.1 ft and 5 ft. Apparently the roof surface temperature tends to approach a constant value at increasing x values on a windward roof, judging from the flat response.

As shown in Table XIII the change in Δt with wind velocity is small for the two shelter systems. This is quite surprising to find a variation of Δt with wind velocity as low as 0.09 for the full size shelter. In the model system the variations of Δt with V was always in the range 0.6 to 0.9 which was not at variance with other experimental works reviewed. For the intermediate size shelter temperature rise decreased with velocity to the 0.74 power, a value in line with the model behavior.

Returning to Figure 28 where is shown the range of variation of the dimensionless parameters for the test systems, in the full size system the equation fit is for values of π_3 between 10^5 and 10^6. These values were encountered at relatively low velocities due to the large x values. In usual forced convection heat transfer studies for these values of

Reynolds number the flow in the boundary region is turbulent. A turbulent forced convection system is usually typified by a dependence on velocity to the 0.8 power. This is the accepted value for a parallel wind stream with skin friction-produced turbulent transfer. Parmlee and Huebscher (49) pointed out that the heat transfer rate from a plate surface depends on length of the surface.

With an inclined surface, corrugations on the roof, rough leading edge, a gradient and unsteady wind pattern, one would immediately suspect that turbulence occurred over the full size shelter roof. Flat plate experiments have indicated that non-laminar conditions always occur at Reynolds numbers larger than 10^5. Few plate experiments have made use of long plates which give large Reynolds number at low velocities. The slight dependence of surface-air temperature difference on velocity offers evidence that heat transfer rate becomes somewhat unaffected by velocity in regions sufficiently far from the leading edge of the surface. At least this result was substantiated for the windward shelter roof which had three separate observational systems namely, the three roof treatments studied in the full size system. Many heat transfer systems encountered in engineering practice are represented by long surfaces as Parmlee and Huebscher pointed out. Theoretical analysis have substantiated experimental findings for turbulent transfer for R_{ex} up to 10^6 but for greater values there is a scarcity of information. In the full size system mean wind velocity varied over a range 270 to 489 ft per min which was wide enough variation to place

some validity on the velocity effects observed.

For the intermediate shelter the decrease in Δt with velocity to the 0.74 power is indicative that a turbulent flow regime occurred for this roof side.

Treatment Effects for Intermediate and Full Size Shelters

No comparison of roof height, surface texture, or slope effect can be made for the intermediate and full size shelters. However differences due to material absorption and emission represented by the three types of roofing used on the full size shelter can be investigated. These surface treatments were white paint on corrugated steel, commercial aluminum roofing and plain, aged, galvanized steel.

The plotted curves, Figure 34, for the three roof materials represent solutions to the prediction equations fitted to this data for each of the three full size roof covering materials. Constant values were assigned to all variables except x.

Material absorption and emission have a pronounced effect on temperature rise. Under conditions of radiative heating and wind cooling comparative values of the temperature rise for the different materials used on the 48 ft x 48 ft shelter are shown in Figure 34. For an 11 mph wind, incident radiant intensity of 450 Btu/hr-ft^2, and 90° F air temperature, the temperature rise for plain galvanized steel was 30 F, 18 F for aluminum, and 12 F for white-painted steel.

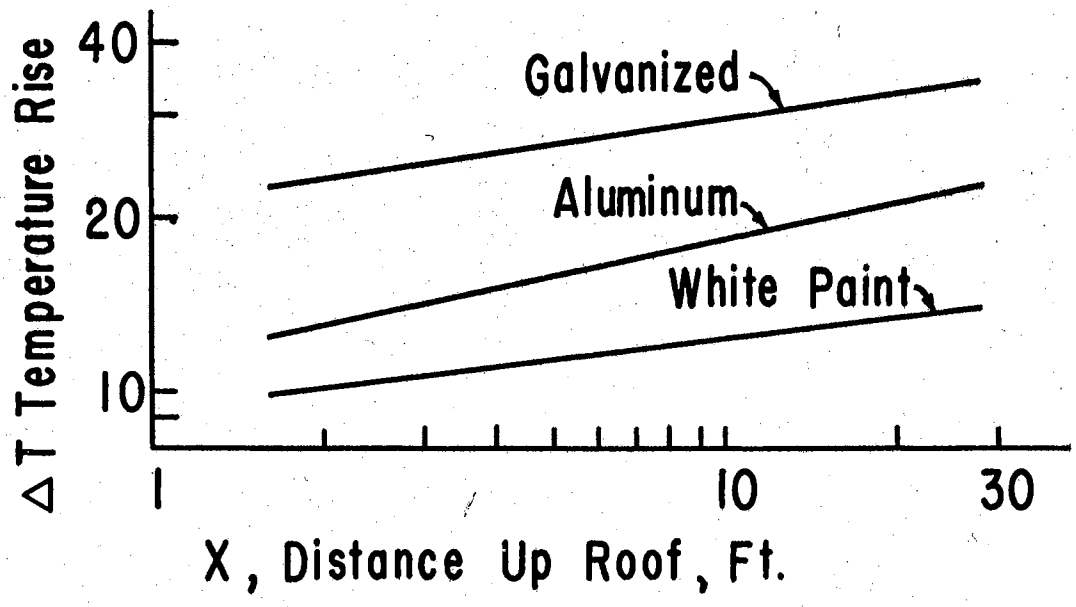

Figure No. 34. Temperature rise for three kinds of roofing on the full size shelter. Curves represent plots of regression equations for specific values of certain quantities as given for Figure 30.

System Compatibility and Similarity

The regression estimates given in preceding sections represent the best fit curves for the experimental observations for a statistical model of the form

$$k\,\Delta t/Hx = K(t_a/\Delta t)^{b1}(V\rho x/\mu)^{b2}(x/t)^{b3}.$$

Treatments in each test system were characterized by values of K, b_1, b_2, and b_3. High correlation coefficients gave confidence to each fit for the particular range of values of the observations for the specific conditions. It remains to be shown to what extent model, intermediate, and full size systems were compatible or similar in behavior.

Compatibility among systems as defined in Chapter II was the requirement that the same set of independent dimensionless groups of quantities necessary for one system be necessary and sufficient to adequately define the action or behavior of the other systems.

For the present study four parameters were considered as the main variables. Five additional parameters designated configuration and roof materials properties. For the chosen dimensionless groups designating configuration and material properties, π_5 to π_9, similarity or equality was established for these five groups by geometrical scaling and material selection for model and full size systems.

The multiple regression analyses give one test of compatitility. In each experiment in the model system a prediction

form was developed in which over 98% of the variation in π_1 was accounted for by π_2, π_3, and π_4. When the same analysis was used on the intermediate and full size shelter system data the same equation form was found suitable to describe the action with high correlations. It appears that the four main parameters characterize each system equally well. This is evidence of compatibility. No new dimensionless group would contribute much to improving the equation fit for any system. Compatibility assures nothing more than reliable chosen estimators for π_1.

Similarity is a more severe condition to be considered. A test for similarity among systems is to find whether observations in one system accurately predict observations taken in another system. The acid test is to use a prediction equation derived in one system for predicting values in another. Even though the magnitude of the groups in one system are different from those in another, if the prediction equation describes a general law it would characterize both systems equally well.

For the three test systems there was little overlap in values of the parameters. As was shown in Figure 28 only for the model and intermediate system was there overlap in values of all four parameters. Therefore these two systems can be compared by application of a prediction equation in a region where extrapolation is not necessary. To test similarity the prediction derived from model Treatment No. 8, Table IV, was used with values of the pertinent quantities taken

from the intermediate size shelter data. A predicted value of Δt resulted from using observed values of x, H, V, etc., from intermediate shelter data to compute a Δt value with the coefficient and exponents obtained for model Treatment No. 8. This equation was solved for Δt at several points over the intermediate shelter roof. In Figure 35 are plotted predicted Δt values versus observed Δt values to show the adequacy of the prediction equation for describing the intermediate shelter behavior. The predictions give evidence of similarity for these two systems.

The model system was operated with an artificial source of thermal radiation which was assummed to be equivalent in effect to the natural solar heating of the sun to which the intermediate and full size shelters were exposed. The model prediction of intermediate shelter behavior serves the purpose of testing the equivalence of the two kinds of radiation. Even though the energy spectrum for the two kinds of radiative heating was known to be different, the absorptive property of the roofing materials was assumed to be nonselective as was discussed in Chapter IV. The reliability of a prediction equation developed from model observations to predict behavior of a shelter heated by solar irradiation indicates that effective absorption for the two kinds of heat sources was not unequal enough to bias the model tests. This can be concluded for the plain, aged, galvanized roofing, at least.

With system equality for π_5 to π_9 for model and full size shelter systems, an application of a model prediction of

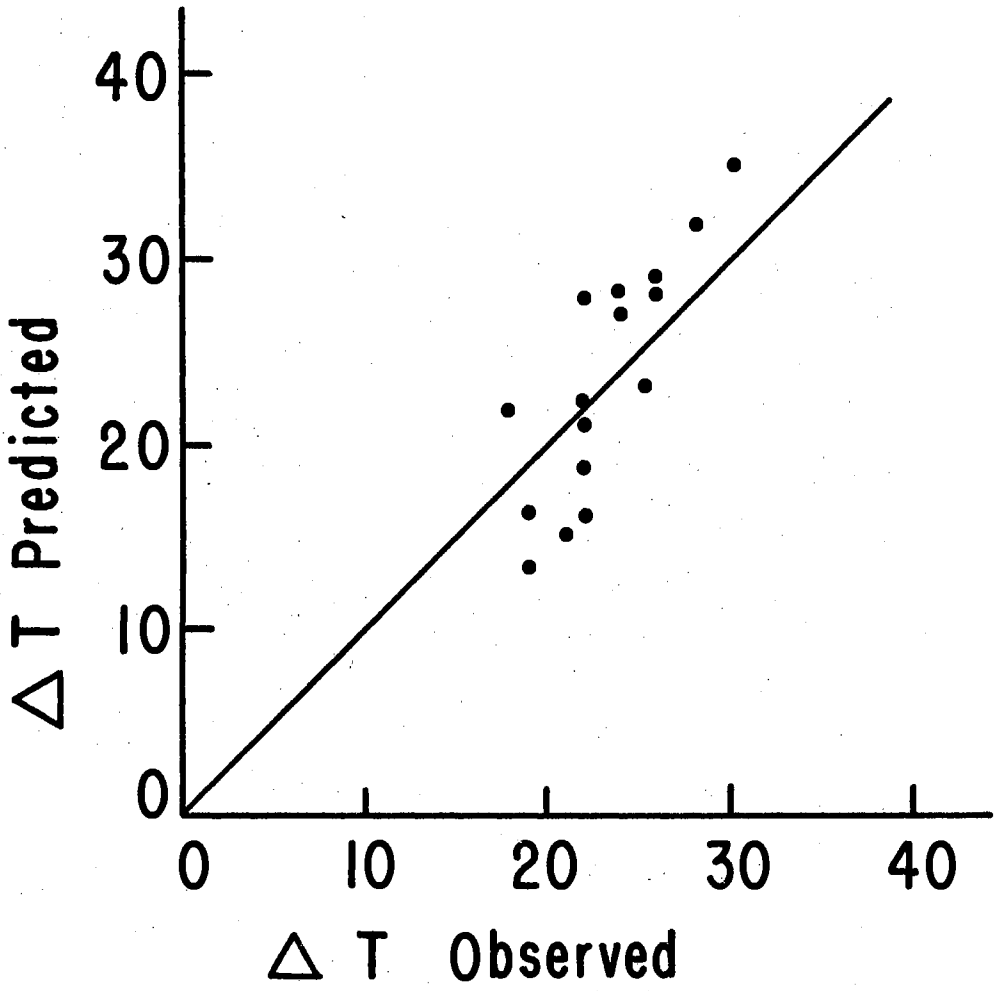

Figure No. 35. Temperature rise of intermediate size shelter as predicted by model equation. Model Treatment No. 8 regression equation applied to intermediate shelter Treatment No. 12 observations.

full size shelter behavior was made for aluminum as shown in Figure 36. It is seen that the model prediction fails to characterize full size shelter behavior, the error increasing with magnitude of Δt. Actually Δt increased with magnitude of x in the experiments, so the prediction is poorer for the large Δt values taken at large x values than for smaller Δt value taken at corresponding smaller x values in the full size system. Even though compatibility was shown to exist among all the systems, similarity was not achieved in all the experiments.

The lack of similarity can also be interpreted from the differences in exponents for the dimensionless parameters obtained from the regression analyses as was given in previous sections. For the range of values of π_1, π_2, π_3 and π_4 experienced in the model system there was evidence of a laminar flow condition on the windward roof. In the full size system with the associated large values for π_3 and π_4, different flow conditions were apparently present.

When the model prediction equation is applied to full size shelter observations, the prediction equation is solved with inserted values for the independent quantities which force the equation to be used in an extremely extrapolated region. Only one equation form was fitted to the experimental observations. It is possible that some other equation form could be found to give a good fit for its own range of values as well as for an extended range as would be encountered in another system. This is a recurrent problem in empirical curve

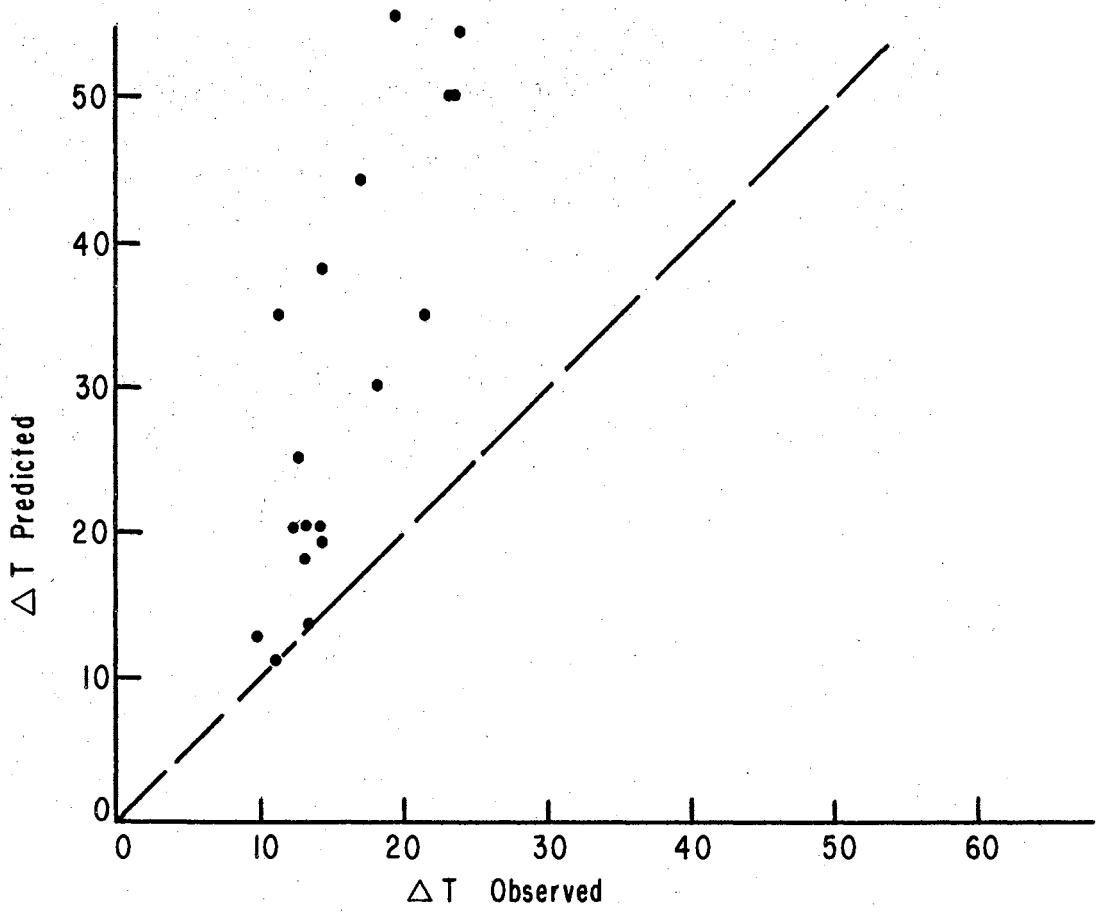

Figure No. 36. Temperature rise on full size shelter as predicted by model equation. Points were randomly chosen from full size shelter Treatment No. 9 and used with the regression equation for model Treatment No. 1 .

fitting.

It might be interesting to determine whether a prediction equation developed from full size shelter data would reliably define the model system behavior. This test could be done in the same manner as the test for model prediction of full size behavior. Because of lack of similarity was exemplified by the first test and the values of the exponents, this test was not tried.

Summarizing, this section presented a discussion of the evidence obtained which verified the compatibility of the three test systems. It was found that a model prediction equation was sufficient to define the thermal behavior of the intermediate size shelter system. This effected a test of similarity. For model and full size system similarity was not achieved. The dependence of Δt on certain parameters characterized by exponents reviewed in a previous section substantiated the lack of system similarity for model and full size systems.

The adequacy of model prediction for describing the intermediate size shelter behavior provided a check on the effective radiant heat source used for the model studies. It was concluded that the model environment was a valid replica of the shelters in the natural outdoor environment.

Regression Analyses for Pooled Groups of Data

If the model system and full size system were truly compatible, observations in either system were samples of a

TABLE XIV

REGRESSION ESTIMATES FOR WINDWARD ROOF BASED ON POOLED MODEL PLUS FULL SIZE AND MODEL PLUS INTERMEDIATE SHELTER DATA

Description	Treatment[1]	K	b_1	b_2	b_3	Number of Observations	Multiple Correlation Coefficient, R^2
		(Model + Fullsize Shelter)					
Aluminum, h=0.264L	1 + 9	3.187	-0.6417	-0.2640	-0.6056	128+96	0.994
Plain Galv. h=0.264L	2 + 11	2.555	-0.6392	-0.1734	-0.7397	128+96	0.991
White Paint h=0.264L	3 + 10	4.046	-0.6694	-0.0798	-0.8472	128+96	0.992
		(Model + 8 ft x 8 ft Shelter)					
Plain Galv. h=0.75L	8 + 12	17.43	-0.4319	-0.5982	-0.2730	128+160	0.963

Note: 1. Table IV contains treatment schedule.
2. Values of K, b_1, b_2, and b_3 apply to equation (1).

pooling does not conform to the usual heat transfer analyses because laminar heat transfer and turbulent heat transfer are separately distinguishable in theory and experiment. The main reason for developing an equation for pooled data is its utility for defining the action of a roof cooling system for a wide range of values of the dimensionless parameters.

The argument against a pooling of the data is two-fold. Unless a more elaborate equation form is used, the distinction between laminar and turbulent heat transfer is dissolved in the process. Secondly, some accuracy of prediction is sacrificed when compared to utilization of two separate prediction equations, each applied to its particular range of values of the parameters. A regression equation for a restricted range of values is a stronger estimator of system behavior over the region than a same order regression for an extended range based on all values unless the response in the extended range is similar to the limited range. There was a lack of physical similarity for the model and full size system as was pointed out previously.

Admittedly, similarity to full size shelter behavior was not achieved in the model although compatibility was established. To correctly unify all the experimental results into a general prediction form applicable to different circumstances for shelters that would be encountered in actual use would fulfill the overall objective of this investigation. Irrespective of the known differences in system behavior for values of the dimensionless parameters represented by the model system and

the full size system values, a desirable and not unrealistic advantage to lumping results and finding the best fit is the utility of a general prediction equation applicable to a wide range of conditions and circumstances that may be encountered in shelter design work.

In the full size shelter system the dimensionless parameters π_3, and π_4 experienced the widest range of variation. In the model system π_2 varied more widely. By pooling the data from 128 observations in the model system with 96 observations in the full size system the resulting regression estimators conform to the effect of the variables without distinction of their origin in either system. A pooled data equation is the simplest approach to describing the cooling effect of a roof for a wide range of values of H, V, and x without stipulating the range of magnitude of the quantities as would be necessary to characterize the boundary layer. The multiple correlation coefficient R^2 serves as a test of the validity of an equation fit. R^2 values for the pooled data equations were high as was shown in Table XIV. However, they were not quite as high as for individual equations for each system.

Rearranging the prediction form gave Δt as an explicit function of the other variables as was expressed in equation (2). A plot of Δt predicted vs. Δt observed for pooled model plus full size shelter data is given in Figure 37 and 38 for aluminum and galvanized roofing. Remembering that full size shelter observations were taken with a three minute time-averaged velocity reading the observed values of Δt for

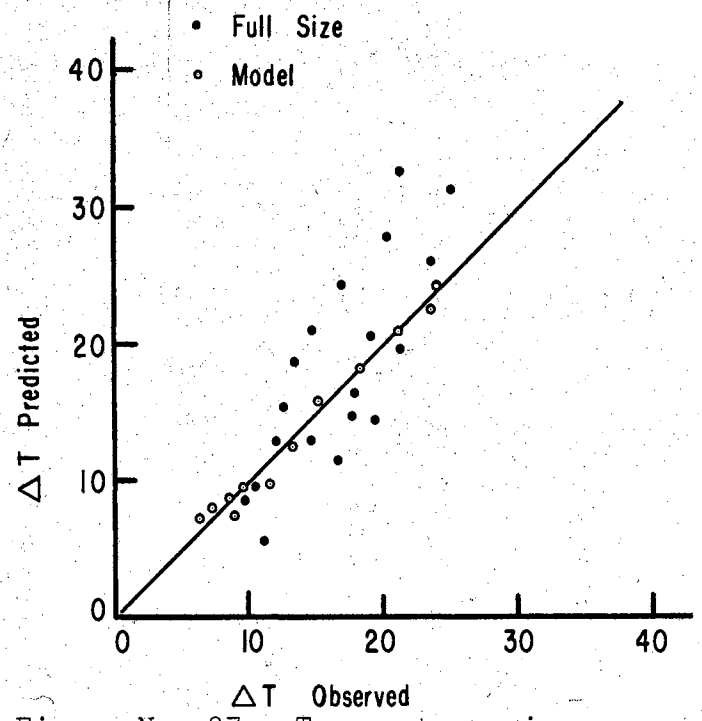

Figure No. 37. Temperature rise as predicted by pooled data equation for model and full size shelter. Plot for aluminum roofing treatment. Random selection of data points are plotted. Pooled model Treatment No. 1 and full size shelter Treatment No. 9. Coefficient and exponents from Table XIV.

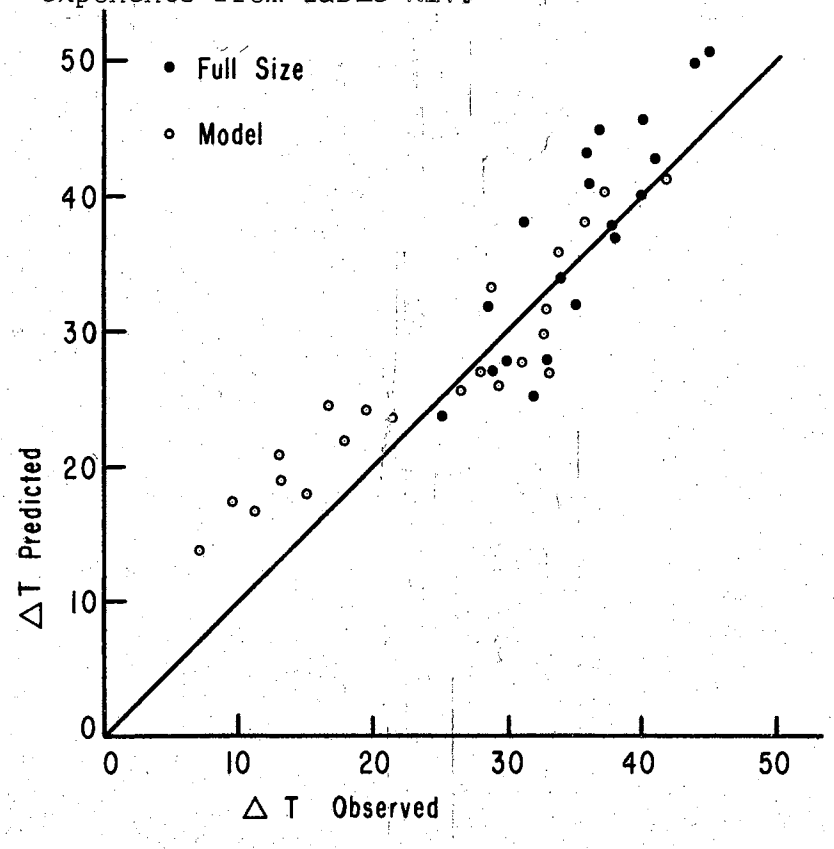

Figure No. 38. Temperature rise as predicted by pooled data equation for galvanized roofing.

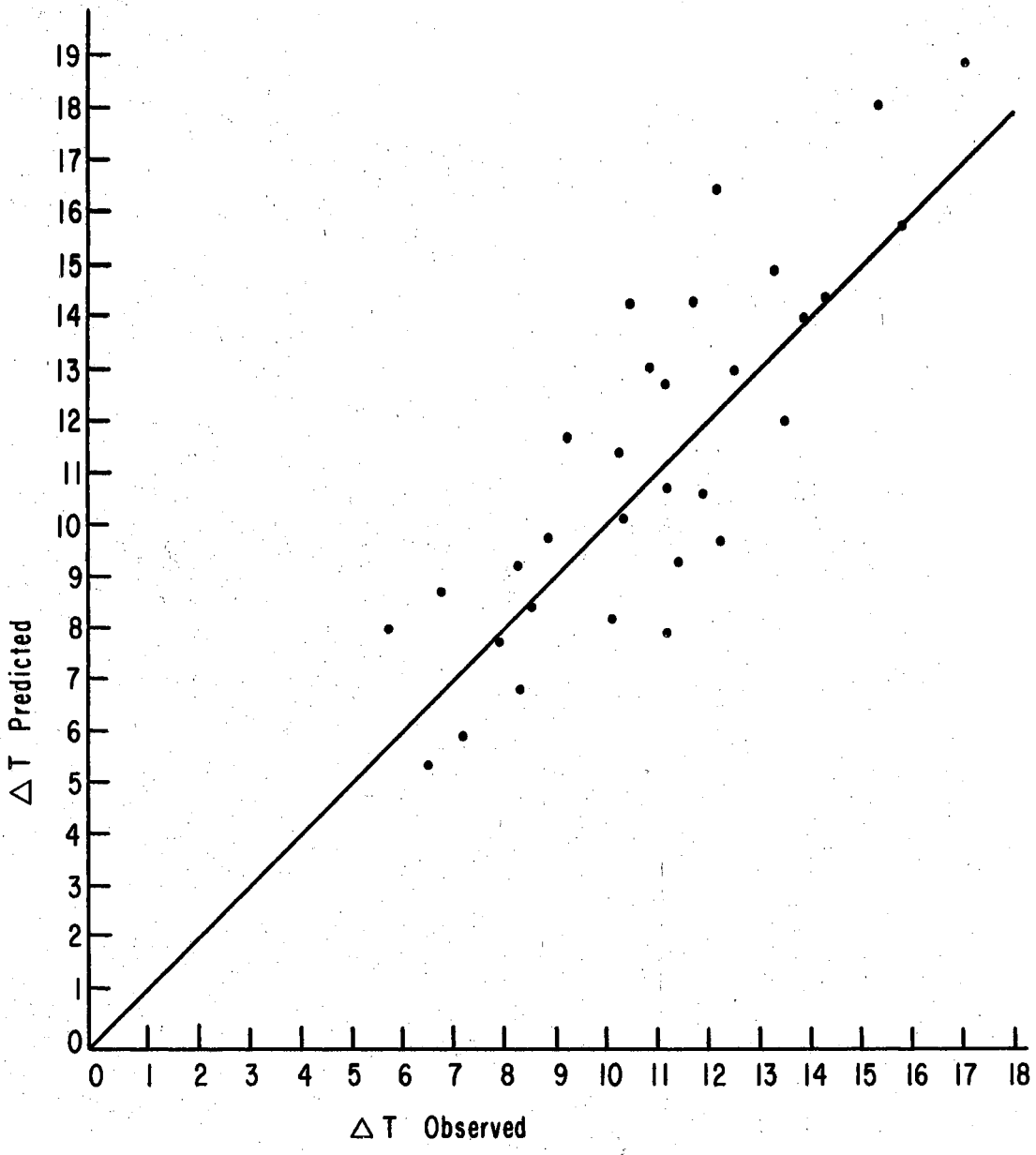

Figure No. 39. Temperature rise of windward roof for pooled data for white-painted roof treatment . Regression equation solution for pooled data of model Treatment No. 3 and full size shelter Treatment No. 10. Coefficient and exponents from Table XIV.

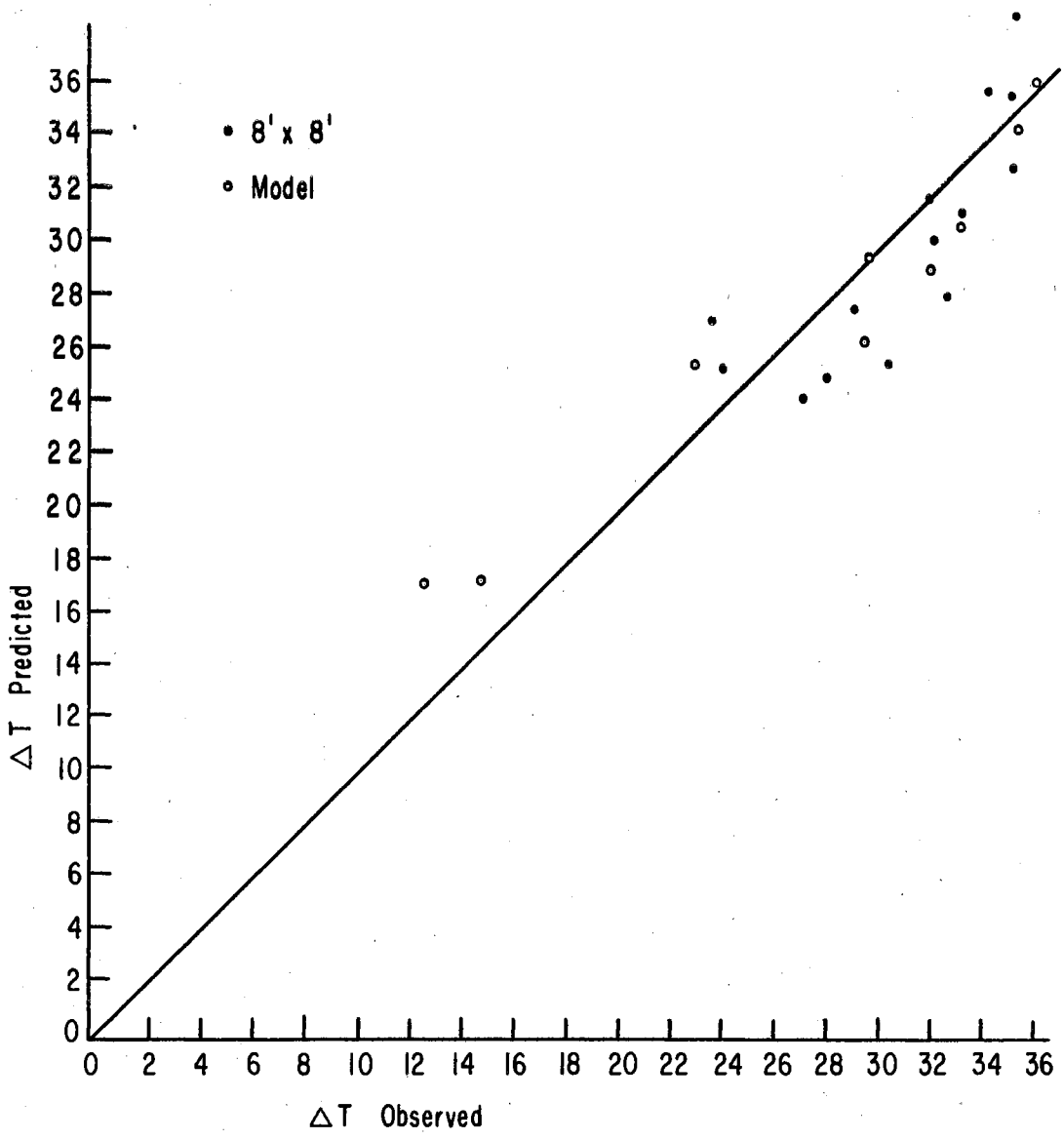

Figure No. 40. Temperature rise for pooled model and intermediate (8 ft x 8 ft) shelter data. Regression equation solution for pooled model Treatment No. 8 and intermediate shelter Treatment No. 12. Coefficient and exponents from Table XIV.

the prototype system are scattered more than model values taken with controlled conditions. The plotted points were randomly chosen from the experimental data points. These model and full size pooled data plots were taken from observations where $\pi_7 = h/L = 0.264$.

Even though the white painted model roof samples were not truly representative of the full size paint treatment, the model and full size data for white painted roofing were pooled and the regression estimates found for their response. Higher than normal absorption values for the model white painted roof samples were evidently counteracted to a certain extent by the behavior of the full size shelter data. The ability of the pooled equation for describing the full size shelter behavior is illustrated in Figure 39.

A plot of predicted versus observed values of Δt resulting from use of the pooled model plus intermediate size shelter data is given in Figure 40. This pooled equation is applicable to the model and intermediate size shelter treatments in which ratio of roof height to length was 0.750. Again a suitable prediction of temperature rise is indicated.

The pooled data equations give multiple regression estimates of the coefficients and exponents which best define the temperature rise of the windward roof of a solar heated wind cooled roof with estimates based on sampling of the quantities over the entire range of variation encountered in the investigation. For a roof height $h/L = 0.75$ the model plus intermediate size shelter regression estimates give usable predictions for

plain galvanized roofing. For roof height h/L = 0.264 the pooled model plus full size shelter observations yield coefficients which were developed for aluminum, white painted, and plain galvanized roofing. These pooled data equations should be applicable to other roof configurations of slope angle and material texture because the model comparisons showed that these configuration variables have small effect on the thermal behavior of a roof. Especially for longer roofs where a turbulent flow region would probably occur, extraneous influences have less effect than in a laminar boundary region. It was pointed out in the literature review that free stream turbulence and surface conditions influence the thermal behavior in the laminar boundary region but apparently have little or no influence in the turbulent region.

Figure 41 presents solutions to the pooled data regression equations with H as a variable and fixed values for other quantities. Plots are shown for two distances up roof slope and for two kinds of material. A similar plot with wind velocity as a variable is given in Figure 42.

Free Convection Effects

Throughout this study it was assumed that forced convection heat transfer occurred over the surfaces without need to consider free convection effects. This assumption was valid because measurements of temperature rise were only made when there was forced wind flow present. The listing of pertinent quantities was formulated to contain those quantities which

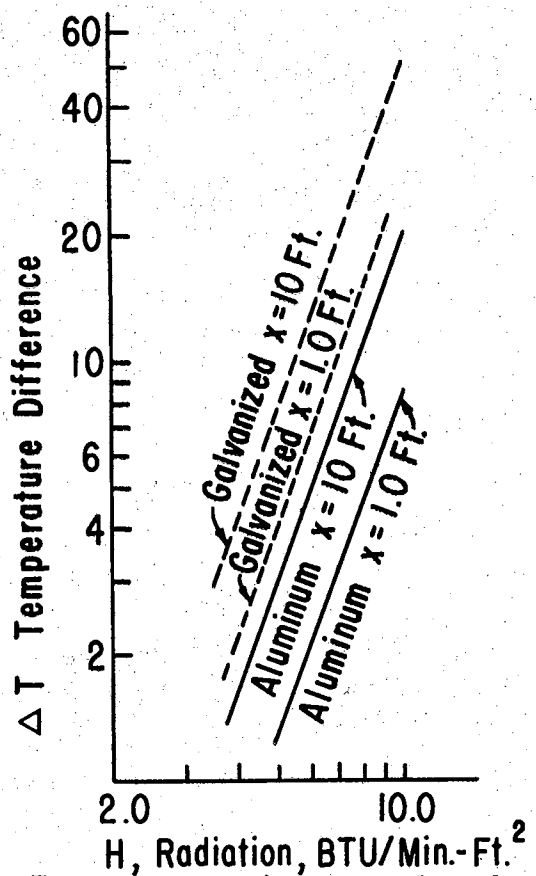

Figure No. 41. Temperature rise as related to incident radiation intensity for aluminum and galvanized roofing. Curves represent solutions to pooled data equations for conditions V=1000 ft/min, t_a=550R, ρ=0.075 lbs/ft^3. Coefficients and exponents from Table XIV.

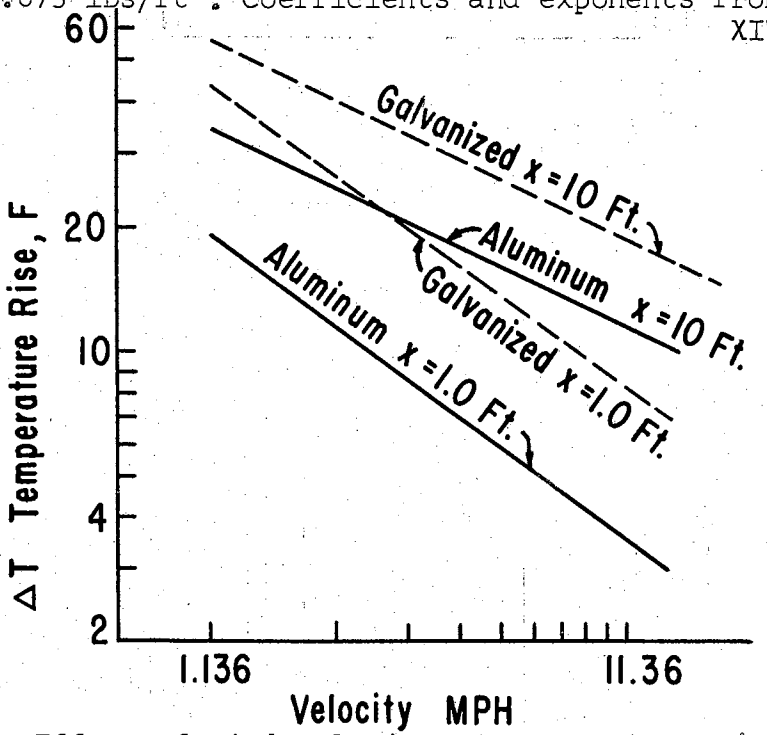

Figure No. 42. Effect of wind velocity on temperature rise for galvanized and aluminum roofing at two points along roof slope. Pooled data equations for H=7.5 Btu/min-ft^2, t_a=550R, ρ=0.075 lbs/ft^3. Coefficients and exponents from Table XIV.

have known significance in forced convection theory.

Free convection caused by the tendency of warm air to rise from a surface has been correlated to pertinent variables by past dimensional and experimental methods. Equations have been developed by McAdams and others to describe free convection from horizontal and from vertical plates. For the three test systems the free convection heat transfer coefficient is computed in this section to find whether the three test systems were appreciably different as far as free convection effects are concerned.

Free convection theory has shown that the rate of heat transfer depends greatly on surface length and surface-fluid temperature difference. The test systems for this study had widely differing surface lengths. However, in all three systems temperature differences seldom exceeded 50 F. Following the procedure given by Jakob and Hawkins (29) the free convection coefficient was computed for the three surfaces for an assumed value of Δt of 30 F, air properties evaluated at 120 F (representative mean fluid-surface temperature) and the surface length particular to each system. The equations for a heated vertical plate were used since they represent the extreme free convection system. For the full size, intermediate size, and model systems the values of free convection coefficients computed were 0.59, 0.59, and 0.68 Btu per hr ft^2 F, respectively, the first two values falling in the turbulent regime and the third in the laminar regime of the surface film. This computation shows that small

differences in free convection potential occurred in the three test systems. Forced movement of air in the surface film greatly increases heat transfer at the surface, making the free convection potential seemingly insignificant as far as it would apply in this study for forced air flow.

Relation of the Experimental Values of Surface Temperature Rise to a Heat Transfer Coefficient

The magnitude of incoming radiation incident on the roof surface for any of the test conditions was metered with the nonselective flat plate radiometer. Part of the incident radiation striking the roof surface was reflected away and part of it absorbed. The absorbed energy caused a rise in roof temperature. The sum of convection loss on top and bottom sides of the roof plus the radiation loss was equal to the absorbed incident radiation energy. Because no quantitative measure of heat flow from the roof material to the moving air stream was made, it was not possible to calculate a heat transfer coefficient in the usual sense. A convection transfer coefficient h_c for a small unit surface area is defined as the rate of heat flow per unit temperature difference of surface and free stream temperature.

$$h_c = q/(t_s - t_a) \text{ Btu/hr ft}^2 \text{ F}$$

where h_c is usually independent of q and $(t_s - t_a)$. The radiation loss from a surface can be expressed with a coefficient

h_r; if t_a represents temperatures of the surround

$$q_r = h_r(t_s - t_a)$$

however, for this case h_r is a function of t_s and t_a and also the location of the temperatures on the absolute scale. A combined heat transfer coefficient which expresses the total rate of loss from surface is then

$$q = (h_c + h_r)\ (t_s - t_a).$$

For the thin roof material there was heat loss from both sides of the surface so that four coefficients apply to the situation, two for top side and two for bottom side,

$$q = (h_{c_t} + h_{r_t} + h_{c_b} + h_{r_b})\ (t_s - t_a).$$

The rate of heat gain per unit area of the roof is

$$q_g = \alpha H$$

where α is the absorption coefficient and H is the intensity of incoming radiation to the roof. At equilibrium the gain equals the loss so that

$$\alpha H = (h_{c_t} + h_{r_t} + h_{c_b} + h_{r_b})\ (t_s - t_a).$$

Rearranging, one gets

$$\alpha H/(t_s - t_a) = (h_{c_t} + h_{r_t} + h_{c_b} + h_{r_b})$$

and since $t_s - t_a = \Delta t$, a similar form with a combined

coefficient $h_s = (h_{c_t} + h_{r_t} + h_{c_b} + h_{r_b})\ 1/\alpha$

and

$$H/\Delta t = h_s. \qquad \text{Btu/hr ft}^2\ \text{F}$$

This is a synthetic heat exchange coefficient which is a measure of the combined absorption, radiation, and convection loss from both sides of a thin piece of roof metal. It is a function of the temperature difference, absolute temperature of the system, and the usual variables for a convection coefficient. Early in the model experiments it was noticed that Δt did not vary linearly with H.

To evaluate the change in magnitude of h_s with wind velocity, experimental values of $h_s = H/\Delta t$ are plotted against wind velocity in Figure 43 using model data in which radiation intensity was held constant for the wide range of wind velocities. In Figure 44 is shown the change in h_s with intensity of incident radiation for the model roof, at a constant velocity. These plots give visual demonstration of model system response to only one variable at a time. More accurate description of system behavior is achieved by use of the prediction equations which take into account all the pertinent variables.

McAdams (44) gives tabulated values of total normal emissivity for numerous building materials. He points out that the emissivity values can be used for absorptivity values without consequential error for many heat transfer calculations. For grey, oxidized galvanized steel a value 0.28 is

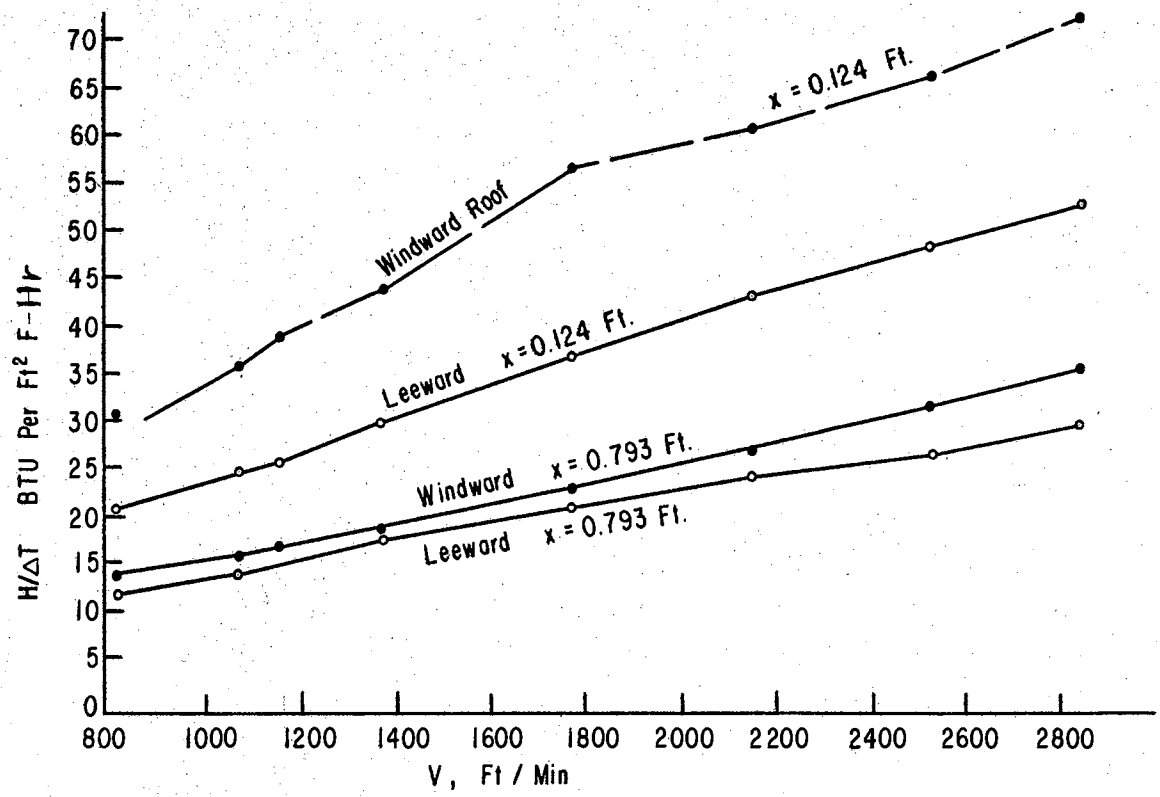

Figure No. 43. Rate of heat transfer from model roof as affected by wind velocity. Model run with H=11.77 Btu/min ft^2. Treatment No. 5.

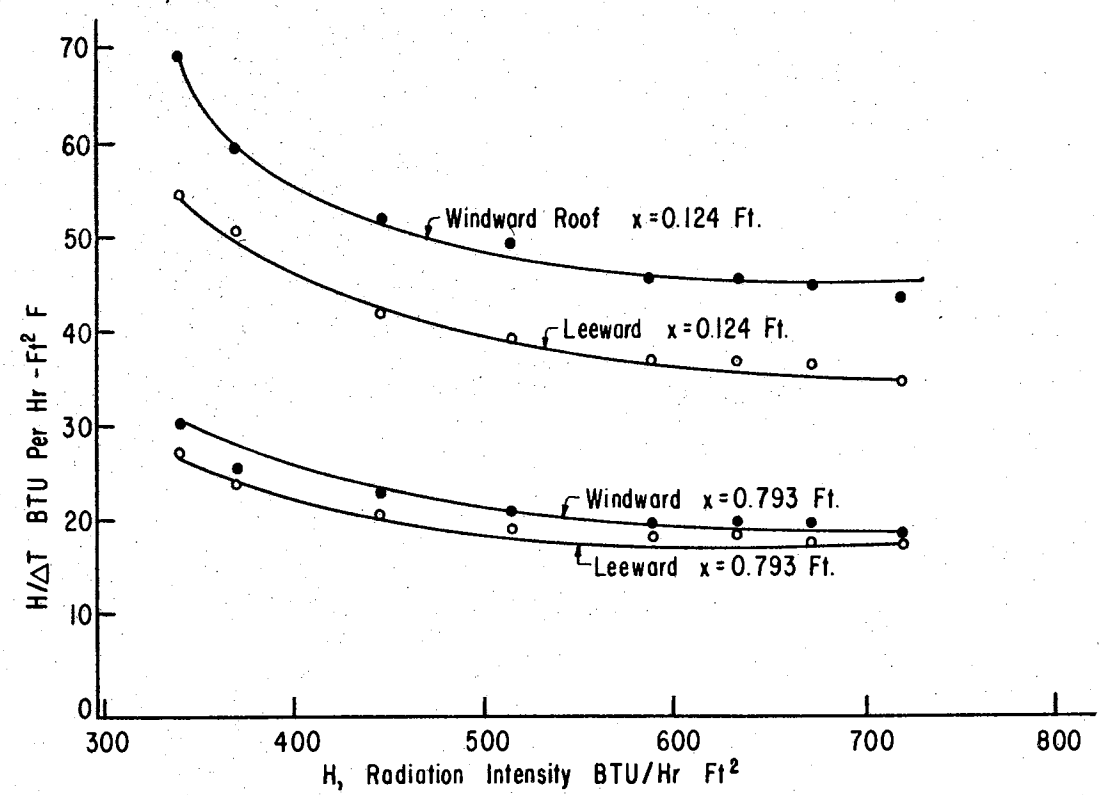

Figure No. 44. Rate of heat transfer from model roof as affected by radiation intensity. Model run with V=1371 ft/min. Treatment No. 5.

listed. Using this as a representative α value, the values of $H/\Delta t$ when multiplied by 0.28 fall in a range of about 20 to 2.8 Btu/hr ft^2 F. This is the range for h_s encountered in the investigation. For a combined coefficient for heat loss from two sides of a piece of roofing material this range of values is in accord with heat transfer coefficients developed for building materials as reported by Rowley, et. al. (55) and others.

It should be noticed that for the open shelter construction, cooling of the leeward roof is almost as pronounced as on the windward roof. Especially near the ridge the rate of heat loss on the two sides appears to equalize as demonstrated by Figures 43 and 44.

Possible Improvement of the Prediction Equation

The equation form (1) was found to be adequate to represent behavior of each system individually with a poorer correlation resulting from application of the equation to pooled data from combinations of test systems. The four dimensionless groups π_1, π_2, π_3, and π_4 lack any physical quantity characteristic of the gross size of the shelter system. Only the quantity x is related to roof size in that its magnitude is limited by roof length. Because each shelter system displayed somewhat different characteristic behavior as exemplified by the exponents and coefficients resulting from the multiple regression analyses, perhaps the inclusion of a new independent dimensionless group whose magnitude typifies the

gross length of the shelter roof would generalize the prediction equation form to provide a stronger predictor of the cooling process for any size of shelter.

In the chosen dimensionless groups for the study the ratio of roof thickness to roof length, $\pi_{10} = t/L$, was hypothesized to be an unimportant parameter. Since roof thickness used in the all three test systems was equal, the value of π_{10} for each system is characteristic of the roof length. The inclusion of the new parameter π_{10} could be taken into account by using it as an added estimator of the chosen dependent parameter

$$\pi_1 = f(\pi_2, \pi_3, \pi_4, \pi_{10}). \qquad \pi_4 = x/t$$

In this case five variables would have to be handled in the curve fitting or equation finding analysis.

In retrospect to the experimental results there is a good indication that the inclusion of π_{10} in the analysis would have given even stronger definition of the thermal behavior of the roof. Nothing is added by π_{10} which would aid correlations of the quantities for a given test system where π_{10} remained a constant value, however a great deal is added when correlations would be made among test systems, each characterized by a particular π_{10} value.

By reviewing the observed behavior of the three test shelters some insight on the significance of a new estimator of the thermal behavior is gained. The model shelter with a roof length of about 1 foot apparently displayed characteristic

laminar flow over the entire roof area for a wide range of wind velocities and intensities of radiative heating. The intermediate size shelter with a roof approximately five feet long yielded data characteristic of some condition intermediate between generally accepted laminar and turbulent boundary behavior for the range of velocities encountered in its operation. The full size shelter with a roof twenty-seven feet long displayed heat transfer characteristics in which the rate of heat transfer had small dependence on wind velocity. The possibility of improving the prediction ability of the equation form by the addition of a new parameter must be left for further study.

CHAPTER VII

SUMMARY AND CONCLUSIONS

Summary

The general objective of the study was to develop a basis for predicting the temperature rise for the forced convective cooling of the roof of a gabled open type animal shelter exposed to combined solar radiative heating and cooling by a natural gradient wind stream. The major variables taken into account were wind velocity at eave height, intensity of incident radiation striking the roof, roof slope angle, eave height, and corrugation pitch size. Only the open type, unceiled shelter exposed to a wind direction normal to eave direction was investigated.

The study involved measurements of the temperature rise of the roof surface of 48 ft x 48 ft shelter building exposed to natural solar heating and wind cooling, similar measurements on an 8 ft x 8 ft shelter, and on a model shelter with a roof length of one ft operated in a wind tunnel. Most of the experimental observations were made with the model shelter under conditions with controlled wind velocity and radiation from a bank of infrared lamps which provided the source of thermal radiation. In all three test systems the behavior of the windward roof was studied and in addition the behavior

of the leeward roof in the model system was investigated.

Dimensional analysis was used to formulate groups of dimensionless parameters from a list of all physical quantities which were thought to have pertinent influence on the thermal behavior of the shelter roof system for the specified condition of radiative heating and wind cooling. From the twenty physical quantities contained in the listing, fifteen dimensionless parameters were formed with four groups containing the quantities wind velocity, radiation intensity, distance up roof slope, and others; these four groups were found to be the primary variables for describing the thermal behavior of the shelter roof. Five of the fifteen dimensionless groups contained component quantities sufficient to characterize the configuration of the shelter and properties of the roof material. Five groups were considered unimportant as variables by their nature. One dimensionless group, the ratio of roof metal thickness to roof length dimension, was assumed unimportant for thin metal roofing. In the data analysis no variations were detected which would have given reason to believe that some pertinent quantities were neglected in the dimensionless groupings.

Experiments were conducted with the model shelter in the wind tunnel where close control on radiation intensity and wind velocity was effected. Wind velocity was varied over a range of 800 to 3400 ft/min and radiation intensity ranged from 5 to 12 Btu/min-ft^2. Slope angles tested with the model shelter were 3/12, 4/12, and 5/12. Three roof textures were studied: two sizes of corrugation and a flat specimen. Two

roof heights were used: one with ratio of height to roof length equal to 0.264 and one with height to length ratio of 0.75. Aluminum, white-painted galvanized steel, and plain, aged, galvanized steel roofing panels were studied. Measurements of the temperature rise of the roof panels were taken at several points along the roof slope on both roof sides on the model shelter for eight combinations of shelter configuration and material selection. The experiments were designed to give sufficient data for each shelter treatment to yield a prediction relation characteristic of the particular treatment.

The full size shelter had a corrugated metal roof with aluminum, white-painted steel, and plain galvanized steel. Ratio of eave height to roof length was 0.264, and roof slope angle was 4/12. Measurements of the windward roof temperature rise were taken on three days with cloud-free skies and a brisk wind blowing over the roof normal to the eave direction.

The intermediate size shelter had a flat, plain galvanized roof with a roof height to length ratio of 0.75 and 4/12 slope angle. Measurements of the pertinent variables were made on two days.

For a given treatment of shelter configuration and roof material, data analysis revealed that an equation form

$$k\Delta t/Hx = K(t_a/\Delta t)^{b1}(V\rho x/\mu)^{b2}(x/t)^{b3}$$

would correlate the quantities with high precision. After logarithmic transformations of the experimental observational values of the dimensionless groups comprising the equation,

multiple regression analyses were used for estimating the values K, b_1, b_2, and b_3 characteristic of each shelter treatment. All computations of the numerical values of the dimensionless groups and the regression analyses were made with an IBM 650 Computer utilizing appropriate programming. A set of exponents and the coefficient were found for each individual model shelter treatment, for the intermediate size whelter response, and for each of the three full size shelter treatments. Multiple correlation coefficients were in excess of 0.97 in each case, giving evidence of a valid choice of parameters for the prediction form. The high correlation coefficients resulting from the equation fitting for each shelter data taken individually gave assurance that compatibility existed among the shelter systems. Compatibility was defined as the requirement that the same set of dimensionless groups be adequate to define the response of the individual systems.

A test of similarity was effected by using prediction equations developed wholly from model test observations to predict the response of the intermediate size shelter and full size shelter. A model equation proved to be a valid predictor of the thermal behavior of the intermediate size shelter roof, but failed to predict the temperature rise observed on the full size shelter. Although similarity was established for model and intermediate size shelter operation it was not achieved for model and full size tests. Compatibility was, however, established and verified for the three test systems.

By comparison of the experimentally derived values of the

exponents of the dimensionless groups in the present study with results from other studies of a similar nature as reported in the literature review, there was an indication that the model system was operated under conditions which were conducive of a laminar boundary layer development on the shelter windward roof.

The exponents resulting from regression estimates for the windward roof of the intermediate size shelter were partially descriptive of laminar boundary conditions and partially akin to values found in other experimental works with known turbulent exchange. Exponents found applicable to the full size roof behavior were more characteristic of a turbulent exchange than laminar, with the condition of the boundary layer again predicted only by comparison of exponents to values of exponents in other studies.

Behavior of the leeward roof of the model shelter was strikingly similar to the windward roof for all model tests. Because of the exposure to a wake region no straightforward interpretation of the heat transfer process for the leeward side was realized.

Comparisons of shelter treatment effects were made to learn the effect of the configuration and roof material characteristics. Algebraic rearrangement of the prediction equation form produced a more explicit relation between the temperature rise at a point on the roof and the other quantities. It was found that small differences in temperature rise can be attributed to the configuration variables roof

slope, height, and texture for the values of these variables tested.

In the rearranged form the exponent for certain quantities served as a measure of their effect on the dependent quantity. Of particular interest was the rate of change in temperature rise with changes in wind velocity, radiation intensity, and distance up roof from eave edge.

Regression analyses were also run on pooled model plus full size shelter data and model plus intermediate shelter data to define a general prediction equation applicable to a wide range of variation in the magnitude of the dimensionless groups of quantities. The pooled model plus intermediate shelter equation was applicable to the case with ratio of roof eave height to roof length of 0.75 and the pooled model plus full size shelter data applicable to the case with ratio of roof eave height to length of 0.264. Multiple correlation coefficients derived for the pooled equation fits were in excess of 0.96, values less than the correlations for individual equation fits which were developed for each test shelter system independently. The correlations were, however, high enough to insure predictions of surface temperature rise of the roof within tolerable accuracy limits.

A computation of the free convection potential for each test system indicated that negligible differences as far as free convection effects are concerned existed among the three test shelters. While the roof surface lengths varied greatly the differences in surface and air temperature experienced were

relative small.

In order to relate the experimental results of the present study to more familiar heat transfer terms a heat transfer index was computed to reference the thermal behavior of the roof system to a heat transfer coefficient. It was found that the observed values of temperature rise of the roof exposed to heating from above and to cooling on both top and bottom sides were of the same order of magnitude as that which conventional heat flow calculation procedures would indicate.

Possible improvement in the prediction equation would be to use one additional parameter, π_{10}, to estimate the dependent variable, π_1, in equation form (1). The pi term, π_{10}, would provide a parameter whose magnitude depends directly on roof length which when taken into the analysis might describe a general prediction form with greater predictive ability than equation (1). This possibility was not pursued in this study.

Conclusions

From the results of the investigation certain conclusions can be drawn:

1. The equation form adequate to correlate the physical quantities pertinent in the thermal behavior of a thin metal roof inclined to the main windstream is

$$k\Delta t/Hx = K(t_a/\Delta t)^{b1}(V\rho x/\mu)^{b2}(x/t)^{b3}$$

where

k = air conductivity, Btu/hr ft F

Δt= difference in surface temperature, t_s at distance x from eave and air temperature, t_a, F

H = intensity of incoming radiation incident on roof plane, Btu/hr ft^2

x = distance up roof slope, ft

t_a= air temperature, absolute

V = velocity of wind at eave height ft/hr

ρ = air density lbs_m/ft^3

μ = air viscosity lbs_m/ft hr

t = roof metal thickness, ft.

This equation form was found to be adequate to account for the thermal behavior of a model shelter roof approximately one ft long, a shelter with a roof approximately 5 ft long, and a shelter with a roof 27 ft long. Strongest predictions were obtained by analyzing each test shelter separately to find the exponents and coefficients applicable to the shelter data.

Exponents b_1, b_2 and b_3 and the coefficient K for predicting temperature rise adequate for the widest range in variation of the variables was developed from combined shelter system data. These pooled data results were developed for three kinds of roofing material for a roof eave height-to-length ratio of 0.264 as represented by model and full size shelter treatments and for a height-to-length ratio of 0.75 as represented by a model and intermediate size shelter treatment. For 0.264 eave height to roof length ratio the values for K, b_1, b_2 and b_3 are respectively 3.187, -0.6417,

-0.2640 and -.06056 for aluminum roofing, 2.555, -0.6392, -0.1734 and -0.7397 for plain galvanized roofing, and 4.046, -0.6694, -0.0798, -0.8472 for white painted roofing. For the 0.75 eave height-to-length ratio the values of K, b_1, b_2, and b_3 are respectively 17.43, -0.4319, -0.5982 and -0.2730.

2. Dimensional analysis and model techniques offer an expedient means of analyzing the behavior of thermal systems. The model approach has in the past been adapted to fluid flow problems without widespread use in shelter heat transfer studies. Especially when control on certain variables can be effected in a model system the advantages of utilizing more than one physical system are multiplied. Dimensional compatibility and similarity provide the necessary criteria for establishing correct correspondence among test systems. In the present investigation where several physical quantities were thought to have significant influence on the thermal behavior of the shelter roof, dimensional analysis provided a systematic approach to an experimental design for evaluating the effects of variables.

3. Corrugation size has little effect on the cooling rate for an inclined roof. Except for disturbances at the eave edge, wind flow parallel to corrugation direction is probably not influenced to a significant degree by the presence or lack of corrugations. Perhaps with wind flow across the corrugations, thermal exhange would be influenced by corrugation configuration.

4. From the model tests, little if any differences in temperature rise were noted for changes in roof slope angle

in the range 3/12 to 5/12. Convective heat transfer appears equally prevalent for any of the three slope angles tested. In terms of the behavior of an actual shelter structure, the angle of incidence of direct solar irradiation is affected by the slope angle of the roof. In shelter design, attention should be given to the angle of direct solar radiation for selecting the slope angle. The present study revealed that convective cooling is uninfluenced by roof slope angle. Therefore, the selection of the roof slope angle should be based on a choice of roof slope which minimizes the angle of incidence of direct beam solar radiation at the hottest part of the day.

5. The temperature rise of the leeward roof is only slightly larger than the windward roof. When correlated in an equation form similar to the equation for the windward roof with certain quantities defined appropriately for the leeward roof side, the temperature rise of the leeward roof of the model shelter was strikingly similar to the temperature rise on the windward side. The variation of temperature with distance up roof slope was similar on the two roof sides. The coolest region of the roof was near the eave with an increase in temperature with distance up roof slope. In all instances in the model investigation, the leeward roof temperatures were within five or fewer degrees F of the windward roof temperatures under conditions of equal radiative heating.

6. Shelter roof eave height has only a slight influence

on thermal behavior. The model treatments with h = 0.75L experienced a slightly larger temperature rise than those with h = 0.264L. Wind velocity was measured at eave height in the experiments. In an actual shelter, higher roofs are in a zone of higher wind velocity which enhances cooling significantly.

7. Material absorption and emission have a pronounced effect on temperature rise. Under conditions of radiative heating and wind cooling comparative values for the different materials used on the 48 ft x 48 ft shelter were, for an 11 mph wind, incident radiant intensity of 450 Btu/hr-ft^2, and 90 F air temperature, a temperature rise for plain galvanized steel of 30 F, 18 F for aluminum, and 12 F for white-painted steel. This confirms the findings of other investigators on the importance of highly reflective materials for low heat gain.

8. The rate of heat transfer tends to become independent of wind velocity and distance from leading edge at regions far from the leading edge of a heated surface. This result was substantiated by observation of the temperature rise on the three kinds of roofing used on the full size shelter. With temperature measurements taken at distances from one to twenty-two ft from the eave the temperature rise was found to vary with wind velocity to the 0.09 power and distance from the leading edge to the 0.11 power in one case and 0.20 power in another.

SELECTED BIBLIOGRAPHY

1. Berry, F. A., Bollay, E., and Beers, N. R. Handbook of Meteorology. New York: McGraw-Hill Book Co., Inc., 1945.

2. Bond, T. E. and Kelly, C. F. "Effectiveness of Artifical Shade Materials," Ag. Eng., 39:758-760, 1958.

3. Bond, T. E., Kelly, C. F., and Ittner, N. R. "Radiation Studies of Painted Shade Materials," Ag. Eng. 35:389-392, 1954.

4. Bosworth, R. C. L. Heat Transfer Phenomena. New York: John Wiley and Sons, Inc., 1952.

5. Brooks, F. A. An Introduction to Physical Microclimatology. University of California: Davis, California., 1959.

6. Brunt, David. Physical and Dynamical Meteorology. Cambridge University Press: Cambridge, 1939.

7. Colburn, A. P. "A Method of Correlating Forced Convective Heat Transfer," Transactions, American Institute of Chemical Engineers, 29:174-210, 1933.

8. Colburn, A. P. "Heat Transfer by Natural and Forced Convection," Bulletin No. 84, Purdue University Engineering Experiment Station, Lafayette, Indiana, 1942.

9. Corcoran, W. H., Opfell, J. B. and Sage, B. H. Momentum Transfer in Fluids. New York: Academic Press, Inc., 1956.

10. Dale, A. C. and Giese, Henry. "Effect of Roofing Materials on Temperatures in Farm Buildings Under Summer Conditions," Ag. Eng. 34:168-177, 1953.

11. Drake, R. M. "Investigation of Variation of Point Unit Heat Transfer Coefficients For Laminar Flow over an Inclined Flat Plate," Journal of Applied Mechanics, (Bound in ASME Transactions, Vol. 71, 1949).

12. Dryden, H. L. Air Flow In The Boundary Layer Near A Plate, National Advisory Comm. Aeronautics, Report No. 562, 1936.

13. Dryden, H. L. "Fifty Years of Boundary Layer Theory and Experiment," Science, 121:375-380, 1955.

14. Edwards, A. and Furber, B. N. "The Influence of Free Stream Turbulence on Heat Transfer by Convection From an Isolated Region of a Plane on Parallel Air Flow," Proceedings, Inst. Mech. Engineers, 170:28, 14 pp. 1956.

15. Elias, Franz. The Transference of Heat From A Hot Plate to An Air Stream, National Advisory Comm. Aeronautics, Technical Memoirs No. 614, 1931. (Translation of ABH. D. Aerodyn. Inst. D. Techn. Hochschule Aachen, No. 9, pp. 10-39, 1930.)

16. Evans, B. H. "Natural Air Flow Around Buildings," Texas Engineering Experiment Station, Research Report No. 59, 1957.

17. Giedt, W. H. Principles of Engineering Heat Transfer. New York: D. Van Nostrand Co., Inc., 1957.

18. Gieger, Rudolf. The Climate Near the Ground. Harvard Univ. Press: Cambridge, Mass., 1957.

19. Gier, J. T. and Dunkle, R. V. "Total Hemispherical Radiometers," Transactions, American Society of Electrical Engineers, 70:339-343, 1951.

20. Goldstein, S. Modern Developments in Fluid Mechanics. Vol. 1 and 2. Oxford: Clarendon Press, 1938.

21. Guide. American Society of Heating and Ventilating Engineers, Vol. 25, Published by ASHVE, New York, 1947.

22. Hinze, J. O. Turbulence, An Introduction to Its Mechanism and Theory. New York: McGraw-Hill Book Co., 1959.

23. Houghten, F. C. and McDermott, Paul. "Wind Velocity Gradients Near A Surface and Their Effect on Film Conductance," Transactions, American Society of Heating and Ventilating Engineers, 37:301-322, 1931.

24. Houghten, F. C. and Zobel, C. G. F. "Coefficients of Heat Transfer as Measured Under Natural Weather Conditions," Transactions, American Society of Heating and Ventilating Engineers, 34:397-414, 1928.

25. Houghten, F. C. and Zobel, C. G. F. "Heat Transfer Through Roofs Under Summer Conditions," Transactions, American Society of Heating and Ventilating Engineers, 34:415-438, 1928.

26. Irminger, J. O. V., and Nokkentved, Chr. Wind-Pressure on Buildings. Experimental Researches, (second series). Translated by Alexander C. Jarvis and O. Brodsgaard. Danmarks Naturvidenskabelige Samfund, Ingeniorvidenskabelige Skrifter. A, Nr. 23. Copenhagen, Denmark, 1936.

27. Ittner, N. R. and Kelly, C. F. "Cattle Shades," Journal of Animal Science, 10:184-194, 1951.

28. Jakob, Max and Dow, W. M. "Heat Transfer From a Cylindrical Surface to Air in Parallel Flow With and Without Unheated Starting Sections," Transactions, American Society of Mechanical Engineers, 68:123-134, 1946.

29. Jakob, Max and Hawkins, G. A., Elements of Heat Transfer. New York: John Wiley and Sons, Inc., 1957.

30. Jakob, Max. Heat Transfer. Vol. 1. New York: John Wiley and Sons, Inc., 1949.

31. Jensen, Martin. Shelter Effect. The Danish Technical Press: Copenhagen, Denmark, 1954.

32. Karman von, Th. "The Analogy Between Fluid Friction and Heat Transfer," Transactions, American Society of Mechanical Engineers, 61:705-710, 1939.

33. Karman von, Th. "Turbulence and Skin Friction," Journal of Aeronautical Sciences, 1:1-20, 1934.

34. Keast, David and Wiener, F. M. "An Empirical Method for Estimating Wind Profiles over Open Level Ground," Transactions, American Geophysical Union, 39:858-864, No. 39, 1958.

35. Kelly, C. F., Bond, T. E. and Heitman, H. "The Role of Thermal Radiation in Animal Ecology," Ecology, 35:562-569, 1954.

36. Kelly, C. F. and Ittner, N. R. "Artifical Shades for Livestock in Hot Climates," Ag.Eng. 29:239-242, 1948.

37. Klebanoff, P. S. and Diehl, Z. W. Fully Developed Turbulent Boundary Layers With Zero Pressure Gradient, National Advisory Comm. Aeronautics, Technical Note No. 2475, 1951.

38. Langhaar, Henry L. Dimensional Analysis and Theory of Models. New York: John Wiley and Sons, Inc., 1951.

39. Latzko, H. Heat Transfer in A Turbulent Liquid or Gas Stream, National Advisory Comm. Aeronautics, Technical Memoirs No. 1068, 1944. (Translation of A Dissertation Presented to the Phil. Faculty of the University of Vienna, 1921).

40. Mackey, C. O. and Wright, L. T. "The Sol-Air Thermometer ... A New Instrument," Transactions, American Society of Heating and Ventilating Engineers, 52:271-282, 1946.

41. Mackey, C. O. and Watson, E. B. "Summer Weather Data and Sol-Air Temperatures - Study of Data for New York, New York," Transactions, American Society of Heating and Ventilating Engineers, 51:75-91, 1945.

42. Mackey, C. O. "Summer Weather Data and Sol-Air Temperatures - Study of Data for Lincoln, Nebraska," Transactions, American Society of Heating and Ventilating Engineers, 51:93-110, 1945.

43. Maher, Thomas F. An Investigation of the Transportation of Fog or Mist When Sprayed into an Air Stream. Unpublished PhD Thesis, Oklahoma State University, Stillwater, Oklahoma, 1961.

44. McAdams, W. H. Heat Transmission. New York: McGraw-Hill Book Co., Inc., 1954.

45. Moon, P. "Proposed Standard Solar Radiation Curves for Engineering Use," Journal of The Franklin Institute, 230:583-617, No. 5, 1940.

46. Murphy, Glenn. Similitude in Engineering. New York, Ronald Press Co., 1950.

47. Nelson, G. L., Mahoney, G. W. A., Berousek, E. R. and Graybill, F. "Hot Weather Shelters For Livestock," Ag. Eng. 35:638-645, 1954.

48. O'Neill, P. G. G. "Experiments to Simulate a Natural Wind Velocity Gradient in the Compressed Air Tunnel," NPL/aero 312, Mimo., Teddington, Meddlex, England, National Physics Laboratory, 1956.

49. Parmlee, G. V. and Huebscher, R. G. "Forced Convection Heat Transfer From Flat Surfaces," Transactions, American Society of Heating and Ventilating Engineers, 53:245, 1947.

50. Pohlhausen, E. "Heat Exchange Between Solid Bodies and Fluids By Slight Friction and Low Heat Conductivity," Z. Angew. Mathem. Mechan., 1:120, 1921.

51. Prandtl, Ludwig. Essentials of Fluid Dynamics. New York: Hafner Publishing Co., 1952.

52. Reynolds, Osborne. "On The Extent and Action of The Heating Surface For Steam Boilers," Proceedings, Manchester Literary and Philosophical Society, 14:7, 1874.

53. Rice, Charles E. Wind Forces on Open or Umbrella Type Shelters. Unpublished Masters Thesis, Oklahoma State University, Stillwater, Oklahoma, 1961.

54. Rouse, Hunter, (Editor). Advanced Mechanics of Fluids. New York: John Wiley and Sons, Inc., 1959.

55. Rowley, F. B., Algren, A. B. and Blackshaw, J. L. "Effect of Air Velocities on Surface Coefficients," Transactions, American Society of Heating and Ventilating Engineers, 36:123-136, 1930.

56. Rowley, F. B., Algren, A. B. and Blackshaw, J. L. "Surface Conductance Coefficients as Affected by Air Velocity, Temperature, and Surface Character," Transactions, American Society of Heating and Ventilating Engineers, 36:429-446, 1930.

57. Rowley, F. B. and Eckley, W. A. "Surface Coefficients as Affected by Direction of Wind," Transactions, American Society of Heating and Ventilating Engineers, 38:33-46, 1932.

58. Seban, R. A. and Doughty, D. L. "Heat Transfer to Turbulent Boundary Layers With Variable Free-Stream Velocity," Transactions, American Society of Mechanical Engineers, 78:217-223, 1956.

59. Slegel, L. and Hawkins, G. A. "Heat Transfer From A Vertical Plate to an Air Stream," Research Series No. 97, Purdue University Engineering Experiment Station, Lafayette, Indiana, 1946.

60. Sutton, O. G. Micrometeorology. New York: McGraw-Hill Book Co., Inc., 1953.

61. Weitz, C. E. Lamp Bulletin. General Electric Co., Lamp Division, Cleveland, Ohio, 1950.

Personal Correspondence

62. Kelly, C. F. Personal correspondence, September 21, 1960.

APPENDIX A

CURVES OF THERMAL CONDUCTIVITY AND VISCOSITY OF AIR USED FOR COMPUTATION OF DIMENSIONLESS PARAMETERS AND CURVES FOR CALIBRATION OF RADIATION INTENSITY APPLICABLE TO MODEL TESTS

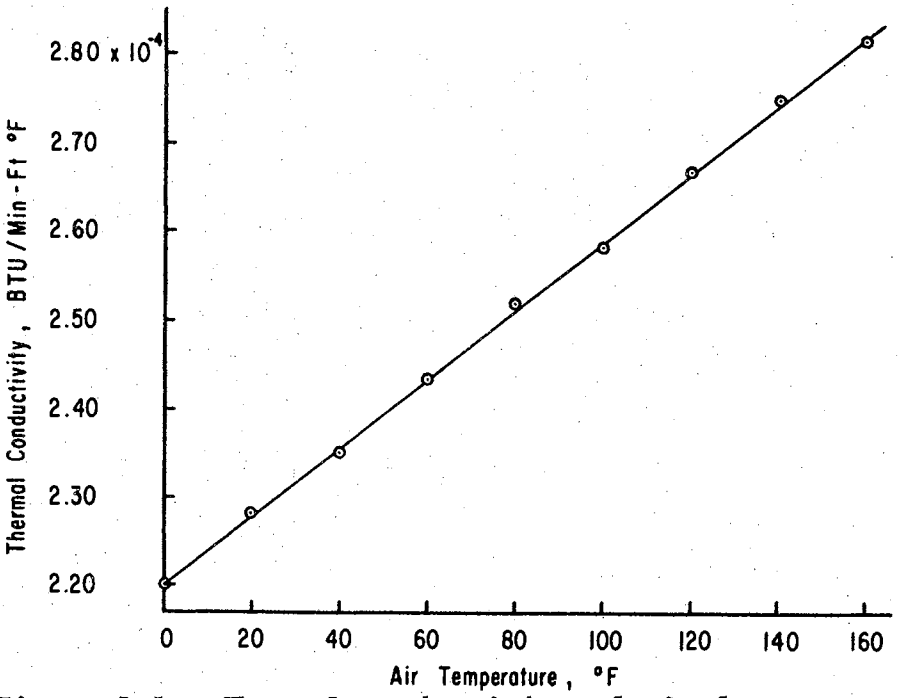

Figure A.1. Thermal conductivity of air for computation of dimensionless numbers. Plotted from data by Jakob and Hawkins (29, p. 12).

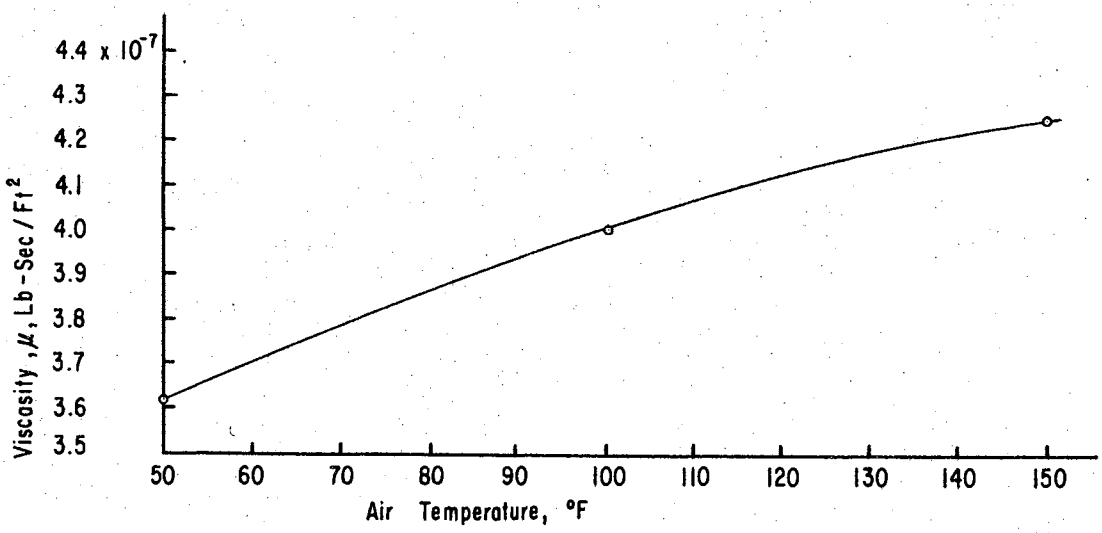

Figure A.2. Viscosity of air for use in computing dimensionless numbers. From data by Eshbach, O. W. Handbook of Engineering Fundamentals. 2nd ed. New York: John Wiley and Sons, Inc., 1958, page 606.

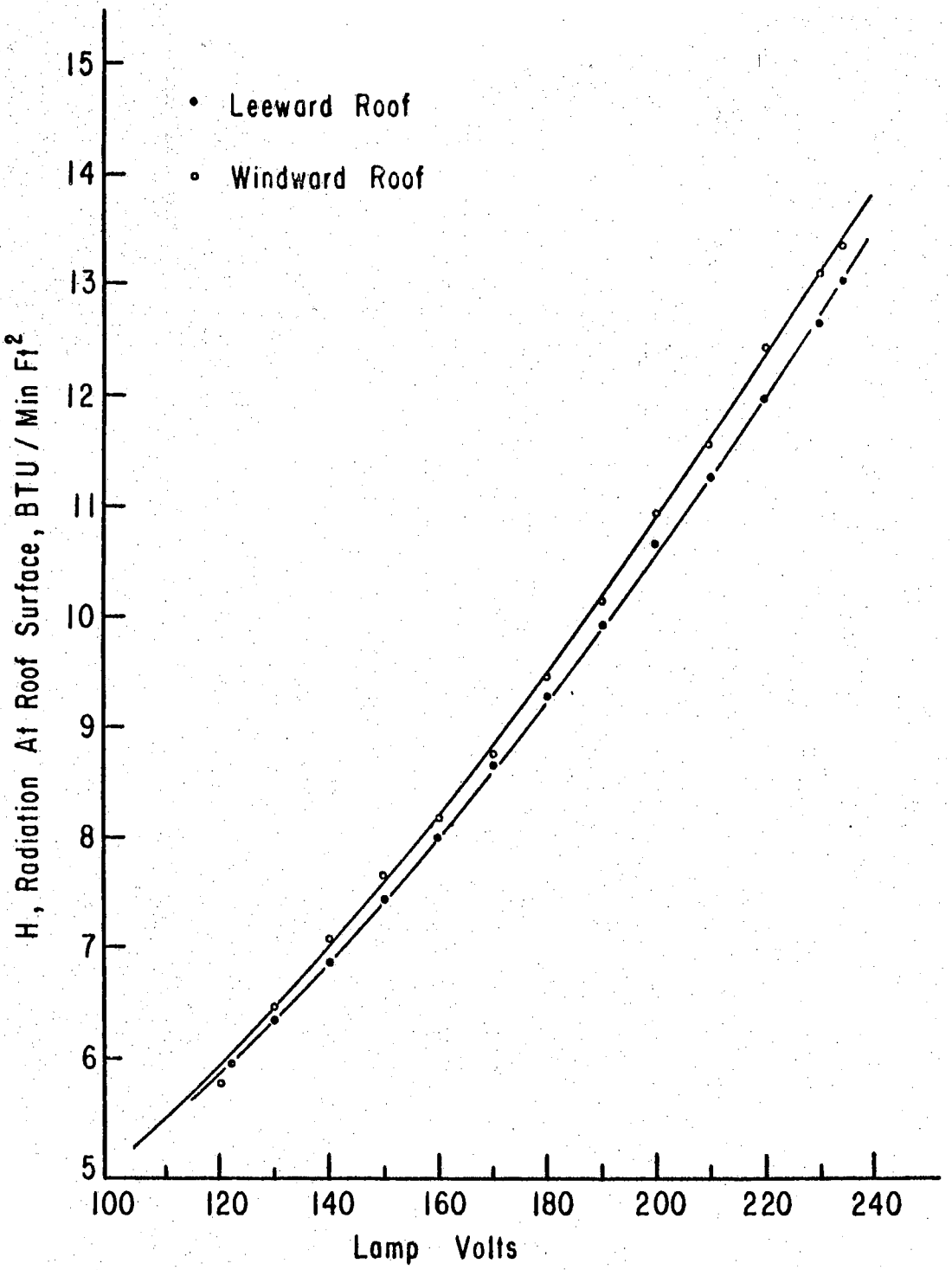

Figure A.3. Calibration curves for radiation incident on model roof for treatment conditions pi-five=5/12, pi-seven=0.264.

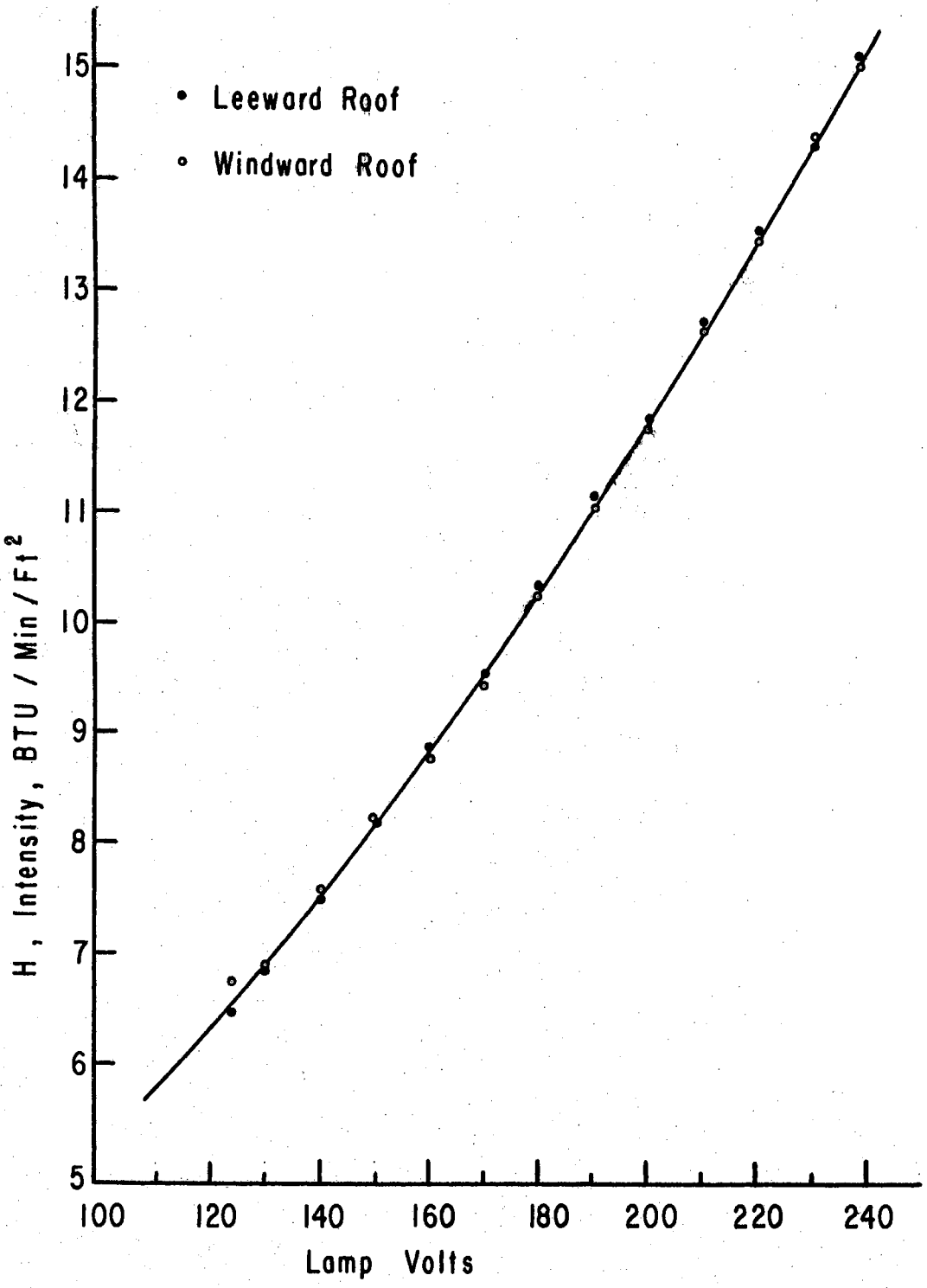

Figure A.4. Calibration curves for radiation incident on model roof for treatment conditions pi-five=4/12, pi-seven=0.75.

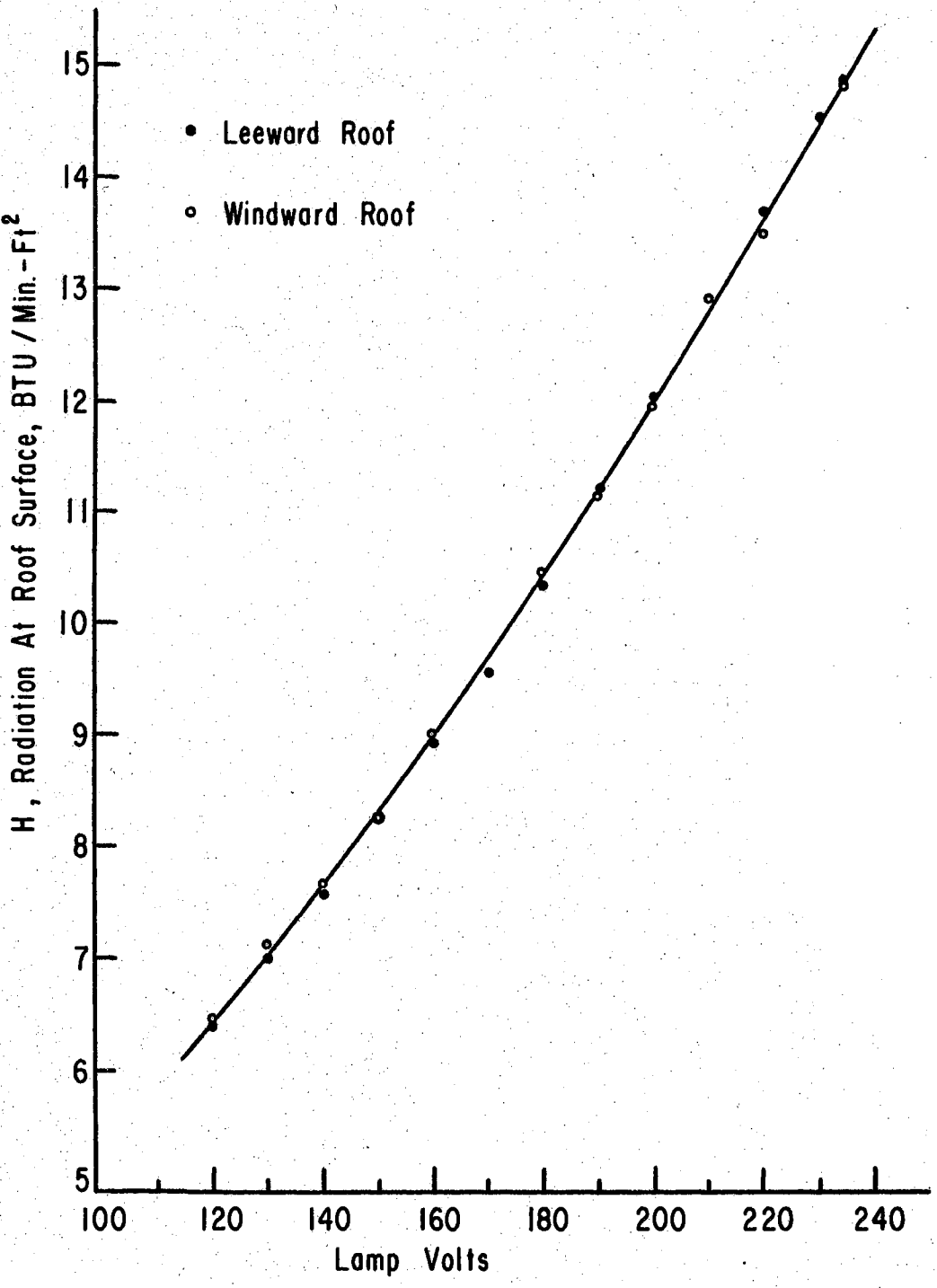

Figure A.5. Calibration curves for radiation incident on model roof for treatment conditions pi-five=3/12, pi-seven=0.264.

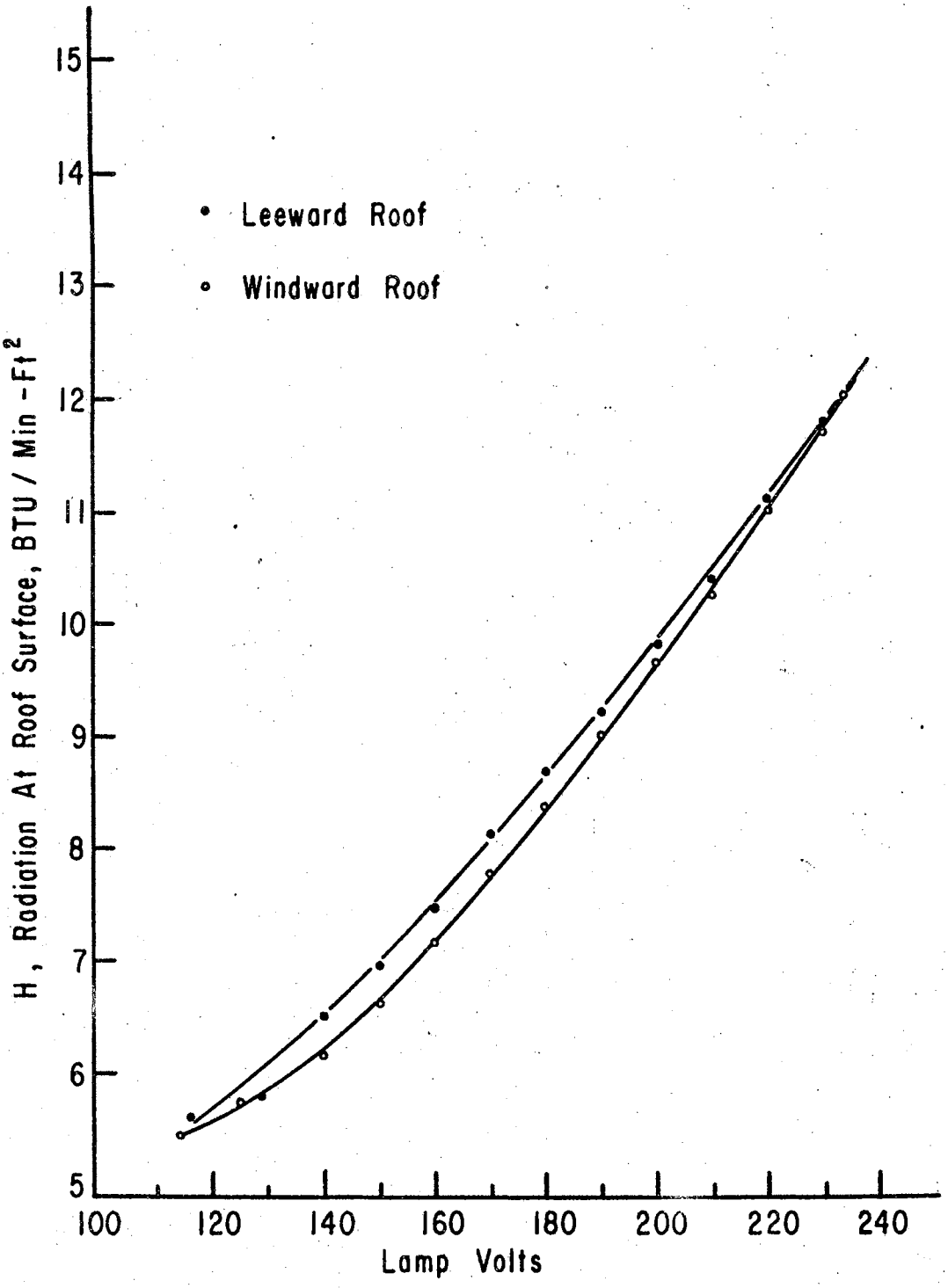

Figure A.6. Calibration curves for radiation incident on model roof for treatment conditions pi-five=4/12, pi-seven=0.264.

APPENDIX B

VALUES OF THE DIMENSIONLESS PARAMETERS FOR THE EXPERIMENTAL OBSERVATIONS FOR THE THREE TEST SHELTER SYSTEMS

Explanation of the Contents of the Tables and Data Coding Scheme

For each observation of surface temperature made in the investigation there was an associated value of air temperature, other air properties, wind velocity, radiation intensity, and distance of roof slope to point temperature was measured. Rather than a presentation of values of surface temperature, air temperature, wind velocity, etc., the values of the dimensionless groups $\pi_1 = k\Delta t/Hx$, $\pi_2 = t_a/\Delta t$, $\pi_3 = V\rho x/\mu$, and $\pi_4 = x/t$ as computed by the IBM 650 Computer are presented in this appendix. Each table contains the values corresponding to a particular shelter treatment defined by values of π_5 to π_9 as was given in Table IV. In all three test systems the roof thickness t was 0.00157 feet so that a tabulated value of π_4 can be solved to yield the value of x, distance of roof slope to point t_s was measured.

Each value of the four π terms listed in the table is identified with a code number located in the left-most column in the table. The first two digits from left to right in a code number identify the test system and treatment as defined in Table B.I. Third digit has no meaning. For the model system the fourth digit from the left denotes the test conditions, i.e. for the model system a one in the fourth place indicates observations made with wind velocity constant and radiation intensity changing from run to run. A two in the fourth place indicates observations made with radiation intensity constant and wind velocity different for each run.

Usually eight runs were made; the fifth digit denotes run number. The sixth digit tells the roof side; a one denotes the windward roof, a two the leeward roof. The seventh place was not used. Digits in the eighth and ninth place denote a thermocouple junction number. Junctions one to eight were located along the windward roof, and nine to sixteen along the leeward roof.

For the 8 ft x 8 ft shelter and the full size system the coding scheme is similar to the model coding scheme with a few exceptions. For the intermediate size shelter and the full size shelter the fourth digit from the left gives the day of the observations. The date has no special signifiance. No control on test conditions was possible for these observations.

TABLE B.I

SHELTER TREATMENT SCHEDULE IDENTIFYING DATA CODE

Shelter Treatment No.	Two Left-Most Digits in Code Number	Pi Term Values $\pi_5=\theta$	$\pi_6=r/L$	$\pi_7=h/L$	$\pi_8=\alpha$ $\pi_9=\epsilon$
		Model Shelter			
1	04	4/12	0.0989	0.264	AL*
2	02	4/12	0.0989	0.264	G
3	05	4/12	0.0989	0.264	PS
4	03	4/12	flat	0.264	G
5	06	4/12	0.1978	0.264	G
6	07	3/12	0.0989	0.264	G
7	08	5/12	0.0989	0.264	G
8	01	4/12	0.0989	0.750	G
		Intermediate Size Shelter			
12	30	4/12	flat	0.750	G
		Full Size Shelter			
9	52	4/12	0.0989	0.264	AL
10	51	4/12	0.0989	0.264	PS
11	53	4/12	0.0989	0.264	G

*AL means aluminum roofing, PS white painted steel, G plain, galvanized steel in aged condition. Numerical value of absorptivity and emissivity not needed.

TABLE B.II

VALUES OF THE FOUR DIMENSIONLESS GROUPS FOR MODEL TREATMENT NO. 1 WINDWARD ROOF

CODE	k Δt/Hx	$t_a/\Delta t$	$V\rho x/\mu$	x/t
0401110010	0.0006475	263.3	13,400	39.80
0401110020	0.0004752	181.6	26,490	78.66
0401110030	0.0003537	131.6	49,080	145.7
0401110040	0.0002552	107.4	83,350	247.4
0401110050	0.0002132	95.76	111,900	332.4
0401110060	0.0001949	83.60	140,300	416.5
0401110070	0.0001786	75.24	170,100	505.0
0401110080	0.0001541	75.24	197,100	585.3
0401210010	0.0007107	250.9	13,400	39.80
0401210020	0.0004453	202.6	26,490	78.66
0401210030	0.0003328	146.3	49,080	145.7
0401210040	0.0002341	122.5	83,350	247.4
0401210050	0.0002066	103.3	111,900	332.4
0401210060	0.0001876	90.86	140,300	416.5
0401210070	0.0001733	81.07	170,100	505.0
0401210080	0.0001519	79.84	197,100	585.3
0401310010	0.0005400	351.1	13,400	39.80
0401310020	0.0003643	263.3	26,490	78.66
0401310030	0.0002950	175.5	49,080	145.7
0401310040	0.0002258	135.0	83,350	247.4
0401310050	0.0002025	112.0	111,900	332.4
0401310060	0.0001823	99.39	140,300	416.5
0401310070	0.0001702	87.79	170,100	505.0
0401310080	0.0001468	87.79	197,100	585.3
0401410010	0.0006997	309.7	13,400	39.80
0401410020	0.0004374	250.7	26,490	78.66
0401410030	0.0003260	181.5	49,080	145.7
0401410040	0.0002185	159.5	83,350	247.4
0401410050	0.0001872	138.5	111,900	332.4
0401410060	0.0001770	117.0	140,300	416.5
0401410070	0.0001654	103.2	170,100	505.0
0401410080	0.0001427	103.2	197,100	585.3
0401510010	0.0006679	375.9	13,400	39.80
0401510020	0.0003380	375.9	26,490	78.66
0401510030	0.0002476	277.0	49,080	145.7
0401510040	0.0002072	194.9	83,350	247.4
0401510050	0.0001828	164.4	111,900	332.4
0401510060	0.0001595	150.3	140,300	416.5
0401510070	0.0001466	134.9	170,100	505.0
0401510080	0.0001265	134.9	197,100	585.3
0401610010	0.0004470	751.9	13,400	39.80
0401610020	0.0002909	584.8	26,490	78.66
0401610030	0.0001744	526.3	49,080	145.7
0401610040	0.0001130	478.5	83,350	247.4
0401610050	0.0001223	328.9	111,900	332.4
0401610060	0.0001159	277.0	140,300	416.5
0401610070	0.0001107	239.2	170,100	505.0
0401610080	0.00009556	239.2	197,100	585.3
0401710010	0.0004114	657.8	13,400	39.80
0401710020	0.0002082	657.8	26,490	78.66
0401710030	0.0001545	478.4	49,080	145.7
0401710040	0.0001571	276.9	83,350	247.4
0401710050	0.0001477	219.2	111,900	332.4
0401710060	0.0001326	194.9	140,300	416.5
0401710070	0.0001175	181.4	170,100	505.0
0401710080	0.0001014	181.4	197,100	585.3
0401810010	0.0006133	328.8	13,400	39.80
0401810020	0.0003880	263.0	26,490	78.66
0401810030	0.0003141	175.3	49,080	145.7
0401810040	0.0002281	142.2	83,350	247.4
0401810050	0.0002019	119.5	111,900	332.4
0401810060	0.0001795	107.3	140,300	416.5
0401810070	0.0001661	95.67	170,100	505.0
0401810080	0.0001433	95.67	197,100	585.3

CODE	k Δt/Hx	$t_a/\Delta t$	$V\rho x/\mu$	x/t
0402110010	0.004829	36.82	2,229	39.80
0402110020	0.002666	33.75	4,406	78.66
0402110030	0.001623	29.91	8,163	145.7
0402110040	0.001140	25.07	13,860	247.4
0402110050	0.0009663	22.03	18,620	332.4
0402110060	0.0008616	19.72	23,330	416.5
0402110070	0.0007745	18.09	28,290	505.0
0402110080	0.0006798	17.79	32,780	585.3
0402210010	0.002634	67.69	3,966	39.80
0402210020	0.001521	59.32	7,837	78.66
0402210030	0.001005	48.43	14,520	145.7
0402210040	0.0007442	38.53	24,650	247.4
0402210050	0.0006428	33.20	33,120	332.4
0402210060	0.0005905	28.85	41,500	416.5
0402210070	0.0005376	26.13	50,320	505.0
0402210080	0.0004777	25.38	58,320	585.3
0402310010	0.002127	83.83	5,124	39.80
0402310020	0.001247	72.35	10,120	78.66
0402310030	0.0008302	58.68	18,760	145.7
0402310040	0.0006302	45.53	31,850	247.4
0402310050	0.0005418	39.41	42,800	332.4
0402310060	0.0004937	34.52	53,620	416.5
0402310070	0.0005323	26.40	65,020	505.0
0402310080	0.0003996	30.35	75,350	585.3
0402410010	0.001722	103.6	6,202	39.80
0402410020	0.001025	88.06	12,250	78.66
0402410030	0.0006918	70.45	22,700	145.7
0402410040	0.0005324	53.91	38,550	247.4
0402410050	0.0004609	46.35	51,800	332.4
0402410060	0.0004195	40.64	64,900	416.5
0402410070	0.0003832	36.69	78,690	505.0
0402410080	0.0003399	35.70	91,190	585.3
0402510010	0.001350	132.1	7,678	39.80
0402510020	0.0008374	107.8	15,170	78.66
0402510030	0.0005811	83.90	28,110	145.7
0402510040	0.0004454	64.46	47,730	247.4
0402510050	0.0003760	56.83	64,130	332.4
0402510060	0.0003453	49.40	80,350	416.5
0402510070	0.0003167	44.41	97,420	505.0
0402510080	0.0002801	43.32	112,900	585.3
0402610010	0.001181	150.8	9,910	39.80
0402610020	0.0007177	125.7	19,580	78.66
0402610030	0.0004889	99.62	36,270	145.7
0402610040	0.0003585	79.99	61,600	247.4
0402610050	0.0003072	69.47	82,760	332.4
0402610060	0.0002840	59.99	103,600	416.5
0402610070	0.0002634	53.33	125,700	505.0
0402610080	0.0002319	52.27	145,700	585.3
0402710010	0.001013	176.0	10,830	39.80
0402710020	0.0006665	135.4	21,410	78.66
0402710030	0.0004520	107.8	39,670	145.7
0402710040	0.0003368	85.20	67,360	247.4
0402710050	0.0002830	75.47	90,520	332.4
0402710060	0.0002646	64.42	113,400	416.5
0402710070	0.0002422	58.05	137,500	505.0
0402710080	0.0002112	57.42	159,300	585.3
0402810010	0.003951	45.17	2,748	39.80
0402810020	0.002221	40.66	5,431	78.66
0402810030	0.001374	35.47	10,060	145.7
0402810040	0.0009833	29.20	17,080	247.4
0402810050	0.0008369	25.53	22,950	332.4
0402810060	0.0007551	22.58	28,760	416.5
0402810070	0.0006281	22.39	34,870	505.0
0402810080	0.0005971	20.33	40,410	585.3

TABLE B.III

VALUES OF THE FOUR DIMENSIONLESS GROUPS FOR MODEL TREATMENT NO. 2 WINDWARD ROOF

CODE	$k\Delta t/Hx$	$t_a/\Delta t$	$v\rho x/\mu$	x/t
0201110010	0.002684	141.2	8,126	39.80
0201110020	0.001752	109.5	16,050	78.66
0201110030	0.001312	78.93	29,740	145.7
0201110040	0.001011	60.31	50,510	247.4
0201110050	0.0008628	52.62	67,870	332.4
0201110060	0.0007224	50.16	85,030	416.5
0201110070	0.0006125	48.79	103,100	505.0
0201110080	0.0005958	43.28	119,400	585.3
0201210010	0.003131	107.3	8,126	39.80
0201210020	0.002028	83.87	16,050	78.66
0201210030	0.001573	58.34	29,740	145.7
0201210040	0.001188	45.49	50,510	247.4
0201210050	0.001019	39.46	67,870	332.4
0201210060	0.0008499	37.80	85,030	416.5
0201210070	0.0007157	37.02	103,100	505.0
0201210080	0.0007028	32.53	119,400	585.3
0201310010	0.003252	89.46	8,126	39.80
0201310020	0.002166	67.94	16,050	78.66
0201310030	0.001658	47.92	29,740	145.7
0201310040	0.001229	38.07	50,510	247.4
0201310050	0.001064	32.73	67,870	332.4
0201310060	0.0008805	31.57	85,030	416.5
0201310070	0.0007561	30.32	103,100	505.0
0201310080	0.0007372	26.83	119,400	585.3
0201410010	0.003669	68.84	8,126	39.80
0201410020	0.002333	54.79	16,050	78.66
0201410030	0.001812	38.08	29,740	145.7
0201410040	0.001339	30.33	50,510	247.4
0201410050	0.001143	26.45	67,870	332.4
0201410060	0.0009576	25.21	85,030	416.5
0201410070	0.0008157	24.40	103,100	505.0
0201410080	0.0007966	21.56	119,400	585.3
0201510010	0.003945	55.94	8,126	39.80
0201510020	0.002599	42.96	16,050	78.66
0201510030	0.001964	30.69	29,740	145.7
0201510040	0.001454	24.41	50,510	247.4
0201510050	0.001244	21.22	67,870	332.4
0201510060	0.001036	20.34	85,030	416.5
0201510070	0.0008841	19.67	103,100	505.0
0201510080	0.0008607	17.43	119,400	585.3
0201610010	0.004053	50.66	8,126	39.80
0201610020	0.002632	39.49	16,050	78.66
0201610030	0.001776	31.59	29,740	145.7
0201610040	0.001452	22.75	50,510	247.4
0201610050	0.001250	19.67	67,870	332.4
0201610060	0.001048	18.71	85,030	416.5
0201610070	0.0008922	18.14	103,100	505.0
0201610080	0.0008739	15.98	119,400	585.3
0201710010	0.004172	46.71	8,126	39.80
0201710020	0.002680	36.79	16,050	78.66
0201710030	0.002041	26.07	29,740	145.7
0201710040	0.001523	20.58	50,510	247.4
0201710050	0.001307	17.84	67,870	332.4
0201710060	0.001092	17.05	85,030	416.5
0201710070	0.0009264	16.57	103,100	505.0
0201710080	0.0008981	14.75	119,400	585.3
0201810010	0.004368	40.39	8,126	39.80
0201810020	0.002792	31.98	16,050	78.66
0201810030	0.002108	22.86	29,740	145.7
0201810040	0.001558	18.21	50,510	247.4
0201810050	0.001341	15.75	67,870	332.4
0201810060	0.001130	14.92	85,030	416.5
0201810070	0.0009682	14.36	103,100	505.0
0201810080	0.0009449	12.70	119,400	585.3

CODE	$k\Delta t/Hx$	$t_a/\Delta t$	$v\rho x/\mu$	x/t
0202110010	0.006932	26.38	4,576	39.80
0202110020	0.004179	22.15	9,043	78.66
0202110030	0.003026	16.51	16,750	145.7
0202110040	0.002285	12.87	28,450	247.4
0202110050	0.001973	11.09	38,220	332.4
0202110060	0.001669	10.47	47,890	416.5
0202110070	0.001510	9.544	58,070	505.0
0202110080	0.001386	8.971	67,290	585.3
0202210010	0.005199	35.18	6,500	39.80
0202210020	0.003233	28.63	12,840	78.66
0202210030	0.002385	20.94	23,790	145.7
0202210040	0.001798	16.36	40,400	247.4
0202210050	0.001582	13.83	54,290	332.4
0202210060	0.001328	13.16	68,010	416.5
0202210070	0.001162	12.40	82,470	505.0
0202210080	0.001100	11.30	95,580	585.3
0202310010	0.004350	42.03	7,865	39.80
0202310020	0.002768	33.42	15,540	78.66
0202310030	0.002098	23.80	28,790	145.7
0202310040	0.001569	18.74	48,890	247.4
0202310050	0.001350	16.20	65,690	332.4
0202310060	0.001143	15.28	82,300	416.5
0202310070	0.0009803	14.70	99,790	505.0
0202310080	0.0009568	12.99	115,600	585.3
0202410010	0.003534	51.74	10,260	39.80
0202410020	0.002304	40.16	20,290	78.66
0202410030	0.001726	28.93	37,590	145.7
0202410040	0.001290	22.80	63,830	247.4
0202410050	0.001098	19.93	85,770	332.4
0202410060	0.0009288	18.81	107,400	416.5
0202410070	0.0007928	18.18	130,300	505.0
0202410080	0.0007742	16.06	151,000	585.3
0202510010	0.003092	59.14	12,250	39.80
0202510020	0.002046	45.22	24,220	78.66
0202510030	0.001541	32.42	44,870	145.7
0202510040	0.001148	25.62	76,190	247.4
0202510050	0.0009847	22.23	102,300	332.4
0202510060	0.0008216	21.27	128,200	416.5
0202510070	0.0007098	20.30	155,500	505.0
0202510080	0.0006910	17.99	180,200	585.3
0202610010	0.002752	66.44	14,240	39.80
0202610020	0.001788	51.74	28,140	78.66
0202610030	0.001373	36.36	52,130	145.7
0202610040	0.001016	28.93	88,520	247.4
0202610050	0.0008748	25.03	118,900	332.4
0202610060	0.0007307	23.91	149,000	416.5
0202610070	0.0006294	22.90	180,600	505.0
0202610080	0.0005963	20.86	209,400	585.3
0202710010	0.002548	71.75	15,630	39.80
0202710020	0.001651	56.06	30,890	78.66
0202710030	0.001253	39.86	57,240	145.7
0202710040	0.0009349	31.47	97,190	247.4
0202710050	0.0008138	26.90	130,500	332.4
0202710060	0.0006722	25.99	163,600	416.5
0202710070	0.0005705	25.26	198,400	505.0
0202710080	0.0005223	23.81	229,900	585.3
0202810010	0.002378	76.81	17,590	39.80
0202810020	0.001530	60.41	34,770	78.66
0202810030	0.001123	44.43	64,410	145.7
0202810040	0.0008528	34.46	109,300	247.4
0202810050	0.0007324	29.87	146,900	332.4
0202810060	0.0005975	29.22	184,100	416.5
0202810070	0.0004955	29.06	223,200	505.0
0202810080	0.0004414	28.15	258,700	585.3

TABLE B.IV

VALUES OF THE FOUR DIMENSIONLESS GROUPS FOR MODEL TREATMENT NO. 3 WINDWARD ROOF

CODE	$k\Delta t/Hx$	$t_a/\Delta t$	$V\rho x/\mu$	x/t
0501110010	0.002477	152.6	8.538	39.80
0501110020	0.001540	124.2	16.870	78.66
0501110030	0.001043	98.92	31.250	145.7
0501110040	0.0007514	80.93	53.070	247.4
0501110050	0.0006778	66.77	71.310	332.4
0501110060	0.0006628	54.50	89.340	416.5
0501110070	0.0006079	49.00	108.300	505.0
0501110080	0.0005246	49.00	125.500	585.3
0501210010	0.002406	144.3	8.538	39.80
0501210020	0.001481	118.7	16.870	78.66
0501210030	0.001030	92.10	31.250	145.7
0501210040	0.0007637	73.17	53.070	247.4
0501210050	0.0006930	60.02	71.310	332.4
0501210060	0.0006774	49.00	89.340	416.5
0501210070	0.0006202	44.14	108.300	505.0
0501210080	0.0005351	44.14	125.500	585.3
0501310010	0.002430	118.7	8.538	39.80
0501310020	0.001475	98.92	16.870	78.66
0501310030	0.001032	76.31	31.250	145.7
0501310040	0.0007645	60.70	53.070	247.4
0501310050	0.0007048	49.00	71.310	332.4
0501310060	0.0006916	39.86	89.340	416.5
0501310070	0.0006257	36.33	108.300	505.0
0501310080	0.0005399	36.33	125.500	585.3
0501410010	0.002578	97.14	8.538	39.80
0501410020	0.001542	82.19	16.870	78.66
0501410030	0.001075	63.60	31.250	145.7
0501410040	0.0007994	50.40	53.070	247.4
0501410050	0.0007352	40.78	71.310	332.4
0501410060	0.0007212	33.18	89.340	416.5
0501410070	0.0006539	30.18	108.300	505.0
0501410080	0.0005643	30.18	125.500	585.3
0501510010	0.002538	86.20	8.538	39.80
0501510020	0.001574	70.32	16.870	78.66
0501510030	0.001084	55.10	31.250	145.7
0501510040	0.0008102	43.45	53.070	247.4
0501510050	0.0007501	34.93	71.310	332.4
0501510060	0.0007356	28.43	89.340	416.5
0501510070	0.0006648	25.94	108.300	505.0
0501510080	0.0005764	25.82	125.500	585.3
0501610010	0.002629	77.46	8.538	39.80
0501610020	0.001600	64.39	16.870	78.66
0501610030	0.001103	50.42	31.250	145.7
0501610040	0.0008215	39.88	53.070	247.4
0501610050	0.0007619	32.00	71.310	332.4
0501610060	0.0007392	26.32	89.340	416.5
0501610070	0.0006817	23.54	108.300	505.0
0501610080	0.0005909	23.44	125.500	585.3
0501710010	0.002711	71.27	8.538	39.80
0501710020	0.001646	59.39	16.870	78.66
0501710030	0.001125	46.89	31.250	145.7
0501710040	0.0008258	37.64	53.070	247.4
0501710050	0.0007618	30.37	71.310	332.4
0501710060	0.0007531	24.52	89.340	416.5
0501710070	0.0006866	22.18	108.300	505.0
0501710080	0.0005925	22.18	125.500	585.3
0501810010	0.002742	65.23	8.538	39.80
0501810020	0.001658	54.58	16.870	78.66
0501810030	0.001141	42.79	31.250	145.7
0501810040	0.0008499	33.85	53.070	247.4
0501810050	0.0007887	27.15	71.310	332.4
0501810060	0.0007701	22.19	89.340	416.5
0501810070	0.0007036	20.03	108.300	505.0
0501810080	0.0006072	20.03	125.500	585.3

CODE	$k\Delta t/Hx$	$t_a/\Delta t$	$V\rho x/\mu$	x/t
0502110010	0.004403	41.44	4.959	39.80
0502110020	0.002556	36.12	9.800	78.66
0502110030	0.001697	29.37	18.150	145.7
0502110040	0.001268	23.14	30.830	247.4
0502110050	0.001132	19.29	41.420	332.4
0502110060	0.001099	15.86	51.900	416.5
0502110070	0.0009980	14.40	62.930	505.0
0502110080	0.0008658	14.33	72.930	585.3
0502210010	0.003618	50.42	6.588	39.80
0502210020	0.002159	42.75	13.010	78.66
0502210030	0.001473	33.82	24.110	145.7
0502210040	0.001092	26.85	40.950	247.4
0502210050	0.0009726	22.45	55.020	332.4
0502210060	0.0009688	17.99	68.940	416.5
0502210070	0.0008797	16.34	83.590	505.0
0502210080	0.0007683	16.14	96.870	585.3
0502310010	0.003003	60.76	8.383	39.80
0502310020	0.001831	50.44	16.560	78.66
0502310030	0.001258	39.60	30.680	145.7
0502310040	0.0009280	31.63	52.100	247.4
0502310050	0.0008378	26.08	70.010	332.4
0502310060	0.0008481	20.56	87.720	416.5
0502310070	0.0007721	18.63	106.300	505.0
0502310080	0.0006685	18.56	123.200	585.3
0502410010	0.002628	69.44	9.597	39.80
0502410020	0.001641	56.28	18.960	78.66
0502410030	0.001118	44.55	35.130	145.7
0502410040	0.0008291	35.40	59.650	247.4
0502410050	0.0007601	28.74	80.150	332.4
0502410060	0.0007633	22.85	100.400	416.5
0502410070	0.0006994	20.56	121.700	505.0
0502410080	0.0006012	20.64	141.100	585.3
0502510010	0.002355	77.49	11.690	39.80
0502510020	0.001433	64.42	23.100	78.66
0502510030	0.0009697	51.41	42.790	145.7
0502510040	0.0007193	40.81	72.660	247.4
0502510050	0.0006620	33.00	97.630	332.4
0502510060	0.0006687	26.08	122.300	416.5
0502510070	0.0005999	23.97	148.300	505.0
0502510080	0.0005107	24.30	171.800	585.3
0502610010	0.002150	84.87	13.180	39.80
0502610020	0.001312	70.35	26.050	78.66
0502610030	0.0009231	54.00	48.270	145.7
0502610040	0.0006644	44.18	81.970	247.4
0502610050	0.0006171	35.40	110.100	332.4
0502610060	0.0006197	28.14	137.900	416.5
0502610070	0.0005595	25.70	167.300	505.0
0502610080	0.0004828	25.70	193.900	585.3
0502710010	0.001911	95.48	15.690	39.80
0502710020	0.001191	77.49	31.000	78.66
0502710030	0.0008112	61.45	57.430	145.7
0502710040	0.0006040	48.60	97.530	247.4
0502710050	0.0005476	39.90	131.000	332.4
0502710060	0.0005545	31.45	164.100	416.5
0502710070	0.0004869	29.54	199.000	505.0
0502710080	0.0004132	30.03	230.700	585.3
0502810010	0.001774	102.8	17.750	39.80
0502810020	0.001105	83.54	35.080	78.66
0502810030	0.0007272	68.55	65.000	145.7
0502810040	0.0005491	53.46	110.300	247.4
0502810050	0.0004945	44.18	148.300	332.4
0502810060	0.0004990	34.94	185.800	416.5
0502810070	0.0004331	33.21	225.300	505.0
0502810080	0.0003621	34.27	261.100	585.3

TABLE B.V

VALUES OF THE FOUR DIMENSIONLESS GROUPS FOR MODEL TREATMENT NO. 4 WINDWARD ROOF

CODE	$k\Delta t/Hx$	$t_a/\Delta t$	$V\rho x/\mu$	x/t
0301110010	0.002506	144.4	9,442	39.80
0301110020	0.001761	104.0	18,650	78.66
0301110030	0.001255	78.81	34,560	145.7
0301110040	0.0008961	65.02	58,690	247.4
0301110050	0.0007836	55.33	78,860	332.4
0301110060	0.0007119	48.61	98,800	416.5
0301110070	0.0006091	46.86	119,800	505.0
0301110080	0.0005066	48.61	138,800	585.3
0301210010	0.002986	110.7	9,442	39.80
0301210020	0.002025	82.61	18,650	78.66
0301210030	0.001492	60.52	34,560	145.7
0301210040	0.001062	50.04	58,690	247.4
0301210050	0.0009204	43.01	78,860	332.4
0301210060	0.0008500	37.17	98,800	416.5
0301210070	0.0007210	36.14	119,800	505.0
0301210080	0.0005962	37.71	138,800	585.3
0301310010	0.003271	84.01	9,442	39.80
0301310020	0.002162	64.30	18,650	78.66
0301310030	0.001585	47.35	34,560	145.7
0301310040	0.001137	38.87	58,690	247.4
0301310050	0.0009854	33.39	78,860	332.4
0301310060	0.0009075	28.93	98,800	416.5
0301310070	0.0007775	27.85	119,800	505.0
0301310080	0.0006494	28.77	138,800	585.3
0301410010	0.003480	68.57	9,442	39.80
0301410020	0.002387	50.60	18,650	78.66
0301410030	0.001713	38.04	34,560	145.7
0301410040	0.001222	31.39	58,690	247.4
0301410050	0.001058	27.00	78,860	332.4
0301410060	0.0009715	23.47	98,800	416.5
0301410070	0.0008445	22.27	119,800	505.0
0301410080	0.0007007	23.16	138,800	585.3
0301510010	0.003680	56.59	9,442	39.80
0301510020	0.002489	42.33	18,650	78.66
0301510030	0.001802	31.55	34,560	145.7
0301510040	0.001287	26.03	58,690	247.4
0301510050	0.001106	22.54	78,860	332.4
0301510060	0.001032	19.28	98,800	416.5
0301510070	0.0008795	18.66	119,800	505.0
0301510080	0.0007372	19.21	138,800	585.3
0301610010	0.003759	51.51	9,442	39.80
0301610020	0.002524	38.82	18,650	78.66
0301610030	0.001850	28.58	34,560	145.7
0301610040	0.001317	23.64	58,690	247.4
0301610050	0.001141	20.32	78,860	332.4
0301610060	0.001056	17.51	98,800	416.5
0301610070	0.0009066	16.83	119,800	505.0
0301610080	0.0007544	17.45	138,800	585.3
0301710010	0.003884	47.29	9,442	39.80
0301710020	0.002573	36.13	18,650	78.66
0301710030	0.001871	26.81	34,560	145.7
0301710040	0.001346	21.95	58,690	247.4
0301710050	0.001171	18.78	78,860	332.4
0301710060	0.001076	16.31	98,800	416.5
0301710070	0.0009296	15.57	119,800	505.0
0301710080	0.0007781	16.05	138,800	585.3
0301810010	0.004028	41.31	9,442	39.80
0301810020	0.002653	31.74	18,650	78.66
0301810030	0.001930	23.55	34,560	145.7
0301810040	0.001388	19.28	58,690	247.4
0301810050	0.001213	16.42	78,860	332.4
0301810060	0.001121	14.18	98,800	416.5
0301810070	0.0009676	13.55	119,800	505.0
0301810080	0.0008023	14.10	138,800	585.3

CODE	$k\Delta t/Hx$	$t_a/\Delta t$	$V\rho x/\mu$	x/t
0302110010	0.006355	28.41	5,060	39.80
0302110020	0.003990	22.90	10,000	78.66
0302110030	0.002757	17.89	18,520	145.7
0302110040	0.001984	14.63	31,450	247.4
0302110050	0.001713	12.62	42,260	332.4
0302110060	0.001597	10.80	52,950	416.5
0302110070	0.001400	10.16	64,210	505.0
0302110080	0.001187	10.33	74,410	585.3
0302210010	0.004655	38.76	7,760	39.80
0302210020	0.003026	30.17	15,330	78.66
0302210030	0.002153	22.89	28,410	145.7
0302210040	0.001558	18.63	48,240	247.4
0302210050	0.001346	16.04	64,810	332.4
0302210060	0.001253	13.75	81,200	416.5
0302210070	0.001090	13.04	98,460	505.0
0302210080	0.0009037	13.58	114,100	585.3
0302310010	0.004384	41.15	8,526	39.80
0302310020	0.002820	32.37	16,840	78.66
0302310030	0.002051	24.02	31,210	145.7
0302310040	0.001476	19.66	53,000	247.4
0302310050	0.001285	16.80	71,210	332.4
0302310060	0.001182	14.58	89,220	416.5
0302310070	0.001028	13.82	108,100	505.0
0302310080	0.0008528	14.38	125,300	585.3
0302410010	0.003432	52.52	11,540	39.80
0302410020	0.002321	39.29	22,810	78.66
0302410030	0.001689	29.14	42,270	145.7
0302410040	0.001208	24.00	71,770	247.4
0302410050	0.001033	20.88	96,440	332.4
0302410060	0.0009580	17.98	120,800	416.5
0302410070	0.0008330	17.05	146,500	505.0
0302410080	0.0006956	17.62	169,700	585.3
0302510010	0.003126	57.61	13,430	39.80
0302510020	0.002063	44.17	26,530	78.66
0302510030	0.001541	31.93	49,160	145.7
0302510040	0.001093	26.50	83,480	247.4
0302510050	0.0009318	23.14	112,100	332.4
0302510060	0.0008541	20.15	140,500	416.5
0302510070	0.0007419	19.13	170,400	505.0
0302510080	0.0006124	20.00	197,400	585.3
0302610010	0.002596	71.74	18,390	39.80
0302610020	0.001740	54.17	36,350	78.66
0302610030	0.001265	40.21	67,340	145.7
0302610040	0.0008918	33.60	114,300	247.4
0302610050	0.0007688	29.01	153,600	332.4
0302610060	0.0006974	25.52	192,500	416.5
0302610070	0.0005890	24.92	233,400	505.0
0302610080	0.0004724	26.81	270,500	585.3
0302710010	0.002582	69.89	18,390	39.80
0302710020	0.001719	53.11	36,350	78.66
0302710030	0.001253	39.34	67,340	145.7
0302710040	0.0008911	32.58	114,300	247.4
0302710050	0.0007568	28.55	153,600	332.4
0302710060	0.0006885	25.05	192,500	416.5
0302710070	0.0005839	24.36	233,400	505.0
0302710080	0.0004622	26.55	270,500	585.3
0302810010	0.005437	33.36	6,046	39.80
0302810020	0.003491	26.29	11,940	78.66
0302810030	0.002450	20.21	22,130	145.7
0302810040	0.001782	16.37	37,580	247.4
0302810050	0.001354	16.02	50,500	332.4
0302810060	0.001445	11.99	63,270	416.5
0302810070	0.001258	11.35	76,720	505.0
0302810080	0.001051	11.73	88,910	585.3

TABLE B.VI

VALUES OF THE FOUR DIMENSIONLESS GROUPS FOR MODEL TREATMENT NO. 5 WINDWARD ROOF

CODE	$k\Delta t/Hx$	$t_a/\Delta t$	$V\rho x/\mu$	x/t
0601110010	0.002621	144.5	8,393	39.80
0601110020	0.001757	109.1	16,580	78.66
0601110030	0.001180	87.70	30,720	145.7
0601110040	0.0008891	68.58	52,170	247.4
0601110050	0.0007550	60.11	70,100	332.4
0601110060	0.0007110	50.95	87,820	416.5
0601110070	0.0006310	47.34	106,400	505.0
0601110080	0.0005889	46.11	123,400	585.3
0601210010	0.002995	116.3	8,393	39.80
0601210020	0.002043	86.33	16,580	78.66
0601210030	0.001387	68.62	30,720	145.7
0601210040	0.001037	54.06	52,170	247.4
0601210050	0.0008653	48.22	70,100	332.4
0601210060	0.0008151	40.86	87,820	416.5
0601210070	0.0007390	37.17	106,400	505.0
0601210080	0.0006554	36.16	123,400	585.3
0601310010	0.003568	81.01	8,393	39.80
0601310020	0.002353	62.17	16,580	78.66
0601310030	0.001565	50.44	30,720	145.7
0601310040	0.001165	39.90	52,170	247.4
0601310050	0.0009840	35.17	70,100	332.4
0601310060	0.0009198	30.03	87,820	416.5
0601310070	0.0008310	27.42	106,400	505.0
0601310080	0.0007318	26.86	123,400	585.3
0601410010	0.003848	65.23	8,393	39.80
0601410020	0.002493	50.94	16,580	78.66
0601410030	0.001705	40.21	30,720	145.7
0601410040	0.001283	31.46	52,170	247.4
0601410050	0.001084	27.71	70,100	332.4
0601410060	0.001000	23.98	87,820	416.5
0601410070	0.0009136	21.65	106,400	505.0
0601410080	0.0007979	21.39	123,400	585.3
0601510010	0.004140	52.93	8,393	39.80
0601510020	0.002676	41.44	16,580	78.66
0601510030	0.001814	33.00	30,720	145.7
0601510040	0.001352	26.08	52,170	247.4
0601510050	0.001148	22.85	70,100	332.4
0601510060	0.001069	19.58	87,820	416.5
0601510070	0.0009596	18.00	106,400	505.0
0601510080	0.0008615	17.30	123,400	585.3
0601610010	0.004158	49.06	8,393	39.80
0601610020	0.002703	38.19	16,580	78.66
0601610030	0.001844	30.21	30,720	145.7
0601610040	0.001368	23.98	52,170	247.4
0601610050	0.001160	21.05	70,100	332.4
0601610060	0.001071	18.19	87,820	416.5
0601610070	0.0009803	16.40	106,400	505.0
0601610080	0.0008562	16.20	123,400	585.3
0601710010	0.004234	45.72	8,393	39.80
0601710020	0.002765	35.42	16,580	78.66
0601710030	0.001858	28.45	30,720	145.7
0601710040	0.001391	22.38	52,170	247.4
0601710050	0.001183	19.59	70,100	332.4
0601710060	0.001099	16.82	87,820	416.5
0601710070	0.0009927	15.37	106,400	505.0
0601710080	0.0008787	14.98	123,400	585.3
0601810010	0.004285	41.79	8,393	39.80
0601810020	0.002829	32.03	16,580	78.66
0601810030	0.001920	25.47	30,720	145.7
0601810040	0.001432	20.11	52,170	247.4
0601810050	0.001222	17.54	70,100	332.4
0601810060	0.001142	14.98	87,820	416.5
0601810070	0.001037	13.61	106,400	505.0
0601810080	0.0009016	13.50	123,400	585.3

CODE	$k\Delta t/Hx$	$t_a/\Delta t$	$V\rho x/\mu$	x/t
0602110010	0.006422	28.47	4,771	39.80
0602110020	0.004010	23.07	9,428	78.66
0602110030	0.002650	18.85	17,460	145.7
0602110040	0.002011	14.62	29,650	247.4
0602110050	0.001726	12.68	39,850	332.4
0602110060	0.001580	11.06	49,920	416.5
0602110070	0.001424	10.12	60,540	505.0
0602110080	0.001256	9.896	70,160	585.3
0602210010	0.005295	34.55	6,117	39.80
0602210020	0.003388	27.32	12,080	78.66
0602210030	0.002295	21.77	22,390	145.7
0602210040	0.001714	17.16	38,020	247.4
0602210050	0.001452	15.08	51,090	332.4
0602210060	0.001361	12.84	64,010	416.5
0602210070	0.001225	11.77	77,610	505.0
0602210080	0.001087	11.44	89,940	585.3
0602310010	0.004919	37.16	7,328	39.80
0602310020	0.003181	29.08	14,480	78.66
0602310030	0.002155	23.16	26,820	145.7
0602310040	0.001615	18.20	45,550	247.4
0602310050	0.001390	15.74	61,200	332.4
0602310060	0.001292	13.51	76,680	416.5
0602310070	0.001168	12.33	92,980	505.0
0602310080	0.001033	12.02	107,700	585.3
0602410010	0.004236	43.15	7,799	39.80
0602410020	0.002800	33.03	15,410	78.66
0602410030	0.001912	26.10	28,550	145.7
0602410040	0.001439	20.42	48,480	247.4
0602410050	0.001231	17.77	65,140	332.4
0602410060	0.001145	15.24	81,610	416.5
0602410070	0.001039	13.86	98,960	505.0
0602410080	0.0009107	13.65	114,600	585.3
0602510010	0.003381	53.99	10,090	39.80
0602510020	0.002109	43.81	19,940	78.66
0602510030	0.001567	31.82	36,950	145.7
0602510040	0.001181	24.86	62,740	247.4
0602510050	0.001006	21.73	84,300	332.4
0602510060	0.0009369	18.62	105,600	416.5
0602510070	0.0008454	17.02	128,000	505.0
0602510080	0.0007527	16.49	148,400	585.3
0602610010	0.002972	61.37	12,230	39.80
0602610020	0.002022	45.64	24,170	78.66
0602610030	0.001371	36.32	44,780	145.7
0602610040	0.001033	28.40	76,050	247.4
0602610050	0.0008630	25.30	102,100	332.4
0602610060	0.0008031	21.70	128,000	416.5
0602610070	0.0007161	20.07	155,200	505.0
0602610080	0.0006319	19.63	179,800	585.3
0602710010	0.002732	66.69	14,250	39.80
0602710020	0.001832	50.33	28,160	78.66
0602710030	0.001222	40.73	52,170	145.7
0602710040	0.0009122	32.14	88,590	247.4
0602710050	0.0009775	22.32	119,000	332.4
0602710060	0.0007051	24.70	149,100	416.5
0602710070	0.0006084	23.61	180,800	505.0
0602710080	0.0005297	23.40	209,500	585.3
0602810010	0.002493	73.06	16,210	39.80
0602810020	0.001694	54.42	32,030	78.66
0602810030	0.001147	43.36	59,340	145.7
0602810040	0.0008408	34.86	100,700	247.4
0602810050	0.0007076	30.83	135,300	332.4
0602810060	0.0006333	27.49	169,600	416.5
0602810070	0.0005357	26.80	205,600	505.0
0602810080	0.0004646	26.66	238,300	585.3

TABLE B.VII

VALUES OF THE FOUR DIMENSIONLESS GROUPS FOR MODEL TREATMENT NO. 6 WINDWARD ROOF

CODE	k Δt/Hx	$t_a/\Delta t$	$V\rho x/\mu$	x/t
0701110010	0.0031S4	101.9	8,154	39.80
0701110020	0.001934	84.18	16,110	78.66
0701110030	0.001557	56.42	29,850	145.7
0701110040	0.001180	43.83	50,690	247.4
0701110050	0.0009951	38.71	68,110	332.4
0701110060	0.0008174	37.61	85,330	416.5
0701110070	0.0007028	36.08	103,400	505.0
0701110080	0.0006436	33.99	119,900	585.3
0701210010	0.003221	87.03	8,154	39.80
0701210020	0.002111	67.20	16,110	78.66
0701210030	0.001745	43.87	29,850	145.7
0701210040	0.001299	34.69	50,690	247.4
0701210050	0.001100	30.51	68,110	332.4
0701210060	0.0008780	30.51	85,330	416.5
0701210070	0.0007574	29.16	103,400	505.0
0701210080	0.0006930	27.50	119,900	585.3
0701310010	0.003812	62.48	8,154	39.80
0701310020	0.002383	50.58	16,110	78.66
0701310030	0.001911	34.04	29,850	145.7
0701310040	0.001421	26.95	50,690	247.4
0701310050	0.001213	23.49	68,110	332.4
0701310060	0.0009858	23.09	85,330	416.5
0701310070	0.0008378	22.40	103,400	505.0
0701310080	0.0007748	20.90	119,900	585.3
0701410010	0.004030	50.58	8,154	39.80
0701410020	0.002544	40.54	16,110	78.66
0701410030	0.001960	28.40	29,850	145.7
0701410040	0.001556	21.07	50,690	247.4
0701410050	0.001319	18.50	68,110	332.4
0701410060	0.001045	18.63	85,330	416.5
0701410070	0.0008954	17.94	103,400	505.0
0701410080	0.0008144	17.02	119,900	585.3
0701510010	0.004272	41.51	8,154	39.80
0701510020	0.002770	32.40	16,110	78.66
0701510030	0.002352	20.59	29,850	145.7
0701510040	0.001820	15.67	50,690	247.4
0701510050	0.001534	13.83	68,110	332.4
0701510060	0.001154	14.67	85,330	416.5
0701510070	0.0009680	14.43	103,400	505.0
0701510080	0.0008467	14.24	119,900	585.3
0701610010	0.004467	37.70	8,154	39.80
0701610020	0.002902	29.36	16,110	78.66
0701610030	0.002778	16.56	29,850	145.7
0701610040	0.001911	14.17	50,690	247.4
0701610050	0.001615	12.47	68,110	332.4
0701610060	0.001202	13.39	85,330	416.5
0701610070	0.001021	12.99	103,400	505.0
0701610080	0.0009049	12.65	119,900	585.3
0701710010	0.004458	34.73	8,154	39.80
0701710020	0.002875	27.25	16,110	78.66
0701710030	0.002451	17.25	29,850	145.7
0701710040	0.001893	13.15	50,690	247.4
0701710050	0.001597	11.60	68,110	332.4
0701710060	0.001177	12.56	85,330	416.5
0701710070	0.001003	12.16	103,400	505.0
0701710080	0.0008759	12.02	119,900	585.3
0701810010	0.004553	30.91	8,154	39.80
0701810020	0.002920	24.38	16,110	78.66
0701810030	0.002502	15.36	29,850	145.7
0701810040	0.001941	11.65	50,690	247.4
0701810050	0.001648	10.22	68,110	332.4
0701810060	0.001214	11.07	85,330	416.5
0701810070	0.001032	10.74	103,400	505.0
0701810080	0.0008911	10.74	119,900	585.3

CODE	k Δt/Hx	$t_a/\Delta t$	$V\rho x/\mu$	x/t
0702110010	0.0005604	26.39	6,346	39.80
0702110020	0.0003545	20.87	12,540	78.66
0702110030	0.0002851	14.00	23,230	145.7
0702110040	0.0002139	10.99	39,450	247.4
0702110050	0.0001786	9.802	53,000	332.4
0702110060	0.0001430	9.766	66,410	416.5
0702110070	0.0001266	9.098	80,520	505.0
0702110080	0.0001100	9.037	93,320	585.3
0702210010	0.007060	20.71	4,815	39.80
0702210020	0.004671	15.84	9,515	78.66
0702210030	0.003834	10.42	17,620	145.7
0702210040	0.002726	8.630	29,930	247.4
0702210050	0.002144	8.167	40,210	332.4
0702210060	0.001688	8.281	50,380	416.5
0702210070	0.001504	7.661	61,090	505.0
0702210080	0.001285	7.739	70,800	585.3
0702310010	0.004972	29.43	7,166	39.80
0702310020	0.003211	23.06	14,160	78.66
0702310030	0.002769	14.43	26,230	145.7
0702310040	0.002130	11.05	44,540	247.4
0702310050	0.001743	10.05	59,850	332.4
0702310060	0.001323	10.56	74,980	416.5
0702310070	0.001156	9.975	90,920	505.0
0702310080	0.0009921	10.03	105,300	585.3
0702410010	0.004258	34.36	8,738	39.80
0702410020	0.002711	27.31	17,260	78.66
0702410030	0.002273	17.57	31,990	145.7
0702410040	0.001776	13.24	54,320	247.4
0702410050	0.001499	11.67	72,980	332.4
0702410060	0.001128	12.38	91,440	416.5
0702410070	0.0009786	11.78	110,800	505.0
0702410080	0.0008519	11.67	128,400	585.3
0702510010	0.004038	36.23	9,296	39.80
0702510020	0.002585	28.63	18,360	78.66
0702510030	0.002198	18.18	34,030	145.7
0702510040	0.001701	13.83	57,780	247.4
0702510050	0.001417	12.35	77,640	332.4
0702510060	0.001050	13.31	97,270	416.5
0702510070	0.0008877	12.99	117,900	505.0
0702510080	0.0008052	12.35	136,600	585.3
0702610010	0.003681	39.76	10,760	39.80
0702610020	0.002363	31.34	21,270	78.66
0702610030	0.002056	19.44	39,410	145.7
0702610040	0.001591	14.79	66,930	247.4
0702610050	0.001315	13.31	89,930	332.4
0702610060	0.0009582	14.59	112,600	416.5
0702610070	0.0008444	13.66	136,600	505.0
0702610080	0.0007249	13.73	158,300	585.3
0702710010	0.003269	44.80	12,500	39.80
0702710020	0.002085	35.54	24,700	78.66
0702710030	0.001771	22.59	45,770	145.7
0702710040	0.001347	17.48	77,710	247.4
0702710050	0.001128	15.54	104,400	332.4
0702710060	0.0008427	16.61	130,800	416.5
0702710070	0.0007188	16.05	158,600	505.0
0702710080	0.0006315	15.77	183,800	585.3
0702810010	0.002472	59.29	17,820	39.80
0702810020	0.001584	46.81	35,220	78.66
0702810030	0.001283	31.20	65,260	145.7
0702810040	0.0009546	24.70	110,800	247.4
0702810050	0.0008256	21.26	148,900	332.4
0702810060	0.0005828	24.04	186,500	416.5
0702810070	0.0004915	23.51	226,200	505.0
0702810080	0.0004110	24.25	262,100	585.3

TABLE B.VIII

VALUES OF THE FOUR DIMENSIONLESS GROUPS FOR MODEL TREATMENT NO. 7 WINDWARD ROOF

CODE	k Δt/Hx	$t_a/\Delta t$	V ρx/μ	x/t
0801110010	0.003155	114.2	8.068	39.80
0801110020	0.001936	94.20	15.940	78.66
0801110030	0.001338	73.56	29.530	145.7
0801110040	0.0009938	58.36	50.150	247.4
0801110050	0.0008521	50.65	67.380	332.4
0801110060	0.0007571	45.50	84.430	416.5
0801110070	0.0006985	40.68	102.300	505.0
0801110080	0.0006301	38.91	118.600	585.3
0801210010	0.003280	94.22	8.068	39.80
0801210020	0.002067	75.64	15.940	78.66
0801210030	0.001446	58.37	29.530	145.7
0801210040	0.001111	44.75	50.150	247.4
0801210050	0.0009449	39.20	67.380	332.4
0801210060	0.0008525	34.65	84.430	416.5
0801210070	0.0007666	31.78	102.300	505.0
0801210080	0.0006888	30.51	118.600	585.3
0801310010	0.003711	70.68	8.068	39.80
0801310020	0.002248	59.03	15.940	78.66
0801310030	0.001587	45.14	29.530	145.7
0801310040	0.001209	34.88	50.150	247.4
0801310050	0.001017	30.87	67.380	332.4
0801310060	0.0008680	28.88	84.430	416.5
0801310070	0.0008274	24.98	102.300	505.0
0801310080	0.0007439	23.98	118.600	585.3
0801410010	0.004011	57.15	8.068	39.80
0801410020	0.002462	47.13	15.940	78.66
0801410030	0.001748	35.81	29.530	145.7
0801410040	0.001311	28.13	50.150	247.4
0801410050	0.001129	24.31	67.380	332.4
0801410060	0.001011	21.66	84.430	416.5
0801410070	0.0009216	19.60	102.300	505.0
0801410080	0.0008272	18.85	118.600	585.3
0801510010	0.004289	46.72	8.068	39.80
0801510020	0.002624	38.65	15.940	78.66
0801510030	0.001854	29.52	29.530	145.7
0801510040	0.001392	23.15	50.150	247.4
0801510050	0.001183	20.27	67.380	332.4
0801510060	0.001062	18.02	84.430	416.5
0801510070	0.0009672	16.33	102.300	505.0
0801510080	0.0008701	15.66	118.600	585.3
0801610010	0.004332	43.33	8.068	39.80
0801610020	0.002705	35.12	15.940	78.66
0801610030	0.001918	26.73	29.530	145.7
0801610040	0.001444	20.91	50.150	247.4
0801610050	0.001234	18.21	67.380	332.4
0801610060	0.001111	16.13	84.430	416.5
0801610070	0.001010	14.64	102.300	505.0
0801610080	0.0009053	14.10	118.600	585.3
0801710010	0.004465	39.51	8.068	39.80
0801710020	0.002741	32.56	15.940	78.66
0801710030	0.001946	24.76	29.530	145.7
0801710040	0.001479	19.19	50.150	247.4
0801710050	0.001269	16.63	67.380	332.4
0801710060	0.001132	14.88	84.430	416.5
0801710070	0.001029	13.50	102.300	505.0
0801710080	0.0009311	12.88	118.600	585.3
0801810010	0.004633	34.22	8.068	39.80
0801810020	0.002823	28.43	15.940	78.66
0801810030	0.002007	21.58	29.530	145.7
0801810040	0.001490	17.11	50.150	247.4
0801810050	0.001261	15.05	67.380	332.4
0801810060	0.001139	13.30	84.430	416.5
0801810070	0.001039	12.02	102.300	505.0
0801810080	0.0009394	11.48	118.600	585.3

CODE	k Δt/Hx	$t_a/\Delta t$	V ρx/μ	x/t
0802110010	0.006826	23.53	4.944	39.80
0802110020	0.003994	20.35	9.769	78.66
0802110030	0.002722	16.12	18.090	145.7
0802110040	0.002054	12.58	30.730	247.4
0802110050	0.001740	11.05	41.290	332.4
0802110060	0.001564	9.817	51.730	416.5
0802110070	0.001443	8.771	62.730	505.0
0802110080	0.001260	8.670	72.690	585.3
0802210010	0.005180	31.01	6.827	39.80
0802210020	0.003115	26.09	13.490	78.66
0802210030	0.002197	19.96	24.990	145.7
0802210040	0.001647	15.69	42.430	247.4
0802210050	0.001401	13.72	57.010	332.4
0802210060	0.001255	12.23	71.430	416.5
0802210070	0.001155	10.96	86.620	505.0
0802210080	0.001032	10.58	100.300	585.3
0802310010	0.004358	36.87	8.668	39.80
0802310020	0.002683	30.30	17.120	78.66
0802310030	0.001873	23.43	31.730	145.7
0802310040	0.001412	18.30	53.880	247.4
0802310050	0.001185	16.22	72.390	332.4
0802310060	0.001071	14.32	90.700	416.5
0802310070	0.0009776	12.95	109.900	505.0
0802310080	0.0008580	12.73	127.400	585.3
0802410010	0.003992	40.27	9.682	39.80
0802410020	0.002436	33.39	19.130	78.66
0802410030	0.001748	25.12	35.440	145.7
0802410040	0.001304	19.83	60.180	247.4
0802410050	0.001120	17.18	80.860	332.4
0802410060	0.001001	15.33	101.300	416.5
0802410070	0.0009223	13.73	122.800	505.0
0802410080	0.0007689	14.22	142.300	585.3
0802510010	0.003596	44.71	11.090	39.80
0802510020	0.002251	36.14	21.910	78.66
0802510030	0.001615	27.20	40.600	145.7
0802510040	0.001191	21.71	68.940	247.4
0802510050	0.001018	18.91	92.630	332.4
0802510060	0.0009116	16.85	116.000	416.5
0802510070	0.0008190	15.47	140.700	505.0
0802510080	0.0007046	15.52	163.000	585.3
0802610010	0.003352	47.97	12.640	39.80
0802610020	0.002097	38.80	24.990	78.66
0802610030	0.001498	29.31	46.300	145.7
0802610040	0.001103	23.45	78.620	247.4
0802610050	0.0009341	20.61	105.600	332.4
0802610060	0.0008387	18.32	132.300	416.5
0802610070	0.0007446	17.02	160.400	505.0
0802610080	0.0006528	16.75	185.900	585.3
0802710010	0.002986	53.87	14.640	39.80
0802710020	0.001881	43.27	28.940	78.66
0802710030	0.001332	32.99	53.620	145.7
0802710040	0.0009805	26.39	91.040	247.4
0802710050	0.0008356	23.05	122.300	332.4
0802710060	0.0007397	20.78	153.200	416.5
0802710070	0.0006485	19.55	185.800	505.0
0802710080	0.0005637	19.41	215.300	585.3
0802810010	0.002742	58.72	16.980	39.80
0802810020	0.001711	47.61	33.560	78.66
0802810030	0.001215	36.19	62.180	145.7
0802810040	0.0008923	29.03	105.500	247.4
0802810050	0.0007516	25.65	141.800	332.4
0802810060	0.0006611	23.28	177.700	416.5
0802810070	0.0005740	22.11	215.500	505.0
0802810080	0.0004829	22.68	249.700	585.3

TABLE B.IX

VALUES OF THE FOUR DIMENSIONLESS GROUPS FOR MODEL TREATMENT NO. 8 WINDWARD ROOF

CODE	$k\Delta t/Hx$	$t_a/\Delta t$	$V\rho x/\mu$	x/t
0101110010	0.003059	111.5	8,850	39.80
0101110020	0.001967	87.78	17,480	78.66
0101110030	0.001584	58.84	32,390	145.7
0101110040	0.001158	47.38	55,010	247.4
0101110050	0.0009693	42.16	73,910	332.4
0101110060	0.0008589	37.97	92,600	416.5
0101110070	0.0007737	34.77	112,200	505.0
0101110080	0.0006589	35.22	130,100	585.3
0101210010	0.003641	78.73	8,850	39.80
0101210020	0.002276	63.73	17,480	78.66
0101210030	0.001769	44.24	32,390	145.7
0101210040	0.001300	35.45	55,010	247.4
0101210050	0.001096	31.30	73,910	332.4
0101210060	0.0009569	28.63	92,600	416.5
0101210070	0.0008356	27.03	112,200	505.0
0101210080	0.0007028	27.74	130,100	585.3
0101310010	0.003829	63.76	8,850	39.80
0101310020	0.002445	50.52	17,480	78.66
0101310030	0.001917	34.77	32,390	145.7
0101310040	0.001400	28.04	55,010	247.4
0101310050	0.001178	24.79	73,910	332.4
0101310060	0.001028	22.69	92,600	416.5
0101310070	0.0009161	21.00	112,200	505.0
0101310080	0.0007781	21.33	130,100	585.3
0101410010	0.004062	51.51	8,850	39.80
0101410020	0.002589	40.90	17,480	78.66
0101410030	0.002048	27.90	32,390	145.7
0101410040	0.001495	22.51	55,010	247.4
0101410050	0.001272	19.69	73,910	332.4
0101410060	0.001112	17.97	92,600	416.5
0101410070	0.0009852	16.74	112,200	505.0
0101410080	0.0008342	17.06	130,100	585.3
0101510010	0.004352	41.85	8,850	39.80
0101510020	0.002736	33.69	17,480	78.66
0101510030	0.002173	22.89	32,390	145.7
0101510040	0.001586	18.47	55,010	247.4
0101510050	0.001343	16.23	73,910	332.4
0101510060	0.001176	14.80	92,600	416.5
0101510070	0.001050	13.66	112,200	505.0
0101510080	0.0009019	13.73	130,100	585.3
0101610010	0.004405	38.55	8,850	39.80
0101610020	0.002791	30.79	17,480	78.66
0101610030	0.002207	21.01	32,390	145.7
0101610040	0.001616	16.90	55,010	247.4
0101610050	0.001366	14.88	73,910	332.4
0101610060	0.001178	13.77	92,600	416.5
0101610070	0.001059	12.63	112,200	505.0
0101610080	0.0008902	12.97	130,100	585.3
0101710010	0.004581	34.81	8,850	39.80
0101710020	0.002830	28.51	17,480	78.66
0101710030	0.002250	19.35	32,390	145.7
0101710040	0.001655	15.49	55,010	247.4
0101710050	0.001406	13.57	73,910	332.4
0101710060	0.001230	12.38	92,600	416.5
0101710070	0.001094	11.47	112,200	505.0
0101710080	0.0009367	11.57	130,100	585.3
0101810010	0.004577	32.10	8,850	39.80
0101810020	0.002871	25.89	17,480	78.66
0101810030	0.002328	17.23	32,390	145.7
0101810040	0.001693	13.96	55,010	247.4
0101810050	0.001421	12.38	73,910	332.4
0101810060	0.001241	11.30	92,600	416.5
0101810070	0.001106	10.47	112,200	505.0
0101810080	0.0009358	10.67	130,100	585.3

CODE	$k\Delta t/Hx$	$t_a/\Delta t$	$V\rho x/\mu$	x/t
0102110010	0.006806	21.51	5,010	39.80
0102110020	0.004186	17.69	9,900	78.66
0102110030	0.003325	12.02	18,340	145.7
0102110040	0.002452	9.604	31,140	247.4
0102110050	0.001970	8.893	41,840	332.4
0102110060	0.001652	8.467	52,420	416.5
0102110070	0.001495	7.714	63,560	505.0
0102110080	0.001260	7.898	73,660	585.3
0102210010	0.005671	25.81	6,476	39.80
0102210020	0.003542	20.92	12,790	78.66
0102210030	0.002705	14.78	23,710	145.7
0102210040	0.002025	11.63	40,260	247.4
0102210050	0.001682	10.41	54,090	332.4
0102210060	0.001419	9.856	67,770	416.5
0102210070	0.001273	9.063	82,170	505.0
0102210080	0.001066	9.334	95,230	585.3
0102310010	0.005035	29.09	7,560	39.80
0102310020	0.003136	23.63	14,930	78.66
0102310030	0.002493	16.04	27,670	145.7
0102310040	0.001833	12.85	46,990	247.4
0102310050	0.001503	11.66	63,140	332.4
0102310060	0.001255	11.14	79,110	416.5
0102310070	0.001138	10.14	95,920	505.0
0102310080	0.0009539	10.44	111,100	585.3
0102410010	0.004565	32.10	8,797	39.80
0102410020	0.002814	26.35	17,380	78.66
0102410030	0.002259	17.71	32,200	145.7
0102410040	0.001664	14.16	54,680	247.4
0102410050	0.001368	12.82	73,470	332.4
0102410060	0.001165	12.01	92,050	416.5
0102410070	0.001033	11.17	111,600	505.0
0102410080	0.0008692	11.46	129,300	585.3
0102510010	0.003845	38.10	11,270	39.80
0102510020	0.002422	30.61	22,270	78.66
0102510030	0.001949	20.53	41,270	145.7
0102510040	0.001424	16.55	70,080	247.4
0102510050	0.001192	14.71	94,160	332.4
0102510060	0.001015	13.79	117,900	416.5
0102510070	0.0008962	12.88	143,000	505.0
0102510080	0.0007451	13.37	165,700	585.3
0102610010	0.003403	43.09	13,570	39.80
0102610020	0.002142	34.64	26,810	78.66
0102610030	0.001730	23.14	49,670	145.7
0102610040	0.001250	18.86	84,350	247.4
0102610050	0.001050	16.72	113,300	332.4
0102610060	0.0008910	15.72	142,000	416.5
0102610070	0.0007871	14.68	172,100	505.0
0102610080	0.0006623	15.05	199,500	585.3
0102710010	0.003015	48.65	16,050	39.80
0102710020	0.001918	38.71	31,720	78.66
0102710030	0.001541	25.99	58,760	145.7
0102710040	0.001121	21.04	99,780	247.4
0102710050	0.0009308	18.87	134,000	332.4
0102710060	0.0007773	18.04	167,900	416.5
0102710070	0.0006737	17.16	203,600	505.0
0102710080	0.0005569	17.91	236,000	585.3
0102810010	0.002794	52.53	18,390	39.80
0102810020	0.001750	42.44	36,350	78.66
0102810030	0.001420	28.22	67,350	145.7
0102810040	0.001028	22.96	114,300	247.4
0102810050	0.0008447	20.80	153,600	332.4
0102810060	0.0006927	20.25	192,500	416.5
0102810070	0.0005931	19.50	233,400	505.0
0102810080	0.0004798	20.80	270,500	585.3

TABLE B.X

VALUES OF THE FOUR DIMENSIONLESS GROUPS FOR THE LOW AIR TEMPERATURE RUN MODEL TREATMENT NO. 8 WINDWARD AND LEEWARD ROOF

CODE	k △t/Hx	$t_a/\triangle t$	V ρx/μ	x/t
0103110010	0.002529	117.3	10,060	39.80
0103110020	0.001786	84.09	19,880	78.66
0103110030	0.001446	56.06	36,830	145.7
0103110040	0.001060	45.05	62,540	247.4
0103110050	0.0008945	39.73	84,040	332.4
0103110060	0.0007871	36.04	105,200	416.5
0103110070	0.0007233	32.34	127,600	505.0
0103110080	0.0006081	33.19	147,900	585.3
0103210010	0.003000	99.15	10,060	39.80
0103210020	0.001964	76.61	19,880	78.66
0103210030	0.001558	52.13	36,830	145.7
0103210040	0.001145	41.79	62,540	247.4
0103210050	0.0009509	37.45	84,040	332.4
0103210060	0.0008377	33.93	105,200	416.5
0103210070	0.0007418	31.60	127,600	505.0
0103210080	0.0006201	32.62	147,900	585.3
0103310010	0.002992	93.75	10,060	39.80
0103310020	0.001907	74.45	19,880	78.66
0103310030	0.001544	49.63	36,830	145.7
0103310040	0.001150	39.24	62,540	247.4
0103310050	0.0009555	35.15	84,040	332.4
0103310060	0.0008368	32.04	105,200	416.5
0103310070	0.0007556	29.26	127,600	505.0
0103310080	0.0006445	29.60	147,900	585.3
0103410010	0.003514	67.57	10,060	39.80
0103410020	0.002276	52.79	19,880	78.66
0103410030	0.001804	35.94	36,830	145.7
0103410040	0.001319	28.95	62,540	247.4
0103410050	0.001110	25.59	84,040	332.4
0103410060	0.0009628	23.57	105,200	416.5
0103410070	0.0008458	22.13	127,600	505.0
0103410080	0.0007107	22.72	147,900	585.3
0103510010	0.003852	52.79	10,060	39.80
0103510020	0.002436	42.23	19,880	78.66
0103510030	0.001907	29.12	36,830	145.7
0103510040	0.001407	23.24	62,540	247.4
0103510050	0.001157	21.02	84,040	332.4
0103510060	0.001008	19.26	105,200	416.5
0103510070	0.0008855	18.09	127,600	505.0
0103510080	0.0007204	19.19	147,900	585.3
0103610010	0.003979	44.07	10,060	39.80
0103610020	0.002521	35.20	19,880	78.66
0103610030	0.002022	23.68	36,830	145.7
0103610040	0.001469	19.20	62,540	247.4
0103610050	0.001238	16.95	84,040	332.4
0103610060	0.001088	15.40	105,200	416.5
0103610070	0.0009573	14.44	127,600	505.0
0103610080	0.0007954	14.99	147,900	585.3
0103710010	0.004208	36.48	10,060	39.80
0103710020	0.002666	29.14	19,880	78.66
0103710030	0.002125	19.73	36,830	145.7
0103710040	0.001544	15.99	62,540	247.4
0103710050	0.001294	14.20	84,040	332.4
0103710060	0.001122	13.06	105,200	416.5
0103710070	0.0009879	12.24	127,600	505.0
0103710080	0.0008359	12.48	147,900	585.3
0103810010	0.004673	27.25	10,060	39.80
0103810020	0.002911	22.13	19,880	78.66
0103810030	0.002306	15.08	36,830	145.7
0103810040	0.001661	12.33	62,540	247.4
0103810050	0.001380	11.04	84,040	332.4
0103810060	0.001205	10.09	105,200	416.5
0103810070	0.001055	9.512	127,600	505.0
0103810080	0.0008816	9.825	147,900	585.3

CODE	k △t/Hx	$t_a/\triangle t$	V ρx/μ	x/t
0103120090	0.004824	61.53	10,060	39.80
0103120100	0.002977	50.45	19,880	78.66
0103120110	0.001671	48.51	36,830	145.7
0103120120	0.001164	41.02	62,540	247.4
0103120130	0.0009579	37.10	84,040	332.4
0103120140	0.0008545	33.19	105,200	416.5
0103120150	0.001029	22.72	127,600	505.0
0103120160	0.0008842	22.83	147,900	585.3
0103220090	0.005000	59.49	10,060	39.80
0103220100	0.002709	55.57	19,880	78.66
0103220110	0.001719	47.26	36,830	145.7
0103220120	0.001201	39.81	62,540	247.4
0103220130	0.0009861	36.12	84,040	332.4
0103220140	0.0008939	31.80	105,200	416.5
0103220150	0.001057	22.17	127,600	505.0
0103220160	0.0009122	22.17	147,900	585.3
0103320090	0.004710	59.56	10,060	39.80
0103320100	0.002664	53.29	19,880	78.66
0103320110	0.001680	45.61	36,830	145.7
0103320120	0.001176	38.35	62,540	247.4
0103320130	0.0009687	34.67	84,040	332.4
0103320140	0.0008791	30.49	105,200	416.5
0103320150	0.0008255	26.78	127,600	505.0
0103320160	0.0007010	27.21	147,900	585.3
0103420090	0.005529	42.94	10,060	39.80
0103420100	0.003059	39.28	19,880	78.66
0103420110	0.001894	34.24	36,830	145.7
0103420120	0.001296	29.46	62,540	247.4
0103420130	0.001094	25.98	84,040	332.4
0103420140	0.0009807	23.14	105,200	416.5
0103420150	0.0009196	20.35	127,600	505.0
0103420160	0.0007744	20.85	147,900	585.3
0103520090	0.006018	33.78	10,060	39.80
0103520100	0.003289	31.28	19,880	78.66
0103520110	0.002027	27.39	36,830	145.7
0103520120	0.001439	22.72	62,540	247.4
0103520130	0.001172	20.77	84,040	332.4
0103520140	0.001043	18.63	105,200	416.5
0103520150	0.0009677	16.56	127,600	505.0
0103520160	0.0008214	16.83	147,900	585.3
0103620090	0.006194	28.31	10,060	39.80
0103620100	0.003450	25.73	19,880	78.66
0103620110	0.002174	22.03	36,830	145.7
0103620120	0.001531	18.43	62,540	247.4
0103620130	0.001259	16.67	84,040	332.4
0103620140	0.001127	14.86	105,200	416.5
0103620150	0.001041	13.26	127,600	505.0
0103620160	0.0008896	13.40	147,900	585.3
0103720090	0.006600	23.26	10,060	39.80
0103720100	0.003585	21.67	19,880	78.66
0103720110	0.002241	18.71	36,830	145.7
0103720120	0.001524	16.20	62,540	247.4
0103720130	0.001257	14.61	84,040	332.4
0103720140	0.001148	12.77	105,200	416.5
0103720150	0.001080	11.19	127,600	505.0
0103720160	0.0009245	11.29	147,900	585.3
0103820090	0.006984	18.23	10,060	39.80
0103820100	0.003814	16.89	19,880	78.66
0103820110	0.002388	14.56	36,830	145.7
0103820120	0.001681	12.18	62,540	247.4
0103820130	0.001389	10.97	84,040	332.4
0103820140	0.001255	9.693	105,200	416.5
0103820150	0.001168	8.593	127,600	505.0
0103820160	0.0009876	8.771	147,900	585.3

TABLE B.XI

VALUES OF THE FOUR DIMENSIONLESS GROUPS FOR MODEL TREATMENT NO. 1 LEEWARD ROOF

CODE	$k\Delta t/Hx$	$t_a/\Delta t$	$V\rho x/\mu$	x/t
0401120090	0.001165	146.3	13,400	39.80
0401120100	0.0006062	142.3	26,490	78.66
0401120110	0.0003891	119.7	49,080	145.7
0401120120	0.0002760	99.37	83,350	247.4
0401120130	0.0002132	95.76	111,900	332.4
0401120140	0.0001949	83.60	140,300	416.5
0401120150	0.0001990	67.52	170,100	505.0
0401120160	0.0001783	65.02	197,100	585.3
0401220090	0.0009815	181.7	13,400	39.80
0401220100	0.0005481	164.6	26,490	78.66
0401220110	0.0003420	142.4	49,080	145.7
0401220120	0.0002613	109.7	83,350	247.4
0401220130	0.0002026	105.3	111,900	332.4
0401220140	0.0001843	92.45	140,300	416.5
0401220150	0.0001920	73.19	170,100	505.0
0401220160	0.0001749	69.34	197,100	585.3
0401320090	0.0009720	195.1	13,400	39.80
0401320100	0.0005283	181.6	26,490	78.66
0401320110	0.0003441	150.5	49,080	145.7
0401320120	0.0002548	119.7	83,350	247.4
0401320130	0.0002068	109.7	111,900	332.4
0401320140	0.0001892	95.78	140,300	416.5
0401320150	0.0001957	76.34	170,100	505.0
0401320160	0.0001787	72.16	197,100	585.3
0401420090	0.0008644	250.7	13,400	39.80
0401420100	0.0004374	250.7	26,490	78.66
0401420110	0.0003260	181.5	49,080	145.7
0401420120	0.0002450	142.3	83,350	247.4
0401420130	0.0002020	128.4	111,900	332.4
0401420140	0.0001927	107.4	140,300	416.5
0401420150	0.0001849	92.38	170,100	505.0
0401420160	0.0001707	86.32	197,100	585.3
0401520090	0.0008110	309.6	13,400	39.80
0401520100	0.0004587	277.0	26,490	78.66
0401520110	0.0002867	239.2	49,080	145.7
0401520120	0.0002072	194.9	83,350	247.4
0401520130	0.0001599	187.9	111,900	332.4
0401520140	0.0001504	159.5	140,300	416.5
0401520150	0.0001616	122.4	170,100	505.0
0401520160	0.0001460	116.9	197,100	585.3
0401620090	0.0005109	657.9	13,400	39.80
0401620100	0.0001616	1052.	26,490	78.66
0401620110	0.0001395	657.9	49,080	145.7
0401620120	0.0001438	375.9	83,350	247.4
0401620130	0.0001300	309.6	111,900	332.4
0401620140	0.0001098	292.4	140,300	416.5
0401620150	0.0001208	219.3	170,100	505.0
0401620160	0.0001172	194.9	197,100	585.3
0401720090	0.0007200	375.9	13,400	39.80
0401720100	0.0003643	375.9	26,490	78.66
0401720110	0.0002247	328.9	49,080	145.7
0401720120	0.0001820	239.2	83,350	247.4
0401720130	0.0001477	219.2	111,900	332.4
0401720140	0.0001228	210.5	140,300	416.5
0401720150	0.0001337	159.4	170,100	505.0
0401720160	0.0001224	150.3	197,100	585.3
0401820090	0.001073	187.9	13,400	39.80
0401820100	0.0005626	181.4	26,490	78.66
0401820110	0.0003560	154.7	49,080	145.7
0401820120	0.0002713	119.5	83,350	247.4
0401820130	0.0002157	111.9	111,900	332.4
0401820140	0.0001978	97.44	140,300	416.5
0401820150	0.0001933	82.21	170,100	505.0
0401820160	0.0001746	78.53	197,100	585.3

CODE	$k\Delta t/Hx$	$t_a/\Delta t$	$V\rho x/\mu$	x/t
0402120090	0.006416	27.71	2,229	39.80
0402120100	0.003281	27.42	4,406	78.66
0402120110	0.001946	24.95	8,163	145.7
0402120120	0.001331	21.49	13,860	247.4
0402120130	0.001071	19.87	18,620	332.4
0402120140	0.0009552	17.79	23,330	416.5
0402120150	0.0008676	16.15	28,290	505.0
0402120160	0.0007624	15.86	32,780	585.3
0402220090	0.003984	44.74	3,966	39.80
0402220100	0.002033	44.36	7,837	78.66
0402220110	0.001217	39.99	14,520	145.7
0402220120	0.0008475	33.84	24,650	247.4
0402220130	0.0006792	31.42	33,120	332.4
0402220140	0.0006035	28.23	41,500	416.5
0402220150	0.0005749	24.44	50,320	505.0
0402220160	0.0005121	23.67	58,320	585.3
0402320090	0.003174	56.19	5,124	39.80
0402320100	0.001435	62.87	10,120	78.66
0402320110	0.0009778	49.82	18,760	145.7
0402320120	0.0006845	41.91	31,850	247.4
0402320130	0.0005539	38.55	42,800	332.4
0402320140	0.0004970	34.29	53,620	416.5
0402320150	0.0004790	29.34	65,020	505.0
0402320160	0.0004340	27.94	75,350	585.3
0402420090	0.002634	67.74	6,202	39.80
0402420100	0.001333	67.74	12,250	78.66
0402420110	0.0008210	59.36	22,700	145.7
0402420120	0.0005867	48.92	38,550	247.4
0402420130	0.0004771	44.77	51,800	332.4
0402420140	0.0004292	39.72	64,900	416.5
0402420150	0.0004152	33.87	78,690	505.0
0402420160	0.0003766	32.21	91,190	585.3
0402520090	0.002059	86.65	7,678	39.80
0402520100	0.001059	85.25	15,170	78.66
0402520110	0.0006549	74.44	28,110	145.7
0402520120	0.0004672	61.46	47,730	247.4
0402520130	0.0003760	56.83	64,130	332.4
0402520140	0.0003420	49.86	80,350	416.5
0402520150	0.0003380	41.62	97,420	505.0
0402520160	0.0003146	38.58	112,900	585.3
0402620090	0.001789	99.62	9,910	39.80
0402620100	0.0009228	97.77	19,580	78.66
0402620110	0.0005719	85.15	36,270	145.7
0402620120	0.0004074	70.39	61,600	247.4
0402620130	0.0003234	65.99	82,760	332.4
0402620140	0.0002969	57.39	103,600	416.5
0402620150	0.0002927	47.99	125,700	505.0
0402620160	0.0002687	45.12	145,700	585.3
0402720090	0.001620	110.0	10,830	39.80
0402720100	0.0008203	110.0	21,410	78.66
0402720110	0.0004889	99.67	39,670	145.7
0402720120	0.0003531	81.27	67,360	247.4
0402720130	0.0002951	72.36	90,520	332.4
0402720140	0.0002678	63.64	113,400	416.5
0402720150	0.0002634	53.36	137,500	505.0
0402720160	0.0002457	49.37	159,300	585.3
0402820090	0.005470	32.62	2,748	39.80
0402820100	0.002768	32.62	5,431	78.66
0402820110	0.001660	29.36	10,060	145.7
0402820120	0.001151	24.93	17,080	247.4
0402820130	0.0009299	22.98	22,950	332.4
0402820140	0.0008229	20.72	28,760	416.5
0402820150	0.0007585	18.54	34,870	505.0
0402820160	0.0006683	18.16	40,410	585.3

TABLE B.XII

VALUES OF THE FOUR DIMENSIONLESS GROUPS FOR MODEL TREATMENT NO. 2 LEEWARD ROOF

CODE	$k\Delta t/Hx$	$t_a/\Delta t$	$V\rho x/\mu$	x/t
0201120090	0.004239	89.46	8,126	39.80
0201120100	0.002324	82.58	16,050	78.66
0201120110	0.001505	68.81	29,740	145.7
0201120120	0.001011	60.31	50,510	247.4
0201120130	0.0007528	60.31	67,870	332.4
0201120140	0.0006616	54.77	85,030	416.5
0201120150	0.0006515	45.87	103,100	505.0
0201120160	0.0006246	41.29	119,400	585.3
0201220090	0.005073	66.27	8,126	39.80
0201220100	0.002852	59.64	16,050	78.66
0201220110	0.001779	51.61	29,740	145.7
0201220120	0.001188	45.49	50,510	247.4
0201220130	0.0008848	45.49	67,870	332.4
0201220140	0.0007840	40.97	85,030	416.5
0201220150	0.0007799	33.97	103,100	505.0
0201220160	0.0007411	30.85	119,400	585.3
0201320090	0.005365	54.22	8,126	39.80
0201320100	0.003017	48.79	16,050	78.66
0201320110	0.001895	41.93	29,740	145.7
0201320120	0.001264	37.02	50,510	247.4
0201320130	0.0009410	37.02	67,870	332.4
0201320140	0.0008235	33.76	85,030	416.5
0201320150	0.0007988	28.70	103,100	505.0
0201320160	0.0007704	25.68	119,400	585.3
0201420090	0.005927	42.61	8,126	39.80
0201420100	0.003285	38.91	16,050	78.66
0201420110	0.002081	33.14	29,740	145.7
0201420120	0.001369	29.66	50,510	247.4
0201420130	0.001019	29.66	67,870	332.4
0201420140	0.0009082	26.58	85,030	416.5
0201420150	0.0008936	22.28	103,100	505.0
0201420160	0.0008574	20.03	119,400	585.3
0201520090	0.006328	34.87	8,126	39.80
0201520100	0.003514	31.78	16,050	78.66
0201520110	0.002200	27.40	29,740	145.7
0201520120	0.001474	24.08	50,510	247.4
0201520130	0.001111	23.76	67,870	332.4
0201520140	0.0009857	21.39	85,030	416.5
0201520150	0.0009619	18.08	103,100	505.0
0201520160	0.0009250	16.22	119,400	585.3
0201620090	0.006348	32.35	8,126	39.80
0201620100	0.003561	29.18	16,050	78.66
0201620110	0.002214	25.33	29,740	145.7
0201620120	0.001476	22.37	50,510	247.4
0201620130	0.001080	22.75	67,870	332.4
0201620140	0.0009758	20.11	85,030	416.5
0201620150	0.0009555	16.94	103,100	505.0
0201620160	0.0009129	15.30	119,400	585.3
0201720090	0.006530	29.84	8,126	39.80
0201720100	0.003672	26.85	16,050	78.66
0201720110	0.002279	23.35	29,740	145.7
0201720120	0.001517	20.66	50,510	247.4
0201720130	0.001129	20.66	67,870	332.4
0201720140	0.001002	18.58	85,030	416.5
0201720150	0.0009836	15.61	103,100	505.0
0201720160	0.0009524	13.91	119,400	585.3
0201820090	0.006832	25.83	8,126	39.80
0201820100	0.003806	23.46	16,050	78.66
0201820110	0.002377	20.27	29,740	145.7
0201820120	0.001585	17.90	50,510	247.4
0201820130	0.001183	17.85	67,870	332.4
0201820140	0.001048	16.08	85,030	416.5
0201820150	0.001030	13.49	103,100	505.0
0201820160	0.0009896	12.12	119,400	585.3

CODE	$k\Delta t/Hx$	$t_a/\Delta t$	$V\rho x/\mu$	x/t
0202120090	0.01033	17.70	4,576	39.80
0202120100	0.005658	16.36	9,043	78.66
0202120110	0.003471	14.39	16,750	145.7
0202120120	0.002285	12.87	28,450	247.4
0202120130	0.001684	13.00	38,220	332.4
0202120140	0.001458	11.98	47,890	416.5
0202120150	0.001416	10.17	58,070	505.0
0202120160	0.001340	9.280	67,290	585.3
0202220090	0.007952	23.00	6,500	39.80
0202220100	0.004437	20.86	12,840	78.66
0202220110	0.002729	18.30	23,790	145.7
0202220120	0.001820	16.16	40,400	247.4
0202220130	0.001354	16.16	54,290	332.4
0202220140	0.001156	15.12	68,010	416.5
0202220150	0.001124	12.81	82,470	505.0
0202220160	0.001095	11.35	95,580	585.3
0202320090	0.006796	26.90	7,865	39.80
0202320100	0.003800	24.34	15,540	78.66
0202320110	0.002376	21.01	28,790	145.7
0202320120	0.001585	18.55	48,890	247.4
0202320130	0.001180	18.55	65,690	332.4
0202320140	0.001042	16.76	82,300	416.5
0202320150	0.001007	14.31	99,790	505.0
0202320160	0.0009845	12.63	115,600	585.3
0202420090	0.005641	32.42	10,260	39.80
0202420100	0.003181	29.09	20,290	78.66
0202420110	0.001995	25.03	37,590	145.7
0202420120	0.001366	21.52	63,830	247.4
0202420130	0.001049	20.86	85,770	332.4
0202420140	0.0009451	18.49	107,400	416.5
0202420150	0.0009240	15.59	130,300	505.0
0202420160	0.0008667	14.35	151,000	585.3
0202520090	0.004927	37.11	12,250	39.80
0202520100	0.002751	33.63	24,220	78.66
0202520110	0.001717	29.09	44,870	145.7
0202520120	0.001170	25.14	76,190	247.4
0202520130	0.0008870	24.68	102,300	332.4
0202520140	0.0007957	21.96	128,200	416.5
0202520150	0.0007955	18.12	155,500	505.0
0202520160	0.0007534	16.50	180,200	585.3
0202620090	0.004248	43.05	14,240	39.80
0202620100	0.002390	38.71	28,140	78.66
0202620110	0.001494	33.42	52,130	145.7
0202620120	0.001011	29.09	88,520	247.4
0202620130	0.0007527	29.09	118,900	332.4
0202620140	0.0006528	26.77	149,000	416.5
0202620150	0.0006401	22.51	180,600	505.0
0202620160	0.0006355	19.57	209,400	585.3
0202720090	0.003908	46.79	15,630	39.80
0202720100	0.002184	42.37	30,890	78.66
0202720110	0.001401	35.64	57,240	145.7
0202720120	0.0009349	31.47	97,190	247.4
0202720130	0.0006998	31.29	130,500	332.4
0202720140	0.0006203	28.17	163,600	416.5
0202720150	0.0006240	23.09	198,400	505.0
0202720160	0.0006101	20.38	229,900	585.3
0202820090	0.003568	51.20	17,590	39.80
0202820100	0.001977	46.75	34,770	78.66
0202820110	0.001271	39.24	64,410	145.7
0202820120	0.0008638	34.03	109,300	247.4
0202820130	0.0006551	33.39	146,900	332.4
0202820140	0.0005878	29.70	184,100	416.5
0202820150	0.0006026	23.89	223,200	505.0
0202820160	0.0005731	21.68	258,700	585.3

TABLE B. XIII

VALUES OF THE FOUR DIMENSIONLESS GROUPS FOR MODEL TREATMENT NO. 3 LEEWARD ROOF

CODE	k △t/Hx	$t_a/\triangle t$	V ρx/μ	x/t
0501120090	0.003538	106.8	8,538	39.80
0501120100	0.001934	98.92	16,870	78.66
0501120110	0.001237	83.46	31,250	145.7
0501120120	0.0008425	72.18	53,070	247.4
0501120130	0.0006694	67.61	71,310	332.4
0501120140	0.0006019	60.02	89,340	416.5
0501120150	0.0005801	51.36	108,300	505.0
0501120160	0.0005342	48.12	125,500	585.3
0501220090	0.003577	97.12	8,538	39.80
0501220100	0.001908	92.10	16,870	78.66
0501220110	0.001261	75.23	31,250	145.7
0501220120	0.001381	40.46	53,070	247.4
0501220130	0.001074	38.70	71,310	332.4
0501220140	0.0006215	53.41	89,340	416.5
0501220150	0.0005946	46.05	108,300	505.0
0501220160	0.0005484	43.07	125,500	585.3
0501320090	0.003726	77.41	8,538	39.80
0501320100	0.001967	74.19	16,870	78.66
0501320110	0.001298	60.70	31,250	145.7
0501320120	0.0009036	51.36	53,070	247.4
0501320130	0.0007113	48.56	71,310	332.4
0501320140	0.0006348	43.43	89,340	416.5
0501320150	0.0006129	37.09	108,300	505.0
0501320160	0.0005656	34.68	125,500	585.3
0501420090	0.003844	65.15	8,538	39.80
0501420100	0.002016	62.85	16,870	78.66
0501420110	0.001331	51.37	31,250	145.7
0501420120	0.0009351	43.08	53,070	247.4
0501420130	0.0007352	40.78	71,310	332.4
0501420140	0.0006675	35.85	89,340	416.5
0501420150	0.0006391	30.88	108,300	505.0
0501420160	0.0005866	29.03	125,500	585.3
0501520090	0.003971	55.10	8,538	39.80
0501520100	0.002113	52.40	16,870	78.66
0501520110	0.001364	43.81	31,250	145.7
0501520120	0.0009419	37.37	53,070	247.4
0501520130	0.0007452	35.16	71,310	332.4
0501520140	0.0006769	30.89	89,340	416.5
0501520150	0.0006518	26.45	108,300	505.0
0501520160	0.0006042	24.63	125,500	585.3
0501620090	0.004039	50.42	8,538	39.80
0501620100	0.002140	48.15	16,870	78.66
0501620110	0.001374	40.49	31,250	145.7
0501620120	0.0009625	34.04	53,070	247.4
0501620130	0.0007619	32.00	71,310	332.4
0501620140	0.0006919	28.13	89,340	416.5
0501620150	0.0006577	24.40	108,300	505.0
0501620160	0.0006090	22.74	125,500	585.3
0501720090	0.004048	47.73	8,538	39.80
0501720100	0.002158	45.30	16,870	78.66
0501720110	0.001392	37.91	31,250	145.7
0501720120	0.0009712	32.01	53,070	247.4
0501720130	0.0007704	30.03	71,310	332.4
0501720140	0.0006944	26.59	89,340	416.5
0501720150	0.0006610	23.04	108,300	505.0
0501720160	0.0006146	21.38	125,500	585.3
0501820090	0.004146	43.13	8,538	39.80
0501820100	0.002200	41.14	16,870	78.66
0501820110	0.001434	34.06	31,250	145.7
0501820120	0.0009952	28.91	53,070	247.4
0501820130	0.0007887	27.15	71,310	332.4
0501820140	0.0007158	23.87	89,340	416.5
0501820150	0.0006799	20.73	108,300	505.0
0501820160	0.0006299	19.31	125,500	585.3

CODE	k △t/Hx	$t_a/\triangle t$	V ρx/μ	x/t
0502120090	0.006553	27.84	4,959	39.80
0502120100	0.003454	26.72	9,800	78.66
0502120110	0.002163	23.04	18,150	145.7
0502120120	0.001488	19.72	30,830	247.4
0502120130	0.001181	18.49	41,420	332.4
0502120140	0.001086	16.05	51,900	416.5
0502120150	0.001014	14.18	62,930	505.0
0502120160	0.0008983	13.81	72,930	585.3
0502220090	0.005529	32.99	6,588	39.80
0502220100	0.002884	32.00	13,010	78.66
0502220110	0.001818	27.40	24,110	145.7
0502220120	0.001246	23.54	40,950	247.4
0502220130	0.0009849	22.17	55,020	332.4
0502220140	0.0009068	19.22	68,940	416.5
0502220150	0.0008635	16.65	83,590	505.0
0502220160	0.0007730	16.05	96,870	585.3
0502320090	0.004539	40.20	8,383	39.80
0502320100	0.002418	38.19	16,560	78.66
0502320110	0.001557	32.01	30,680	145.7
0502320120	0.001070	27.42	52,100	247.4
0502320130	0.0008419	25.95	70,010	332.4
0502320140	0.0007665	22.75	87,720	416.5
0502320150	0.0007344	19.58	106,300	505.0
0502320160	0.0006708	18.50	123,200	585.3
0502420090	0.004061	44.93	9,597	39.80
0502420100	0.002159	42.77	18,960	78.66
0502420110	0.001398	35.64	35,130	145.7
0502420120	0.0009609	30.55	59,650	247.4
0502420130	0.0007519	29.05	80,150	332.4
0502420140	0.0006882	25.34	100,400	416.5
0502420150	0.0006671	21.56	121,700	505.0
0502420160	0.0006128	20.25	141,100	585.3
0502520090	0.003413	53.46	11,690	39.80
0502520100	0.001848	49.97	23,100	78.66
0502520110	0.001193	41.77	42,790	145.7
0502520120	0.0008291	35.40	72,660	247.4
0502520130	0.0006539	33.41	97,630	332.4
0502520140	0.0005936	29.37	122,300	416.5
0502520150	0.0005757	24.98	148,300	505.0
0502520160	0.0005339	23.24	171,800	585.3
0502620090	0.003174	57.49	13,180	39.80
0502620100	0.001710	54.00	26,050	78.66
0502620110	0.001118	44.55	48,270	145.7
0502620120	0.0007797	37.65	81,970	247.4
0502620130	0.0006130	35.64	110,100	332.4
0502620140	0.0005545	31.45	137,900	416.5
0502620150	0.0005353	26.86	167,300	505.0
0502620160	0.0005014	24.75	193,900	585.3
0502720090	0.002867	63.65	15,690	39.80
0502720100	0.001485	62.17	31,000	78.66
0502720110	0.0009883	50.44	57,430	145.7
0502720120	0.0006864	42.77	97,530	247.4
0502720130	0.0005353	40.81	131,000	332.4
0502720140	0.0004827	36.12	164,100	416.5
0502720150	0.0004707	30.55	199,000	505.0
0502720160	0.0004526	27.42	230,700	585.3
0502820090	0.002594	70.35	17,750	39.80
0502820100	0.001364	67.68	35,080	78.66
0502820110	0.0008858	56.28	65,000	145.7
0502820120	0.0006260	46.90	110,300	247.4
0502820130	0.0004863	44.93	148,300	332.4
0502820140	0.0004403	39.60	185,800	416.5
0502820150	0.0004304	33.41	225,300	505.0
0502820160	0.0004155	29.87	261,100	585.3

TABLE B.XIV

VALUES OF THE FOUR DIMENSIONLESS GROUPS FOR MODEL TREATMENT NO. 4 LEEWARD ROOF

CODE	k Δt/Hx	$t_a/\Delta t$	V ρ x/μ	x/t
0301120090	0.003899	92.89	9,442	39.80
0301120100	0.002149	85.27	18,650	78.66
0301120110	0.001407	70.29	34,560	145.7
0301120120	0.0009633	60.48	58,690	247.4
0301120130	0.0008003	54.18	78,860	332.4
0301120140	0.0006986	49.54	98,800	416.5
0301120150	0.0006585	43.34	119,800	505.0
0301120160	0.0005966	41.28	138,800	585.3
0301220090	0.004701	70.33	9,442	39.80
0301220100	0.002507	66.72	18,650	78.66
0301220110	0.001614	55.96	34,560	145.7
0301220120	0.001144	46.47	58,690	247.4
0301220130	0.0009356	42.31	78,860	332.4
0301220140	0.0008075	39.13	98,800	416.5
0301220150	0.0007661	34.01	119,800	505.0
0301220160	0.0006870	32.73	138,800	585.3
0301320090	0.005275	52.08	9,442	39.80
0301320100	0.002830	49.14	18,650	78.66
0301320110	0.001830	41.01	34,560	145.7
0301320120	0.001290	34.26	58,690	247.4
0301320130	0.001029	31.95	78,860	332.4
0301320140	0.0009025	29.10	98,800	416.5
0301320150	0.0008441	25.65	119,800	505.0
0301320160	0.0007534	24.80	138,800	585.3
0301420090	0.005495	43.43	9,442	39.80
0301420100	0.002920	41.36	18,650	78.66
0301420110	0.001913	34.06	34,560	145.7
0301420120	0.001333	28.79	58,690	247.4
0301420130	0.001074	26.59	78,860	332.4
0301420140	0.0009452	24.12	98,800	416.5
0301420150	0.0008950	21.01	119,800	505.0
0301420160	0.0008066	20.12	138,800	585.3
0301520090	0.005800	35.90	9,442	39.80
0301520100	0.003097	34.03	18,650	78.66
0301520110	0.002010	28.29	34,560	145.7
0301520120	0.001389	24.10	58,690	247.4
0301520130	0.001115	22.34	78,860	332.4
0301520140	0.0009785	20.33	98,800	416.5
0301520150	0.0009331	17.59	119,800	505.0
0301520160	0.0008378	16.90	138,800	585.3
0301620090	0.005881	32.92	9,442	39.80
0301620100	0.003146	31.15	18,650	78.66
0301620110	0.002023	26.14	34,560	145.7
0301620120	0.001407	22.14	58,690	247.4
0301620130	0.001145	20.24	78,860	332.4
0301620140	0.001003	18.45	98,800	416.5
0301620150	0.0009535	16.00	119,800	505.0
0301620160	0.0008557	15.39	138,800	585.3
0301720090	0.006144	29.90	9,442	39.80
0301720100	0.003288	28.27	18,650	78.66
0301720110	0.002103	23.86	34,560	145.7
0301720120	0.001460	20.24	58,690	247.4
0301720130	0.001183	18.58	78,860	332.4
0301720140	0.001046	16.78	98,800	416.5
0301720150	0.0009853	14.69	119,800	505.0
0301720160	0.0008766	14.25	138,800	585.3
0301820090	0.006362	26.16	9,442	39.80
0301820100	0.003349	25.14	18,650	78.66
0301820110	0.002166	20.99	34,560	145.7
0301820120	0.001491	17.95	58,690	247.4
0301820130	0.001217	16.37	78,860	332.4
0301820140	0.001060	15.00	98,800	416.5
0301820150	0.001013	12.95	119,800	505.0
0301820160	0.0009132	12.39	138,800	585.3

CODE	k Δt/Hx	$t_a/\Delta t$	V ρ x/μ	x/t
0302120090	0.009617	18.77	5,060	39.80
0302120100	0.005039	18.13	10,000	78.66
0302120110	0.003202	15.40	18,520	145.7
0302120120	0.002225	13.05	31,450	247.4
0302120130	0.001802	11.99	42,260	332.4
0302120140	0.001601	10.77	52,950	416.5
0302120150	0.001505	9.455	64,210	505.0
0302120160	0.001298	9.455	74,410	585.3
0302220090	0.007170	25.17	7,760	39.80
0302220100	0.003800	24.03	15,330	78.66
0302220110	0.002450	20.11	28,410	145.7
0302220120	0.001705	17.02	48,240	247.4
0302220130	0.001363	15.85	64,810	332.4
0302220140	0.001191	14.47	81,200	416.5
0302220150	0.001135	12.52	98,460	505.0
0302220160	0.001023	11.98	114,100	585.3
0302320090	0.006728	26.81	8,526	39.80
0302320100	0.003594	25.40	16,840	78.66
0302320110	0.002339	21.06	31,210	145.7
0302320120	0.001629	17.81	53,000	247.4
0302320130	0.001318	16.38	71,210	332.4
0302320140	0.001149	14.99	89,220	416.5
0302320150	0.001092	13.01	108,100	505.0
0302320160	0.0009753	12.58	125,300	585.3
0302420090	0.005335	33.78	11,540	39.80
0302420100	0.002803	32.54	22,810	78.66
0302420110	0.001865	26.39	42,270	145.7
0302420120	0.001295	22.38	71,770	247.4
0302420130	0.001053	20.48	96,440	332.4
0302420140	0.0009353	18.41	120,800	416.5
0302420150	0.0008865	16.02	146,500	505.0
0302420160	0.0007904	15.51	169,700	585.3
0302520090	0.004825	37.33	13,430	39.80
0302520100	0.002562	35.57	26,530	78.66
0302520110	0.001689	29.12	49,160	145.7
0302520120	0.001180	24.54	83,480	247.4
0302520130	0.0009602	22.46	112,100	332.4
0302520140	0.0008346	20.62	140,500	416.5
0302520150	0.0008035	17.66	170,400	505.0
0302520160	0.0007188	17.04	197,400	585.3
0302620090	0.003964	46.98	18,390	39.80
0302620100	0.002095	44.99	36,350	78.66
0302620110	0.001361	37.38	67,340	145.7
0302620120	0.0009652	31.04	114,300	247.4
0302620130	0.0007730	28.85	153,600	332.4
0302620140	0.0006773	26.28	192,500	416.5
0302620150	0.0006554	22.40	233,400	505.0
0302620160	0.0006061	20.90	270,500	585.3
0302720090	0.003908	46.19	18,390	39.80
0302720100	0.002063	44.26	36,350	78.66
0302720110	0.001624	30.35	67,340	145.7
0302720120	0.001038	27.95	114,300	247.4
0302720130	0.0008422	25.66	153,600	332.4
0302720140	0.0007859	21.95	192,500	416.5
0302720150	0.0006883	20.66	233,400	505.0
0302720160	0.0005939	20.66	270,500	585.3
0302820090	0.008292	21.87	6,046	39.80
0302820100	0.004385	20.93	11,940	78.66
0302820110	0.002831	17.50	22,130	145.7
0302820120	0.001683	17.33	37,580	247.4
0302820130	0.001171	18.53	50,500	332.4
0302820140	0.001373	12.61	63,270	416.5
0302820150	0.001296	11.02	76,720	505.0
0302820160	0.001148	10.74	88,910	585.3

TABLE B. XV

VALUES OF THE FOUR DIMENSIONLESS GROUPS FOR MODEL TREATMENT NO. 5 LEEWARD ROOF

CODE	$k\Delta t/Hx$	$t_a/\Delta t$	$V\rho x/\mu l$	x/t
0601120090	0.004038	93.85	8.393	39.80
0601120100	0.002223	86.28	16.580	78.66
0601120110	0.001412	73.28	30.720	145.7
0601120120	0.001003	60.79	52.170	247.4
0601120130	0.0008144	55.72	70.100	332.4
0601120140	0.0007245	49.99	87.820	416.5
0601120150	0.0006980	42.79	106.400	505.0
0601120160	0.0006457	39.92	123.400	585.3
0601220090	0.004297	81.10	8.393	39.80
0601220100	0.002405	73.32	16.580	78.66
0601220110	0.001565	60.82	30.720	145.7
0601220120	0.001120	50.02	52.170	247.4
0601220130	0.0009199	45.36	70.100	332.4
0601220140	0.0008089	41.17	87.820	416.5
0601220150	0.0007903	34.75	106.400	505.0
0601220160	0.0007262	32.63	123.400	585.3
0601320090	0.005245	55.12	8.393	39.80
0601320100	0.002900	50.44	16.580	78.66
0601320110	0.001846	42.77	30.720	145.7
0601320120	0.001304	35.64	52.170	247.4
0601320130	0.001068	32.40	70.100	332.4
0601320140	0.0009559	28.90	87.820	416.5
0601320150	0.0009120	24.98	106.400	505.0
0601320160	0.0008310	23.65	123.400	585.3
0601420090	0.005726	43.84	8.393	39.80
0601420100	0.003135	40.52	16.580	78.66
0601420110	0.001987	34.50	30.720	145.7
0601420120	0.001411	28.60	52.170	247.4
0601420130	0.001146	26.22	70.100	332.4
0601420140	0.001022	23.46	87.820	416.5
0601420150	0.0009802	20.18	106.400	505.0
0601420160	0.0009001	18.96	123.400	585.3
0601520090	0.006108	35.88	8.393	39.80
0601520100	0.003340	33.21	16.580	78.66
0601520110	0.002116	28.29	30.720	145.7
0601520120	0.001510	23.34	52.170	247.4
0601520130	0.001227	21.38	70.100	332.4
0601520140	0.001104	18.96	87.820	416.5
0601520150	0.001059	16.30	106.400	505.0
0601520160	0.0009646	15.45	123.400	585.3
0601620090	0.006104	33.42	8.393	39.80
0601620100	0.003321	31.09	16.580	78.66
0601620110	0.002115	26.34	30.720	145.7
0601620120	0.001497	21.91	52.170	247.4
0601620130	0.001210	20.18	70.100	332.4
0601620140	0.001097	17.76	87.820	416.5
0601620150	0.001046	15.36	106.400	505.0
0601620160	0.0009522	14.57	123.400	585.3
0601720090	0.006261	30.92	8.393	39.80
0601720100	0.003406	28.76	16.580	78.66
0601720110	0.002155	24.54	30.720	145.7
0601720120	0.001537	20.26	52.170	247.4
0601720130	0.001248	18.57	70.100	332.4
0601720140	0.001127	16.41	87.820	416.5
0601720150	0.001069	14.26	106.400	505.0
0601720160	0.0009772	13.47	123.400	585.3
0601820090	0.006428	27.86	8.393	39.80
0601820100	0.003507	25.84	16.580	78.66
0601820110	0.002249	21.74	30.720	145.7
0601820120	0.001583	18.19	52.170	247.4
0601820130	0.001274	16.82	70.100	332.4
0601820140	0.001139	15.02	87.820	416.5
0601820150	0.001095	12.89	106.400	505.0
0601820160	0.001013	12.02	123.400	585.3

CODE	$k\Delta t/Hx$	$t_a/\Delta t$	$V\rho x/\mu l$	x/t
0602120090	0.009394	19.46	4.771	39.80
0602120100	0.005082	18.21	9.428	78.66
0602120110	0.003200	15.60	17.460	145.7
0602120120	0.002253	13.05	29.650	247.4
0602120130	0.001856	11.79	39.850	332.4
0602120140	0.001694	10.31	49.920	416.5
0602120150	0.001572	9.167	60.540	505.0
0602120160	0.001366	9.105	70.160	585.3
0602220090	0.007754	23.59	6.117	39.80
0602220100	0.004252	21.77	12.080	78.66
0602220110	0.002696	18.53	22.390	145.7
0602220120	0.001907	15.43	38.020	247.4
0602220130	0.001591	13.76	51.090	332.4
0602220140	0.001446	12.09	64.010	416.5
0602220150	0.001365	10.56	77.610	505.0
0602220160	0.001212	10.26	89.940	585.3
0602320090	0.007344	24.89	7.328	39.80
0602320100	0.003993	23.16	14.480	78.66
0602320110	0.002566	19.46	26.820	145.7
0602320120	0.001808	16.26	45.550	247.4
0602320130	0.001468	14.90	61.200	332.4
0602320140	0.001335	13.08	76.680	416.5
0602320150	0.001278	11.26	92.980	505.0
0602320160	0.001152	10.79	107.700	585.3
0602420090	0.006354	28.76	7.799	39.80
0602420100	0.003440	26.88	15.410	78.66
0602420110	0.002211	22.57	28.550	145.7
0602420120	0.001577	18.64	48.480	247.4
0602420130	0.001276	17.15	65.140	332.4
0602420140	0.001132	15.42	81.610	416.5
0602420150	0.001090	13.21	98.960	505.0
0602420160	0.001003	12.38	114.600	585.3
0602520090	0.005090	35.87	10.090	39.80
0602520100	0.002800	32.99	19.940	78.66
0602520110	0.001829	27.27	36.950	145.7
0602520120	0.001296	22.65	62.740	247.4
0602520130	0.001059	20.64	84.300	332.4
0602520140	0.0009663	18.06	105.600	416.5
0602520150	0.0009288	15.49	128.000	505.0
0602520160	0.0008596	14.44	148.400	585.3
0602620090	0.004304	42.38	12.230	39.80
0602620100	0.002351	39.26	24.170	78.66
0602620110	0.001530	32.56	44.780	145.7
0602620120	0.001104	26.56	76.050	247.4
0602620130	0.0008998	24.27	102.100	332.4
0602620140	0.0008194	21.27	128.000	416.5
0602620150	0.0007942	18.10	155.200	505.0
0602620160	0.0007341	16.89	179.800	585.3
0602720090	0.003826	47.64	14.250	39.80
0602720100	0.002109	43.73	28.160	78.66
0602720110	0.001362	36.54	52.170	145.7
0602720120	0.0009892	29.64	88.590	247.4
0602720130	0.0007935	27.50	119.000	332.4
0602720140	0.0007247	24.03	149.100	416.5
0602720150	0.0007161	20.05	180.800	505.0
0602720160	0.0006551	18.92	209.500	585.3
0602820090	0.003484	52.29	16.210	39.80
0602820100	0.001884	48.93	32.030	78.66
0602820110	0.001250	39.80	59.340	145.7
0602820120	0.0009177	31.93	100.700	247.4
0602820130	0.0007280	29.96	135.300	332.4
0602820140	0.0006627	26.27	169.600	416.5
0602820150	0.0006542	21.95	205.600	505.0
0602820160	0.0006110	20.28	238.300	585.3

TABLE B.XVI

VALUES OF THE FOUR DIMENSIONLESS GROUPS FOR MODEL TREATMENT NO. 6 LEEWARD ROOF

CODE	$k\Delta t/Hx$	$t_a/\Delta t$	$V\rho x/\mu$	x/t
0701120090	0.004914	65.48	8,154	39.80
0701120100	0.002763	58.93	16,110	78.66
0701120110	0.001723	50.99	29,850	145.7
0701120120	0.001161	44.57	50,690	247.4
0701120130	0.0008862	43.47	68,110	332.4
0701120140	0.0007595	40.48	85,330	416.5
0701120150	0.0006885	36.83	103,400	505.0
0701120160	0.0006230	35.12	119,900	585.3
0701220090	0.005386	52.04	8,154	39.80
0701220100	0.003019	46.98	16,110	78.66
0701220110	0.001903	40.21	29,850	145.7
0701220120	0.001291	34.92	50,690	247.4
0701220130	0.0009862	34.03	68,110	332.4
0701220140	0.0008427	31.78	85,330	416.5
0701220150	0.0007574	29.16	103,400	505.0
0701220160	0.0006715	28.38	119,900	585.3
0701320090	0.005920	40.23	8,154	39.80
0701320100	0.003314	36.37	16,110	78.66
0701320110	0.002046	31.80	29,850	145.7
0701320120	0.001392	27.51	50,690	247.4
0701320130	0.001063	26.82	68,110	332.4
0701320140	0.0009130	24.93	85,330	416.5
0701320150	0.0008307	22.59	103,400	505.0
0701320160	0.0007321	22.12	119,900	585.3
0701420090	0.006026	33.82	8,154	39.80
0701420100	0.003418	30.17	16,110	78.66
0701420110	0.002159	25.78	29,850	145.7
0701420120	0.001463	22.40	50,690	247.4
0701420130	0.001116	21.85	68,110	332.4
0701420140	0.0009574	20.34	85,330	416.5
0701420150	0.0008682	18.50	103,400	505.0
0701420160	0.0007727	17.94	119,900	585.3
0701520090	0.006441	27.53	8,154	39.80
0701520100	0.003614	24.83	16,110	78.66
0701520110	0.002252	21.51	29,850	145.7
0701520120	0.001514	18.84	50,690	247.4
0701520130	0.001126	18.84	68,110	332.4
0701520140	0.0009473	17.89	85,330	416.5
0701520150	0.0008497	16.45	103,400	505.0
0701520160	0.0007763	15.53	119,900	585.3
0701620090	0.006589	25.55	8,154	39.80
0701620100	0.003703	23.01	16,110	78.66
0701620110	0.002345	19.61	29,850	145.7
0701620120	0.001554	17.42	50,690	247.4
0701620130	0.001164	17.31	68,110	332.4
0701620140	0.0009870	16.30	85,330	416.5
0701620150	0.0008914	14.89	103,400	505.0
0701620160	0.0008123	14.10	119,900	585.3
0701720090	0.006731	23.00	8,154	39.80
0701720100	0.003760	20.84	16,110	78.66
0701720110	0.002356	17.95	29,850	145.7
0701720120	0.001575	15.81	50,690	247.4
0701720130	0.001175	15.77	68,110	332.4
0701720140	0.0009996	14.80	85,330	416.5
0701720150	0.0009025	13.52	103,400	505.0
0701720160	0.0008124	12.96	119,900	585.3
0701820090	0.006803	20.68	8,154	39.80
0701820100	0.003818	18.65	16,110	78.66
0701820110	0.002379	16.16	29,850	145.7
0701820120	0.001597	14.17	50,690	247.4
0701820130	0.001185	14.21	68,110	332.4
0701820140	0.001001	13.42	85,330	416.5
0701820150	0.0008950	12.39	103,400	505.0
0701820160	0.0008137	11.76	119,900	585.3

CODE	$k\Delta t/Hx$	$t_a/\Delta t$	$V\rho x/\mu$	x/t
0702120090	0.008241	17.74	6,346	39.80
0702120100	0.004643	15.93	12,540	78.66
0702120110	0.002919	13.68	23,230	145.7
0702120120	0.001940	12.12	39,450	247.4
0702120130	0.001470	11.90	53,000	332.4
0702120140	0.001257	11.11	66,410	416.5
0702120150	0.001134	10.15	80,520	505.0
0702120160	0.001010	9.839	93,320	585.3
0702220090	0.01008	14.50	4,815	39.80
0702220100	0.006298	11.75	9,515	78.66
0702220110	0.003489	11.45	17,620	145.7
0702220120	0.002298	10.24	29,930	247.4
0702220130	0.001733	10.10	40,210	332.4
0702220140	0.001467	9.525	50,380	416.5
0702220150	0.001309	8.801	61,090	505.0
0702220160	0.001145	8.686	70,800	585.3
0702320090	0.007582	19.30	7,166	39.80
0702320100	0.004254	17.40	14,160	78.66
0702320110	0.002649	15.09	26,230	145.7
0702320120	0.001759	13.38	44,540	247.4
0702320130	0.001319	13.28	59,850	332.4
0702320140	0.001118	12.50	74,980	416.5
0702320150	0.001006	11.45	90,920	505.0
0702320160	0.0008968	11.09	105,300	585.3
0702420090	0.006538	22.37	8,738	39.80
0702420100	0.003684	20.09	17,260	78.66
0702420110	0.002273	17.57	31,990	145.7
0702420120	0.001551	15.17	54,320	247.4
0702420130	0.001157	15.13	72,980	332.4
0702420140	0.0009766	14.31	91,440	416.5
0702420150	0.0008812	13.08	110,800	505.0
0702420160	0.0008052	12.35	128,400	585.3
0702520090	0.006208	23.57	9,296	39.80
0702520100	0.003503	21.13	18,360	78.66
0702520110	0.002176	18.36	34,030	145.7
0702520120	0.001485	15.85	57,780	247.4
0702520130	0.001115	15.71	77,640	332.4
0702520140	0.0009425	14.83	97,270	416.5
0702520150	0.0008466	13.62	117,900	505.0
0702520160	0.0007716	12.89	136,600	585.3
0702620090	0.005714	25.61	10,760	39.80
0702620100	0.003225	22.96	21,270	78.66
0702620110	0.001988	20.10	39,410	145.7
0702620120	0.001365	17.24	66,930	247.4
0702620130	0.001026	17.07	89,930	332.4
0702620140	0.0008637	16.19	112,600	416.5
0702620150	0.0007340	15.71	136,600	505.0
0702620160	0.0007043	14.13	158,300	585.3
0702720090	0.004807	30.46	12,500	39.80
0702720100	0.002738	27.06	24,700	78.66
0702720110	0.001763	22.68	45,770	145.7
0702720120	0.001188	19.82	77,710	247.4
0702720130	0.0008848	19.82	104,400	332.4
0702720140	0.0007508	18.64	130,800	416.5
0702720150	0.0006820	16.92	158,600	505.0
0702720160	0.0006240	15.96	183,800	585.3
0702820090	0.003626	40.43	17,820	39.80
0702820100	0.002071	35.81	35,220	78.66
0702820110	0.001298	30.84	65,260	145.7
0702820120	0.0008883	26.55	110,800	247.4
0702820130	0.0006611	26.55	148,900	332.4
0702820140	0.0005565	25.17	186,500	416.5
0702820150	0.0005109	22.61	226,200	505.0
0702820160	0.0004726	21.09	262,100	585.3

TABLE B.XVII

VALUES OF THE FOUR DIMENSIONLESS GROUPS FOR MODEL TREATMENT NO. 7 LEEWARD ROOF

CODE	k Δt/Hx	$t_a/\Delta t$	$V\rho x/\mu$	x/t
0801120090	0.004498	80.14	8,058	39.80
0801120100	0.002582	70.65	15,940	78.66
0801120110	0.001522	64.69	29,530	145.7
0801120120	0.001037	55.93	50,150	247.4
0801120130	0.0008200	52.64	67,380	332.4
0801120140	0.0007507	45.89	84,430	416.5
0801120150	0.0007038	40.37	102,300	505.0
0801120160	0.0006256	39.19	118,600	585.3
0801220090	0.004892	63.18	8,068	39.80
0801220100	0.002679	58.37	15,940	78.66
0801220110	0.001666	50.66	29,530	145.7
0801220120	0.001148	43.31	50,150	247.4
0801220130	0.0008751	42.29	67,380	332.4
0801220140	0.0008415	35.10	84,430	416.5
0801220150	0.0007892	30.86	102,300	505.0
0801220160	0.0006849	30.69	118,600	585.3
0801320090	0.005376	50.67	8,068	39.80
0801320100	0.002891	45.91	15,940	78.66
0801320110	0.001800	39.79	29,530	145.7
0801320120	0.001225	34.43	50,150	247.4
0801320130	0.0009939	31.59	67,380	332.4
0801320140	0.0009100	27.54	84,430	416.5
0801320150	0.0008544	24.19	102,300	505.0
0801320160	0.0007439	23.98	118,600	585.3
0801420090	0.005675	40.39	8,068	39.80
0801420100	0.003174	36.55	15,940	78.66
0801420110	0.001970	31.79	29,530	145.7
0801420120	0.001345	27.41	50,150	247.4
0801420130	0.001098	24.99	67,380	332.4
0801420140	0.0009910	22.11	84,430	416.5
0801420150	0.0009283	19.46	102,300	505.0
0801420160	0.0008213	18.98	118,600	585.3
0801520090	0.006080	32.96	8,068	39.80
0801520100	0.003379	30.01	15,940	78.66
0801520110	0.002099	26.08	29,530	145.7
0801520120	0.001440	22.38	50,150	247.4
0801520130	0.001170	20.50	67,380	332.4
0801520140	0.001055	18.15	84,430	416.5
0801520150	0.0009849	16.03	102,300	505.0
0801520160	0.0008600	15.84	118,600	585.3
0801620090	0.006079	30.88	8,068	39.80
0801620100	0.003430	27.70	15,940	78.66
0801620110	0.002128	24.09	29,530	145.7
0801620120	0.001461	20.66	50,150	247.4
0801620130	0.001188	18.92	67,380	332.4
0801620140	0.001078	16.63	84,430	416.5
0801620150	0.001018	14.52	102,300	505.0
0801620160	0.0008911	14.33	118,600	585.3
0801720090	0.006304	27.98	8,068	39.80
0801720100	0.003555	25.11	15,940	78.66
0801720110	0.002206	21.84	29,530	145.7
0801720120	0.001521	18.65	50,150	247.4
0801720130	0.001234	17.11	67,380	332.4
0801720140	0.001120	15.05	84,430	416.5
0801720150	0.001053	13.20	102,300	505.0
0801720160	0.0009200	13.04	118,600	585.3
0801820090	0.006552	24.20	8,068	39.80
0801820100	0.003644	22.02	15,940	78.66
0801820110	0.002241	19.33	29,530	145.7
0801820120	0.001538	16.58	50,150	247.4
0801820130	0.001250	15.18	67,380	332.4
0801820140	0.001133	13.36	84,430	416.5
0801820150	0.001065	11.73	102,300	505.0
0801820160	0.0009313	11.58	118,600	585.3

CODE	k Δt/Hx	$t_a/\Delta t$	$V\rho x/\mu$	x/t
0802120090	0.009234	17.39	4,944	39.80
0802120100	0.005043	16.12	9,769	78.66
0802120110	0.003055	14.36	18,090	145.7
0802120120	0.002088	12.37	30,730	247.4
0802120130	0.001696	11.33	41,290	332.4
0802120140	0.001543	9.946	51,730	416.5
0802120150	0.001438	8.801	62,730	505.0
0802120160	0.001233	8.860	72,690	585.3
0802220090	0.007192	22.33	6,827	39.80
0802220100	0.004303	18.89	13,490	78.66
0802220110	0.002472	17.75	24,990	145.7
0802220120	0.001730	14.93	42,430	247.4
0802220130	0.001423	13.51	57,010	332.4
0802220140	0.001313	11.68	71,430	416.5
0802220150	0.001217	10.39	86,620	505.0
0802220160	0.001044	10.46	100,300	585.3
0802320090	0.006217	25.84	8,668	39.80
0802320100	0.003454	23.53	17,120	78.66
0802320110	0.002131	20.59	31,730	145.7
0802320120	0.001465	17.63	53,880	247.4
0802320130	0.001215	15.83	72,390	332.4
0802320140	0.001100	13.94	90,700	416.5
0802320150	0.001030	12.29	109,900	505.0
0802320160	0.0008788	12.43	127,400	585.3
0802420090	0.005424	29.63	9,682	39.80
0802420100	0.003038	26.78	19,130	78.66
0802420110	0.001848	23.76	35,440	145.7
0802420120	0.001235	20.93	60,180	247.4
0802420130	0.0009596	20.06	80,860	332.4
0802420140	0.0008387	18.31	101,300	416.5
0802420150	0.0008094	15.65	122,800	505.0
0802420160	0.0007399	14.77	142,300	585.3
0802520090	0.004937	32.57	11,090	39.80
0802520100	0.002776	29.31	21,910	78.66
0802520110	0.001706	25.74	40,600	145.7
0802520120	0.001152	22.45	68,940	247.4
0802520130	0.0008866	21.71	92,630	332.4
0802520140	0.0007863	19.54	116,000	416.5
0802520150	0.0007662	16.54	140,700	505.0
0802520160	0.0006943	15.75	163,000	585.3
0802620090	0.004540	35.41	12,640	39.80
0802620100	0.002529	32.17	24,990	78.66
0802620110	0.001556	28.21	46,300	145.7
0802620120	0.001073	24.09	78,620	247.4
0802620130	0.0008356	23.04	105,600	332.4
0802620140	0.0007572	20.29	132,300	416.5
0802620150	0.0007566	16.75	160,400	505.0
0802620160	0.0006777	16.13	185,900	585.3
0802720090	0.004022	39.99	14,640	39.80
0802720100	0.002267	35.91	28,940	78.66
0802720110	0.001390	31.61	53,620	145.7
0802720120	0.0009658	26.80	91,040	247.4
0802720130	0.0007626	25.26	122,300	332.4
0802720140	0.0006756	22.75	153,200	416.5
0802720150	0.0006941	18.26	185,800	505.0
0802720160	0.0006052	18.08	215,300	585.3
0802820090	0.003626	44.41	16,980	39.80
0802820100	0.002051	39.73	33,560	78.66
0802820110	0.001273	34.54	62,180	145.7
0802820120	0.0008629	30.02	105,500	247.4
0802820130	0.0006823	28.26	141,800	332.4
0802820140	0.0006261	24.58	177,700	416.5
0802820150	0.0006293	20.17	215,500	505.0
0802820160	0.0005451	20.09	249,700	585.3

TABLE B.XVIII

VALUES OF THE FOUR DIMENSIONLESS GROUPS FOR MODEL TREATMENT NO. 8 LEEWARD ROOF

CODE	k△t/Hx	$t_a/\triangle t$	V♀x/△	x/t
0101120090	0.004589	74.37	8.850	39.80
0101120100	0.002548	67.78	17.480	78.66
0101120110	0.001602	58.20	32.390	145.7
0101120120	0.001128	48.68	55.010	247.4
0101120130	0.0009311	43.89	73.910	332.4
0101120140	0.0008650	37.71	92.600	416.5
0101120150	0.0008239	32.65	112.200	505.0
0101120160	0.0007066	32.85	130.100	585.3
0101220090	0.005194	55.19	8.850	39.80
0101220100	0.002899	50.03	17.480	78.66
0101220110	0.001799	43.52	32.390	145.7
0101220120	0.001257	36.67	55.010	247.4
0101220130	0.001045	32.84	73.910	332.4
0101220140	0.0009620	28.47	92.600	416.5
0101220150	0.0009073	24.90	112.200	505.0
0101220160	0.0007756	25.13	130.100	585.3
0101320090	0.005789	42.17	8.850	39.80
0101320100	0.003206	38.53	17.480	78.66
0101320110	0.001979	33.68	32.390	145.7
0101320120	0.001393	28.18	55.010	247.4
0101320130	0.001140	25.62	73.910	332.4
0101320140	0.001036	22.50	92.600	416.5
0101320150	0.0009880	19.47	112.200	505.0
0101320160	0.0008401	19.76	130.100	585.3
0101420090	0.006055	34.56	8.850	39.80
0101420100	0.003360	31.51	17.480	78.66
0101420110	0.002112	27.06	32.390	145.7
0101420120	0.001495	22.51	55.010	247.4
0101420130	0.001234	20.29	73.910	332.4
0101420140	0.001127	17.74	92.600	416.5
0101420150	0.001065	15.48	112.200	505.0
0101420160	0.0009059	15.71	130.100	585.3
0101520090	0.006324	28.80	8.850	39.80
0101520100	0.003459	26.65	17.480	78.66
0101520110	0.002182	22.79	32.390	145.7
0101520120	0.001526	19.20	55.010	247.4
0101520130	0.001254	17.39	73.910	332.4
0101520140	0.001147	15.17	92.600	416.5
0101520150	0.001101	13.03	112.200	505.0
0101520160	0.0009574	12.94	130.100	585.3
0101620090	0.006561	25.88	8.850	39.80
0101620100	0.003657	23.50	17.480	78.66
0101620110	0.002285	20.29	32.390	145.7
0101620120	0.001621	16.85	55.010	247.4
0101620130	0.001324	15.35	73.910	332.4
0101620140	0.001220	13.29	92.600	416.5
0101620150	0.001149	11.64	112.200	505.0
0101620160	0.0009872	11.70	130.100	585.3
0101720090	0.006604	24.14	8.850	39.80
0101720100	0.003688	21.88	17.480	78.66
0101720110	0.002332	18.67	32.390	145.7
0101720120	0.001651	15.53	55.010	247.4
0101720130	0.001339	14.25	73.910	332.4
0101720140	0.001213	12.55	92.600	416.5
0101720150	0.001165	10.78	112.200	505.0
0101720160	0.001015	10.67	130.100	585.3
0101820090	0.006825	21.52	8.850	39.80
0101820100	0.003759	19.78	17.480	78.66
0101820110	0.002366	16.96	32.390	145.7
0101820120	0.001658	14.25	55.010	247.4
0101820130	0.001385	12.70	73.910	332.4
0101820140	0.001270	11.05	92.600	416.5
0101820150	0.001201	9.641	112.200	505.0
0101820160	0.001027	9.729	130.100	585.3

CODE	k△t/Hx	$t_a/\triangle t$	V♀x/△	x/t
0102120090	0.01106	13.22	5.010	39.80
0102120100	0.005964	12.42	9.900	78.66
0102120110	0.003672	10.88	18.340	145.7
0102120120	0.002554	9.219	31.140	247.4
0102120130	0.002070	8.467	41.840	332.4
0102120140	0.001805	7.748	52.420	416.5
0102120150	0.001615	7.141	63.560	505.0
0102120160	0.001398	7.122	73.660	585.3
0102220090	0.009296	15.75	6.476	39.80
0102220100	0.004970	14.90	12.790	78.66
0102220110	0.003083	12.97	23.710	145.7
0102220120	0.002140	11.00	40.260	247.4
0102220130	0.001752	10.00	54.090	332.4
0102220140	0.001541	9.078	67.770	416.5
0102220150	0.001397	8.257	82.170	505.0
0102220160	0.001219	8.168	95.230	585.3
0102320090	0.007525	19.46	7.560	39.80
0102320100	0.004172	17.76	14.930	78.66
0102320110	0.002622	15.25	27.670	145.7
0102320120	0.001833	12.85	46.990	247.4
0102320130	0.001517	11.56	63.140	332.4
0102320140	0.001340	10.44	79.110	416.5
0102320150	0.001223	9.436	95.920	505.0
0102320160	0.001085	9.176	111.100	585.3
0102420090	0.006889	21.27	8.797	39.80
0102420100	0.003808	19.47	17.380	78.66
0102420110	0.002388	16.76	32.200	145.7
0102420120	0.001673	14.08	54.680	247.4
0102420130	0.001351	12.98	73.470	332.4
0102420140	0.001197	11.69	92.050	416.5
0102420150	0.001129	10.22	111.600	505.0
0102420160	0.0009859	10.10	129.300	585.3
0102520090	0.005588	26.22	11.270	39.80
0102520100	0.003080	24.07	22.270	78.66
0102520110	0.001889	21.18	41.270	145.7
0102520120	0.001295	18.20	70.080	247.4
0102520130	0.001026	17.08	94.160	332.4
0102520140	0.0009386	14.92	117.900	416.5
0102520150	0.0008918	12.95	143.000	505.0
0102520160	0.0008071	12.34	165.700	585.3
0102620090	0.004869	30.11	13.570	39.80
0102620100	0.002730	27.18	26.810	78.66
0102620110	0.001715	23.35	49.670	145.7
0102620120	0.001215	19.41	84.350	247.4
0102620130	0.0009639	18.21	113.300	332.4
0102620140	0.0008725	16.06	142.000	416.5
0102620150	0.0008613	13.42	172.100	505.0
0102620160	0.0007563	13.18	199.500	585.3
0102720090	0.004233	34.66	16.050	39.80
0102720100	0.002366	31.38	31.720	78.66
0102720110	0.001503	26.65	58.760	145.7
0102720120	0.001072	22.00	99.780	247.4
0102720130	0.0008612	20.39	134.000	332.4
0102720140	0.0007879	17.79	167.900	416.5
0102720150	0.0007893	14.65	203.600	505.0
0102720160	0.0006811	14.65	236.000	585.3
0102820090	0.004011	36.59	18.390	39.80
0102820100	0.002198	33.79	36.350	78.66
0102820110	0.001390	28.83	67.350	145.7
0102820120	0.0009791	24.11	114.300	247.4
0102820130	0.0007652	22.96	153.600	332.4
0102820140	0.0007138	19.65	192.500	416.5
0102820150	0.0007217	16.02	233.400	505.0
0102820160	0.0006228	16.02	270.500	585.3

TABLE B. XIX

VALUES OF THE FOUR DIMENSIONLESS GROUPS FOR 8 FT X 8 FT SHELTER TREATMENT NO. 12 WINDWARD ROOF, FIRST DAY

CODE	k △t/Hx	$t_a/\triangle t$	V/x/	x/t
3001110010	0.008202	29.17	8.734	53.05
3001110020	0.002252	26.25	35.330	214.6
3001110030	0.001418	26.93	54.730	332.4
3001110040	0.001289	23.13	70.040	425.4
3001110050	0.0008467	25.61	96.360	585.3
3001110060	0.0005993	26.93	129.500	786.6
3001110070	0.0003980	23.87	219.900	1.336.
3001110080	0.0003033	23.34	295.200	1.793.
3001110090	0.0002473	22.83	370.100	2.248.
3001110100	0.0002013	23.13	448.800	2.726.
3001210010	0.008135	29.04	9.146	53.05
3001210020	0.002211	26.42	37.000	214.6
3001210030	0.001391	27.10	57.310	332.4
3001210040	0.001171	25.15	73.340	425.4
3001210050	0.0007700	27.81	100.900	585.3
3001210060	0.0005275	30.21	135.500	786.6
3001210070	0.0003908	24.00	230.300	1.336.
3001210080	0.0002845	24.56	309.100	1.793.
3001210090	0.0002110	26.42	387.500	2.248.
3001210100	0.0001837	25.03	469.900	2.726.
3001310010	0.008583	27.03	6.620	53.05
3001310020	0.002393	23.96	26.780	214.6
3001310030	0.001545	23.96	41.480	332.4
3001310040	0.001372	21.08	53.090	425.4
3001310050	0.0009575	21.96	73.030	585.3
3001310060	0.0006383	24.52	98.150	786.6
3001310070	0.0004893	18.82	166.700	1.336.
3001310080	0.0003450	19.89	223.800	1.793.
3001310090	0.0002648	20.67	280.500	2.248.
3001310100	0.0002141	21.08	340.100	2.726.
3001410010	0.007032	32.91	9.632	53.05
3001410020	0.002064	27.72	38.970	214.6
3001410030	0.001332	27.72	60.360	332.4
3001410040	0.001096	26.33	77.240	425.4
3001410050	0.0007569	27.72	106.200	585.3
3001410060	0.0005039	30.98	142.800	786.6
3001410070	0.0003839	23.94	242.600	1.336.
3001410080	0.0002730	25.08	325.600	1.793.
3001410090	0.0002074	26.33	408.200	2.248.
3001410100	0.00002634	27.00	494.900	2.726.

CODE	k △t/Hx	$t_a/\triangle t$	V/x/	x/t
3001510010	0.007352	31.04	10.740	53.05
3001510020	0.002084	27.06	43.480	214.6
3001510030	0.001276	28.52	67.350	332.4
3001510040	0.001132	25.12	86.190	425.4
3001510050	0.0007644	27.06	118.500	585.3
3001510060	0.0005396	28.52	159.300	786.6
3001510070	0.0004121	21.98	270.700	1.336.
3001510080	0.0003070	21.98	363.300	1.793.
3001510090	0.0002347	22.96	455.400	2.248.
3001510100	0.0001683	26.38	552.200	2.726.
3001610010	0.008099	27.72	10.170	53.05
3001610020	0.002318	23.94	41.170	214.6
3001610030	0.001360	26.33	63.780	332.4
3001610040	0.001275	21.94	81.620	425.4
3001610050	0.0008500	23.94	112.200	585.3
3001610060	0.0006325	23.94	150.800	786.6
3001610070	0.0004400	20.25	256.300	1.336.
3001610080	0.0003089	21.49	344.000	1.793.
3001610090	0.0002414	21.94	431.300	2.248.
3001610100	0.0001949	22.41	522.900	2.726.
3001710010	0.007575	29.31	9.297	53.05
3001710020	0.002184	25.12	37.610	214.6
3001710030	0.001410	25.12	58.260	332.4
3001710040	0.001338	20.69	74.550	425.4
3001710050	0.001010	19.91	102.500	585.3
3001710060	0.0006244	23.98	137.800	786.6
3001710070	0.0004678	18.84	234.100	1.336.
3001710080	0.0003361	19.54	314.200	1.793.
3001710090	0.0002731	19.18	393.900	2.248.
3001710100	0.0002170	19.91	477.600	2.726.
3001810010	0.008701	25.71	8.113	53.05
3001810020	0.002360	23.43	32.820	214.6
3001810030	0.001591	22.43	50.840	332.4
3001810040	0.001402	19.89	65.060	425.4
3001810050	0.0009618	21.08	89.510	585.3
3001810060	0.0006441	23.43	120.200	786.6
3001810070	0.0005140	17.28	204.300	1.336.
3001810080	0.0003515	18.82	274.200	1.793.
3001810090	0.0002854	18.49	343.800	2.248.
3001810100	0.0002230	19.52	416.800	2.726.

TABLE B.XX

VALUES OF THE FOUR DIMENSIONLESS GROUPS FOR 8 FT X 8 FT SHELTER TREATMENT NO. 12 WINDWARD ROOF, SECOND DAY

CODE	$k\Delta t/Hx$	$t_a/\Delta t$	$V\rho x/\mu$	x/t
3002110010	0.008699	25.71	8,150	53.05
3002110020	0.002569	21.51	32,970	214.6
3002110030	0.001692	21.08	51,070	332.4
3002110040	0.001481	18.82	65,360	425.4
3002110050	0.0009039	22.43	89,920	585.3
3002110060	0.0006411	23.53	120,800	786.6
3002110070	0.0005054	17.57	205,200	1,336.
3002110080	0.0003765	17.57	275,500	1,793.
3002110090	0.0002903	18.17	345,400	2,248.
3002110100	0.0002353	18.49	418,700	2,726.
3002210010	0.008690	24.63	8,897	53.05
3002210020	0.002597	20.37	35,990	214.6
3002210030	0.001741	19.61	55,750	332.4
3002210040	0.001512	17.65	71,350	425.4
3002210050	0.0009159	21.18	98,160	585.3
3002210060	0.0006407	22.54	131,900	786.6
3002210070	0.0005296	16.05	224,000	1,336.
3002210080	0.0003886	16.29	300,700	1,793.
3002210090	0.0002670	18.91	377,000	2,248.
3002210100	0.0002478	16.81	457,100	2,726.
3002310010	0.007654	27.16	8,823	53.05
3002310020	0.002183	23.54	35,690	214.6
3002310030	0.001503	22.07	55,280	332.4
3002310040	0.001346	19.26	70,750	425.4
3002310050	0.0008894	21.18	97,330	585.3
3002310060	0.0005957	23.54	130,800	786.6
3002310070	0.0004659	17.71	222,200	1,336.
3002310080	0.0003367	18.26	298,200	1,793.
3002310090	0.0002547	19.26	373,800	2,248.
3002310100	0.0002024	19.98	453,300	2,726.
3002410010	0.007276	27.93	10,280	53.05
3002410020	0.002224	22.58	41,600	214.6
3002410030	0.001466	22.11	64,440	332.4
3002410040	0.001193	21.22	82,460	425.4
3002410050	0.0008157	22.58	113,400	585.3
3002410060	0.0005611	23.58	152,400	786.6
3002410070	0.0004713	17.11	259,000	1,336.
3002410080	0.0003285	18.29	347,600	1,793.
3002410090	0.0002485	19.29	435,700	2,248.
3002410100	0.0001975	20.02	528,300	2,726.

CODE	$k\Delta t/Hx$	$t_a/\Delta t$	$V\rho x/\mu$	x/t
3002610010	0.009048	23.23	6,714	53.05
3002610020	0.002637	19.71	27,160	214.6
3002610030	0.001733	19.35	42,070	332.4
3002610040	0.001502	17.44	53,840	425.4
3002610050	0.001020	18.67	74,080	585.3
3002610060	0.0006795	20.87	99,550	786.6
3002610070	0.0005192	16.07	169,100	1,336.
3002610080	0.0003681	16.89	226,900	1,793.
3002610090	0.0002750	18.04	284,500	2,248.
3002610100	0.0002422	16.89	345,000	2,726.
3002710010	0.008739	24.12	8,449	53.05
3002710020	0.002209	23.58	34,180	214.6
3002710030	0.001648	20.41	52,940	332.4
3002710040	0.001386	18.95	67,750	425.4
3002710050	0.0009721	19.65	93,210	585.3
3002710060	0.0006430	22.11	125,200	786.6
3002710070	0.0005204	16.08	212,800	1,336.
3002710080	0.0003760	16.58	285,600	1,793.
3002710090	0.0002999	16.58	358,000	2,248.
3002710100	0.0002435	16.84	434,100	2,726.
3002810010	0.009212	22.64	7,403	53.05
3002810020	0.002664	19.35	29,950	214.6
3002810030	0.001782	18.67	46,390	332.4
3002810040	0.001490	17.44	59,370	425.4
3002810050	0.001012	18.67	81,680	585.3
3002810060	0.0006874	20.46	109,700	786.6
3002810070	0.0005525	14.99	186,400	1,336.
3002810080	0.0004058	15.20	250,200	1,793.
3002810090	0.0003237	15.20	313,700	2,248.
3002810100	0.0002708	14.99	380,400	2,726.
3002510010	0.007850	26.63	7,768	53.05
3002510020	0.002522	20.48	31,430	214.6
3002510030	0.001659	20.10	48,680	332.4
3002510040	0.001370	19.02	62,300	425.4
3002510050	0.0009250	20.48	85,710	585.3
3002510060	0.0006089	23.16	115,100	786.6
3002510070	0.0004831	17.18	195,600	1,336.
3002510080	0.0003657	16.91	262,600	1,793.
3002510090	0.0002871	17.18	329,200	2,248.
3002510100	0.0002139	19.02	399,100	2,726.

TABLE B.XXI

VALUES OF THE FOUR DIMENSIONLESS GROUPS FOR THE 48 FT X 48 FT SHELTER TREATMENT NO. 9 WINDWARD ROOF

CODE	k Δt/Hx	$t_a/\Delta t$	$V\rho x/\mu$	x/t
5203510010	0.0003132	36.67	37,360	1,074.
5203510020	0.00006070	51.61	136,900	3,939.
5203510030	0.00005036	27.32	311,800	8,968.
5203510040	0.00003796	23.82	474,600	13,640.
5205510010	0.0002195	51.61	80,310	1,074.
5205510020	0.00009538	32.41	294,400	3,939.
5205510030	0.00004433	30.63	670,300	8,968.
5205510040	0.00003249	27.46	1,020,000	13,640.
5230510010	0.0002414	41.81	59,390	1,074.
5230510020	0.0001070	25.71	217,700	3,939.
5230510030	0.00004660	25.96	495,700	8,968.
5230510040	0.00003787	20.98	754,500	13,640.
5203610010	0.0002249	51.10	61,470	1,074.
5203610020	0.00006247	50.17	225,300	3,939.
5203610030	0.00004104	33.55	513,000	8,968.
5203610040	0.00003070	29.47	780,900	13,640.
5205610010	0.0002708	43.23	58,740	1,074.
5205610020	0.0001093	29.20	215,300	3,939.
5205610030	0.00004754	29.51	490,200	8,968.
5205610040	0.00003289	28.02	746,200	13,640.
5230610010	0.0002516	40.33	46,990	1,074.
5230610020	0.00009032	30.64	172,300	3,939.
5230610030	0.00004278	28.42	392,200	8,968.
5230610040	0.00003393	23.54	597,000	13,640.
5203710010	0.0002555	48.36	66,370	1,074.
5203710020	0.00007879	42.78	243,300	3,939.
5203710030	0.00004233	34.98	553,900	8,968.
5203710040	0.00003218	30.22	843,100	13,640.
5205710010	0.0002059	61.18	87,220	1,074.
5205710020	0.0001043	32.94	319,700	3,939.
5205710030	0.00004094	36.87	727,900	8,968.
5205710040	0.00002636	37.62	1,107,000	13,640.
5230710010	0.0002703	37.33	62,430	1,074.
5230710020	0.0001123	24.50	228,900	3,939.
5230710030	0.00004472	27.03	521,100	8,968.
5230710040	0.00003807	20.87	793,100	13,640.
5203810010	0.0002652	48.81	62,980	1,074.
5203810020	0.00007108	49.68	230,900	3,939.
5203810030	0.00004572	33.93	525,700	8,968.
5203810040	0.00003553	28.68	800,100	13,640.
5205810010	0.0001896	69.61	87,810	1,074.
5205810020	0.00005820	61.87	321,900	3,939.
5205810030	0.00003039	52.04	732,900	8,968.
5205810040	0.00002501	41.55	1,115,000	13,640.
5230810010	0.0002026	50.31	78,010	1,074.
5230810020	0.00009280	29.96	286,000	3,939.
5230810030	0.00003742	32.64	651,100	8,968.
5230810040	0.00003146	25.50	991,000	13,640.

CODE	k Δt/Hx	$t_a/\Delta t$	$V\rho x/\mu$	x/t
5203110010	0.0002281	44.72	40,630	1,074.
5203110020	0.00008683	32.05	148,900	3,939.
5203110030	0.00004211	29.03	339,100	8,968.
5203110040	0.00003172	25.32	516,200	13,640.
5205110010	0.0002094	49.82	85,250	1,074.
5205110020	0.00007091	40.14	312,500	3,939.
5205110030	0.00003966	31.52	711,500	8,968.
5205110040	0.00002723	30.16	1,083,000	13,640.
5230110010	0.0002488	41.04	36,440	1,074.
5230110020	0.0001071	25.99	133,500	3,939.
5230110030	0.00004482	27.29	304,100	8,968.
5230110040	0.00003298	24.37	462,800	13,640.
5203210010	0.0002688	38.61	50,920	1,074.
5203210020	0.0001089	25.98	186,700	3,939.
5203210030	0.00005257	23.65	425,000	8,968.
5203210040	0.00003762	21.71	646,900	13,640.
5205210010	0.0002735	38.44	63,790	1,074.
5205210020	0.00009210	31.13	233,800	3,939.
5205210030	0.00004972	25.33	532,400	8,968.
5205210040	0.00003281	25.22	810,300	13,640.
5230210010	0.0002052	51.16	60,770	1,074.
5230210020	0.00008999	31.83	222,800	3,939.
5230210030	0.00004343	28.96	507,200	8,968.
5230210040	0.00003201	25.82	772,000	13,640.
5203310010	0.0002288	46.30	43,380	1,074.
5203310020	0.00007385	39.13	159,000	3,939.
5203310030	0.00004569	27.78	362,000	8,968.
5203310040	0.00003257	25.60	551,000	13,640.
5205310010	0.0002307	47.32	84,820	1,074.
5205310020	0.00009602	31.02	310,900	3,939.
5205310030	0.00004499	29.08	707,900	8,968.
5205310040	0.00003140	27.37	1,077,000	13,640.
5230310010	0.0002067	50.17	53,120	1,074.
5230310020	0.00009311	30.38	194,700	3,939.
5230310030	0.00004044	30.72	443,300	8,968.
5230310040	0.00003209	25.43	674,800	13,640.
5203410010	0.0003253	34.03	44,270	1,074.
5203410020	0.00007459	40.48	162,300	3,939.
5203410030	0.00004807	27.59	369,500	8,968.
5203410040	0.00003630	24.01	562,400	13,640.
5205410010	0.0001747	63.51	86,860	1,074.
5205410020	0.00007475	40.49	318,400	3,939.
5205410030	0.00003831	34.71	724,900	8,968.
5205410040	0.00002720	32.12	1,103,000	13,640.
5230410010	0.0002676	38.56	60,660	1,074.
5230410020	0.0001079	26.08	222,400	3,939.
5230410030	0.00004606	26.84	506,300	8,968.
5230410040	0.00003635	22.35	770,600	13,640.

TABLE B. XXII

VALUES OF THE FOUR DIMENSIONLESS GROUPS FOR THE 48 FT X 48 FT SHELTER TREATMENT NO. 10 WINDWARD ROOF

CODE	k Δt/Hx	$t_a/\Delta t$	$V\rho x/\mu$	x/t
5103110010	0.0001932	52.81	40,630	1.074.
5103110020	0.00006575	42.33	148,900	3.939.
5103110030	0.00003042	40.18	339,100	8.968.
5103110040	0.00002462	32.62	516,200	13.640.
5105110010	0.0001664	62.69	85,250	1.074.
5105110020	0.00006428	44.28	312,500	3.939.
5105110030	0.00002218	56.36	711,500	8.968.
5105110040	0.00002223	36.95	1,083,000	13.640.
5130110010	0.0002301	44.38	36,440	1.074.
5130110020	0.00006837	40.73	133,500	3.939.
5130110030	0.00002936	41.67	304,100	8.968.
5130110040	0.00002562	31.37	462,800	13.640.
5103210010	0.0002464	42.12	50,920	1.074.
5103210020	0.00008097	34.96	186,700	3.939.
5103210030	0.00003557	34.96	425,000	8.968.
5103210040	0.00002998	27.25	646,900	13.640.
5105210010	0.0002320	45.31	63,790	1.074.
5105210020	0.00005402	53.08	233,800	3.939.
5105210030	0.00002870	43.88	532,400	8.968.
5105210040	0.00002524	32.78	810,300	13.640.
5130210010	0.0002186	48.02	60,770	1.074.
5130210020	0.00007167	39.96	222,800	3.939.
5130210030	0.00002803	44.87	507,200	8.968.
5130210040	0.00002551	32.39	772,000	13.640.
5103310010	0.0002040	51.93	43,380	1.074.
5103310020	0.00007177	40.26	159,000	3.939.
5103310030	0.00002969	42.74	362,000	8.968.
5103310040	0.00002626	31.75	551,000	13.640.
5105310010	0.0002268	48.14	84,820	1.074.
5105310020	0.00007148	41.67	310,900	3.939.
5105310030	0.00002694	48.96	707,900	8.968.
5105310040	0.00002432	35.34	1,077,000	13.640.
5130310010	0.0002124	48.82	53,120	1.074.
5130310020	0.00006621	42.72	194,700	3.939.
5130310030	0.00002908	42.72	443,300	8.968.
5130310040	0.00002538	32.17	674,800	13.640.
5103410010	0.0002774	39.90	44,270	1.074.
5103410020	0.00008276	36.49	162,300	3.939.
5103410030	0.00003300	40.19	369,500	8.968.
5103410040	0.00002844	30.64	562,400	13.640.
5105410010	0.0001668	66.53	86,860	1.074.
5105410020	0.00005471	55.33	318,400	3.939.
5105410030	0.00002189	60.74	724,900	8.968.
5105410040	0.00002095	41.70	1,103,000	13.640.
5130410010	0.0002638	39.12	60,660	1.074.
5130410020	0.00007813	36.03	222,400	3.939.
5130410030	0.00003093	39.97	506,300	8.968.
5130410040	0.00002700	30.09	770,600	13.640.

CODE	k Δt/Hx	$t_a/\Delta t$	$V\rho x/\mu$	x/t
5103510010	0.0002514	45.69	37,360	1.074.
5103510020	0.00007756	40.39	136,900	3.939.
5103510030	0.00003851	35.73	311,800	8.968.
5103510040	0.00002790	32.41	474,600	13.640.
5105510010	0.0002073	54.65	80,310	1.074.
5105510020	0.00006211	49.77	296,400	3.939.
5105510030	0.00002679	50.68	670,300	8.968.
5105510040	0.00002304	38.71	1,020,000	13.640.
5130510010	0.0002267	44.53	59,390	1.074.
5130510020	0.00007692	35.80	217,700	3.939.
5130510030	0.00003335	36.27	495,700	8.968.
5130510040	0.00002858	27.80	754,500	13.640.
5103610010	0.0002001	57.42	61,470	1.074.
5103610020	0.00006472	48.43	225,300	3.939.
5103610030	0.00002645	52.05	513,000	8.968.
5103610040	0.00002907	31.11	780,900	13.640.
5105610010	0.0002330	50.25	58,740	1.074.
5105610020	0.00006815	46.87	215,300	3.939.
5105610030	0.00002792	50.25	490,200	8.968.
5105610040	0.00002297	40.12	746,200	13.640.
5130610010	0.0002331	43.53	46,990	1.074.
5130610020	0.00007317	37.83	172,300	3.939.
5130610030	0.00002859	42.52	392,200	8.968.
5130610040	0.00002665	29.97	597,000	13.640.
5103710010	0.0002266	54.52	66,370	1.074.
5103710020	0.00006970	48.36	243,300	3.939.
5103710030	0.00003115	47.53	553,900	8.968.
5103710040	0.00002589	37.58	843,100	13.640.
5105710010	0.0001629	77.33	87,220	1.074.
5105710020	0.00004876	70.47	319,700	3.939.
5105710030	0.00002223	67.90	727,900	8.968.
5105710040	0.00001852	53.53	1,107,000	13.640.
5130710010	0.0002592	38.92	62,430	1.074.
5130710020	0.00008075	34.09	228,900	3.939.
5130710030	0.00003172	38.11	521,100	8.968.
5130710040	0.00002938	27.03	793,100	13.640.
5103810010	0.0002303	56.21	62,980	1.074.
5103810020	0.00006981	50.59	230,900	3.939.
5103810030	0.00003011	51.52	525,700	8.968.
5103810040	0.00002564	39.74	800,100	13.640.
5105810010	0.0001541	85.67	87,810	1.074.
5105810020	0.00005367	67.09	321,900	3.939.
5105810030	0.00001647	96.01	732,900	8.968.
5105810040	0.00001269	81.89	1,115,000	13.640.
5130810010	0.0002100	48.53	78,010	1.074.
5130810020	0.00006846	40.62	286,000	3.939.
5130810030	0.00002762	44.22	651,100	8.968.
5130810040	0.00002458	32.64	991,000	13.640.

TABLE B.XXIII

VALUES OF THE FOUR DIMENSIONLESS GROUPS FOR THE 48 FT X 48 FT SHELTER TREATMENT NO. 11 WINDWARD ROOF

CODE	k Δt/Hx	$t_a/\Delta t$	$V\rho x/\mu$	x/t
5303110010	0.0005355	19.05	40,630	1.074.
5303110020	0.0001822	15.27	148,900	3.939.
5303110030	0.00007673	15.93	339,100	8.968.
5303110040	0.000007987	100.8	916,200	13.640.
5305110010	0.0004806	21.71	85,250	1.074.
5305110020	0.0001453	19.57	312,500	3.939.
5305110030	0.00006700	18.66	711,500	8.968.
5305110040	0.00005285	15.54	1,083,000	13.640.
5330110010	0.0004789	21.32	36,440	1.074.
5330110020	0.0001867	14.91	133,500	3.939.
5330110030	0.00007912	15.46	304,100	8.968.
5330110040	0.00006126	13.12	462,800	13.640.
5303210010	0.0006161	16.84	50,920	1.074.
5303210020	0.0001945	14.55	186,700	3.939.
5303210030	0.00008948	13.89	425,000	8.968.
5303210040	0.00006599	12.38	646,900	13.640.
5305210010	0.0005564	18.89	63,790	1.074.
5305210020	0.0001733	16.53	233,800	3.939.
5305210030	0.00007368	17.09	532,400	8.968.
5305210040	0.00005717	14.47	810,300	13.640.
5330210010	0.0004642	22.62	60,770	1.074.
5330210020	0.0001778	16.10	222,800	3.939.
5330210030	0.00007814	16.10	507,200	8.968.
5330210040	0.00006100	13.55	772,000	13.640.
5303310010	0.0005586	18.96	43,380	1.074.
5303310020	0.0001804	16.01	159,000	3.939.
5303310030	0.00008521	14.89	362,000	8.968.
5303310040	0.00005959	13.99	551,000	13.640.
5305310010	0.0005202	20.99	84,820	1.074.
5305310020	0.0001696	17.56	310,900	3.939.
5305310030	0.00006866	19.06	707,900	8.968.
5305310040	0.00005650	15.21	1,077,000	13.640.
5330310010	0.0004741	21.87	53,120	1.074.
5330310020	0.0001769	15.99	194,700	3.939.
5330310030	0.00007044	17.64	443,300	8.968.
5330310040	0.00005882	13.88	674,800	13.640.
5303410010	0.0006507	17.01	44,270	1.074.
5303410020	0.0001851	16.31	162,300	3.939.
5303410030	0.00008730	15.19	369,500	8.968.
5303410040	0.00006474	13.46	562,400	13.640.
5305410010	0.0004428	25.06	86,869	1.074.
5305410020	0.0001408	21.49	318,400	3.939.
5305410030	0.00006234	21.33	724,900	8.968.
5305410040	0.00005143	16.98	1,103,000	13.640.
5330410010	0.0005220	19.77	60,660	1.074.
5330410020	0.0001953	14.41	222,400	3.939.
5330410030	0.00007677	16.10	506,300	8.968.
5330410040	0.00006365	12.76	770,600	13.640.

CODE	k Δt/Hx	$t_a/\Delta t$	$V\rho x/\mu$	x/t
5303510010	0.0006614	17.36	37,360	1.074.
5303510020	0.0001686	18.58	136,900	3.939.
5303510030	0.00008740	15.74	311,800	8.968.
5303510040	0.00006424	14.07	474,600	13.640.
5305510010	0.0005083	22.29	80,310	1.074.
5305510020	0.0001658	18.64	294,400	3.939.
5305510030	0.00007089	19.15	670,300	8.968.
5305510040	0.00005602	15.92	1,020,000	13.640.
5330510010	0.0004958	20.36	59,390	1.074.
5330510020	0.0001895	14.53	217,700	3.939.
5330510030	0.00007906	15.30	495,700	8.968.
5330510040	0.00006472	12.28	754,500	13.640.
5303610010	0.0005096	22.55	61,470	1.074.
5303610020	0.0001694	18.50	225,300	3.939.
5303610030	0.00007021	19.61	513,000	8.968.
5303610040	0.00005523	16.38	780,900	13.640.
5305610010	0.0005228	22.40	58,740	1.074.
5305610020	0.0001786	17.87	215,300	3.939.
5305610030	0.00007648	18.34	490,200	8.968.
5305610040	0.00005735	16.07	746,200	13.640.
5330610010	0.0005235	19.38	46,990	1.074.
5330610020	0.0001796	15.40	172,300	3.939.
5330610030	0.00008002	15.19	392,200	8.968.
5330610040	0.00005986	13.34	597,000	13.640.
5303710010	0.0005755	21.47	66,370	1.074.
5303710020	0.0001775	18.98	243,300	3.939.
5303710030	0.00007801	18.98	553,900	8.968.
5303710040	0.00006122	15.89	843,100	13.640.
5305710010	0.0004729	26.64	87,220	1.074.
5305710020	0.0001598	21.49	319,700	3.939.
5305710030	0.00007294	20.69	727,900	8.968.
5305710040	0.00004738	20.93	1,107,000	13.640.
5330710010	0.0005387	18.73	62,430	1.074.
5330710020	0.0001905	14.44	228,900	3.939.
5330710030	0.00008218	14.71	521,100	8.968.
5330710040	0.00006441	12.33	793,100	13.640.
5303810010	0.0005700	22.71	62,980	1.074.
5303810020	0.0001739	20.30	230,900	3.939.
5303810030	0.00007890	19.66	525,700	8.968.
5303810040	0.00006099	16.71	800,100	13.640.
5305810010	0.0003983	33.14	87,810	1.074.
5305810020	0.0001228	29.31	321,900	3.939.
5305810030	0.00005852	27.03	732,900	8.968.
5305810040	0.00004106	25.31	1,115,000	13.640.
5330810010	0.0004741	21.50	78,010	1.074.
5330810020	0.0001779	15.62	286,000	3.939.
5330810030	0.00007039	17.35	651,100	8.968.
5330810040	0.00005913	13.57	991,000	13.640.

VITA

Harry John Braud, Jr.

Candidate for the Degree of

Doctor of Philosophy

Thesis: FORCED CONVECTIVE HEAT TRANSFER FROM AN INCLINED SHELTER ROOF EXPOSED TO SOLAR RADIATION

Major Field: Agricultural Engineering

Biographical:

Personal Data: Born in Ascension Parish, Louisiana, September 9, 1935, the son of Harry J. and Alice Abadie Braud.

Education: Attended grade and high school at Dutchtown, Louisiana; received the Bachelor of Science degree from Louisiana State University in 1957 with a major in Agricultural Engineering; received the Master of Science degree from Louisiana State University in 1959 with a major in Agricultural Engineering; completed the requirements for the Doctor of Philosophy Degree in May, 1962.

Professional Experience: Worked two summers as a part-time student assistant on several agricultural engineering research projects at Louisiana State University from 1956 to 1958; conducted calorimetric research at Louisiana State University while serving as a graduate student on a Louisiana Power and Light Company fellowship in 1957 and 1958; served as laboratory assistant in the hydraulic and surveying laboratories of the Civil Engineering Department at Louisiana State University in 1959; employed as graduate research assistant for the Oklahoma Agricultural Experiment Station from June, 1960 to August, 1961.

Organizations: Member of the American Society of Agricultural Engineers; member of Tau Beta Pi, honorary engineering fraternity; member of Alpha Zeta, honorary agricultural fraternity.